Enantioselective cyclopropanation of heterocycles and the use of high-pressure techniques for the conformational analysis of peptide foldamers

vorgelegt von

Ludwig K. A. Pilsl

aus Regensburg

Regensburg 2014

für Bernadette

“Difficulties are just things to overcome, after all.”

Ernest H. Shackleton (antarctic explorer)

Table of contents

Abbreviations

Ac	acetyl
ACC	aminocyclopropanecarboxylic acid
Ala	alanine
atm	atmosphere
ATR	attenuated total reflection
aq.	aqueous
azabox	aza-bis(oxazoline)
Bn	benzyl
Boc	*tert*-butyloxycarbonyl
box	bis(oxazoline)
bp	boiling point
brsm	based on recovered starting material
CD	circular dichroism
CNS	central nervous system
comb.	combined
conc.	concentrated
Cpe	cispentacin
Cy	cyclohexyl
d	day(s)
DA	donor-acceptor
DCM	dichloromethane
DEAD	diethyl azodicarboxylate
DFT	density functional theory
DMAP	4-dimethylaminopyridine
DMSO	dimethyl sulfoxide
dr	diastereomeric ratio
EA	ethyl acetate
EDC	1-ethyl-3-(3-dimethyl-aminopropyl)carbodiimide
ee	enantiomeric excess
EIC	extracted-ion chromatogram
equiv	equivalent(s)
ESI	electrospray ionization
Et	ethyl
FA	*Felkin-Ahn*
Fmoc	fluorenylmethoxycarbonyl
FT	Fourier transform
GABA	γ-aminobutyric acid
GC	gas chromatography
Gln	glutamine
Glu	glutamic acid
h	hour(s)
HP	high-pressure
HPLC	high-pressure/performance liquid chromatogaphy

HRMS	high resolution mass spectrometry
HSQC	heteronuclear single quantum coherence
IBX	2-iodoxybenzoic acid
IC_{50}	half maximal inhibitory concentration
*i*Pr	*iso*-propyl
IR	infrared spectroscopy
LAH	lithium aluminum hydride
LC	liquid chromatography
Lys	lysine
MCR	multi-component reaction
mGlu	metabotropic glutamate
Me	methyl
min	minute(s)
mp	melting point
MS	mass spectrometry
nd	not determined
NMR	nuclear magnetic resonance
NOESY	nuclear *Overhauser* effect spectroscopy
PE	petroleum ether
PET	polyethylene terephthalate
Ph	phenyl
PLAP	pig liver acetone powder
PPL	porcine pancreatic lipase
ppm	parts per million
Pro	proline
PTFE	polytetrafluoroethylene
quant.	quantitative
R	arbitrary residue
ref.	reference
rt	room temperature
sat.	saturated
SMBC	simulated moving bed chromatography
S_N	nucleophilic substitution
TBAB	tetrabutylammonium bromide
*t*Bu	*tert*-butyl
Tf	trifluoromethanesulfonate
THF	tetrahydrofuran
TIC	total ion current
TLC	thin layer chromatography
tox	tris(oxazoline)
Ts	tosyl
UV	ultraviolet
VT	variable temperature

A Introduction – Synthesis and applications of cyclopropanated furan and pyrrole derivatives

1 Introduction

Cyclopropanated furan and pyrrole derivatives represent a class of highly valuable compounds with unique structural features that have been utilized in a number of elegant synthetic approaches so far. Their versatile reactivity makes them powerful intermediates and allows for various orthogonal functionalizations and transformations. This account will focus on compounds with the general substructures of **1** and **2** (figure **1**).
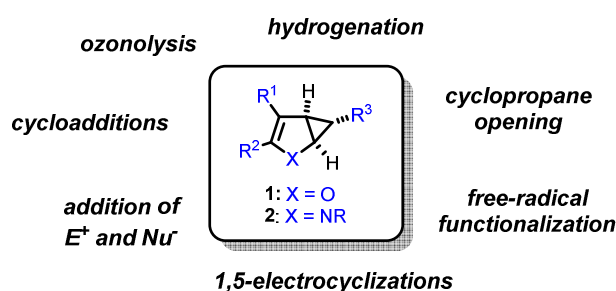
Figure 1. General structure of cyclopropanated furan (X = O) and pyrrole (X = NR) derivatives and possible transformations of them.

Figure **1** illustrates the core structure of the title compounds and the general scope for their further transformation. A brief history of the first literature precedents will be given, followed by recent methods for the preparation of compounds like **1** and **2**, with a special focus on enantioselective reactions. In addition, applications in the synthesis of natural products and other synthetically useful compounds will be presented. Cyclopropanated benzofurans and indoles as well as doubly cyclopropanated furans have also been described, but will not be covered in here.

2 Methods for the preparation of cyclopropanated furan and pyrrole derivatives

The first examples of cyclopropanated furans date back to the 1960s, when *Müller* and co-workers used diazomethane and copper(I)-bromide for the cyclopropanation of furan to synthesize homofuran **1** (X = O, R^1 = R^2 = R^3 = H).[1] While cyclopropanation of furan by photo-induced decomposition of diazo compounds was already reported in 1958 by *Schenck and Steinmetz*,[2, 3] the decomposition of diazoesters catalyzed by dirhodium tetraacetate for cylopropanation reactions of furan itself and derivatives thereof was carried out by *Wenkert et al.* in the 1990s.[4-6] Furthermore, they recognized the intrinsic instability of the unsubstituted furanocyclopropane moiety bearing an ester group at the three-membered ring, which was put to an advantage with the synthesis of highly unsaturated open-chain aldehydes via ring opening / isomerization. More importantly, the authors could already prove that electron-withdrawing groups on the furan ring increase the stability of the cyclopropanated adducts dramatically, thus allowing a multifaceted follow-up chemistry. On the other hand, first efforts for the cylcopropanation of pyrrole derivatives and their application in cycloaddition reactions were conducted by *Fowler* in the early 1970s.[7-9] Copper complexes with homoscorpionate based ligands were shown to be able to catalyze cyclopropanation reactions of furans, although only in racemic form.[10, 11] Current methods for the enantioselective synthesis of cyclopropanated furans (**1**) and pyrrols (**2**) are based on the decomposition of diazo compounds with chiral metal complexes.[12] Copper(I)-complexes with chiral bis(oxazoline) (box, **5-7**) or aza-bis(oxazoline) (azabox, **8-9**) ligands have been shown to be superior catalysts for intermolecular cyclopropanation reactions of furans (scheme **1**).[13-15] However, only very few derivatives are accessible in enantiomerically pure form so far (scheme **1**, *lower part*).
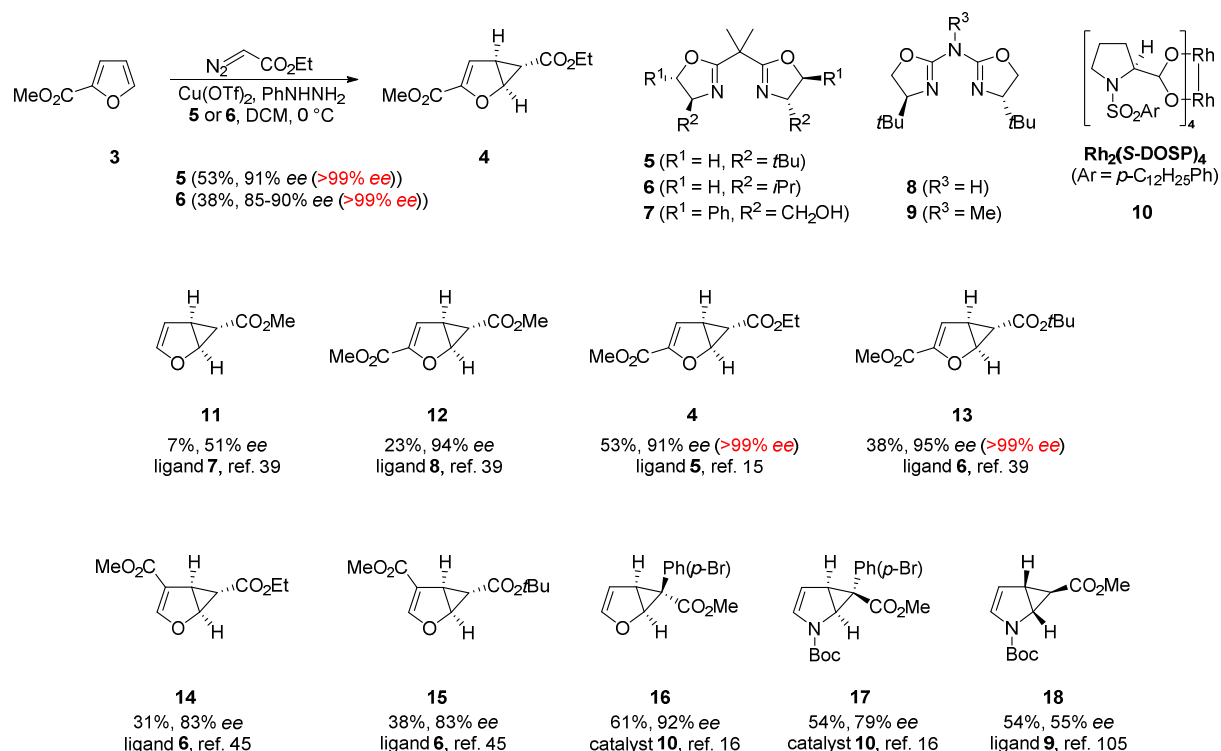
Scheme 1. *Top:* Enantioselective cyclopropanation of 2-methyl furoate **3** reported by *Reiser et al.* Depending on the absolute configuration of the applied ligand, both enantiomers of cyclopropane **4** can be obtained in enantiomerically pure form and multi-gram quantity.[15] *Bottom:* Overview of the most successful results in literature for enantioselectively cyclopropanated of furan and pyrrole derivatives with the applied ligand (or catalyst) and the corresponding reference (*red* values in brackets were obtained after recrystallization).

Chiral rhodium(II)-catalysts like **10** have also emerged for such kind of transformations, however, with limited success (**16, 17**).[16] For the preparation of cyclopropanated pyrroles **2** (see **17** and **18**) no direct asymmetric cyclopropanation reaction is known so far. Nevertheless, other methods for accessing enantiomerically pure **18** have been achieved (see main part chapter **B 1.3.1**).[17, 18] New accomplishments and optimizations of asymmetric cyclopropanation reactions of furan and pyrrole derivatives will be presented in the main part of the present thesis. In the following chapter, possible transformations of the compounds presented above will be discussed.

3 Transformations of cyclopropanated furans and pyrroles

The simplest representatives of the title compounds are homofuran **1** (X = O) and homopyrrole **2** (X = NR). These molecules have been employed in a manifold of cycloaddition reactions, as they exhibit unique properties as masked 1,5-dipoles.[19-22]

Under thermal activation, **1** or **2** can rearrange to form compounds of type **19**, being a highly reactive intermediate that can undergo [5+2] cycloaddition reactions with suitable dienophiles to form seven-membered ring systems **20** with ease (scheme **2**). By density functional theory (DFT) calculations it was shown that homofuran **1** and homopyrrole **2** display relatively low distortion energies for the reaction to **19**, which was claimed to be the main reason for their ability to undergo metal-free [5+2] cycloaddition reactions.[23]
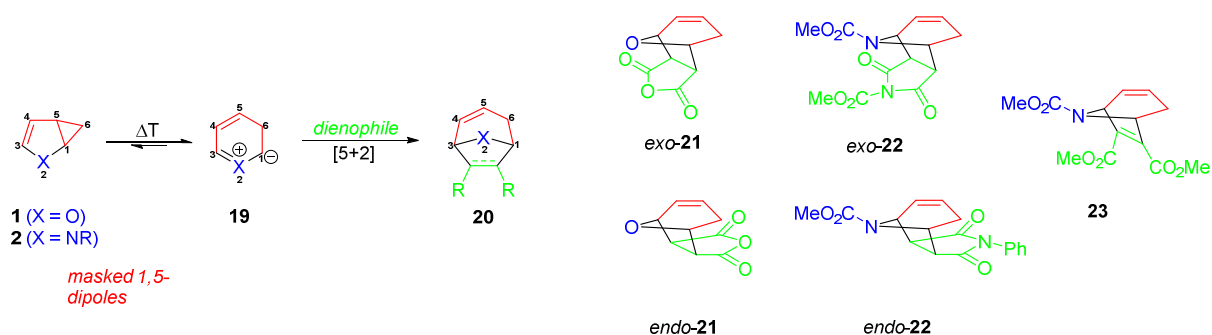
Scheme 2. Reactivity of homofuran **1** (X = O) and homopyrrole **2** (X = NR). Under thermal conditions **1** or **2** can serve as masked 1,5-dipoles for [5+2] cycloaddition reactions, yielding products like **21**-**23**.[7, 8, 23, 24]

Tanny and Fowler could show that also cylopropanated pyrrole derivatives bearing an ethyl ester moiety at the 6-position are able to undergo analogous reactions with suitable nucleophiles.[25] On the other hand, racemic cyclopropanated furan **24** was shown to undergo a [4+2] cycloaddition reaction with diethyl azodicarboxylate (DEAD).[26] Nevertheless, applications of homofuran and homopyrrole derivatives are limited, and cyclopropanated furan and pyrrole esters (**4**, **15**, **18**, **24**) proved to be superior building blocks for synthesis, since access to enantiomerically pure material is feasible and possible transformations are more diverse. Figure **2** gives an overview of accessible target compounds (**25**-**34**) and details on their syntheses and properties will be discussed in the following sections.
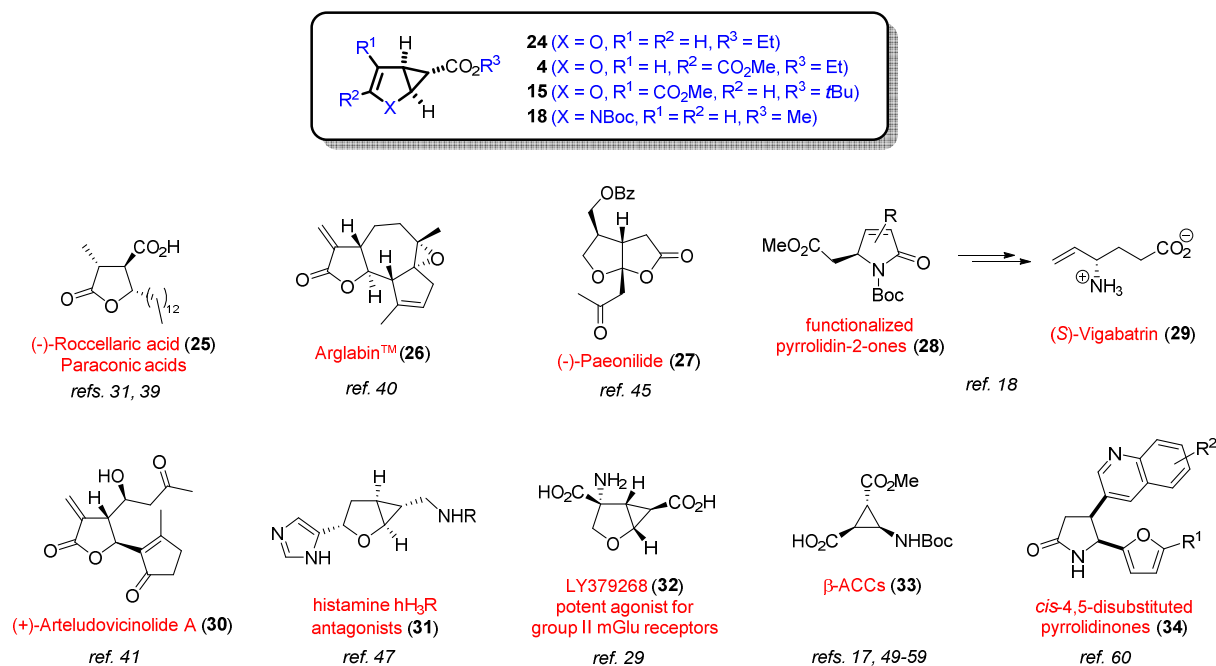
Figure 2. Overview of accessible compounds from cyclopropanated furan and pyrrole esters (mGlu = metabotropic glutamate; ACC = aminocyclopropanecarboxylic acid).

3.1 Transformations of cyclopropanated furan derivatives

A rhodium catalyzed cyclopropanation of furan **35** with diazo compound **36** was used for the total synthesis of racemic 12-hydroxyeicosatetraenoic acid **38** by *Fitzsimmons* and co-workers via an intermediary cyclopropane and open-chain aldehyde **37** (scheme **3**).[27] Hereby, the authors made use of the cyclopropane ring unraveling process introduced earlier by *Wenkert et al.*[28]
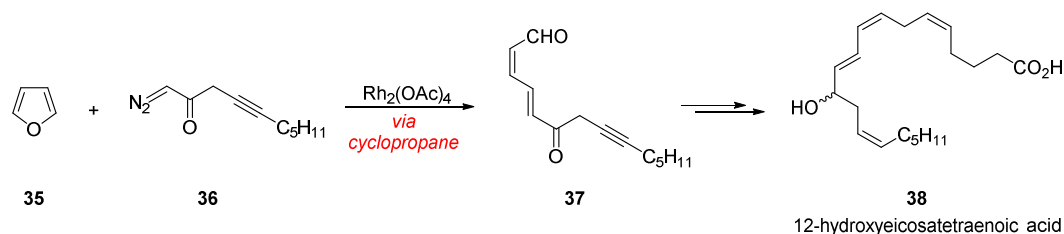
Scheme 3. Synthesis of 12-hydroxyeicosatetraenoic acid **38** by *Fitzsimmons et al.* through cyclopropanation of furan **35** with diazoester **36** and subsequent cyclopropane unraveling.[27]

In 1999, *Monn* and colleagues synthesized bicyclic amino acid LY379268 (**32**) in ten steps from furan ester **24** and found it to be a remarkably potent agonist for group II metabotropic

glutamate (mGlu) receptors.[29, 30] A powerful methodology for the construction of *trans*-4,5-disubstituted γ-butyrolactones **43** from cyclopropanated furan **4** was presented by *Reiser* and co-workers,[13, 15, 31, 32] which enables the access to a manifold of natural products, including Paraconic acids, Eudesmanolides, Elemanolides, Guaianolides and Xanthanolides (scheme **4**).[33-37] After ozonolytic cleavage of the double bond in **4** with reductive work-up, a diastereoselective addition of various nucleophiles (Nu) to the aldehyde function of **39** can be performed, which yields either the *Felkin-Ahn* or *Cram-Chelate* products (depending on the nucleophile) in high selectivity.[36] Base-induced saponification of the oxalic ester moiety in **40** leads to donor-acceptor (DA) substituted cyclopropane **41**, which undergoes a retroaldol/lactonization sequence (via **42**) to yield diversely substituted lactones of type **43**.
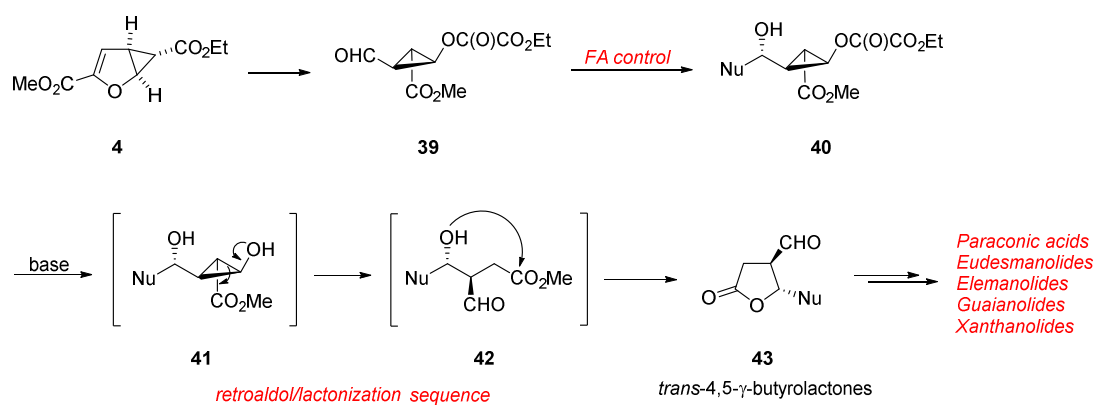
Scheme 4. Synthetic sequence for the stereoselective preparation of *trans*-4,5-disubstituted γ-butyrolactones **43** as precursors for the synthesis of sesquiterpenelactone based natural products (FA = *Felkin-Ahn*).[38]

This method has been applied successfully for the construction of several natural products, amongst them various Paraconic acids (e.g. Roccellaric acid **25**),[31, 39] Arglabin^{TM} **26**[40] and Arteludovicinolide A **30** (see also figure **2**).[41] Another promising method for the application of cyclopropanated furans is the acid-catalyzed cyclopropane ring opening reaction followed by lactonization that is depicted in scheme **5**. It has to be noted that related transformations were reported earlier.[42, 43] As an application of this methodology *cis*-fused 5-oxofuro[2,3-*b*]furans of type **44** and **45** can be generated, with an carboxylic acid function either in 2- or 3-position (**44** and **45**) depending on the furan starting material being used.
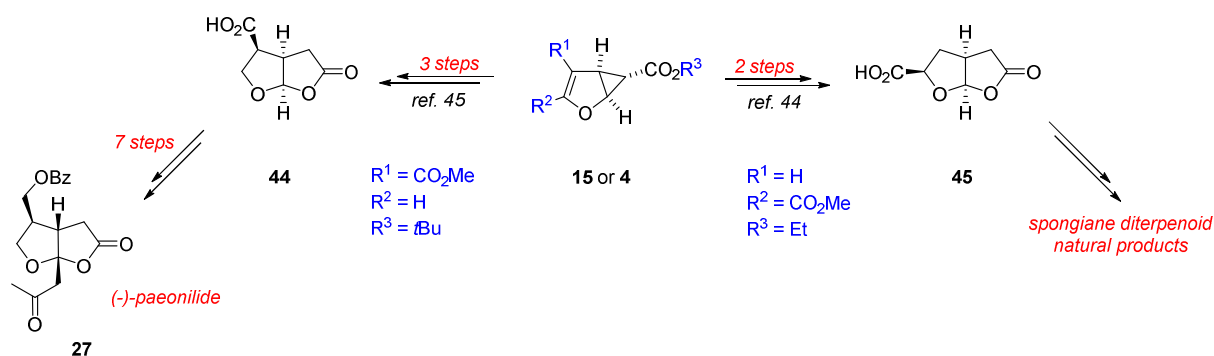
Scheme 5. Facile access to *cis*-fused 5-oxofuro[2,3-*b*]furans of type **44** and **45** based on acid-catalyzed cyclopropane opening and subsequent lactonization starting from 2- or 3-substituted furans.[44, 45]

While bicyclic lactone **45** can serve as starting point into several spongiane diterpenoid natural products (e.g. Norrisolide, Macfarlandin C, Cheloviolene A and B),[46] **44** has been successfully used for the enantioselective synthesis of (-)-Paeonilide **27** in ten steps from cyclopropane **15** (in 83% *ee*, see main part chapter **B 1.2** for details). Recently, tetrahydrofuran derivative **31** and various related compounds were prepared from cyclopropane **4** as potent histamine hH$_3$ receptor antagonists (figure **2**).[47]

3.2 Transformations of cyclopropanated pyrrole derivatives

In contrast to the furan derivatives presented above, cyclopropanated pyrroles have been applied for the construction of a variety of biologically relevant nitrogen containing compounds (figure **2**). For instance, so-called β-aminocyclopropanecarboxylic acids (β-ACCs **33**)[17, 48-52] – conformationally constrained β-amino acids – have been successfully employed in a variety of artificial peptide sequences as rigidifying compounds. The combination of **33** with α-amino acids allowed in peptides the construction of new secondary structural motifs,[53] biologically active ligands toward Neuropeptide Y, Orexin and CPRG receptors [54-57] as well as organocatalysts (see main part chapter **B 4** for details).[58, 59] Comparable to the procedure in scheme **4**, an ozonolytic cleavage of the remaining double bond in **18** was again the key step for the preparation of these valuable unnatural amino acids. Besides opening the pyrrol ring that led to the synthesis of conformationally constrained amino acids **33**, pyrrole derivative **18** could also be employed in transformations that selectively open the cyclopropane ring. For example, **18** can be converted into 4-functionalized pyrrolidin-2-one **28** within four steps. From there, multiple functionalizations

of **28**, as well as the synthesis of (*S*)-Vigabatrin **29** have been accomplished.[18] Cyclopropane **18** was also subjected to a *Povarov* reaction for the construction of complex heterocyclic compounds like **34** and **51** (scheme **6**).[60] In this case aromatic imines, which are in situ formed from aldehydes **46** or **48** and aniline derivatives **47** or **49**, undergo a [4+2] cycloaddition reaction with cyclopropanated pyrrole **18** in order to establish a six-membered ring system.
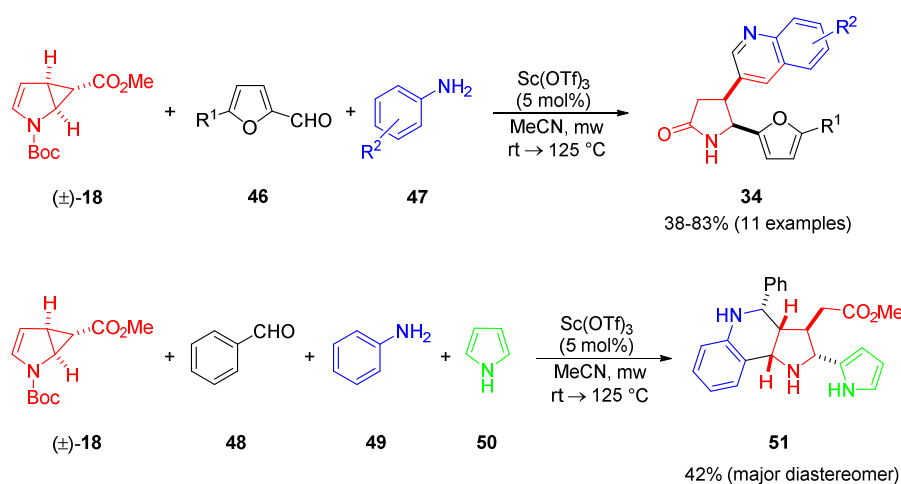
Scheme 6. *Lewis* acid catalyzed multicomponent reactions for the construction of complex heterocyclic compounds **34** and **51** (mw = microwaves, single fragments are color coded for clarity).[60]

Depending on the reaction conditions, these intermediates can react further in different pathways to form either *cis*-4,5-disubstituted pyrrolidinones **34** or compounds like **51**, where pyrrole **50** was added as an external nucleophile for trapping the intermediary iminium ion resulting from cyclopropane opening. *Landais* and *Renaud et al.* were able to add phenylthiol to a cyclopropanated pyrrole (X = NCO_2Me, $R^1 = R^2 = H$, $R^3 = Et$) under UV irradiation via a free-radical mechanism, however, only in 32% yield and a 1:1 mixture of diastereomers for this single example.[61] All in all, the literature examples presented above demonstrate the synthetic utility of cyclopropanated furans and pyrrols. Moreover, it seems obvious that from such a class of important molecules new and creative ideas for their transformations will arise in the future. In the present thesis, attempts for the optimization of heterocycle cyclopropanation, as well as subsequent transformations of the latter were carried out. The results are presented in the following.

B Main part

1 Asymmetric cyclopropanations of furan and pyrrole derivatives

1.1 Synthesis of the ligands for asymmetric cyclopropanation reactions

A central part of the present thesis deals with the asymmetric cyclopropanation of heterocyclic substrates using chiral copper(I)-complexes. Thus, we have focused on the application of the well-established aza-bis(oxazoline) (azabox) ligands **56** that were developed in the *Reiser* group[62, 63] and have already found various successful applications in asymmetric catalysis.[64-66] Structurally related to the parent semicorrines **52**,[67-69] the aza-semicorrines **53**,[70] and the bis(oxazolines) (box, **54**),[71-75] azabox ligands combine several positive aspects like accessibility from the chiral pool (starting from amino alcohols), a high degree of diversity, and the potential of functionalization and/or immobilization on the central nitrogen atom (figure **3**).[76-80] One step further from box and azabox ligands was made by *Tang et al.* and *Gade et al.* with the invention of tripodal tris(oxazoline) (tox) ligands with an additional binding site (figure **3**).[81, 82] However, the basis of box, azabox and tox ligands was made by *Brunner et al.*, who introduced oxazolines to catalysis already in 1989.[83, 84]
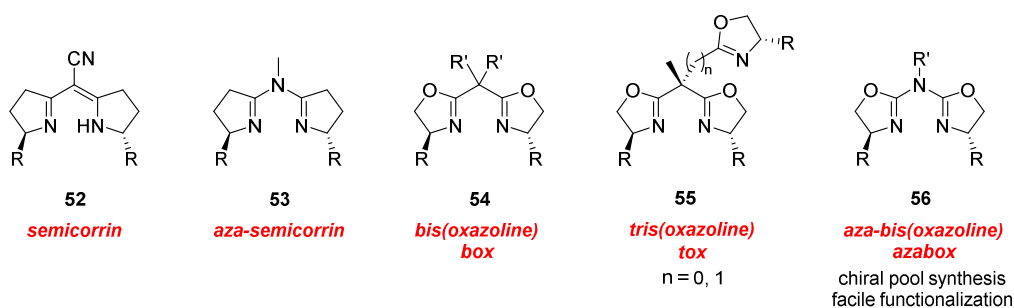
Figure 3. General chemical structures of different N-containing bi- and tridentate ligands for catalysis.

The original synthesis of azabox ligands published in 2000 was based on the direct coupling of two molecules of aminoxazoline **57** promoted by benzaldehyde **48** (*method A*, table **1**).[62] Using this method it was possible to prepare ligands with *tert*-butyl and *iso*-propyl substituents, however, yields were not always satisfying and there was no access to asymmetrically substituted ligands with a higher degree of diversity. In 2003, *Reiser* and

co-workers presented a new solution to such problems (*method B*, table **1**). Thus, by making use of alkylated oxazolidinones **59** as coupling partners with the established aminooxazolines **57** new types of ligands were accessible, partially in better yields.[63] Table **1** gives an overview of all so far synthesized azabox ligands (with free NH), the method of preparation, as well as the corresponding yields of the final coupling step, while figure **4** shows the chemical structures of the corresponding ligands.
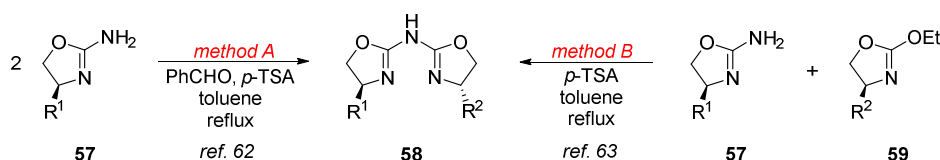
Table 1. Overview of all so far synthesized azabox ligands (with free NH) from the *Reiser* group.

entry	method	R^1	R^2	ligand	yield [%]
1[a]	A	*i*Pr	*i*Pr	**60**	53
2[b]	B	*i*Pr	*i*Pr	**60**	51
3[a]	A	*t*Bu	*t*Bu	**8**	58
4[b]	B	*t*Bu	*t*Bu	**8**	92
5[b,c]	B	*t*Bu	Ph	**63**	64
5[b,c]	B	Ph	Ph	**61**	35
6[d]	B	Bn	Bn	**62**	35
7[e]	B	*i*Pr	H	**64**	69
8[e]	B	*i*Pr	*gem*-di-Me	**65**	57
9[e,f]	B	*t*Bu	H	**66**	62
10[e,f]	B	*t*Bu	*gem*-di-Me	**67**	59
11[g]	A	indanyl	indanyl	**68**	26
12[g]	B	indanyl	indanyl	**68**	68

a) ref. [62]; b) ref. [63]; c) reaction carried out at 50 °C due to thermal lability of **61**; d) ref. [64]; e) ref. [85]; f) ref. [86]; g) ref. [87].

60 (R^1 = R^2 = *i*Pr)
8 (R^1 = R^2 = *t*Bu)
61 (R^1 = R^2 = Ph)
62 (R^1 = R^2 = Bn)
63 (R^1 = *t*Bu, R^2 = Ph)

64 (R^1 = *i*Pr, R^2 = H)
65 (R^1 = *i*Pr, R^2 = Me)
66 (R^1 = *t*Bu, R^2 = H)
67 (R^1 = *t*Bu, R^2 = Me)

68
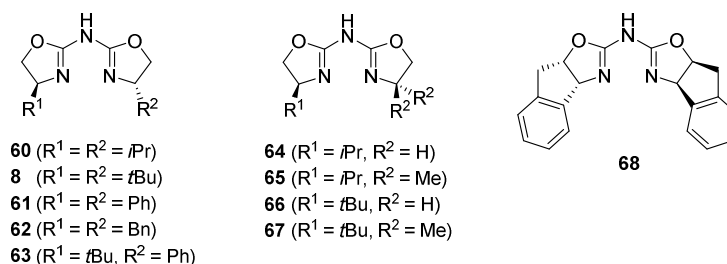
Figure 4. Overview of all so far synthesized azabox ligands (with free NH) from the *Reiser* group.

Scheme **7** gives an overview of the exemplary synthesis of *tert*-butyl-azabox **8** following the improved methodology.[63]
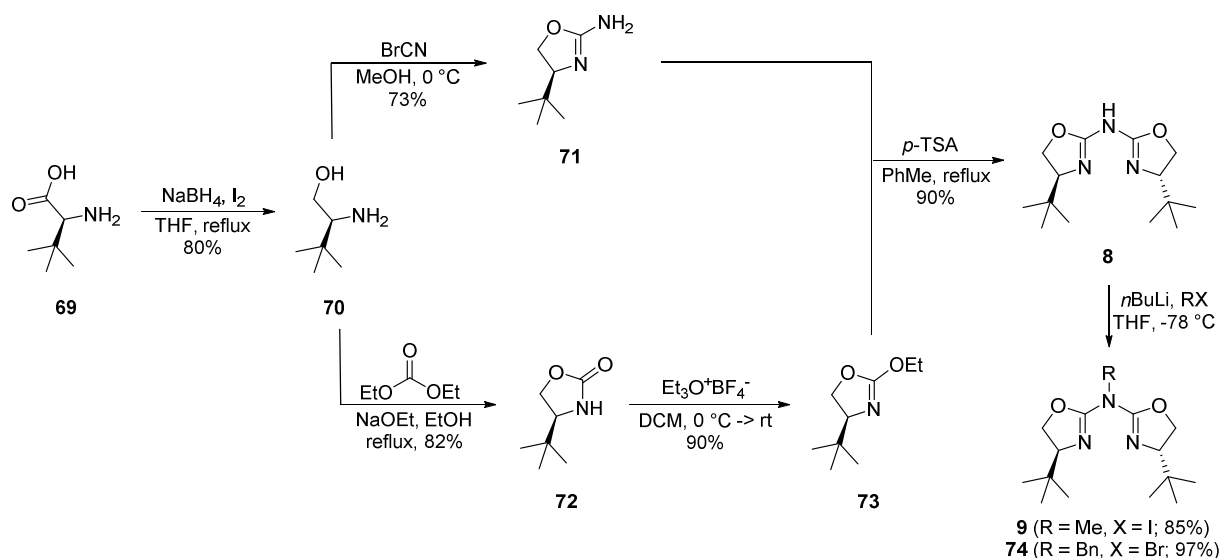
Scheme 7. Exemplary reaction scheme for the synthesis of *tert*-butyl substituted azabox ligand **8** following the improved methodology of *Reiser et al.*, and functionalization of the central N-atom to yield **9** and **74**.

Reduction of the amino acid **69** according to a protocol of *McKennon* and *Meyers*[88] yields amino alcohols **70** in good to excellent yields,[89] which serve as starting point for both coupling partners. On the one hand, **70** is cyclized to the corresponding aminooxazoline **71** by the use of in situ prepared cyanogen bromide (protocol of *Poos et al.*).[90-92] On the other hand, amino alcohol **70** is transformed into ethoxyoxazoline **73** in a two-step procedure. First, **70** is cyclized to the oxazolidinone **72** by the use of diethylcarbonate under basic conditions and then alkylated using *Meerwein's* reagent[93-95] to yield **73**. The final acid catalyzed step couples the aminooxazoline **71** with the ethoxyoxazoline **73** to yield azabox ligands in varying yields, strongly depending on the nature of the substituents (see table **1** for details).

Further functionalization of the central nitrogen atom can be readily achieved by deprotonation with *n*-butyl lithium, followed by trapping with a suitable electrophile (scheme **7**). As the new synthesis of azabox ligands by *Reiser et al.* (scheme **7**; ref. [63]) was based on studies by *Gawley et al.*, who investigated the reactivity of ethoxyoxazolines **75** toward amine nucleophiles (scheme **8**),[96] the idea for developing a simpler approach without the need for an aminooxazoline came to our mind.
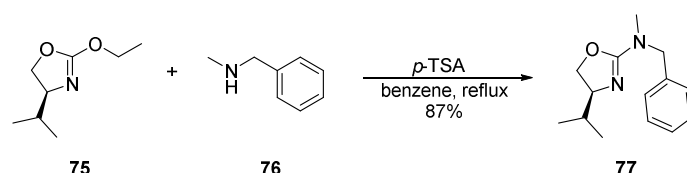
Scheme 8. Reaction of ethoxyoxazoline **75** with secondary amine **76** investigated by *Gawley et al.*[96]

As was already shown by *Gawley* and co-workers, ethoxyoxazolines are capable of reacting with secondary amines, thus, making use of the high reactivity of **78**, they could be applied for a much more convenient synthesis of azabox ligands. Based on these results **78**, should also react with ammonia or primary amines in order to form aminooxazolines of type **79**. These could further react with a second molecule of ethoxyoxazoline **78** to form azabox ligands with free NH or substituted derivatives (**80**), respectively (scheme **9**).
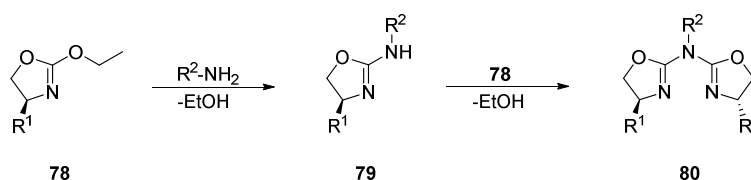
Scheme 9. Proposed strategy for a more convenient synthesis of azabox ligands **80** based on the condensation of ammonia or primary amines with two equivalents of alkylated oxazolidinones **78**.

For the investigation of our proposed strategy we have applied two different nitrogen sources, namely a solution of ammonia in methanol (7 M) and *N*-benzylamine. Main criteria for the choice of amines were manageability (e.g. boiling point) and the potential resulting target molecules. Furthermore, all experiments were carried out with *iso*-propyl substituted ethoxyoxazoline **75**, as its starting material *L*-valine is among the most abundant and inexpensive alternatives herein (compared for instance to *tert*-leucine **69**). Table **2** summarizes the experiments carried out to study the proposed strategy.
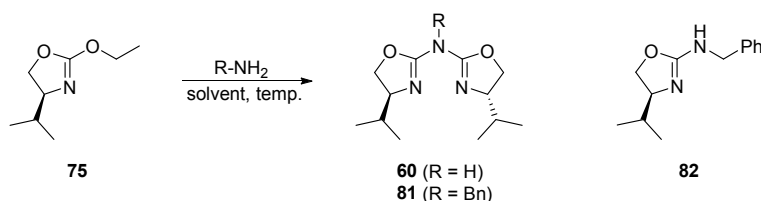
Table 2. Attempts for the preparation of azabox ligands by direct coupling with amines.[1]

entry[a]	N-source	product	solvent	catalyst	temperature [°C]	yield [%][d]
1	NH_3/MeOH	**60**	MeOH	-	50	8
2[b]	NH_3/MeOH	**60**	MeOH	-	50	12
3	NH_3/MeOH	**60**	MeOH	-	80	16
4	$BnNH_2$	**82**	toluene	-	125	17[e]
5	$BnNH_2$	**82**	toluene	*p*-TSA	125	84[e]
6[c]	**82**	-	toluene	*p*-TSA	125	-

a) 1.89 mmol (2 equiv) **75**, 0.95 mmol (1 equiv) R-NH₂, 0.09 mmol (0.1 equiv) *p*-TSA, 5 ml solvent, 24 h; b) ratio **75**/R-NH₂ (2:3); c) 0.95 mmol **82** (1 equiv), 4.75 mmol **75** (5 equiv), 0.10 mmol (0.1 equiv) *p*-TSA, 5 ml toluene, 24 h, reflux; d) isolated yields after column chromatography; e) no azabox formed, yield of mono-substitution product **82**.

Looking at table **2** it can be seen that the reaction did indeed work, but only in rather poor yields. Reactions employing a solution of ammonia in methanol (entries 1-3) resulted in unsubstituted azabox **60** with yields between 8% and 16%. Using *N*-benzylamine as the nucleophile, only the mono-substitution product **82** was obtained instead of the desired azabox **81** (entries 4-5). Moreover, an attempt of transforming secondary amine **82** into the desired *N*-benzyl-azabox **81** with an excess of ethoxyoxazoline **75** failed, probably due to the high steric demand of **82** (entry 6). In regard of the overall low yields for this approach no further investigations were conducted.

Besides the well-known reactivity of ethoxyoxazolines toward nucleophiles, it is also known that 2-chloro- and 2-bromooxazolines are capable of undergoing substitution reactions with a variety of nucleophiles. This was first shown by *Sam* and *Plampin* in 1964 when they investigated the synthesis of new benzoxazole derivatives as skeletal muscle relaxants (scheme **10**).[97]

---

[1] *Results are partially taken from the Bachelors thesis of M. Halder (supervised by L. Pilsl).*
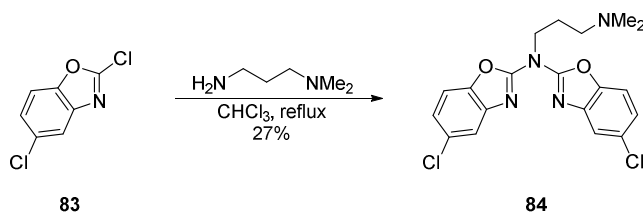
Scheme 10. Synthesis of aza-bis-benzoxazole **84** from 2-chlorobenzoxazole **83** by *Sam* and *Plampin*.

Although, the resulting double coupling product **84** was rather an unwanted by-product in their case, it nevertheless demonstrated the possibilities of such substrates. More recently, *Bellemin-Laponnaz* and *Gade et al.* were reacting 2-bromooxazolines **85** with imidazoles for the synthesis of N-heterocyclic carbene (NHC) ligands (scheme **11**).[98]
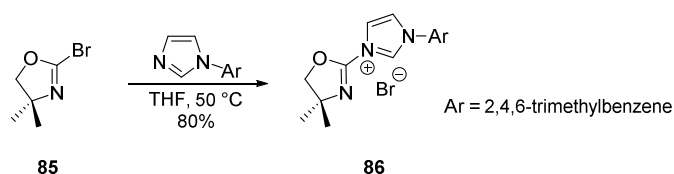
Scheme 11. Synthesis of NHC ligands from 2-bromooxazoline **85** by *Bellemin-Laponnaz* and *Gade et al.*[82]

In terms of such a reactivity pattern, it seemed applicable to try substitution of 2-bromooxazolines with ammonia in order to obtain azabox ligands (scheme **12**). Direct lithiation of the 2-*H*-oxazoline **87**[2] by the use of *tert*-butyllithium, followed by in situ bromination of the lithiated species with 1,2-dibromo-1,1,2,2-tetrafluoroethane is an established methodology for the preparation of bromooxazolines.[99-101]
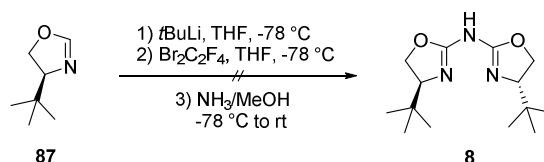
Scheme 12. Attempt for the direct lithiation-bromination-amination strategy for the synthesis of azabox **8** based on 2-*H*-oxazoline **87**.

Due to the fact that bromooxazolines are not permanently stable and tend to isomerize,[100] it was chosen to generate them in situ and directly convert them into the corresponding aminooxazolines/azabox ligands. Subsequent substitution of the bromide with methanolic ammonia was intended to yield an intermediary aminooxazoline of type **79**, which could then further react to the desired azabox ligand **8** (scheme **12**). However, this strategy did not lead to any product formation, and upon the failure of this approach no further efforts were made

---

[2] Oxazoline **87** was provided by M. Knorn.

to study such coupling reactions in more detail. In the course of this project the established synthesis procedure of *Reiser et al.*[63] was applied for the preparation of the required ligands.

1.2 Asymmetric cyclopropanation of furan derivatives

While cyclopropanation products of furan with diazoacetates have been shown to be rather unstable and tend to rearrange (see also introduction),[10, 12, 13, 102, 103] the enantioselective cyclopropanation of furan-2-carboxylic acid methyl ester **3** is a well-established process. It was developed in the *Reiser* group and is regularly performed on a multi-gram scale in our laboratories.[13-15, 31] Since then, this methodology was applied for a variety of γ-butyrolactone-containing natural product syntheses[32, 34-36, 39-41] and other synthetically useful compounds.[47, 60] In contrast, furan-3-carboxylic acid **88** was used as starting point for the synthesis of (-)-Paeonilide by *Harrar* and *Reiser*.[45] The key intermediate for their synthesis was cyclopropanated furoic ester **15** from which on they were able to synthesize **27** in ten steps and an overall yield of 14% (12 steps, 4.4% yield, 7.7% brsm, starting from commercially available furan-3-carboxylic acid **88**). However, due to the lack of complete stereocontrol during the crucial cyclopropanation step, (-)-Paeonilide **27** could only be prepared in a maximum of 83% enantiomeric excess. Scheme **13** depicts an overview of the synthesis of (-)-paeonilide **27** by *Harrar and Reiser*.
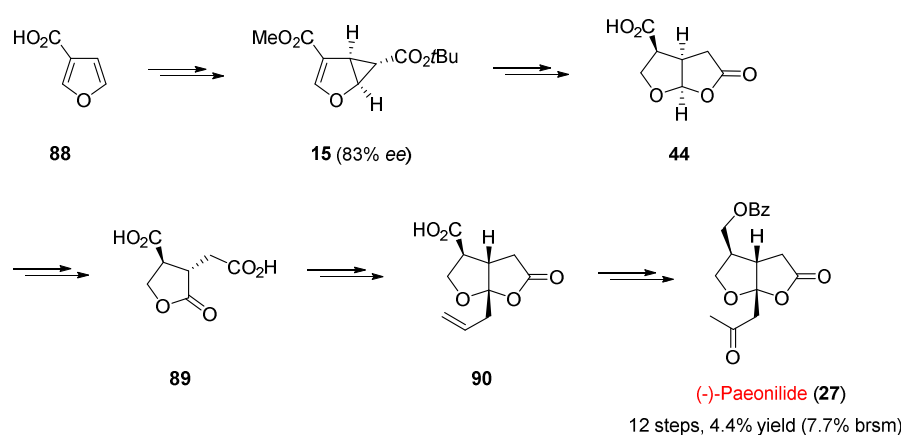
Scheme 13. Enantioselective synthesis of (-)-Paeonilide **27** from 3-furoic acid **88** (via **15**, **44**, **89**, **90**) by *Harrar and Reiser*.[45]

Table **3** summarizes all so far reported attempts for the enantioselective cyclopropanation of **91** (entries 1-8). When applying ethyldiazoacetate (R = Et) a maximum of 31% yield and 83% *ee* could be reached (entry 1), while for *tert*-butyl substituted analogue **15** 38% yield and analogous 83% *ee* could be realized in the best case so far (entry 6). As these results display the state-of-the-art for this important molecule, we envisioned to find a reasonable solution to this problem.

MeO₂C structure and scheme images:

- **91**   R = Et, *t*Bu   **14** (R = Et)   **15** (R = *t*Bu)
- **5** (R¹ = H, R² = *t*Bu)
- **6** (R¹ = H, R² = *i*Pr)
- **92** (R¹ = H, R² = Ph)
- **7** (R¹ = Ph, R² = CH₂OH)
- **93** (R² = Me, R³ = Boc)
- **94** (R² = Me, R³ = Ts)
- **8** (R⁵ = H)
- **9** (R⁵ = Me)
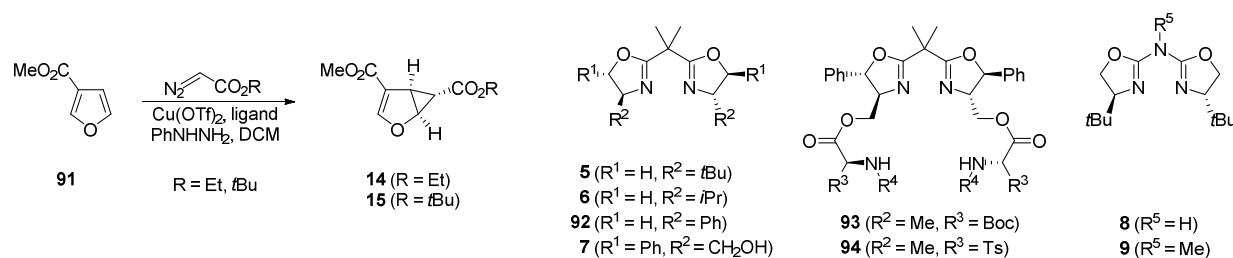
Table 3. Asymmetric cyclopropanation of furan-3-carboxylic acid methyl ester **91**.[14, 39, 45]

entry[a]	R	ligand	temperature [°C]	ratio Cu/ligand	yield [%][f]	*ee* [%][g]
1[b]	Et	**6**	0	0.8	31	83
2[c]	Et	**5**	0	0.8	22	74
3[c]	Et	**7**	0	0.8	27	74
4[d]	Et	**93**	0	0.8	31	68
5[d]	Et	**94**	0	0.8	19	40
6[b]	*t*Bu	**6**	0	0.8	38	83
7[b]	*t*Bu	**7**	0	0.8	38	65
8[b]	*t*Bu	**92**	0	0.8	34	19
9	*t*Bu	**8**	0	0.5	55	92
10	*t*Bu	**9**	0	0.5	38	94
11	*t*Bu	**8**	-10	0.5	31	93
12	*t*Bu	**9**	-10	0.5	21	92
13[e]	*t*Bu	**8**	0	0.5	47	89 (99)[h]

a) 3.97 mmol (500 mg) **91**, 1 mol% Cu(OTf)₂, 2.2 mol% ligand, 1 mol% PhNHNH₂, 1.5 equiv diazoester, 3 ml DCM; b) ref. [45]; c) ref. [39]; d) ref. [14]; e) 102.4 mmol (12.91 g) **91**; f) isolated yield; g) determined by chiral HPLC; h) 19%, > 99% *ee* after single recrystallization from *n*-pentane.

From earlier studies with box and azabox ligands it is known that the derived copper complexes predominantly form 1:2 complexes with two ligand molecules bound to the metal center,[66, 104] thus the ratio for our experiments was set to 0.5 (1 mol% Cu/2.2 mol%

ligand; entries 9-13) in contrast to the former investigations (0.8; entries 1-8). When the two applied ligands **8** and **9** are directly compared to each other one clearly recognizes that the size of the substituent on the central nitrogen atom is rather negligible with regard to selectivity (92-94% *ee*, entries 9-12). However, in terms of yield the ligand with the free NH **8** shows significantly better results compared to its methylated analogue **9** (entries 9/10 and 11/12). Furthermore, the substantial influence of temperature on the performance of the reactions becomes obvious when comparing the yields of entries 9 with 11, and 10 with 12, respectively. A significant drop of the yields for both catalysts becomes evident when the temperature is lowered from 0 °C to -10 °C, independent of the applied ligand (55% to 31% for **8**, and 38% to 21% for **9**). Best results were obtained when using *t*Bu-azabox **8** with free NH at 0 °C, yielding **15** in thus far surpassing 55% and excellent 92% *ee*. This observation intrigued us to perform a large scale experiment under the very same conditions applied in entry 9. Fortunately, when upscaling the reaction only a low decrease in yield and enantioselectivity was observed, giving rise to cyclopropane **15** in 47% isolated yield and 89% *ee*. Most importantly, the product could be recrystallized from *n*-pentane to yield **15** in enantiopure form (table **3**, entry 13, and figure **4**). Figure **4** depicts the analytical chiral HPLC chromatogram of enantiopure (*S,R,S*)-(-)-**15**.
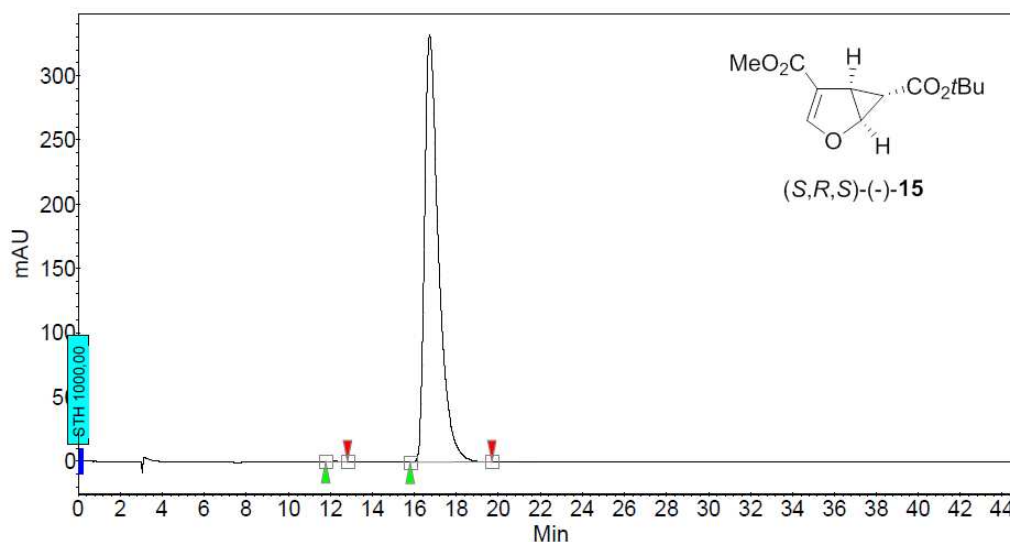
Figure 4. Analytical HPLC chromatogram for enantiomerically pure (*S,R,S*)-(-)-**15**. Phenomenex Lux Cellulose-2, *n*-heptane/*i*PrOH = 99:1, flow = 1.0 ml/min, λ_{max} = 254 nm (t_r = 12.3 min (+), t_r = 16.7 min (-); for racemic data see ref. [45]).

All in all, three significant parameters for the cyclopropanation reaction of 3-furoic acid were modified compared to the original efforts by *Harrar*[45] in order to yield optimum results.

The type of ligand was exchanged from box to azabox ligands, the ratio of metal to ligand (stoichiometry of catalyst) was changed from approximately 1:1 to 1:2, and finally – and also most importantly – suitable conditions for a recrystallization of crude **15** were found, giving access to enantiopure material in gram scale for the first time. Based on the herein presented results, the synthesis of enantiopure (**-**)**-**Paeonilide, as well as its natural enantiomer (+)**-**Paeonilide, is currently ongoing in the *Reiser* group.

1.3 Asymmetric cyclopropanation of *N*-Boc-pyrrole

1.3.1 Synthesis of (*S,S,S*)-(-)-103

In table **4** the state-of-art results for the asymmetric cylopropanation of *N*-Boc-pyrrole **101** are summarized. Eleven different ligands have been employed so far, among them azabox (**8**, **9**, **60**, **95**), regular box (**7**, **96**, **97**), as well as box ligands with secondary binding sites (**93**, **98**, **99**), and a chiral ferrocene based ligand **100** (figure **5**).

60 (R^1 = H, R^2 = *i*Pr)
8 (R^1 = H, R^2 = *t*Bu)
95 (R^1 = Me, R^2 = *i*Pr)
9 (R^1 = Me, R^2 = *t*Bu)

96 (R^3 = Me, R^4 = Ph)
7 (R^3 = Ph, R^4 = OH)
97 (R^3 = Ph, R^4 = OAc)

93 (R^5 = Me, R^6 = Boc)
98 (R^5 = Me, R^6 = Ac)
99 (R^5 = *i*Pr, R^4 = Cbz)

100
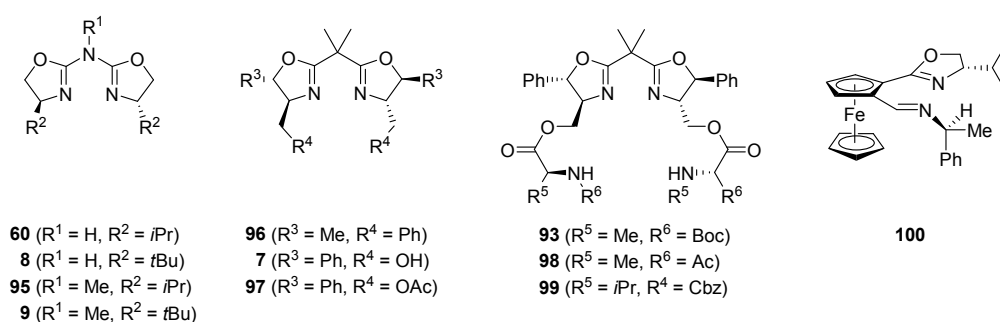
Figure 5. Chemical structures of the employed ligands for asymmetric cyclopropanation approaches of *N*-Boc-pyrrole **101** reported so far.

In all cases besides one (entry 9), methyldiazoacetate was used as the carbene source for those experiments (entries 1-8). When having a look at table **4** it becomes apparent that a level of enantioselectivity better than moderate has not been reached so far. Despite the relatively good yields (max. 63%), the best results in terms of selectivity were obtained when using azabox ligands **8** or **9** (giving 52 and 55% *ee* respectively). This is far from acceptable if one considers using **18** as starting material for amino acid or natural product synthesis.

18 (R = Me)
102 (R = Et)   3
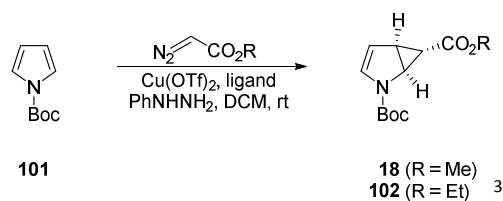
Table 4. Literature results for the asymmetric cyclopropanation of *N*-Boc-pyrrole **101** (for the applied ligands see figure **5**).

entry	R	ligand	yield [%][d]	*ee* [%][e]
1[a]	Me	**60**	63	25
2[a]	Me	**95**	54	25
3[a]	Me	**8**	61	52
4[a]	Me	**9**	54	55
5[b]	Me	**7**	52	46
6[b]	Me	**97**	50	22
7[b]	Me	**99**	57	28
8[b]	Me	**93**	48	34
9[b]	Me	**98**	46	27
8[c]	Me	**96**	17	20
9[c]	Et	**100**	34	5

a) ref. [105]; b) ref. [14]; c) ref. [106]; d) isolated yield; e) determined by chiral HPLC.

Interestingly, none of the investigators tried decreasing the temperature in order to improve selectivity, and only in one case an ester group other than methyl (ethyl, entry 9) was applied. Based on the results from table **4**, it seems obvious that with the levels of enantioselectivity reached so far, the idea for the development of unnatural amino acids or natural products using said method was rendered meaningless. Nevertheless, it has to be noted that access to enantiomerically pure **18** (in either form) has been accomplished by other methods than asymmetric cyclopropanation. In a cooperation between the *Reiser* group and *Merck Darmstadt*, racemic (±)-**18** could be separated by simulated moving bed chromatography (SMBC) to give about 75 g of either enantiomer and excellent enantiomeric excess (scheme **14**).[18, 107] This material was then used for a great variety of applications, especially the

---

3 Several reports claimed that (*R,R,R*)-(+)-**18** was formed with the presented ligands (derived from *L*-amino acids), which would be contrary to the results from furan derivatives. In chapter **B 1.3.4**, it is clearly demonstrated that these claims are wrong, and (*S,S,S*)-(-)-**18** is the major product formed in these reactions.

synthesis of β-amino acids (β-ACCs) for the incorporation into artificial peptides, so-called foldamers (see introduction).
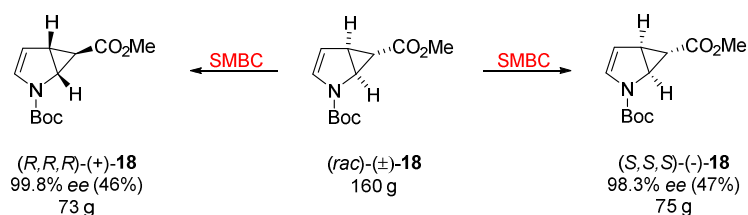
Scheme 14. Resolution of racemic **18** via simulated moving bed chromatography (SMBC).[18]

In addition, enantiomerically pure **18** could also be prepared by kinetic enzymatic resolution of racemic (±)-**18** using lipase L-2.[51] However, due to significant limitations in scale this approach was not followed up intensively. On the other hand stock amounts of enantiomerically pure **18** in the *Reiser* group have almost vanished by now, but nonetheless **18** is still of high importance.[60] These facts made us thinking about whether the initial idea of an asymmetric cylopropanation reaction of *N*-Boc-pyrrole was still the most reasonable strategy. As already mentioned in chapter **B 1.2**, our group has strong expertise in asymmetric cyclopropanation chemistry, facilitating the search for optimal conditions. In the following section the efforts toward enantiomerically pure cyclopropanated pyrrole are presented. Table **5** summarizes all experiments carried out in this investigation. In our studies two major differences were made when compared to the original reports; first *tert*-butyldiazoacetate was used instead of methyl- or ethyldiazoacetate because it is known that the higher degree of steric bulk of the ester group can play a beneficial role for selectivity.[108] Additionally, we reached excellent enantioselectivities using this compound in the furan cyclopropanation trials (chapter **B 1.2**). Secondly, temperatures lower than room temperature were investigated, as it is a well-known fact in catalysis that lower temperatures can have positive effects on selectivity. Other ligands than those applied before were investigated as well, but, as it will be explained later on, only *tert*-butyl substituted azabox ligands gave good results. Noteworthy, all of the herein reported experiments are not only enantioselective but also highly diastereoselective, forming the *exo*-products exclusively. In none of the cases any hint of *endo*-product formation was observed.

Table 5. Asymmetric cyclopropanation of *N*-Boc-pyrrole using *L*-amino acid based azabox ligands (*right*).

entry[a]	ligand	temperature [°C]	yield **103** [%][e]	ee **103** [%][f]	yield **104** [%][e]	ee **104** [%][f]
1[b),c)]	-	25	35	0	7	0
2[c)]	**60**	0	29	35	1	*nd*
3	**60**	-10	24	37	2	*nd*
4	**8**	25	23	83	31	27
5	**8**	0	23	83	25	41
6	**8**	-10	30	90	17	*nd*
7[c)]	**8**	-15	37	68	17	4
8	**8**	-20	37	93	-	*nd*
9	**9**	0	33	81	24	18
10	**9**	-10	38	76	13	*nd*
11[c)]	**9**	-15	34	83	15	37
12	**9**	-20	26	64	2	*nd*
13[c)]	**74**	0	43	72	-	-
14	**74**	-15	19	52	-	-
15	**62**	-10	29	33	10	0
16[d)]	**8**	-15	44 (59 brsm)	87 (> 99)[g]	12	41

a) 2.99 mmol (500 mg) **101**, 1 mol% Cu(OTf)$_2$, 2.2 mol% ligand, 1 mol% PhNHNH$_2$, 1.5 equiv diazoester, 3 ml DCM; b) 5.98 mmol **101**; c) 1.2 equiv diazoester; d) 150.6 mmol (25.2 g) **101**; e) isolated yield; f) determined by chiral HPLC; g) 18%, > 99% *ee* after recrystallization from hexanes.

As can be seen from table **5**, yields are in general rather moderate, with 43% being the maximum for *N*-benzyl substituted *t*Bu-azabox **74** (entry 13). In terms of enantioselectivity, only *tert*-butyl substituted azabox ligands (**8** and **9**) gave satisfying results (up to 93% *ee*). Thus, after screening some of the other available ligands and temperatures, it seemed obvious that *tert*-butyl-azabox **8** was the ideal candidate for an upscaling experiment (entry 16). Not only that enantioselectivities > 90% are accessible with this ligand (entries 6 and 8), but also comparatively good yields of > 30% were achieved at different temperatures. Therefore, *N*-Boc-pyrrole **101** was cyclopropanated with *tert*-butyldiazoacetate under the conditions

shown in entry 16. Noteworthy, on a 150 mmol scale cyclopropane **103** was obtained in remarkably good 44% yield (59% brsm) and 87% *ee*. Even more important was the fact that **103** was found to crystallize from hexanes, giving a multi-gram quantity of enantiopure (*S,S,S*)-(-)-**103** from this reaction. This strategy enables ready access to this important molecule in good amounts and perfect enantiomeric excess. Besides the effects of our new cyclopropanation conditions on monocyclopropanation product **103**, the fact that double cyclopropanated pyrrole **104** is also formed in significant amounts during this process is interesting. Unfortunately, only very low to no degree of enantioselectivity for the double cyclopropanation product **104** (0-41% *ee*) was found. Until now there is no reasonable explanation for this finding. Nevertheless, possible applications of **104** will be discussed in chapter **B 3**.

1.3.2 Structural investigations of the cyclpropanation products

The absolute configuration of the two cyclopropanation products **103** and **104** were determined by X-ray analysis in combination with chiral HPLC and optical rotation measurements (see experimental section for data). Figure **6** illustrates the structures for monocyclopropane **103** and biscyclopropane **104** obtained by X-ray diffraction.
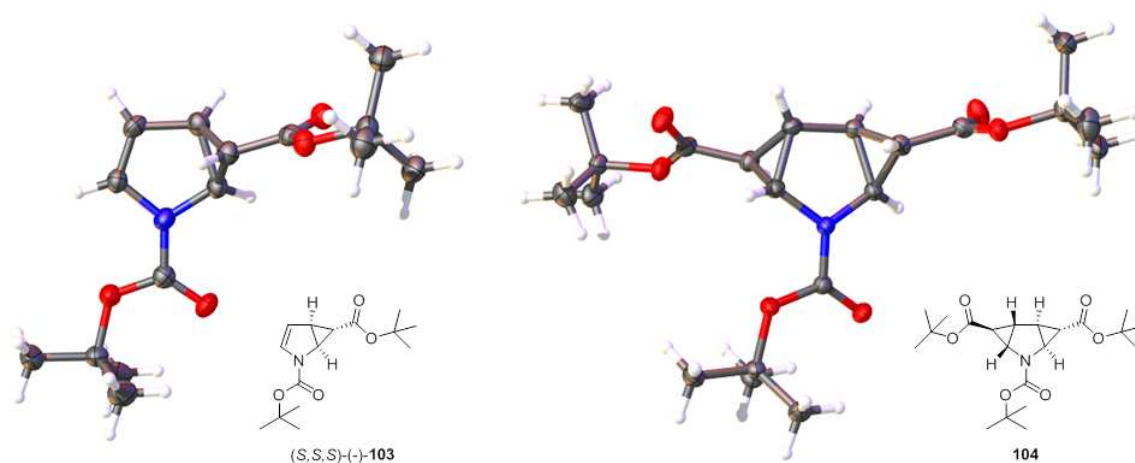
Figure 6. Single crystal X-ray structures of mono-cyclopropanation product (*S,S,S*)-(-)-**103** (*left*), and double cyclopropanation product **104** (*right*). (*C = grey, H = white, O = red, N = blue*).

Especially for double cyclopropanation product **104** the structure shows the strict *exo*-conformation of both cyclopropane rings, resulting in a C_2-symmetric molecule. The

potential applications of this interesting compound, where six stereogenic centers are formed in a single step from non-chiral *N*-Boc-pyrrole **101**, are discussed in a later part of the present thesis (chapter **B 3.1**). When examining ^{1}H-NMR spectra of monocyclopropane **103** one immediately recognizes a strong signal broadening, accompanied by splitting of the corresponding signals. The signal broadening is presumably due to the occurrence of rotational energy barriers of the one, or even both of the *tert*-butyl groups in **103** (restricted rotation around C-N bond due to steric hindrance), leading to the presence of rotational isomers, so-called rotamers. The presence of rotamers can be proven, and distinguished, from the existence of diastereomers by the dynamic behavior of the ^{1}H-NMR signals in temperature-dependent NMR experiments.[109-111]
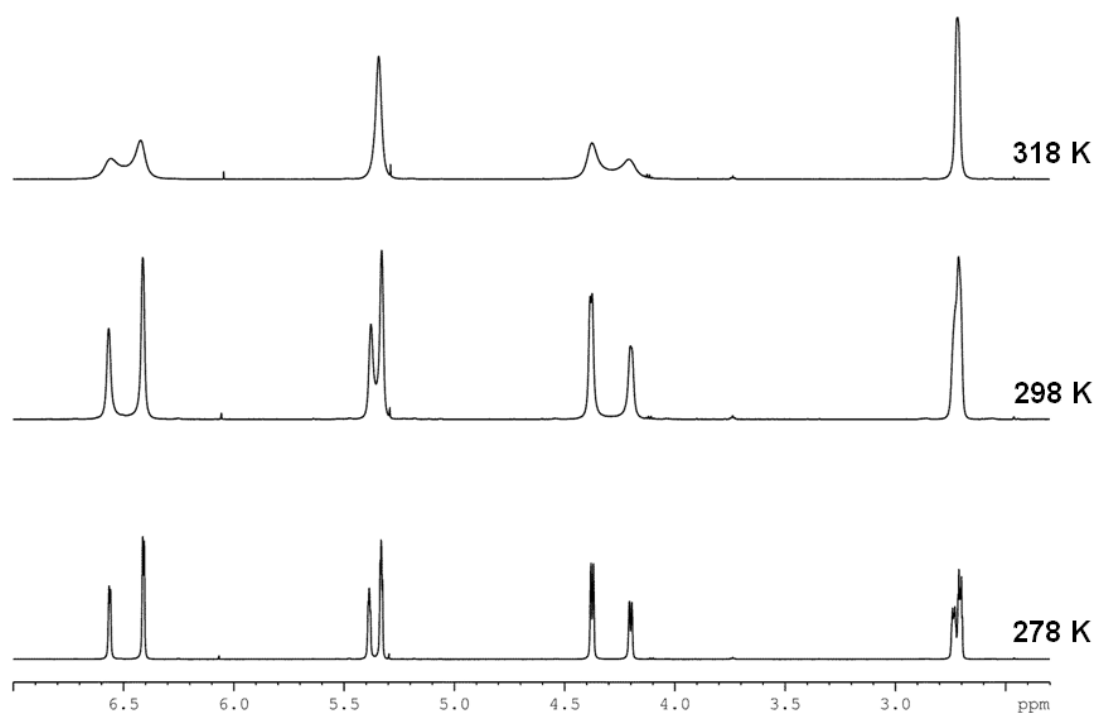
Figure 7. Excerpts from the ^{1}H-NMR spectra of cyclopropane **103** at 278, 298, and 318 K in CDCl$_3$ (600 MHz kryo). The presence of two distinct sets of signals (ratio ~ 0.6:0.4) becomes obvious at 278 K. Upon heating the signals melt together, proving the existence of rotamers (rather than diastereomers).

In this case three ^{1}H-NMR spectra of **103** were recorded at different temperatures (Figure **7**). At low temperature (278 K) it is clearly visible that two distinct sets of signals in a ratio of about 0.6:0.4 appear. This alone does not allow for any conclusions, but if one takes into account that the signals start broadening and melting together at higher temperatures (298 K,

318 K) it is evident that **103** shows strong rotameric behavior, excluding the presence of diastereomers.

1.3.3 Synthesis of (*R,R,R*)-(+)-**103**

As already mentioned above, the synthesis of *tert*-butyl-azabox **8** (as well as **9** and **74**) is based on the non-proteinogenic amino acid *tert*-leucine **69**. From an economical point of view, access to the (*R*)-enantiomer of ligand **8** is not advisable (as *D-tert*-leucine is very expensive), and thus alternative strategies toward enantiopure (*R,R,R*)-(+)-**103** need to be employed. Therefore, different ligands based on *D*-configured amino acids were employed for the asymmetric cyclopropanation of *N*-Boc-pyrrole and the results were compared to the already obtained data (table **6**, entries 1-7).
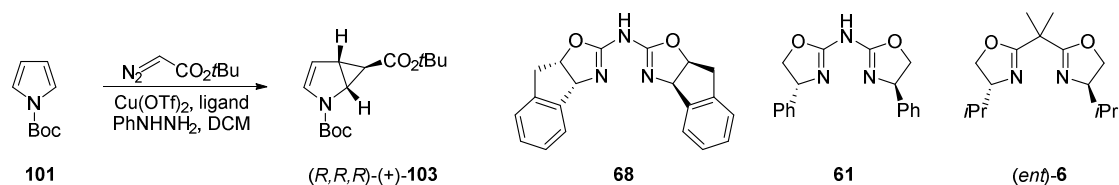
Table 6. Asymmetric cyclopropanation of *N*-Boc-pyrrole using *D*-amino acid based ligands.

entry[a]	ligand	temperature [°C]	yield **103** [%][f]	*ee* **103** [%][g]	yield **104** [%][f]	*ee* **104** [%][g]
1[b]	**68**	0	28	53	33	23
2[c]	**68**	0	17	57	19	26
3	**68**	-10	28	32	0	*nd*
4	**61**	0	28	39	33	1
5	**61**	-10	34	56	27	1
6[d]	**61**	-20	18	41	1.5	5
7[e]	(*ent*)-**6**	0	30	41	20	5

a) 2.99 mmol (500 mg) *N*-Boc-pyrrole, 1 mol% Cu(OTf)$_2$, 2.2 mol% ligand, 1 mol% PhNHNH$_2$, 1.5 equiv diazoester, 3 ml DCM; b) defrosting ice-bath; c) cryostat; d) 1.2 equiv diazoester; e) 5.98 mmol (1.00 g) *N*-Boc-pyrrole; f) isolated yield; g) determined by chiral HPLC.

As can be seen from table **6** results are rather poor, leading to a maximum of 57% *ee* for indanyl substituted azabox **68** (entry 2) and 56% *ee* for phenyl-azabox **61** (entry 5). With (*R,R*)-iso-propyl-bisoxazoline (*i*Pr-box) (*ent*)-**6** only 41% *ee* could be achieved (entry 7). Interestingly, only the indanyl-substituted azabox ligand **68** led to enantiomerically enriched double cyclopropanation product **104** (entries 1 and 2), while the other ligands yielded more

or less racemic product (entries 4-7). The overall best results in terms of yield and selectivity were found for phenyl derivative **61** at -10 °C with 34% isolated yield and 56% *ee* (entry 5). However, upon repeated recrystallization steps from hexanes it was possible to obtain (*R,R,R*)-(+)-**103** in enantiomerically pure form (HPLC chromatograms shown in figure **9**).
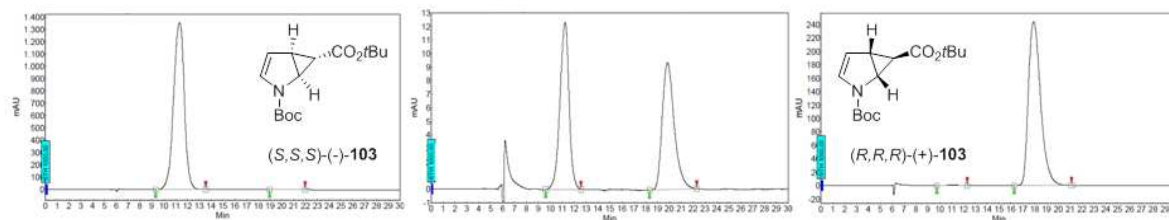
Figure 9. Analytical HPLC chromatograms for (*S,S,S*)-(-)-**103** (*left*), rac-(±)-**103** (*middle*), and (*R,R,R*)-(+)-**103** (*right*). Phenomenex Lux Cellulose-2, *n*-heptane/*i*PrOH = 98:2, flow = 0.5 ml/min, λ_{max} = 254 nm (t_r = 11.3 min (-), t_r = 19.9 min (+)).

1.3.4 Investigations of the stereochemical outcome of the cyclopropanations reactions

Former reports claimed that the asymmetric cyclopropanation of *N*-Boc-pyrrole with methyldiazoacetate leads to inverted stereoinduction (giving (*R,R,R*)-(+)-product from *L-(S,S)*-derived ligands) compared to furan derivatives when using the identical stereochemistry of the ligand ((*S,S,S*)-(-)-product from *L-(S,S)*-derived ligands).[14, 105, 106] This effect was somehow explained by attractive interactions between the oxygen atom of the furan ring with copper, and in the case of **18** with steric repulsion of the bulky Boc-group in **101**, so that an inverted orientation of the substrate binding to the catalyst was claimed. If this was true it would be a very interesting feature due to the fact that (*S,S,S*)-(-)-**103** was the major product for the same substrate when using *tert*-butyl substituted diazoacetate in the analogous experiments instead (proven by X-ray, chiral HPLC, and optical rotation; see chapters **B 1.3.2** and **D 2**). This would mean that only the size of the incoming ester group should be responsible for a complete inversion of the stereochemical outcome of the product, which is hardly believable. Thus, we aimed to reexamine the stereochemistry of the abovementioned cyclopropanation reaction (which is described in the following). The idea of our strategy was to approach methyl-substituted cyclopropane **18** from two different synthetic sites, whilst comparing the stereochemical outcome and therefore proving, or disproving, the original claim (scheme **15**).
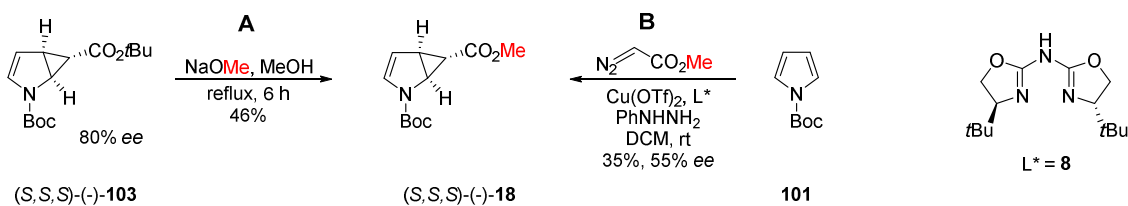
Scheme 15. Strategy for the clarification of the stereochemical outcome of the cyclopropanation of *N*-Boc-pyrrole with methyldiazoacetate. Methyl-substituted cyclopropane **18** was synthesized from two different directions in order to clarify matter. **A**: transesterification of **103** using NaOMe; **B**: asymmetric cylopropanation of **101** using methyldiazoacetate and ligand **8**.

As the absolute configuration of *tert*-butyl-cyclopropane **103** (derived from *L-(S,S)*-configured ligands) was reliably established to be (*S,S,S*)-(-)-**103** using X-ray diffraction, chiral HPLC analysis and optical rotation, a transesterification of **103** into the methyl ester should result in a product **18** bearing the identical stereoinformation as its parent compound **103** (in the worst case epimerization of one stereocenter could occur under basic conditions). Several attempts of transforming the *tert*-butyl ester moiety of **103** into a methyl ester failed or only gave poor results.
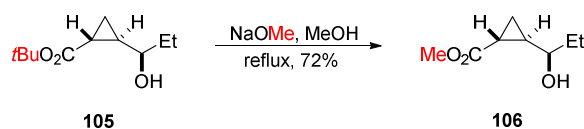
Scheme 16. Transesterification of *tert*-butyl-cyclopropane ester **105** via sodium methoxide by *Fox et al.* [112]

However, a report of *Fox et al.* using sodium methoxide for the transesterification of cyclopropane ester **105** into its methyl derivative **106** (scheme **16**)[112] prompted us to test such conditions for our substrate **103**.
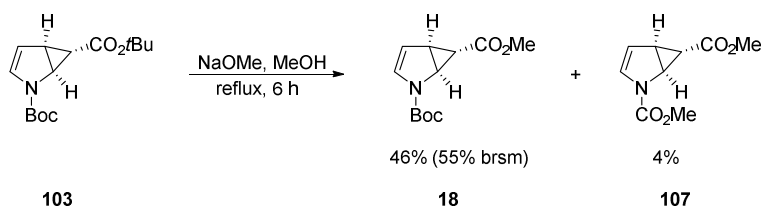
Scheme 17. Transesterification of *tert*-butyl-cyclopropane ester **103** via sodium methoxide using the methodology of *Fox et al.*

Thus, **103** was transformed into its methyl derivative using sodium methoxide in refluxing methanol to give **18** in 45% yield (scheme **17**; **A** in scheme **15**).[4] Substrate **103** was chosen with a moderate degree of enantioselectivity (80% *ee*) on purpose in order to facilitate HPLC

---

[4] Due to the formation of side product **107** from methyl ester **18**, where the Boc-group was transformed into the methyl carbamate, better yields of **18** were not accessible.

analysis. As the transesterification product **18** was obtained with an identical *ee* value as its parent starting material, it can be concluded that no epimerization occurred during the progress of the reaction. Furthermore, the original cyclopropanation of *N*-Boc-pyrrole **101** with methyldiazoacetate was repeated with the aim of comparing the results to those obtained from route **A** (**B** in scheme **15**). In this attempt methylcyclopropane **18** was obtained in 35% yield and 55% enantiomeric excess.[5]
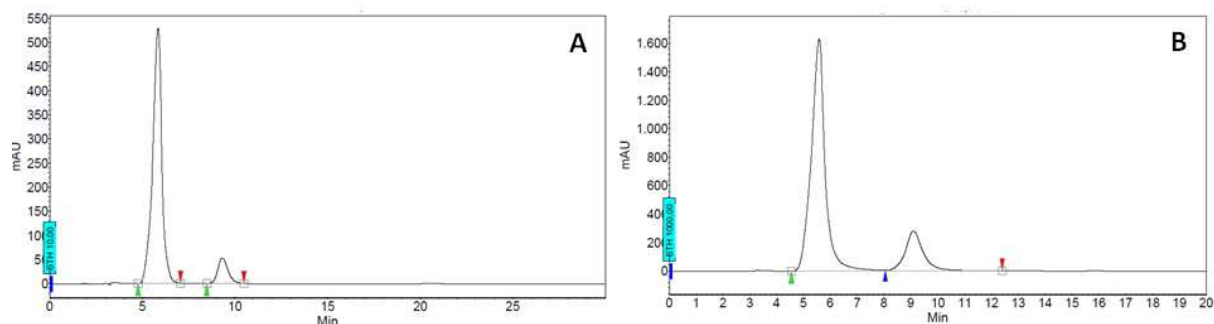
Figure 8. Analytical HPLC chromatograms for methyl-substituted cyclopropane **18** from transesterification (**A**), and from cyclopropanation with methyldiazoacetate (**B**). Chiralcel OD-H, *n*-heptane/*i*PrOH = 99:1, flow = 1.0 ml/min, λ_{max} = 240 nm (t_r = 5.9 min (-), t_r = 9.3 min (+)).

When comparing the HPLC chromatograms for the (identical) product of both reactions (**A** and **B**; figure **8**), it becomes apparent that in both cases the very same product was formed by the two orthogonal reactions, namely (*S,S,S*)-(-)-**18**. Furthermore, the newly obtained results were verified by comparison to the original data of *Glos* and it was thus concluded that no stereoinversion occurs while switching the substrates from furan derivatives to *N*-Boc-pyrrole **101**. In contrast, it could be shown that for all investigated cyclopropanation reactions the (*S,S,S*)-(-)-product is forming from *L-(S,S)*-derived ligands. On the contrary, the corresponding (*R,R,R*)-(+)-cyclopropanes form when using *D-(R,R)*-derived ligands.

---

[5] The original literature report for this reaction was: 61% yield, 52% *ee* (ref. [105]).

2 Transformations of monocyclopropanated pyrrole 103

2.1 Synthesis of (S)-3-pyrrolidineacetic acid ((S)-(+)-homo-β-proline, (S)-(+)-109)

2.1.1 Biological background

The non-proteinogenic γ-amino acid γ-aminobutyric acid (GABA, **108**) has been estimated to be present in 60-70% of all synapses in the mammalian central nervous system (CNS),[113] and represents a major inhibitory neurotransmitter in the CNS of man.[114-116] Since GABA inhibitory neuronal transmission is associated with several neurological disorders, such as anxiety, pain, epilepsy, *Parkinson's* disease, and *Huntington's* disease, there is a special interest in developing specific agonists of postsynaptic GABA$_A$ receptors, as well as in potent inhibitors of the GABA uptake mechanism.[117]

Figure 10. Chemical structures of GABA **108** as well as racemic (±)-homo-β-proline **109** with its two enantiomers (*S*)-(+)- and (*R*)-(-)-**109** (core structure of GABA highlighted in *red*).

On the basis of cyclically constrained GABA analogues for pharmacological studies the non-natural γ-amino acid 3-pyrrolidineacetic acid (homo-β-proline, **109**), which can be classified as a structurally rigidified analogue of GABA was first prepared and analyzed for its pharmacological properties in 1981 by *Schaumburg et al.* (figure **10**, see chapter **B 2.1.2** for syntheses).[118, 119] Since then it was shown that racemic (±)-**109** acts as an inhibitor of GABA$_A$ and GABA$_B$ receptor binding, as well as a glial and neuronal GABA uptake inhibitor.[119-122] Interestingly, the two enantiomers of homo-β-proline were shown to interact in a stereoselective manner with the two GABA receptors.[6][123] While (*S*)-(+)-**109** binds selectively to the GABA$_B$ receptor, its enantiomer (*R*)-(-)-**109** is more than one order of magnitude more potent at GABA$_A$ (compared to its enantiomer). On the other hand, both enantiomers show a remarkably low eudismic ratio (small potency difference) and, interestingly, similar potency compared to the racemate (±)-**109** and the native ligand GABA

---

[6] Meanwhile a third type of GABA receptor, termed GABA$_C$ was identified representing a structural subtype of GABA$_A$ receptors: ref. [123].

itself toward synaptosomal GABA uptake inhibition.[114] Moreover, homo-β-proline **109** and its enantiomers have been widely used as model compounds for structural and functional investigations.[124] Nevertheless, these results only reflect on in vitro activity, which depicts the major disadvantage of compounds like **109**: they do not readily cross the blood-brain-barrier,[125, 126] which renders their potential application as drugs rather meaningless. Therefore, a series of potential pharmaceuticals were developed containing the substructure of **109** bearing a lipophilic moiety (mostly anchored to the endocyclic N-atom), enabling the resulting compounds to cross the blood-brain-barrier and hence showing significantly increased pharmacological activities. One prominent example is the N-modified analogue of homo-β-proline SKF 100561 (**110**, figure **11**), which shows significantly increased GABA uptake inhibition (IC_{50} = 0.12 µM compared to 1.5 µM of the parent amino acid **109**). Furthermore, it displayed anticonvulsant activity upon oral or intraperitoneal administration to rats.[127-129] In addition, **110** was shown to exhibit antitussive properties,[130] whereas in a different study it was presented that **110** potently counteracts the enhancing effect of GABA on dopamine release in rat brain, allowing for the conclusion for coexistence of transporters of GABA and dopamine.[131] Reflecting on the remarkable properties of this molecule, *Young* and co-workers identified it to be a potent histamine H_1-receptor antagonist as well.[132] In 2001, homo-β-proline derivative **111** was reported as the most potent compound in a series of 33 potential GABA uptake inhibitors (IC_{50} = 51 nM), however, its in vivo anticonvulsant properties were rather poor.[117] Figure **11** gives an exemplary overview of some recent pharmacologically active compounds containing **109** as structural motif.
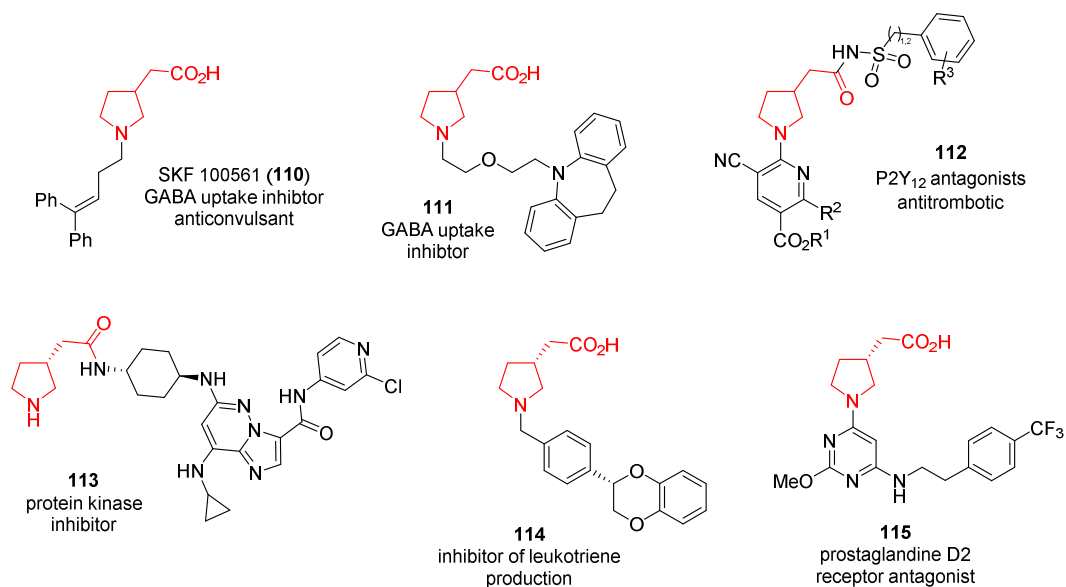
Figure 11. Chemical structures of selected examples of derivatives of homo-β-proline that were designed for pharmaceutical purposes (core structure of **109** highlighted in *red*).

Furthermore, a couple of very recent patents deal with pharmaceutical compounds that incorporate **109** as pharmacophore in a certain manner (figure **11**). While derivatives of type **112** act as P2Y$_{12}$ receptor antagonists[133] and therefore display antitrombotic activity, **115** was prepared as a potential prostaglandine D2 receptor antagonist.[134] On the other hand, **113** acts as a protein kinase inhibitor (both isomers of **109** were incorporated),[135] and **114** as an inhibitor of leukotriene production (inhibitor of leukotriene A$_4$ hydrolase).[136, 137] Besides the presented examples in figure **11**, many more substances containing units of either racemic or enantiopure **109** in their core structure have been reported recently. Moreover, both enantiomers of 3-pyrrolidineacetic acid **109** are not only biologically active by themselves, but also display a key structural element in a broad variety of natural products (figure **12**).
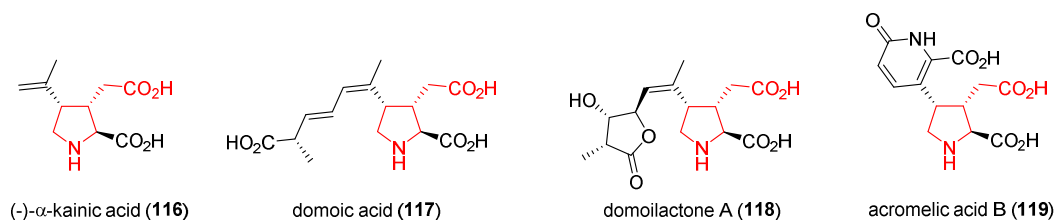

Figure 12. Chemical structures of some structurally related natural products (core structure of **109** highlighted in *red*).[138-140]

The examples shown in figure **12** (**116**-**119**) belong to the family of kainoid amino acids that are structurally based on glutamic acid and display significant biological effects, e.g. insecticidal,[141, 142] anthelmintic,[143-146] and (most importantly) neuroexcitatory properties.[147-151] The compounds presented in figures **11** and **12** clearly demonstrate the importance of homo-β-proline, thus making it an interesting target molecule.

## 2.1.2 Literature syntheses of homo-β-proline 109

Based on our positive results from the asymmetric cyclopropanation of *N*-Boc-pyrrole, we aimed to develop a more efficient synthesis route for (*S*)-3-pyrrolidineacetic acid ((*S*)-(+)-**109**). The following chapter gives a brief overview of the strategies for the synthesis of **109** reported so far. While access to 2-substituted derivatives of pyrrolidine is pretty straightforward (most syntheses start from *L*- or *D*-proline and/or derivatives thereof), methods for the preparation of 3-substituted analogues, especially in enantiomerically pure form, are limited. So far there have been eight synthetic routes reported in literature for either racemic or enantiopure homo-β-proline, with only one of them being enantioselective. The first synthesis of racemic (±)-**109** was reported by *Schaumburg et al.* in 1981, who synthesized **109** in 4% yield over 7 steps starting from glycine ethyl ester hydrochloride (**120**).[118] Key steps in their synthesis were a *Dieckmann* condensation to establish the pyrrolidine skeleton and a *Knoevenagel* condensation of **121** with cyanoacetic acid for the introduction of the side chain in **122** (scheme **18**).
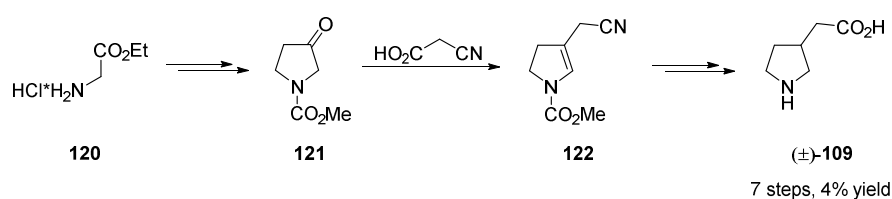
**Scheme 18.** First racemic synthesis of (±)-**109** by *Schaumburg et al.*[118]

The first non-racemic synthesis of (*R*)-(-)-**109** and (*S*)-(+)-**109** was reported in 1990 by *Krogsgaard-Larsen et al.*[114] Based on the addition-cyclization reaction of itaconic acid **123** with (*R*)-1-phenylethylamine and subsequent separation of the resulting diastereomers **124a**

and **124b** via preparative HPLC, they were able to obtain both enantiomers of **109** in 8 steps each and ~ 6% overall yield (scheme **19**).[7]
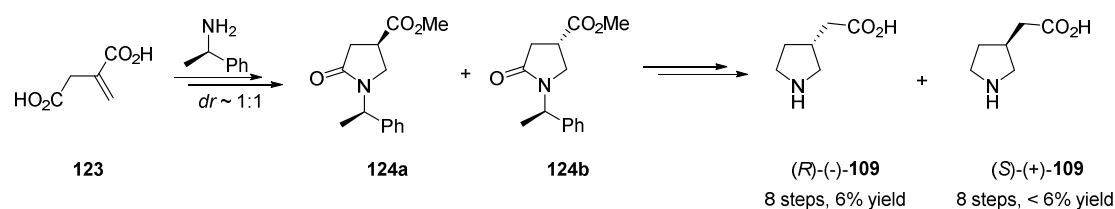
Scheme 19. First synthesis of (*S*)-(+)- and (*R*)-(-)-homo-β-proline from itaconic acid **123** by *Krogsgaard-Larsen et al.*[114]

In 1996, *Coldham* and *Hufton* reported a very short and efficient synthesis of racemic homo-β-proline based on the cyclization reaction of stannane **127** (scheme **20**).[152] Hereby a tin-lithium exchange of stannane **127**, followed by an anionic cyclization reaction and subsequent trapping with an electrophile, represents the crucial step to yield **128** (interestingly, the *N*-benzyl group was replaced by *N*-CO_2Et during this reaction).
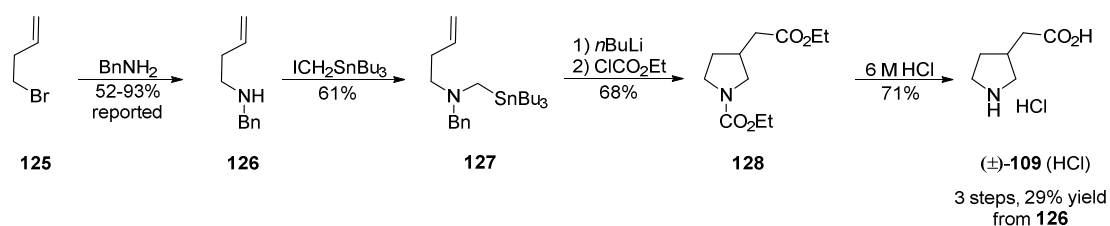
Scheme 20. Synthesis of racemic (±)-**109** according to *Coldham and Hufton*.[152]

Within four synthetic steps they were able to obtain (±)-**109** from commercially available 4-bromobut-1-ene **125** in 15-27% yield (the authors did not give a yield for the first step; from literature it is recognized that **126** can be prepared by the referred strategy in 52-93% yield). However, based on the fact that organotin reagents are not too desirable nowadays, their synthesis strategy may not be of great importance for current studies. In a similar approach to the one reported by *Krogsgaard-Larsen et al.*,[114] *Orena* and co-workers developed several intramolecular cyclization reactions for the generation of the pyrrolidine ring with an appropriate substitution pattern.[153-155] Based on cyclization product **131**, which was obtained in 75% yield and a diastereomeric ratio of 80:20 from **130**, both enantiomers of homo-β-proline were synthezied in 7 steps each (scheme **21**). In this way they were able to obtain (*S*)-(+)-**109** in 11% and (*R*)-(-)-**109** in 3% yield.

---

[7] The authors did not provide a yield for the last synthetic step for (*S*)-(+)-**109**.
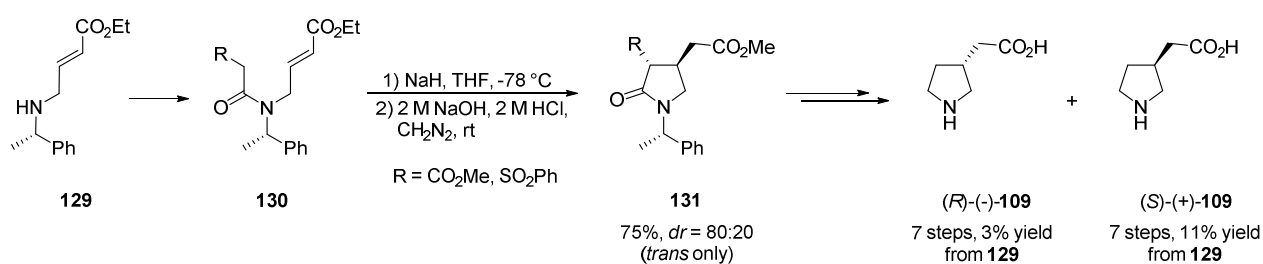
Scheme 21. Synthesis of (*S*)-(+)- and (*R*)-(-)-homo-β-proline by *Orena et al*.

In a slightly older communication, *Orena et al.* presented a formal synthesis of **109** with a Mn(III)-mediated intramolecular cyclization reaction as the key step. By this strategy they were able to prepare synthetic intermediate **135**, the same that was used for the synthesis of **109** by *Krogsgaard-Larsen et al.*[114] from chiral amine **132** in 6 steps and 17% yield (scheme **22**).[153]
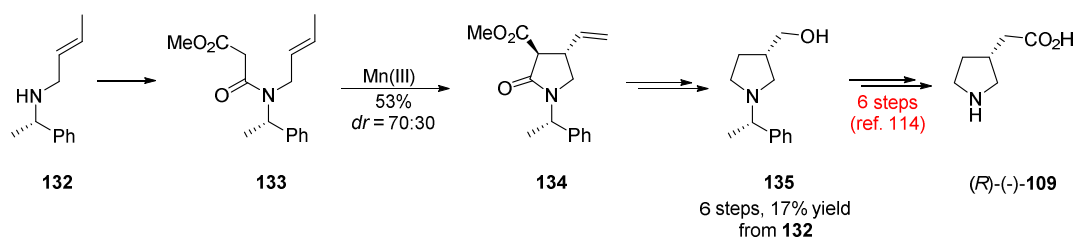
Scheme 22. Formal synthesis of (*S*)-(+)-**109** through Mn(III)-mediated intramolecular cyclization of **133** by *Orena et al*.

On the way to conformationally restricted NO synthase inhibitors, *Eustache* and co-workers synthesized (*S*)-(+)-homo-β-proline **109** from intermediate **136** (obtained from aspartic acid)[156] in order to determine the absolute configuration of their compounds (Scheme **23**).[157] Key steps of the synthesis were the lactamization of a nitro-*Michael*-adduct, followed by transformation into the corresponding thiolactam by *Lawesson's reagent* (including chromatographic separation of diastereomers), and subsequent desulfurization in order to establish the pyrrolidine ring system. Additionally, besides some protection/deprotection steps, a desamination-decarboxylation sequence had to be carried out to finally yield **109** in 9 steps and 5% yield starting from **136**.
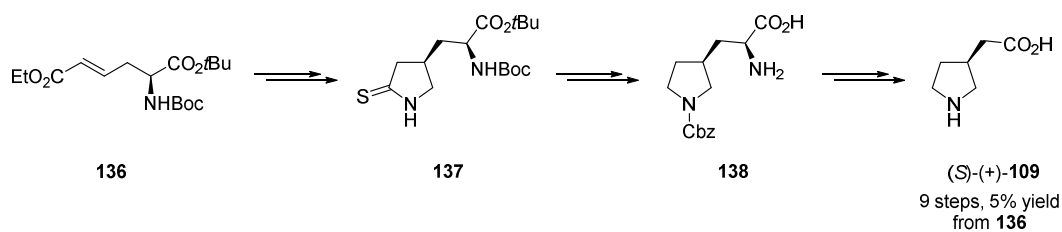
Scheme 23. Synthesis of (*S*)-(+)-homo-β-proline **109** from **136** by *Eustache et al.*[157]

In the same year, *Gmeiner et al.* presented an efficient 11 step synthesis of **109** starting from (*S*)-aspartic acid **139** (scheme **24**).[158] In this chiral pool approach, 1,4-bis-electrophile **140** was rearranged to **141** through an aziridinium ion (not shown) and subsequently cyclized to form the pyrrolidine core. Inversion of the stereocenter by S_N2 type substitution with diethylmalonate, followed by a decarboxylation gave rise to (*R*)-(-)-**109** in an overall yield of 23%. Importantly, (*R*)-aspartic acid could be applied as well for the synthesis of the enantiomeric (*S*)-(+)-**109**.
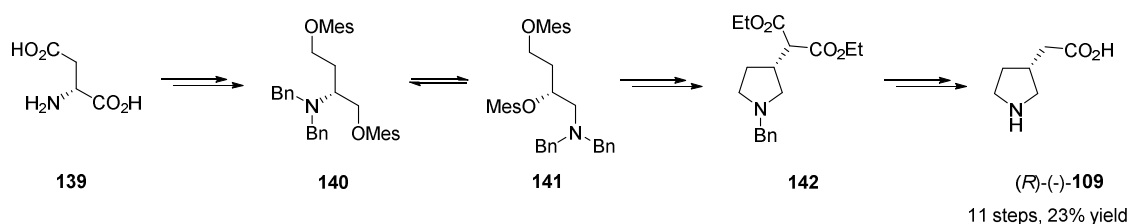
Scheme 24. Synthesis of (*R*)-(-)-homo-β-proline **109** from aspartic acid **139** by *Gmeiner et al.*[158]

In 2004, *Felluga* and co-workers[159] reported a chemoenzymatic synthesis of both enantiomers of homo-β-proline based on the desymmetrization reaction of prochiral nitrodiester **144** (scheme **25**).[159]

Scheme 25. Synthesis of both enantiomers of homo-β-proline via enzymatic desymmetrization of prochiral nitrodiester **144** according to *Felluga et al.*[159]

For the selective saponification of only one of the two ester groups in **144**, two different enzymes had to be applied, namely porcine pancreatic lipase (PPL) for the synthesis of

(*S*)-(+)-**109**, and crude pig liver esterase (PLAP, pig liver acetone powder)[8] for (*R*)-(-)-**109**, respectively. With 38% for (*S*)-(+)-**109**, and 39% for (*R*)-(+)-**109** in a total of 7 steps each, this methodology provides the most efficient strategy to prepare both enantiomers of **109** so far. However, the use of two different enzymes and the noticeable limitations in scale may make this not the most desirable way in terms of economics. The first enantioselective synthesis of (*S*)-(+)-**109** was reported by the group of *Tan* in 2007.[160] During the investigation of organocatalyzed enantioselective *Michael* reactions of dithiomalonates and β-keto thioesters to N-substituted maleimides, they established a 7 step synthesis of **109** (scheme **26**). On the basis of *Michael* adduct **148**, which was obtained in 92% *ee* from the guanidine catalyzed addition of **147** to *N*-benzyl maleimide **146**, the following 6 steps were carried out to yield (*S*)-(+)-**109** in 73% from **148**. Unfortunately, no yield for the crucial addition step was given by the authors, making it difficult to evaluate the overall efficiency of the synthetic sequence.

Scheme 26. Enantioselective synthesis of (*S*)-(+)-**109** by *Tan et al.*, including an organocatalyzed conjugate addition reaction as key step**.**

However, only one enantiomer could be synthesized in a not fully enantioselective manner with this strategy and the use of toxic chromium reagents makes this surely not the method of choice in terms of sustainability. In addition, limitations in scale of the above reported method further restricts its feasibility. In summary, all of the above reported synthetic approaches require several steps, expensive or harmful reagents (Cr, Sn) and are limited in scale. Therefore, we aimed to develop a short and efficient synthesis route giving access to either enantiomer of **109** in enantiopure form and good quantity.

2.1.3 Synthesis of (*S*)-(+)-109

Based on the results from our cyclopropanation experiments, we chose **103** to be a good starting point for our enterprise. Cyclopropane (*S,S,S*)-(-)-**103** can be obtained from *N*-Boc-pyrrole in multigram quantity and > 99% *ee* after recrystallization (see chapter **B 1.3.1**), thus making it a perfect candidate for further synthetic efforts.

---

[8] Surprisingly, application of pure pig liver esterase (PLE) led to formation of **145b** in only 92% *ee*.

Scheme 27. Enantioselective synthesis of **103** from pyrrole **50**.

Based on the experiments from chapter **B 1.3.1** it is well-known that bicycle **103** can be prepared in moderate yield with full enantiocontrol (scheme **27**). Now there are plenty of opportunities of how to apply this highly functionalized cyclopropane for further synthetic ventures. Obviously, the simplest modification of **103** would be the hydrogenation of the enecarbamate double bond to yield the fully saturated system **149**. This can be carried out efficiently using standard conditions (hydrogen, palladium/charcoal) in order to yield **149** in satisfying 85% yield (scheme **28**).
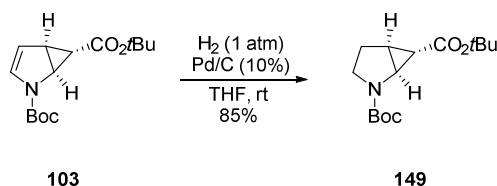

Scheme 28. Hydrogenation of bicyclic enecarbamate **103** using standard conditions.

However, an alternative to the conventional hydrogenation with hydrogen and palladium/charcoal would be the so-called ionic hydrogenation, which has been shown to work efficiently for enamides and enecarbamates.[161-164] In this methodology, the substrate is successively activated by an acidic compound (*Brønsted* or *Lewis* acids) and then reduced by the addition of hydride, mostly from silanes as hydride source. In order to test whether an ionic hydrogenation might produce even higher yields of **149** cyclopropane **103** was treated with trifluoroacetic acid (TFA) and triethylsilane at room temperature. Indeed, chemoselective ionic hydrogenation of the enecarbamate double bond of **103** occurred, accompanied by ring-opening of the donor-acceptor substituted cyclopropane moiety, to give a significant amount of by-product **150** (scheme **29**). After six hours at ambient temperature 33% of hydrogenation product **149** and 23% of ring-opened compound **150** were isolated.
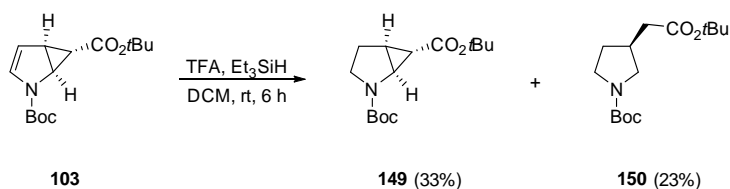
Scheme 29. Ionic hydrogenation of **103** using trifluoroacetic acid in combination with triethylsilane.

This observation can be explained by the occurrence of the desired ionic hydrogenation step of the double bond followed by an acid-catalyzed ring-opening reaction (also traceable by TLC). The corresponding iminium ion should then be trapped by hydride in order to provide **150**. Acid-catalyzed cyclopropane opening is a well-known process in synthetic organic chemistry and innumerable examples have been shown in literature.[165-167] The absolute configuration of ring-opened compound **150** was proven by X-ray analysis (figure **13**) in combination with optical rotation and chiral HPLC analysis (see experimental section).
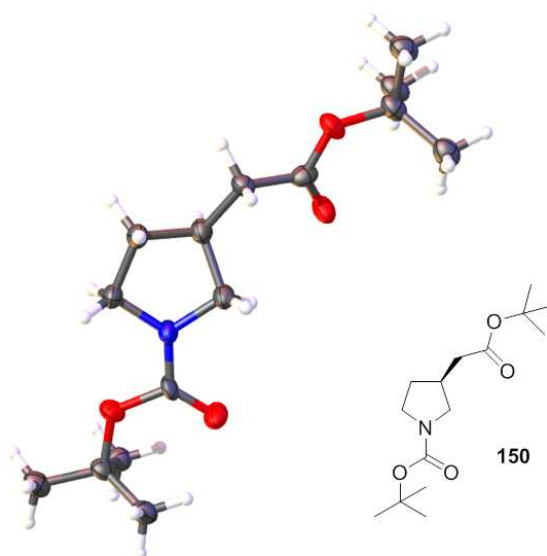

Figure 13. Single crystal X-ray structure of double protected 3-pyrrolidineacetic acid **150** (*left*), and chemical structure of **150** (*right*).

The fact that cyclopropane **149** can be opened readily by the application of acid led us to the idea of making use of it in terms of a total synthesis of homo-β-proline **109** (see chapter **B 2.1.1**). This seems pretty straightforward from **150** (which can be seen as a double protected derivative of **109**), if one can find a way of optimizing the abovementioned reaction to some extent. However, the occurrence of another side-product of the ionic hydrogenation reaction of **103** then attracted our attention. Every time enecarbamate **103** was treated with TFA, two

new spots appeared on TLC. Thus, we examined the chemical behavior of cyclopropane **103** upon treatment with TFA in order to identify these side-products. Interestingly it could be shown that **103** dimerizes upon treatment with TFA to form two diastereomers **151** in a ratio of ~ 3:1 (scheme **30**).
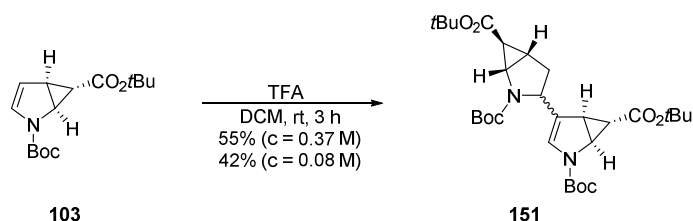
Scheme 30. Concentration-dependent acid-catalyzed dimerization of enecarbamate **103** (combined yields for both diastereomers).

Logically, the reaction turned out to be concentration dependent, giving 42% yield (combined yield of both diastereomers) at a concentration of ~ 0.1 M, and 55% at ~ 0.4 M. In this case the yields could not be optimized due to partial decomposition occurring after prolonged reaction time, which makes sense since dimer **151** contains four *tert*-butyl groups that are regularly cleaved by TFA.[168] The formation of dimer **151** might seem exotic at first, however, it can be explained by having a closer look at the potential mechanism of dimerization for this type of enecarbamate, which was concluded on the basis of the general reactivity pattern of enamides and enecarbamates,[169-171] as well as extensive spectroscopic analyses of the products (scheme **31**).
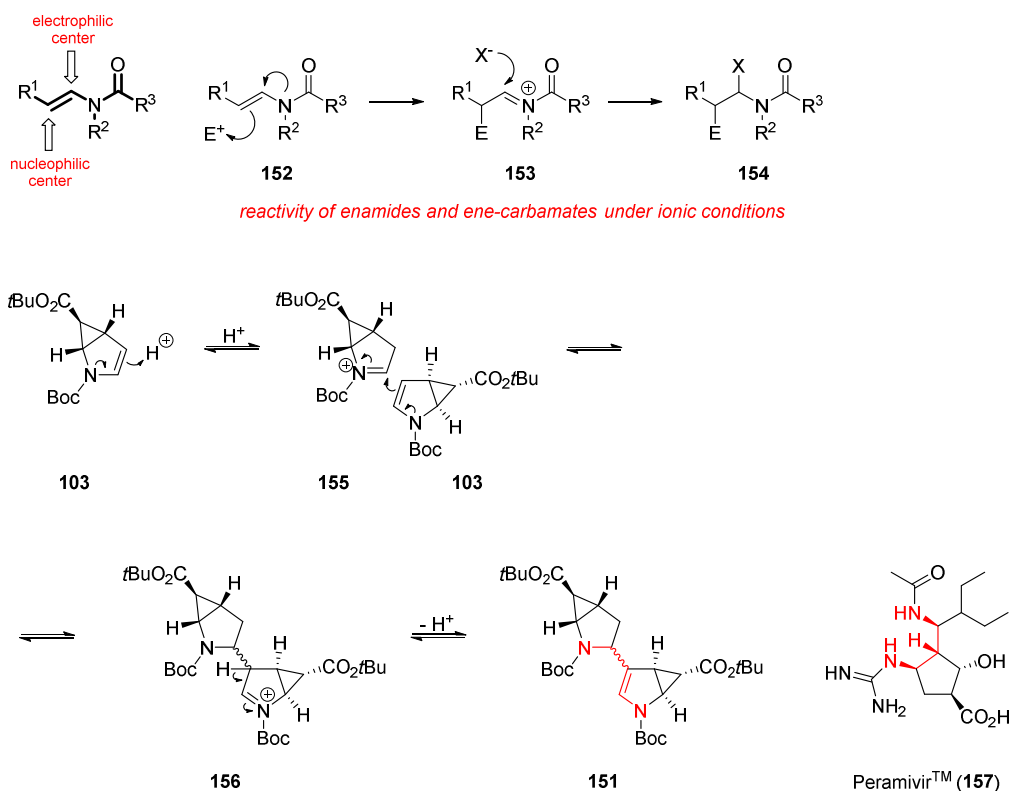
Scheme 31. General reactivity pattern of enamides and enecarbamates (*upper part*), and the proposed mechanism for the acid-catalyzed dimerization of enecarbamate **103**, along with the chemical structure of Peramivir[TM] **157** (1,3-diamino moiety highlighted in *red*).

In general, enamides (and enecarbamates) exhibit an ambivalent reactivity (two opposing reaction pathways), meaning that they can undergo reactions with both electrophiles and nucleophiles. Generally enamides of type **152** react as nucleophiles which attack a suitable electrophile (E$^+$), generating an iminium ion **153** (and **155**) that is then trapped by a nucleophile (Nu$^-$) to yield a double functionalized amide or carbamate **154** (scheme **31**, *upper part*). When having a look on the mechanism of dimerization of **103** it becomes obvious that first the protonation of **103** turns it into the iminium species **155** that acts as the electrophile for the dimer formation. A second molecule of **103** then reacts as nucleophile and attacks the iminium ion **155** to form the dimer **156**. In the final step H$^+$ is eliminated to close the catalytic cycle and yield dimer **151** as product (scheme **31**, *lower part*). Dimer **151** could potentially be of synthetic interest as it bears a 1,3-diamine moiety in its core structure (highlighted in scheme **31**). Optically active 1,3-diamines are valuable targets, as they represent key structural units in many natural products.[172, 173] Moreover, they can be used as chiral auxiliaries and ligands,[174, 175] catalysts in asymmetric synthesis,[176] as well as pharamcophores in medicinal chemistry.[177-181] One prominent example is the commercial drug Peramivir[TM] **157**, which exhibits potent activity against influenza viruses (scheme

31).[182, 183] Furthermore, efficient synthetic strategies toward enantiopure 1,3-diamines are rather limited until now.[184-188]

Coming back to the original purpose to investigate **103** as a promising precursor for the synthesis of homo-β-proline **109**, one has to bear in mind that side reactions like the dimerization mentioned before are rather deleterious for our synthetic endeavor. As already mentioned it is rather likely that the ring-opened product **150** is formed from the hydrogenated compound **149** during the course of the reaction (traceable by TLC). Thus, one can envision carrying out the synthesis in a two-step manner, starting with hydrogenation of the double bond in **103** with conventional methods (H$_2$, Pd/C) followed by acid catalyzed ring opening. In this way side reactions of the enamide can be suppressed and **150** should be accessible in improved yields. Scheme **32** presents the two-step approach for the synthesis of **150**.
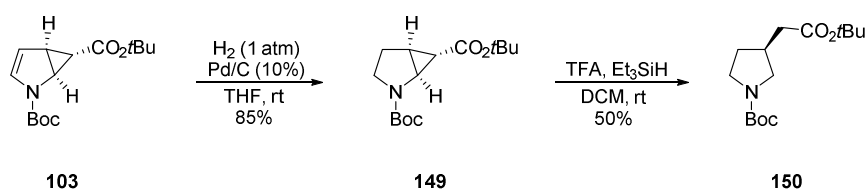
Scheme 32. Two-step synthesis approach of ring-opened product **150** from cyclopropane **103**.

From hydrogenation product **149**, homo-β-proline derivative **150** was obtained in 50% yield. In this case, the yield could not be further optimized as at a certain point new very polar spots occurred on TLC, which might be assigned to partly and fully deprotected **150** (**109**). This observation again led us to the idea to use this feature in terms of directly converting hydrogenation product **149** into homo-β-proline (or its TFA salt). As the ionic hydrogenation/cyclopropane opening conditions already contain TFA, an in situ deprotection of the Boc-group and the *tert*-butyl ester seems plausible. Even a one-step procedure starting from cyclopropane **103**, should in principle be possible; however the occurrence of side-products might influence the outcome of the reaction and also hamper the final purification of the desired polar amino acid **109**.
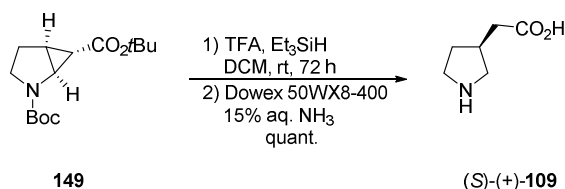
Scheme 33. Synthesis of (*S*)-(+)-homo-β-proline **109** from **149**.

When **149** was treated with TFA and triethylsilane for 72 h at room temperature, the TFA salt of **109** was obtained, that was then transformed into the free amino acid **109** by the use of an acidic ion-exchange resin and elution with aqueous ammonia. (*S*)-(+)-homo-β-proline (*S*)-(+)-**109** was obtained in quantitative yield from cyclopropane **149**. Spectroscopic data of (*S*)-(+)-**109** were in agreement with literature data.[114, 155, 158-160] However, the optical rotation value of **109** was slightly lower than reported before (+7.7 (*c* = 1, H_2O) compared to +9.6 (*c* = 1, H_2O)[114]). Upon investigation of the stereochemical outcome of the TFA mediated cyclopropane opening from **149** to **150**, we found a significant degree of epimerization of the stereocenter in **150**, and the enantiomeric excess was reduced from >99% *ee* for **149** to 73% *ee* for **150** (determined by chiral HPLC, see **E 2**). Further studies for achieving the synthesis of **109** from **103** without loss in stereoinformation are currently ongoing in the *Reiser* group. Nevertheless, it should also be noted that a synthesis of the enantiomeric (*R*)-(-)-**109** from (*R*,*R*,*R*)-(+)-**103** should be straightforward, following the very same synthetic sequence developed for (*S*)-(+)-**109**.

Upon a closer look into literature, it seemed as if the use of **109** as a pharmacophore is rather limited, even though it is obvious that the compound itself and its derivatives are in many cases among the most potent derivatives tested.[117, 119, 122, 127, 131, 189] This fact might be due to the rather displeasing synthesis strategies for **109** thus far published. However, with our new methodology it is possible to get relatively simple access to either racemic or enantioenriched homo-β-proline, which can then be used as a key building block for the preparation of new (and established) pharmaceutically relevant compounds. Furthermore, it may stimulate further investigations with the involvement of **109** as pharmacophore, as before practical access was rather limited. In summary we have developed a short and efficient methodology for the preparation of either enantiomer of 3-pyrrolidineacetic acid (homo-β-proline) **109** based on the enantioselective cyclopropanation of *N*-Boc-pyrrole **101**. The abovementioned cyclopropanation can be carried out on a 150 mmol scale, thus giving rise to

a multigram quantity of enantiopure **103**. In as few as three steps, (*S*)-(+)-**109** (or (±)-**109**/(*R*)-(-)-**109**) can be prepared in 37% yield from *N*-Boc-pyrrole, giving facile access to such biologically and pharmaceutically relevant compounds.

2.2 Further functionalization approaches of monocyclopropane 103

It was demonstrated that cyclopropane **103** reacts efficiently with nucleophiles under acidic conditions (see chapter **B 2.1.3**). After discovery of such a mode of reactivity it was obvious to apply this methodology to other, more challenging nucleophiles besides the enamide (enecarbamate) itself, and the hydride ion (products **149** and **151**), that might lead to an even higher degree of functionalization of this interesting building block.

The *Ugi* multi-component reaction (MCR) is an extremely powerful method for the construction of rather complex molecules that has been applied extensively in organic synthesis and in particular for the generation of large compound libraries.[190]
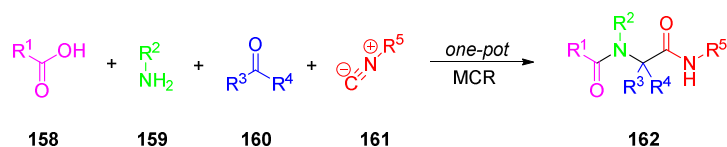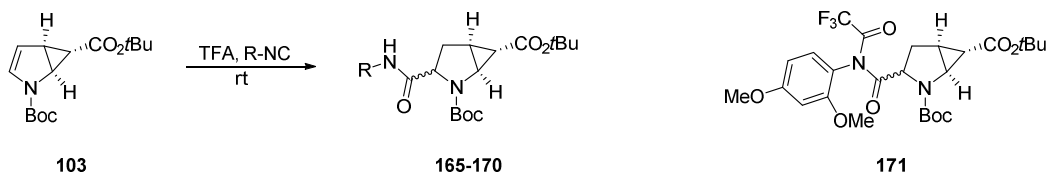

Scheme 34. General scheme for *Ugi* four-component reactions (different building blocks/subunits color coded).

In general, four components are used in this reaction. At first, an imine (or iminium) species is formed by an amine **159** and a carbonyl compound **160** (aldehyde or ketone). However, this first intermediate can also be preformed. Then an isocyanide (isonitrile) **161** attacks the imine and is instantly trapped by the carboxylate **158**. In the last step, an *O,N*-acyl shift occurs to yield the final products of type **162** (Scheme **34**).

A recent publication of *Nenajdenko et al.* attracted our attention,[191] where they presented a MCR with cyclic imines, isonitriles, and organic acids, giving rise to functionalized pyrrolidines in moderate to excellent yields (Scheme **35**).

Scheme 35. Preparation of functionalized pyrrolidines **164** from cyclic imines **163** by a three-component reaction from *Nenajdenko et al.*[191]

Best results were obtained when using TFA as acid, which is also beneficial if one thinks of in situ deprotection of *tert*-butyl-carbamates (Boc groups). In their publication, the isonitriles (*red* in scheme **35**) are attacking the α-position of the pyrrolidine ring (iminium carbon atom) as expected, accompanied by the acylation of the nitrogen atom by TFA (*pink* in scheme **35**). Hydrolysis of the isonitrile forms the final amide derivative. Interestingly, they found that the isonitrile acts as a dehydrating agent that transforms TFA into trifluoroacetic anhydride (TFAA), which subsequently acylates the nitrogen atom.[192] Based on the results of *Nenajdenko et al.*[191] in combination with the obtained reactivity of enecarbamate **103**, it seemed plausible to investigate the behavior of **103** under the abovementioned conditions. Thus, it should be possible to obtain derivatives of **103** with additional functionalization at the α-position and, in principle, also a deprotection/acylation of the nitrogen atom. As enecarbamates (and enamides) are known to display a rather tempered reactivity compared to enamines, one could harness this feature for the selective functionalization of those. In the following, we attempted to perform TFA initiated *Ugi*-type reactions with cyclopropane **103** and several different aliphatic and aromatic isonitriles. The obtained results are summarized in table **7**. In order to avoid the above mentioned dimerization as undesired side-reaction and to favor the intermolecular over the intramolecular reaction, the concentration was kept rather low (c = 0.02 M). It has to be noted that all herein investigated reactions gave highly complex reaction mixtures with partly very poor TLC staining behavior of the products, which severely hampered monitoring of the reaction process as well as the analysis of the crude reaction mixtures. As TLC analysis was hardly comprehensible, and because MCRs with isonitriles usually take several days to progress, reactions were aborted after some days and the crude reaction mixtures were analyzed via NMR and LC-MS. Crude mixtures were purified via flash chromatography where appropriate.

Table 7. Attempts for the TFA initiated *Ugi*-type functionalization of cyclopropane **103**.[9]

entry[a]	R =	product	solvent	time [d]	yield [%][e]	*dr*[h]
1	*t*Bu	**165**	DCM	5	6	*nd*
2[b]	*t*Bu	**165**	DCM	22	69	72:28
3	Cy	**166**	DCM	5	5	71:29
4[b]	Cy	**166**	DCM	22	*traces*	*nd*
5		**167**	DCM	5	*traces*	62:38
6[c]		**167**	THF	7	0[f]	*nd*
7		**168**	DCM	5	*traces*	77:23
8[d]		**168** (**171**)	DCM	9	14 (6)[g]	*nd*
9		**169**	DCM	5	*traces*	55:45
10		**170**	DCM	5	*nd*	*nd*

a) 0.40 mmol **103**, 1.2 equiv R-NC, 5.0 equiv TFA, 20 ml DCM, rt, 5 d; b) 0.68 mmol **103**, 10 equiv R-NC, 4 equiv TFA, 40 ml DCM; c) 0.50 mmol **103**, 2.56 equiv TosMic, 2.0 equiv *p*-TSA, 25 ml THF; d) 1.0 equiv R-NC, 1.0 equiv TFA, 5 ml DCM; e) isolated yield of both diastereomers (combined); f) large amounts of hydrolysis product *N*-(tosylmethyl)formamide isolated; g) 14% **168** + 6% acylation product **171** isolated; h) determined/estimated by LC-MS (ESI-EIC integration);[193] due to severe overlap a concise integration of ^{1}H-NMR signals was not possible.

As can be quickly recognized from table **7**, the proposed reaction worked efficiently for only one substrate, namely *tert*-butyl-isocanide (entry 2). Here, the two diastereomeric addition products were formed in 69% combined yield and a diastereomeric ratio of ~ 3:1. Detailed analysis of the products is described in a later part of this chapter. Interestingly, for all substrates besides 4-methyl-substituted isonitrile (entry 10), product formation could be

---

[9] Aromatic isonitriles of entries 7-10 were provided by M. Knorn.

identified by LC-MS, however, in most cases only in trace amounts. When comparing entries 1 and 2, one might expect that the excess of isonitrile might have favored the outcome of the reaction (1.2 equiv vs. 10 equiv R-NC). On the other hand, the cyclohexyl-substituted isonitrile did not lead to the formation of significant amounts of product while employing the same conditions as in entry 2 (entry 4). This leads to the suspicion that hydrolysis of the isonitrile may not be the limiting factor. For the 2,4-dimethoxy-substituted residue also a minor amount of TFA acylated product **171** could be identified (entry 8), whereas no acylation product was found for the other substrates. Due to a lack of suitable ^{1}H-NMR signals for integration, the values for the diastereomeric ratio of the obtained addition products were determined by integration of LC-MS signals, and should therefore be taken as a rough estimation rather than exact values. Nevertheless, when comparing the data of entry 2 of table **7** with the isolated amounts of diastereomers of **165a** and **165b** it becomes evident that the ratio, at least for this reaction, is quite similar. However, due to limited access to non-commercial isonitriles, no further efforts for optimizing the reaction conditions were carried out. As *tert*-butyl-isocanide was the only of the investigated isonitrile derivatives that worked properly for this kind of reaction, we investigated the structure of the resulting diastereomeric compounds in more detail (table **7**, entry 2; scheme **36**).
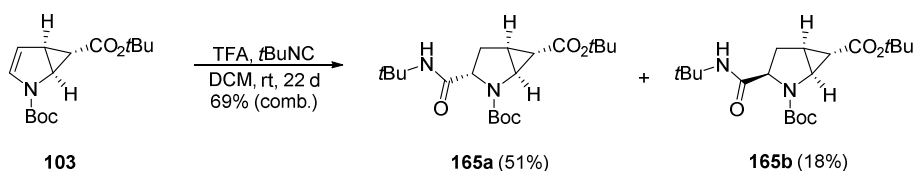
Scheme 36. Synthesis of *tert*-butyl substituted addition products **165a** and **165b** from cyclopropane **103** and *tert*-butyl isocyanide.

The two diastereoisomers **165a** and **165b** that were formed in a ratio of ~ 3:1 could be separated via flash chromatography, and the orientation of the newly formed stereocenter was unambiguously assigned using NOE experiments (minor diastereomer **165b**). The herefore required NMR spectra had to be carried out at low temperature (223 K) because of strong rotameric behavior of **165a** and **165b** leading to significantly broadened signals at ambient temperature. Figure **14** illustrates these observations. As expected, the major product was the one with the new amide substituent in *exo*-position in regard of the cyclopropane ring (**165a**).
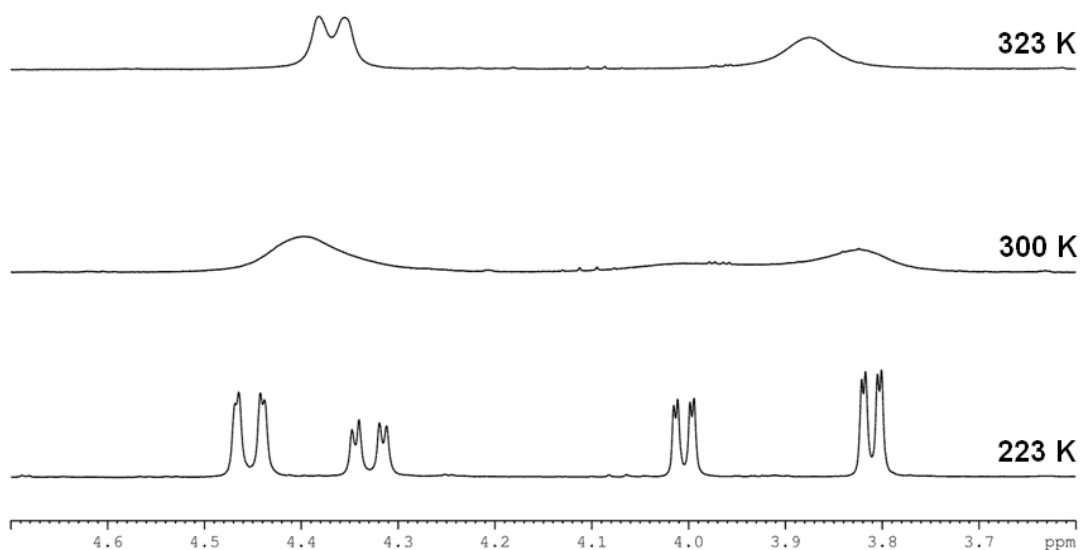
Figure 14. ^{1}H-NMR spectra of the α-CH (in regard of N) region of minor diastereomer **165b** at 223, 300 and 323 K in CDCl$_3$ (400 MHz). The presence of rotamers (ratio ~ 0.6:0.4) becomes obvious at 223 K.

In addition to the functionalizations via Ugi-type of mechanism, it was as well tested to directly add 1,3,5-trimethoxybenzene as a nucleophile to the enecarbamate **103** in an electrophilic aromatic substitution reaction (scheme **37**).
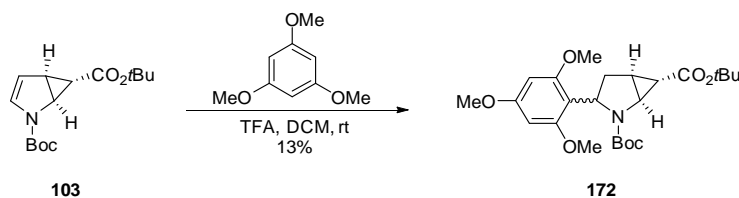

Scheme 37. Synthesis of functionalized derivative **172** from cyclopropane **103**.

Scheme **37** shows that enamide **103** can be functionalized via electrophilic aromatic substitution as well. The rather low yields may be explained by the high steric demand of both reactants. Nevertheless, almost any type of nucleophile may be employed for the functionalization of **103**, giving rise to a great variety of functionalities on this highly substituted pyrrolidine scaffold.

3 Transformations of double cyclopropanated pyrrole 104

3.1 Introduction

As doubly cyclopropanated pyrrole **104** was accumulating in significant amounts during the cyclopropanation reactions discussed before (chapter **B 1.3**), we were hence considering possible applications for it. It was noted before that **104** exhibits C_2-symmetry, which makes it an interesting compound for further derivatizations (figure **15**).
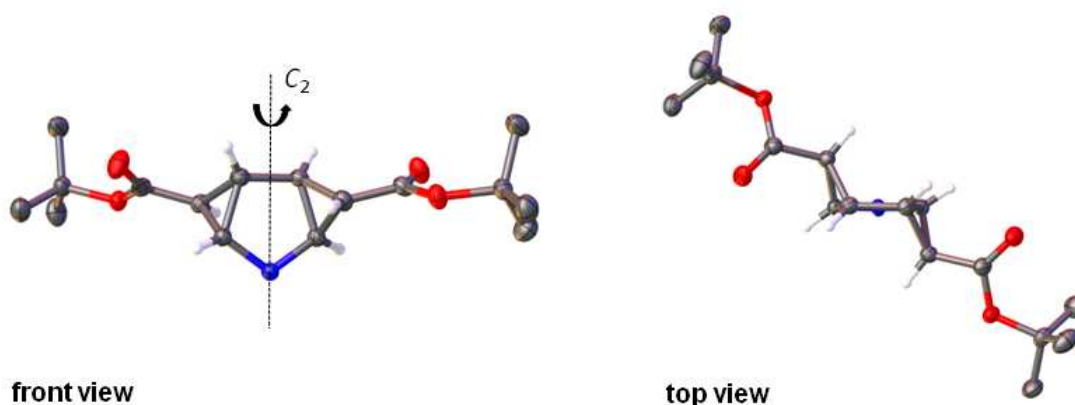
Figure 15. X-ray structure of bis-cyclopropane **104** from front (*left*) and top view (*right*), illustrating the C_2-symmetrical arrangement of the tricyclic core structure (all hydrogen atoms – except for the cyclopropane hydrogens – as well as the Boc protecting group at nitrogen (*blue*) are omitted for the sake of clarity; dotted line demonstrating the hypothetical C_2-symmetry axis).

In the following chapters the investigated attempts for the transformation of tricycle **104** into potentially biologically active pyrrolidine derivatives, as well as into a chiral C_2-symmetrical ligand for metal catalysts are described. The initial task in this part of the thesis was to find a suitable way of opening the two cyclopropane rings in **104**, in order to give C_2-symmetrical pyrrolidines of type **174** (scheme **38**).[194-198] This should be possible in principle, since it is well-known that donor-acceptor (DA) substituted cyclopropanes like **104** can be opened selectively by cleaving the bond in between the donor (D) and the acceptor (A).[165, 199, 200] As an important fact to bear in mind, *Diederich* and co-workers could show that C_2-symmetrical pyrrolidines like **173** exhibit remarkable activity as inhibitors of HIV-1 protease,[201] thus making such molecules highly demanded (scheme **38**).
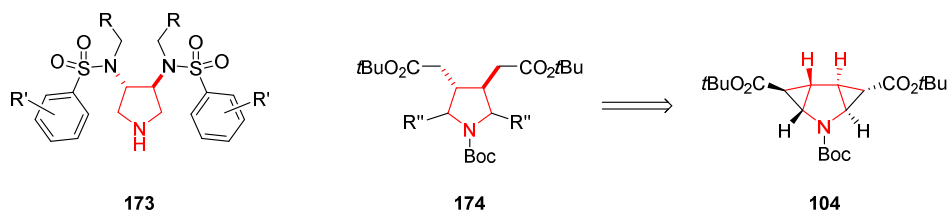
Scheme 38. General structure of potent HIV-1 protease inhibitors, containing a 3,4-disubstituted C_2-symmetrical pyrrolidine skeleton **173**, along with potentially accessible compounds **174** from bis-cyclopropane **104** that are structurally related to **173**.

With this in mind, we started a series of experiments for the selective ring-opening of the DA-cyclopropane bonds in tricycle **104** (or derivatives thereof) by using orthogonal strategies.

3.2 Opening of donor-acceptor substituted bis-cyclopropanes according to *Werz et al*.

From the group of *Werz* it is known that furan based bis-cyclopropane dialdehydes like **176** can be converted into annelated oligoacetals by collapse of the highly unstable *push-pull* cyclopropane system **176**.[202, 203] Within a repeated three-step sequence of double cyclopropanation, reduction and oxidation of furan **35**, all-*anti*-oligoacetals up to the nonamer **175** have been constructed and their structures were thoroughly analyzed by means of X-ray crystallography and DFT calculations (scheme **39**). It was shown that oxidation by 2-iodoxybenzoic acid (IBX)[204] in dimethylsulfoxide (DMSO) was a proper method for oxidizing the bis-cyclopropane diol moiety, and thus inducing cyclopropane ring opening, followed by a ring-closure reaction to form cyclic enol ether compounds like **177**.
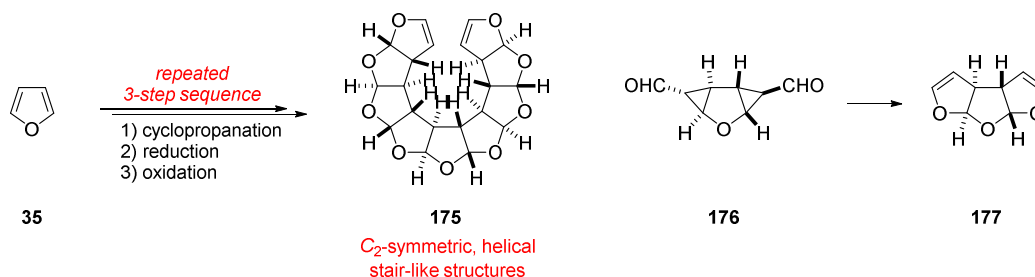
Scheme 39. Preparation of all-*anti*-fused oligoacetals **175** by a repeated three-step sequence starting from furan **35**, reported by *Werz et al*. (*left*). Key step is a ring enlargement reaction from tricyclic bis-cyclopropane aldehyde **176** to bis-enol ether **177** (*right*).

As until then *Werz* and co-workers had only reported such kind of transformations for furan derivatives, it seemed as an attractive strategy to us to envision pyrrolidine based compounds

of that same type (bearing a nitrogen atom in the central ring, instead of oxygen). Thus reduction of the two *tert*-butyl ester moieties of **104** by lithium aluminum hydride (LAH) was straightforward, leading to diol **178** in 95% yield (scheme **40**).
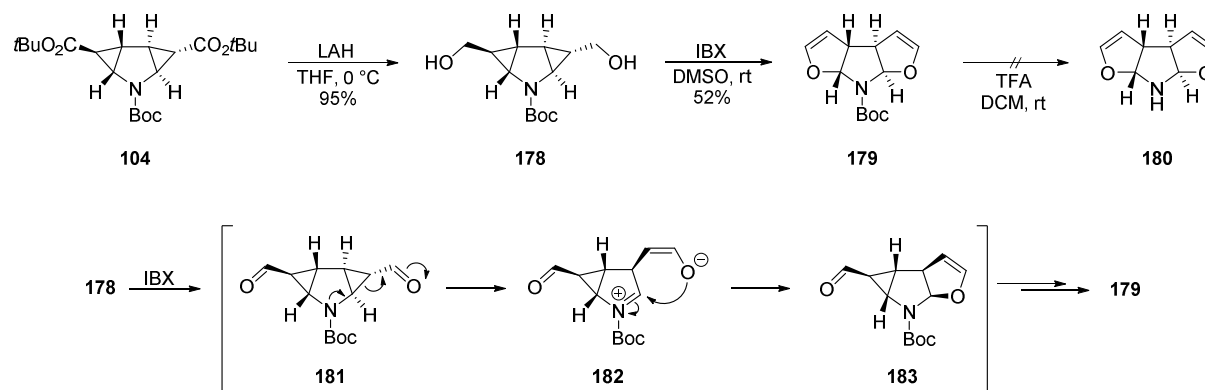
Scheme 40. Synthesis of C_2-symmetric tricyclic compound **179** from diester **104**, attempted deprotection and proposed mechanism of the rearrangement from **178** to **179**. However, calculations from *Werz et al.* suggested that – at least for furan derivatives – the ring enlargement step might occur in a concerted manner.

The second step was the abovementioned oxidation using IBX in DMSO, which led to tricyclic molecule **179** in satisfying 52% yield. Unfortunately, soon after having **179** in hand, the *Werz* group brought out another publication, showing the synthesis of the very same compound (and some derivatives), however, in somewhat inferior yield (42%).[205] An attempt to deprotect the N-atom in **179** in order to yield a potential C_2-symmetrical ligand for metal complexes **180**, failed due to decomposition of the starting material. Another idea for turning this into something useful was to investigate the cylopropane opening behavior in a rearrangement reaction.
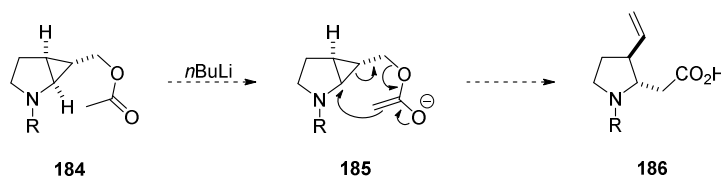
Scheme 41. Proposed mechanism for a base induced rearrangement of acetylated cyclopropane derivatives **184** for the formation of compounds like **186**.

It was thought that diol **178** could be protected by acetyl (Ac) groups and further undergo a rearrangement, which would open the cyclopropane bonds upon enolization with a suitable base. This would lead to interesting compounds like **186**. Scheme **41** depicts the proposed strategy for this idea. A protocol of *Pietruszka et al.* was applied successfully for the

acetylation of diol **178**,[206] giving rise to double acetylated pyrrole **187** in 91% yield within ten minutes reaction time (scheme **42**).
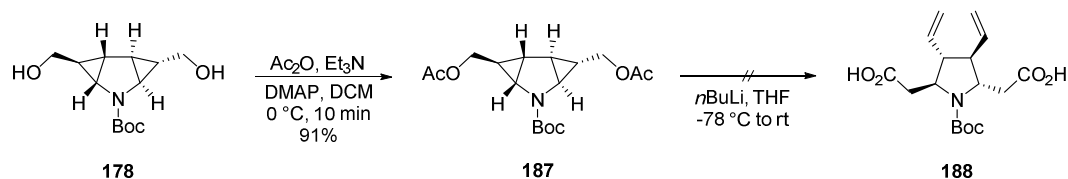

Scheme 42. Acetylation of diol **178** and unsuccessful attempt for the base-induced rearrangement of **187**.

However, the crucial step in this approach failed and only unreacted starting material, along with minor amounts of partially hydrolyzed **187**, were isolated. With the recent publication of *Werz et al.* in mind, and the fact that the subsequent trials were not successful, we turned our attention to other strategies for the opening of the DA-cyclopropane bonds of **104**.

3.3 Hydrogenolysis of donor-acceptor substituted cyclopropanes

Hydrogenolysis of carbon-carbon bonds is a well-known process in chemistry. Especially small rings with a high degree of ring strain, e.g. cyclobutanes or cyclopropanes, are somewhat prone to undergo ring opening reactions. Due to their intrinsic ring strain, catalytic opening of small rings by hydrogenolysis can be carried out at 'rather mild' conditions. Indeed, first examples go back to the early 20th century when *Willstätter* and *Bruce* first hydrogenated cyclopropane **189** and cyclobutane **191** to their corresponding aliphatic alkanes **190** and **192** using a nickel catalyst (scheme **43**).[207] Since then, several examples have appeared in literature revealing that this process is a valuable tool for synthetic chemistry. Scheme **43** presents some outstanding literature precedents for such reactions.
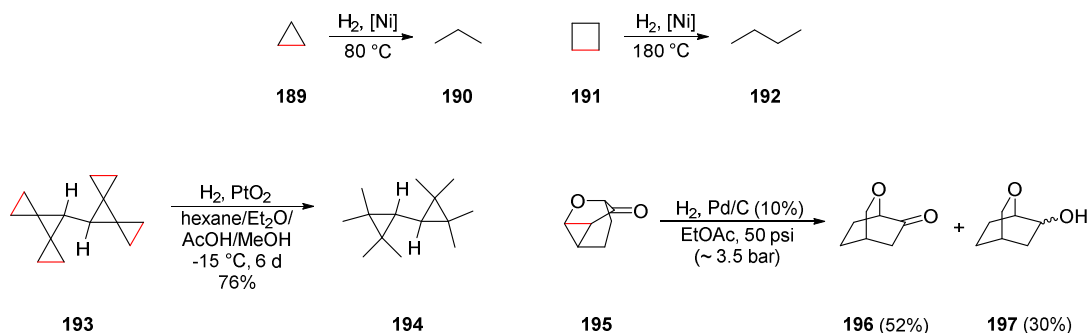
Scheme 43. Literature precedents for the catalytic hydrogenolysis of cyclopropane moieties (bonds to be cleaved are highlighted in *red*).

De Meijere and co-workers presented the catalytic hydrogenolysis of multiple *spiro*-annelated cyclopropanes **193**, using one atmosphere of hydrogen gas on a platinum(IV)-oxid catalyst. These highly strained compounds were shown to react smoothly even at low temperatures to form products like **194** (scheme **43**).[208] Another interesting example is the catalytic hydrogenolysis of DA-cyclopropane **195** with palladium on charcoal at slightly elevated pressures to form **196** and **197**, reported by *Adams and Belley*.[209]

Therefore, it was tested whether such an approach could also be adapted for our doubly cyclopropanated pyrrole derivative **104**. It seems plausible, that in our case, the bond between the donor and the acceptor should be the one to be cleaved most readily (*red* bonds in **104**, scheme **44**), due to the known fact that these bonds are typically the longest, and thus weakest, in such compounds.[210] In theory, one could obtain 3,4-disubstituted C_2-symmetric pyrrolidines **199** in one step via this method. As already mentioned before, derivatives of such compounds exhibit significant biological properties and hence are reasonable target structures.
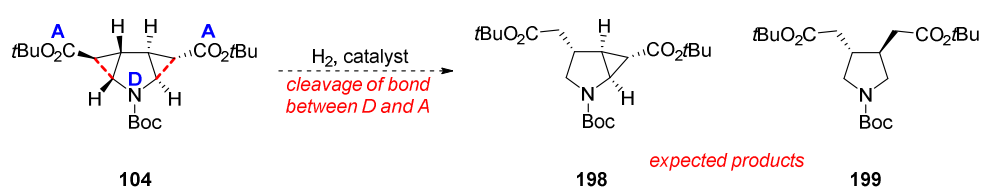
Scheme 44. Theoretical scheme for the hydrogenolysis of DA-cyclopropane **104** and the expected products for this type of transformation **198** and **199** (bonds presumably cleaved are given in *red;* A = acceptor, D = donor).

A first approach for screening several different catalyst systems was conducted using the *ThalesNano H-Cube Pro*™, a continuous flow system for hydrogenation reactions that allows for rapid screening of reaction conditions. Therefore, compound **104** was dissolved in methanol, passed through the reactor for one cycle (at variable conditions, e.g. temperature,

pressure, flow). The crude reaction mixture was analyzed by ^{1}H-NMR spectroscopy. Figure **16** illustrates the experimental setup used for these attempts.
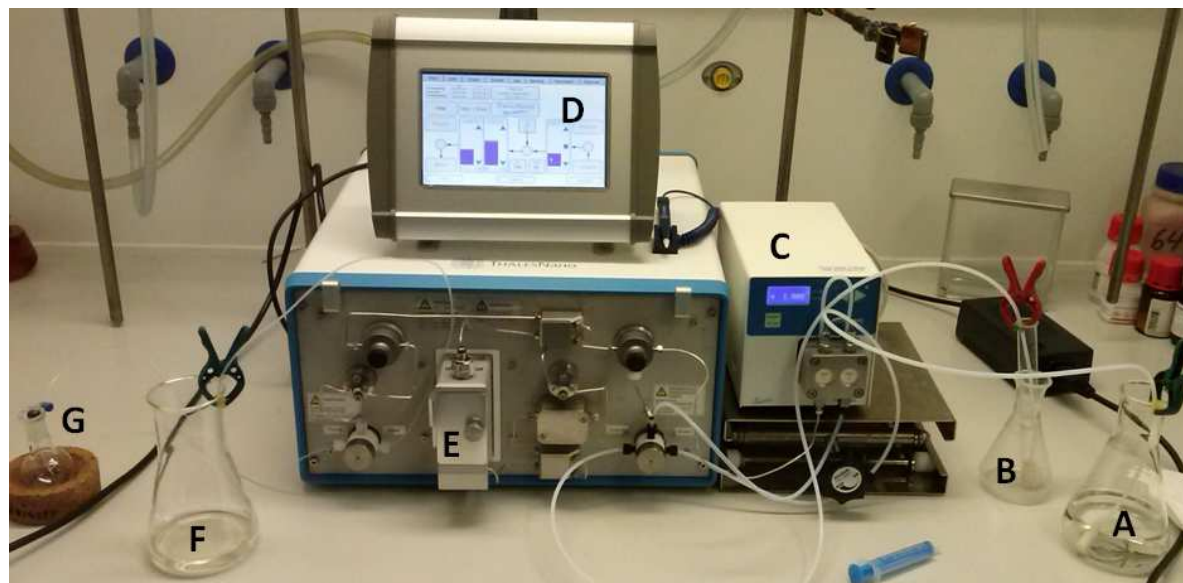
Figure 16. Illustration of the reaction setup for catalyst screening using the *ThalesNano H-Cube Pro*^{TM}. **A**: solvent; **B**: substrate in solvent (MeOH); **C**: HPLC pump; **D**: control element, display for adjusting and monitoring reaction parameters (temperature, pressure, flow, etc.); **E**: reaction chamber containing catalyst cartridge (incl. heating block); **F**: waste drain; **G**: recovered product mixture in solvent.

The obtained results of our screening attempts for the catalytic hydrogenolysis of **104** are summarized in table **8**. It could be shown that the major product of such experiments was none of the expected products (**198** or **199**; scheme **44**), but unsaturated derivative **200**. A discussion about the possible way of formation for **200** will be given in a later part of this chapter (scheme **45**). Looking at entries 1-6 of table **8**, one immediately realizes that neither 10% Pd/C, nor 5% Pt/C were suitable catalysts for the investigated transformation, as there was absolutely no conversion of starting material observable after one cycle (even at temperatures and hydrogen gas pressures of up to 80 °C and 80 bar, respectively). However, when using 5% Rh/C, significant amounts of product (< 10%) could be detected in the crude NMR spectra (40 °C, 40 bar; entry 7, as well as at 60 °C, 60 bar; entry 8). Surprisingly, when forcing the conditions up to 80 °C, 80 bar with the same catalyst system, no conversion of starting material was observed (entry 9).
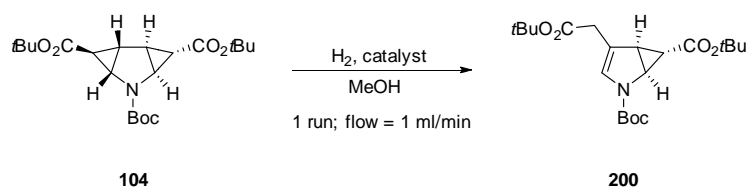
Table 8. Screening of reaction conditions for the catalytic hydrogenolysis of **104** under flow conditions using the *H-Cube^TM*.

entry[a]	catalyst	temperature [°C]	H_2 pressure [bar]	conversion[e]
1	Pd/C (10%)	50	40	0
2	Pd/C (10%)	60	60	0
3	Pd/C (10%)	80	80	0
4	Pt/C (5%)	40	40	0
5	Pt/C (5%)	60	60	0
6	Pt/C (5%)	80	80	0
7	Rh/C (5%)	40	40	4.8
8	Rh/C (5%)	60	60	8.5
9	Rh/C (5%)	80	80	0
10[b]	Rh/C (5%)	60	60	0
11[c]	Rh/C (5%)	40	40	8.3
12[c]	Rh/C (5%)	60	60	9.7
13[c]	Rh/C (5%)	60	80	0
14	Rh/C (5%)	50	50	0
15	Rh/C (5%)	60	60	0
16[d]	Rh/C (5%)	60	60	0

a) 0.05 mmol (20 mg) **104**, 4 ml MeOH; b) flow = 0.3 ml/min, 4 consecutive runs through system; c) fresh catalyst cartridge; d) flow = 0.3 ml/min; e) determined by ^{1}H-NMR of the crude reaction mixture without internal standard.

In order to enrich the amount of product for isolation and purification purposes, there are two obvious options: 1) reducing the flow rate, and 2) raising the amount of consecutive runs through the system in order to increase contact time of the reaction mixture with the catalyst cartridge (reaction chamber; **E** in figure **16**). Hence, the flow rate was set to a minimum value of 0.3 ml/min and the reaction mixture was passed through the system for four consecutive cycles at conditions that gave superior conversion before (60 °C, 60 bar; entry 10). But again no conversion was detectable, which made us curious, as this result did not make any sense at all. Surprisingly, when using a fresh catalyst cartridge of Rh/C (5%), product formation was observed again (entries 11 and 12), indicating a possible, but rather unlikely deactivation of the catalyst system. Unfortunately, follow-up experiments again failed, leading to zero conversion (entries 13-16). This led us to resign from this approach and to rater focus on other methods. The product formed during these attempts could unfortunately not be isolated and fully characterized, due to the limited scale of the experiments and the almost identical R_f values of **200** and the starting material **104**. However, figure **17** illustrates the strategy for its

identification by comparison of ^{1}H-NMR spectra. Mass spectrometry did, in this case, not help, as the starting material and the product would have identical molar masses.
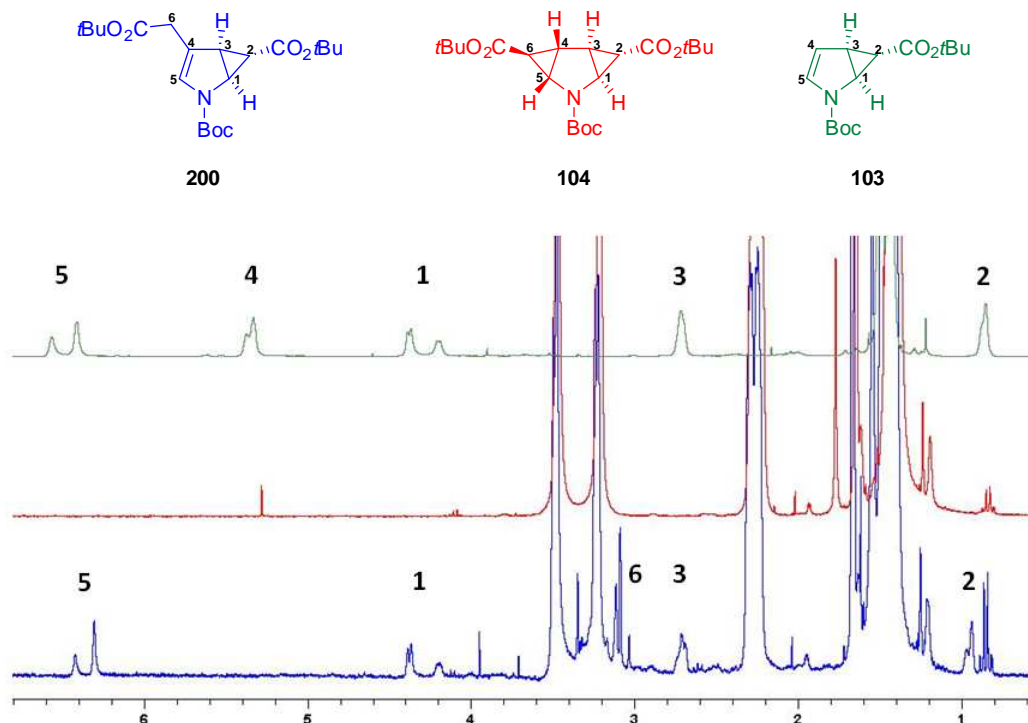

Figure 17. Identification of ring-opened product **200** (*blue*), by comparison of the ^{1}H-NMR spectra of the crude reaction mixture with those for starting material **104** (*red*), and structurally related mono-cyclopropane **103** (*green*). Separation of the crude mixture was not possible and the molar masses of starting material and product are identical (rearrangement).

In scheme **45**, a plausible mechanism for the formation of the obtained product is depicted. Starting from acid-mediated opening of the DA-cyclopropane bond and tautomerism of the enol moiety to the corresponding ester, intermediary iminium species **202** can then react via two orthogonal pathways: 1) Addition of hydride to the iminium ion would lead to an overall hydrogenolysis process (*red* in scheme **45**), whereas 2) elimination of a proton in β-position would lead to the product of an acid-catalyzed rearrangement process (*blue* in scheme **45**).
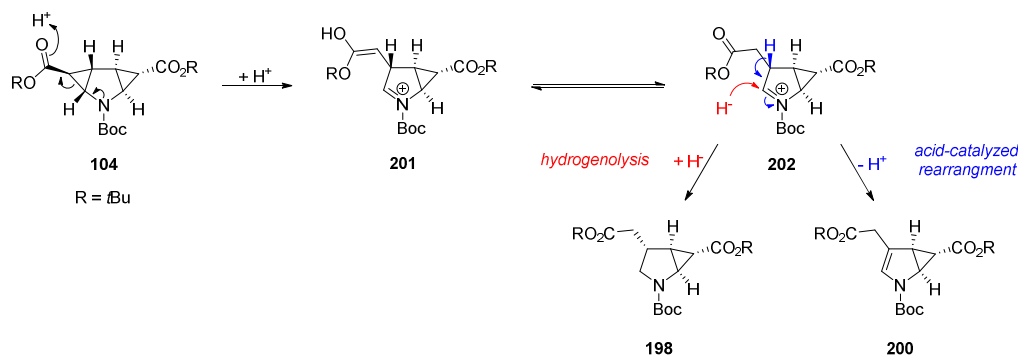
Scheme 45. Plausible mechanism for the above investigated transformation of bis-cyclopropane **104**. In principle two pathways can be envisioned, leading to different types of products. The classical strategy of hydrogenolysis (*red*) would lead to a product like **198**, while an acid-catalyzed rearrangement (*blue*) would give rise to **200**.

Batch experiments were conducted in the following, as it was shown that catalyst deactivation was assumed to be a critical issue in the *H-Cube*^{TM} experiments (table **8**). Thus, in table **9** we tried to reproduce the results from the abovementioned flow experiments, and to accumulate product amount for complete characterization. To our surprise, we found that in these reactions not the unsaturated pyrrolidine **200** but ring-opened methanol adducts of type **203** and **204** were formed, probably due to trapping of the intermediary iminium ion **202** by a molecule of methanol.
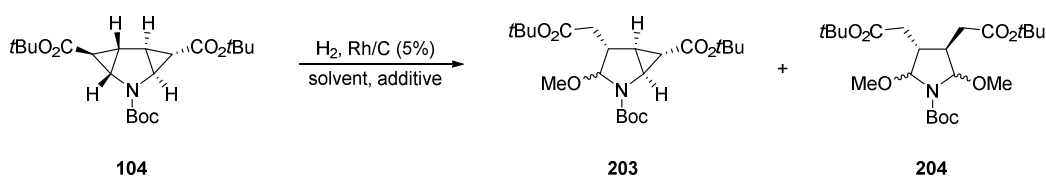
Table 9. Attempts for the hydrogenolytic cleavage of cyclopropane **104** under batch conditions.

| entry[a]	H_2 pressure [bar]	temperature [°C]	additive	time [d]	conversion[f]
1	1	25	-	2	0
2[b]	60	60	-	1	*traces*
3	1	25	10% HOAc (v/v)	19	44
4[c]	1	25	10% HOAc (v/v)	19	32
5[d]	1	65	10% HOAc (v/v)	6	3
6[b]	60	60	10% HOAc (v/v)	6	6
7[e]	-	25	10% HOAc (v/v)	7	7

a) 0.50 mmol (198 mg) **104**, 20 ml MeOH, 10 mol% Rh/C (5%); b) reaction carried out in a sealed autoclave; c) 40 ml MeOH; d) no catalyst used; e) no hydrogen used; f) estimated from ^{1}H-NMR of the crude reaction mixture without internal standard.

The experiments described in table **9** were either performed in regular *Schlenk* flasks with a balloon of hydrogen gas (for ambient pressure experiments; entries 1, 3-5) or in a sealed

autoclave for reactions under pressure (entries 2 and 6). Monitoring of the reaction was severely hampered by the fact that TLC analysis was not sufficient to clearly indicate product formation (nearly identical R_f and staining behavior of starting material **104** and products **203** and **204**). Therefore, ^{1}H-NMR analysis had to be carried out to follow the reaction progress. Without the addition of an additive, there was almost no conversion detectable, even when conditions were forced to 60 °C and 60 bar (entries 1 and 2). Looking at the reaction times, it is noticeable that these processes were extremely slow and the conversion of starting material reached some kind of plateau after a certain time and then stopped completely. Best results were obtained when using 10% (v/v) acetic acid as an additive at ambient temperature and pressure, giving rise to 44% of conversion after 19 days (entry 3). Lower concentrations led to reduced reaction rate (32%, entry 4), whereas higher concentrations were not accomplishable due to the poor solubility of **104**. It could be shown by NMR and MS that methanol adducts **203** and **204** were formed in these transformations, but due to the low conversion and nearly identical R_f values of starting material **104** and the products **203** and **204**, it was practically impossible to completely purify and characterize the products. In none of the cases unsaturated elimination product **198** was observed. In order to check whether Rh/C is crucial for product formation, the attempt was made to convert **104** by simply refluxing it in methanol/acetic acid without catalyst addition (entry 5). However, only very little conversion was obtained after six days, indicating that rhodium indeed plays a role as catalyst. As described above, reaction rate seemed to be a limiting factor. Hence, we applied additional pressure and heat to the reaction conditions of entry **3** in order to accelerate the process. However, after six days of reaction at 60 °C and 60 bars of pressure only 6% conversion were determined (entry **6**). When using Rh/C in MeOH/HOAc at room temperature without hydrogen gas, 7% conversion were observed after seven days (entry **7**). If entries 5 and 7 are taken into account, it seems obvious that the investigated transformation is rather an acid-catalyzed process than a hydrogenation of the cyclopropane bond. Therefore, we turned our focus from hydrogenation approaches to acid-promoted transformations of bis-cyclopropane **104**.

## 3.4 Acid-promoted transformations of DA-cyclopropane 104

As demonstrated earlier in chapter **B 3.3**, hydrogenolysis of the *push-pull* cyclopropane bonds in **104** is not an efficient process as cyclopropane cleavage rather proceeds via an acid-catalyzed ring opening mechanism. Hence, we investigated the effects of different *Brønstedt* and *Lewis* acids on their cyclopropane opening propensities, as well as suitable trapping reagents for the proposed iminium species **202**. Table **10** summarizes the attempts for such kind of transformations. From the previous experiments (entry 5 in table **9**), it is clear that refluxing methanol/acetic acid is not sufficient to induce cyclopropane ring opening. This leads to the conclusion that a suitable catalyst, capable of cyclopropane ring opening, needs to be employed. Indeed, scandium(III)-trifluoromethanesulfonate (scandium triflate; $Sc(OTf)_3$) was shown to be highly efficient in opening both DA-cyclopropane rings in **104** (entries 1-3, see also ref. [60]). After only 5 min of microwave irradiation (heating at 85 °C), full conversion of starting material was observed. Unfortunately, only rearomatization and deprotection products could be isolated in this case (scheme **47**). The same was observed when bis-cyclopropane **104** was refluxed in methanol and activation with *para*-toluenesulfonic acid (*p*-TSA; entry 5). The ratio of the formed aromatic products **208** strongly depended on the reaction times. Under the acidic conditions (and elevated temperatures) an initial deprotection of the Boc group is likely before the ring opening takes place. However, the deprotection may also happen at a later stage. Yet in 1998, *Wenkert* and *Khatuya* reported on acid-mediated ring opening, and subsequent aromatization of doubly cyclopropanated furans **205** to form furan-3,4-diacetates of type **207**.[103] The authors proposed intermediates like **206**, which were claimed to be prone toward elimination (scheme **46**).
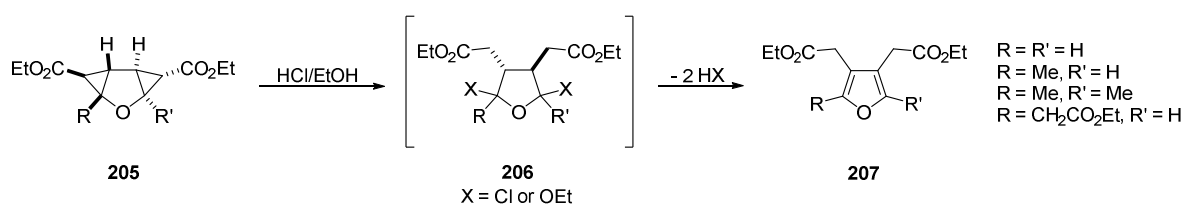
Scheme 46. Synthesis of furan-3,4-diacetates **207** from acid-mediated cyclopropane opening of **205** and subsequent elimination of HX from **206** by *Wenkert* and *Khatuya*.[103]

The fact that mixtures of several different ester functionalities (*t*Bu/Me and Me/Me) were isolated (**208**) leads to the assumption that the transesterification process takes place after the

formation of the pyrrole skeleton. Other *Lewis* acids (LiClO$_4$, FeCl$_3$, AlCl$_3$) did also not yield products other than **208** (entries 6-8). In order to circumvent elimination, and thus rearomatization, the solvent was switched from methanol to less nucleophilic THF (entries 9-17) and the addition of triethylsilane was intended to provide hydride as a suitable nucleophile, which would not undergo elimination once added (see also scheme **47** for a plausible mechanism). However, this approach, though nice on paper, turned out to yield only decomposition products or unreacted starting material.
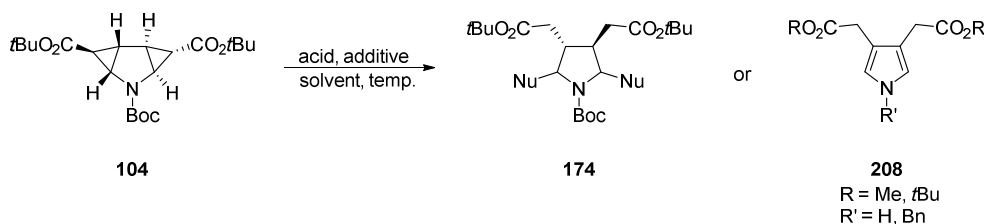

Table 10. Attempts for the acid-catalyzed cyclopropane opening of **104** (mw = microwave).

entry[a]	solvent	acid	temperature [°C]	additive (equiv)	time	conversion [%][h]	product
1	MeOH	Sc(OTf)$_3$	85 (mw)	-	5 min	> 90	**208**
2	MeOH	Sc(OTf)$_3$	85 (mw)	Et$_3$SiH (5)	5 min	> 90	**208**
3	MeOH	Sc(OTf)$_3$	30-80 (mw)	-	30 min (6x5)	~ 80	**208**
4[b]	MeOH	Sc(OTf)$_3$	25	-	6 d	0	-
5[b]	MeOH	*p*-TSA	65	-	18 h	100	**208**
6	MeOH	LiClO$_4$	25	-	72 h	< 5	-
7	MeOH	FeCl$_3$	25	-	72 h	< 5	-
8	MeOH	AlCl$_3$	25	-	72 h	~ 50	**208**
9[b]	THF	Sc(OTf)$_3$	85 (mw)	Et$_3$SiH (5)	10 min	100	*decomposition*
10	THF$_{abs}$	Sc(OTf)$_3$	85 (mw)	-	5 min	100	*decomposition*
11[c]	THF	Sc(OTf)$_3$	85 (mw)	Et$_3$SiH (5)	5 min	~ 20	**208**
12	THF	Sc(OTf)$_3$	25	Et$_3$SiH (5)	30 min	0	-
13	THF	*p*-TSA	25	Et$_3$SiH (5)	72 h	< 5	-
14	THF	*p*-TSA	85 (mw)	Et$_3$SiH (5)	5 min	< 5	-
15[d]	THF	*p*-TSA	25	Et$_3$SiH (5)	24 h	< 5	-
16[e]	THF	TFA	25	Et$_3$SiH (5)	72 h	> 90	*decomposition*
17	THF	Sc(OTf)$_3$	30-80 (mw)	C$_5$H$_{11}$-NH$_2$	30 min (6x5)	0	-
18	MeCN	Sc(OTf)$_3$	150 (mw)	C$_5$H$_{11}$-OH	15 min	100	*not identified*
19[f]	MeCN	Sc(OTf)$_3$	95	*Hantzsch* ester	24 h	0	-
20[f,g]	MeCN	Sc(OTf)$_3$	95	Bn-NH$_2$	3 h	32 (NMR)	**208**

| 21[f)] | THF | Sc(OTf)$_3$ | 85-125 (mw) | Bn-NH$_2$ | 2 h | < 5 | **208** |

a) 0.05 mmol (20 mg) **104**, 40 mol% acid, 1 ml solvent; b) 0.50 mmol (198 mg) **104,** 40 ml solvent; c) 100 μl of water were added; d) 1.1 equiv *p*-TSA used; e) 5 equiv TFA were used; f) catalyst inhibition by amine; g) product inseparable from starting material (**208**: R = *t*Bu, R' = Bn); h) estimated from TLC.

Formation of aromatic compounds **208** in such reactions indicates that there seems to be an intermediary ring-opened methanol adduct of type **203**/**204** present (chapter **B 3.3**), which undergoes subsequent elimination of methanol (and Boc deprotection) to yield ring-opened pyrrole derivatives. A plausible mechanism for this type of transformation is shown in scheme **47**.
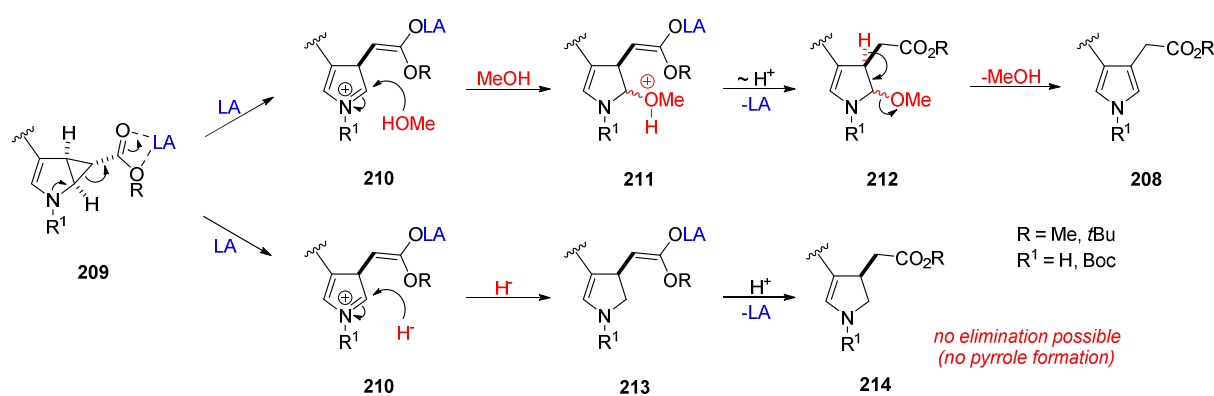
Scheme 47. Plausible mechanism for the acid-catalyzed ring opening and subsequent transformations of proposed intermediate **209**. When methanol acts as the nucleophile (*red*) elimination, and simultaneous pyrrole formation is encouraged (*upper row*). On the other hand, when hydride is used as the nucleophile, no elimination can take place, allowing for maintenance of the stereocenter(s) (LA = *Lewis* acid, *blue*).

After *Lewis* acid activation of the ester moiety a *push-pull* ring opening of the DA-substituted cyclopropane **209** takes place and the intermediary iminium ion **210** is trapped by a molecule of methanol. Intermediate **211** (or **212**) is prone to undergo elimination of methanol again to finally form pyrrole derivatives of type **208** under the applied conditions (scheme **47**, *upper row*). Ideally, one would envision using a nucleophile that is not able to undergo elimination. Thus, hydride may attack the iminium ion **210** to form products of type **213** (or **214**), which cannot undergo elimination and still maintain their stereoinformation (scheme **47**, *lower row*). Unfortunately, results from table **10** suggest that neither of the applied conditions were feasible for sufficient transformation of bis-cyclopropane **104** into the desired products **174** without the occurrence of aromatization. Thus, no further efforts were carried out in this direction.

4 Investigations of peptide foldamers at high pressure

4.1 High pressure as an alternative activation mode in organocatalysis

A general, until now only partly solved problem in organocatalysis is the slow reactivity of many of the catalysts compared to classic metal catalysis, leading to low turnover frequencies and to an instantaneous need for higher catalyst loadings.[211-215] In order to overcome energy barriers for organic transformations, several different modes of activation are feasible, e.g. an increase in temperature, the application of *Lewis* acids, microwave irradiation or ultrasonic sounds.[216, 217] Pressure is an alternative that was somehow ignored by a great part of the scientific community so far (due to plausible reasons, see discussion later); although it bears significant advantages compared to standard activation modes. It is a mild and non-destructive method that allows for activating a broad variety of organic transformations even at low temperatures, giving distinct benefits for selectivity issues. Reactions prone for activation by pressure include aldol, *Michael*, *Mannich* and *Baylis-Hillman* reactions, as well as cycloaddition reactions and cross couplings. In principle, every reaction with a negative *volume of activation* ($\Delta V^{\ddagger}$), which is defined as the difference of the *volume of the transition state* and the *volume of the reactants*, can be accelerated by the influence of pressure.[218-221] Although literature precedents for pressure promoted reactions are rather limited, some remarkable transformations have been accomplished so far.[222-227] It can be assumed that the normally rather sophisticated experimental setup for such reactions excluded more intense application of high pressure in catalysis. However, people are creative and thus developed simple strategies for the generation of high pressures. For instance, *Hayashi* and co-workers reported a very elegant method by freezing water inside a sealed autoclave with a household refrigerator/freezer to -20 °C, which enabled them to generate pressures of up to 2000 bar.[228-231] Some very recent examples include high pressure catalysis combined with photochemistry,[232, 233] as well as the highly enantioselective construction of chiral quaternary stereocenters applying pressures up to 10 kbar, which leads to products that are not accessible under ambient conditions.[234, 235]

4.2 Peptide based organocatalysts

Short peptides have been shown to be remarkably efficient catalysts for organocatalytic transformations and have been applied in a broad scope of transformations. The field of peptide based organocatalysis has been pioneered by *Miller et al.*[236, 237] and extensively augmented by the group of *Wennemers*.[238, 239] Figure **18** depicts two prominent examples from the referred groups (**215** and **216**).
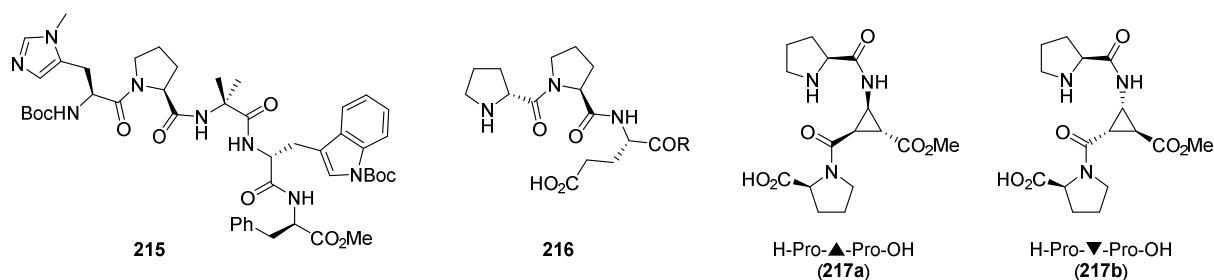

Figure 18. Examples of peptidic organocatalysts from *Miller et al.* (**215**) and *Wennemers et al.* (**216**), along with tripeptide foldamers **217a** and **217b** from the *Reiser* group (▲ designates (+)-*cis*-β-ACC ((+)-**33**), and ▼ designates (-)-*cis*-β-ACC ((-)-**33**)).

Various studies revealed that regular peptides are often too flexible to act efficiently, thus modification by e.g. N-methylation or introduction of conformationally constrained building blocks proved to be vital for the construction of efficient catalyst systems. Tripeptide foldamers like **217a** and **217b**, containing a β-ACC (▲ or ▼) building block in the central position were shown to be efficient catalysts for organocatalytic transformations, including aldol, *Mannich*, and *Michael* reactions.[58, 240] Making use of the rigidity of the central cyclopropane moiety the two functional groups responsible for catalysis, i.e. the secondary amine and the carboxylic acid function can be positioned in close proximity. This feature allows **217a** (containing ▲) to act as a superior catalyst compared to its isomer **217b** (containing ▼). In the following part a plausible explanation for the discrepancy in catalytic activity between **217a** and its isomer **217b**, based on high-pressure (HP) structural studies (including HP-NMR), compared with catalytic results at high- and ambient-pressure conditions is proposed. The synthesis of the two tripeptide foldamers is described in the following section.

4.3 Synthesis of the tripeptide foldamers 217a and 217b

The synthesis of tripeptide foldamers **217a** and **217b** commences with the preparation of the central cyclopropane amino acid *cis*-β-ACC (▲/▼; (±)-**220**) following a method of *Reiser et al.*[50] In this case **33** is prepared in a racemic fashion, as the enantiomers can be separated at a later stage (as diastereomeric dipeptides **221**), hence giving rise to both isomers at once. After *N*-Boc protection of pyrrole **50** using a slightly modified procedure of *Grehn* and *Ragnarsson*,[241] a racemic cyclopropanantion reaction of *N*-Boc-pyrrole **101** was carried out using methyldiazoacetate to form cyclopropane (±)-**18** (scheme **48**). The remaining double bond was subsequently cleaved via ozonolysis and treatment with dimethylsulfide (DMS) to form aldehyde **218**. In the next step, the aldehyde function was oxidized to the carboxylic acid following a procedure of *Dalcanale* and *Montanari*.[242, 243] After a deformylation step mediated by the organic base *N,N*-diethylaminoethylamine (DEAEA), benzyl protection of the free acid concludes the synthesis of racemic (±)-**220**.
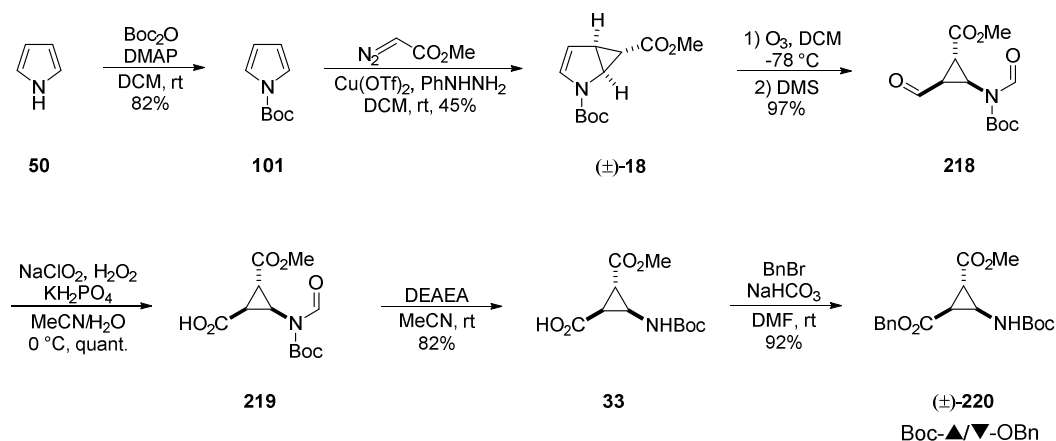

Scheme 48. Synthesis of (±)-**220** from pyrrole **50** following the procedure of *Reiser et al.*[50]

Single crystals of the racemic mixture of **33**, suitable for X-ray analysis could be grown, allowing for a structural proof of the *cis*-relationship of the amine and the carboxylic acid moieties in **33** (figure **19**).
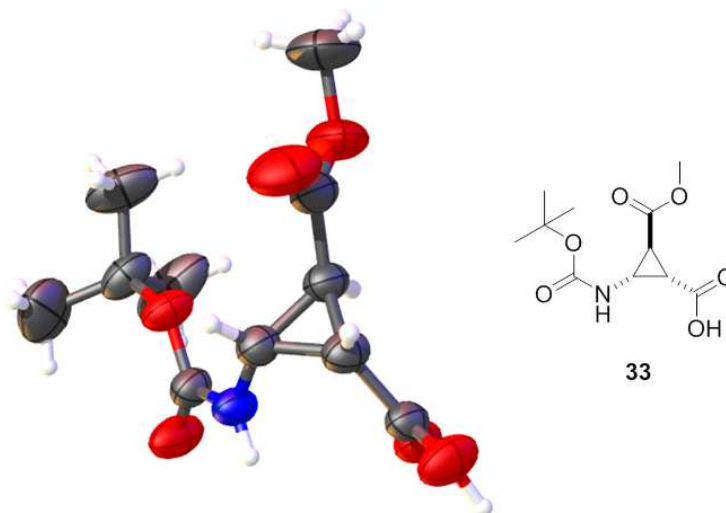
Figure 19. Single crystal X-ray structure of Boc-▼-OH (**33**), clearly showing the *cis*-relationship of the amine and the carboxylic acid function. This structural feature is crucial for further approaches into catalysis, as it allows for spatial proximity of the functional groups responsible for catalytic activity.

After successful synthesis of racemic **220**, the preparation of the tripeptide catalysts followed another report of *Reiser et al.*,[58] which is presented in scheme **49**. As donor-acceptor substituted cyclopropanes are known to undergo rapid ring opening reactions once the N-terminus is deprotected, β-ACC derivatives proved to be tricky substrates for peptide coupling approaches.[48, 244, 245] Nevertheless, it is possible to synthesize dipeptides of type **221** by the deprotection of the *N*-Boc group with a solution of HCl in dry ethylacetate.[54] The resulting ammonium derivatives are stable enough to directly convert them into the corresponding dipeptides via solution phase peptide coupling with *N*-ethyl-*N'*-(3-dimethylaminopropyl)carbodiimide hydrochloride (EDC) and *N*-Boc-*L*-proline. For the separation of the two diastereomeric dipeptides, it is necessary to deprotect the Boc group first, as chromatographic separation proved to be much more convenient at this stage. Thus, the two diastereomerically pure dipeptides could be obtained in 43% (**221a**) and 33% (**221b**) yield from racemic (±)-**220**, respectively. The next steps are then performed in parallel for both isomeric compounds. After Boc protection and hydrogenolytic cleavage of the benzyl groups, the dipeptides are coupled with a second molecule of *L*-proline to form orthogonally protected tripeptides **222a** and **222b**. Final deprotection steps were carried out using HCl/EtOAc with subsequent basic work-up, followed by hydrogenation in order to cleave the benzyl esters. In this way tripeptide H-Pro-▲-Pro-OH (**217a**) was prepared in 5.0% yield over 13 steps (from *N*-Boc-pyrrole), and its isomer H-Pro-▼-Pro-OH (**217b**) in 4.1% (scheme **49**).
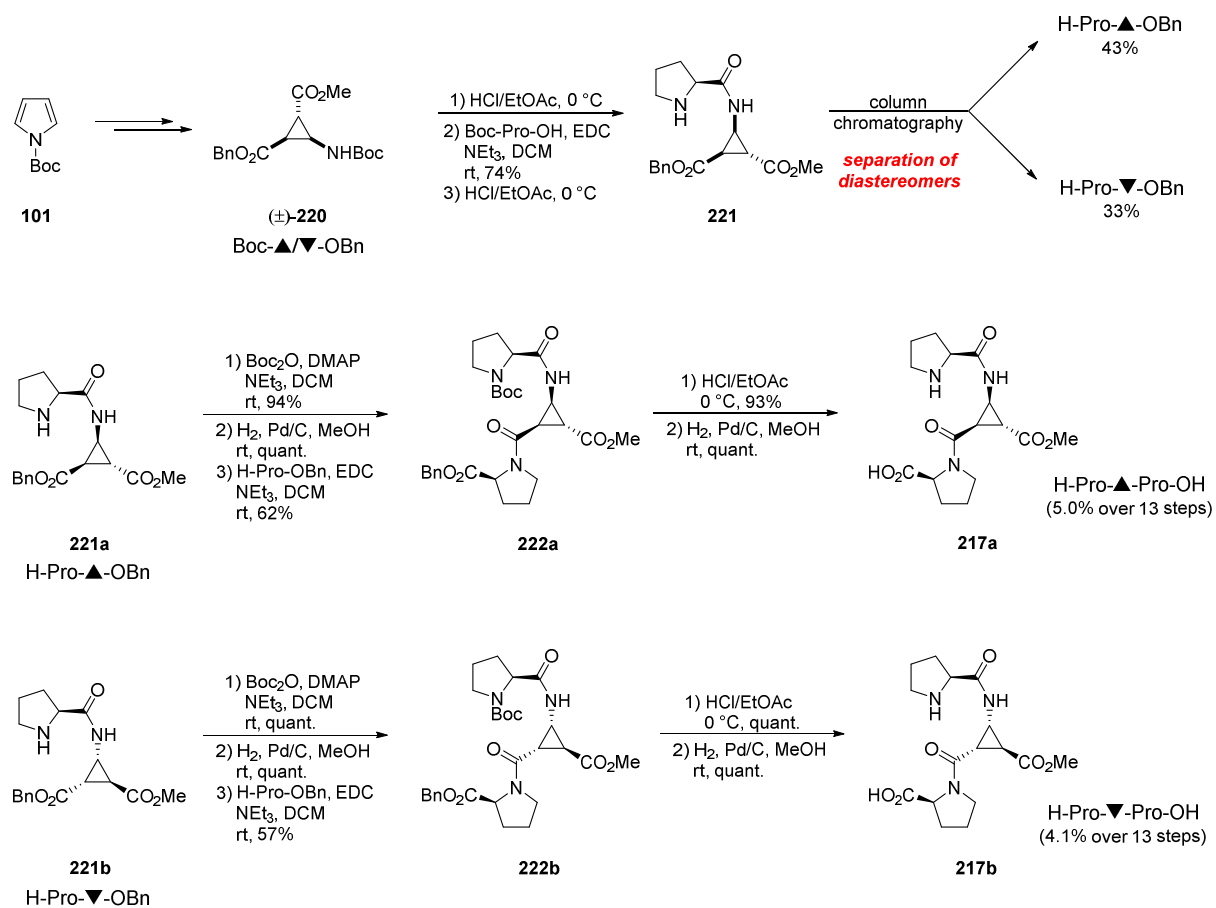
Scheme 49. Synthesis of tripeptide organocatalysts **217a** and **217b** from (±)-**220**, following the procedure of *Reiser et al.* (solely *L*-proline was used for peptide coupling).[58]

4.4 Structural investigations of the tripeptide foldamers 217a and 217b

In order to gain insight into the possible conformations of the two peptidic organocatalysts **217a** and **217b**, we performed detailed structural investigations, including NMR studies combined with molecular modeling approaches. The findings from our structural studies were then compared to the results obtained from catalysis experiments (chapter **B 4.5**). From former studies it is know that H-Pro-▲-Pro-OH (**217a**) is a superior catalyst compared to its isomer H-Pro-▼-Pro-OH (**217b**).[58, 59] With the experiments discussed in the following part we aimed to create a reasonable explanation for the catalytic discrepancy of the two title compounds, and to propose a plausible way of catalytic action for the active species.

When having a look at the proton NMR spectra of the two isomeric compounds **217a** and **217b**, one immediately recognizes a significant difference.[58] While the spectrum looks tidy for **217b**, with nice sharp and separated signals, there is a vast overlap of mostly broadened signals visible for **217a**. Furthermore, one can see multiple distinct sets of signals, which might be assigned to minor populated state conformations. These first insights led to the postulation that **217a** is conformationally highly flexible, while its isomer **217b** is rather fixed to one major conformation, which may be due to an internal hydrogen bond. In order to test our hypothesis, ^{1}H-NMR spectra of both compounds were recorded at varying pressures (30, 1000, 2000 bar), and the relative shifts of the characteristic amide proton (*red* NH in figure **20**) were compared. In general, amide protons of peptides and proteins tend to shift much higher upon an external stimulus (e.g. temperature, solvent titration), when they are not hydrogen bonded. Thus, a minor shift of the amide signal may give hints for H-bonding of the amide proton in question.[246] Figure **20** presents the results of the conducted experiments.
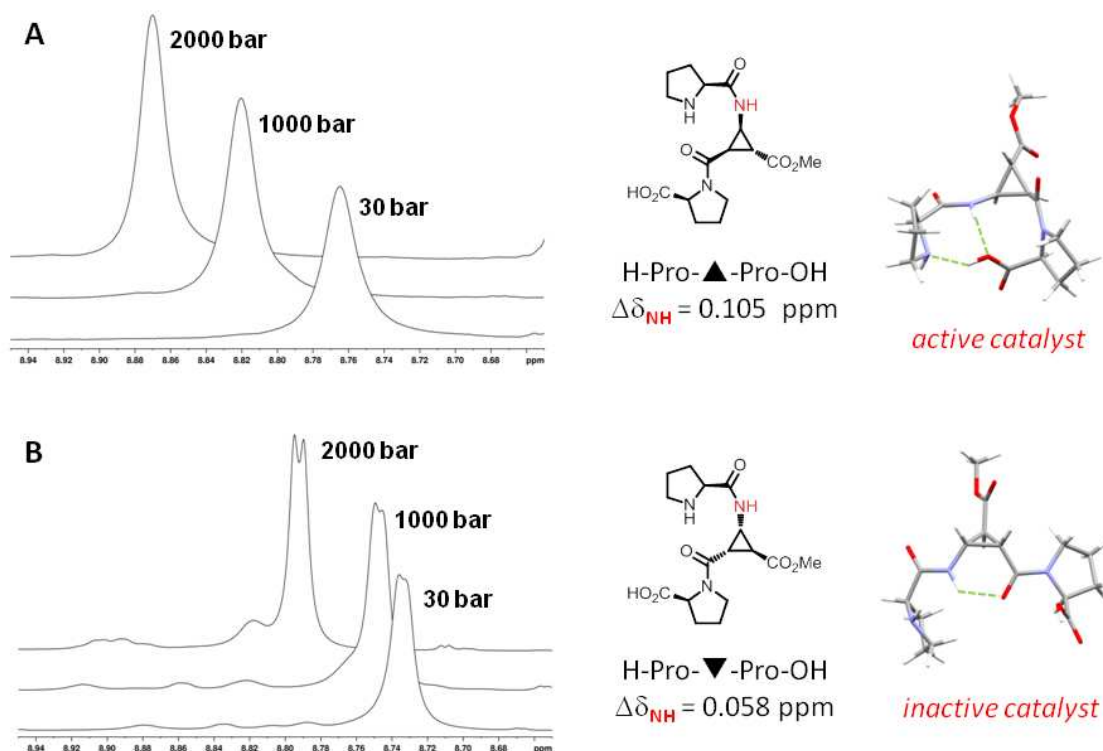
Figure 20. ^{1}H-NMR spectral region of the signal of the amide proton (*red*) of **217a** (**A**) and **217b** (**B**) at varying pressures (30, 1000, 2000 bar). The relatively low shift of the signal of **217b** and the occurrence of peak fine structure are clear hints for strong intramolecular H-bonding (800 MHz, CD$_3$OH, 0.18 M, 298 K).

It is clearly visible from the stacked ^{1}H-NMR spectra depicted in figure **20** that the amide signal shifts to a much larger extent for **217a** ($\Delta\delta_{NH}$ = 0.105 ppm, **A**) compared to **217b** ($\Delta\delta_{NH}$ = 0.058 ppm, **B**). Furthermore, it has to be noticed that the signals are much sharper and start to split into the characteristic doublet of backbone amide protons in peptides (**B**). All together, these observations confirm our hypothesis and lead us to the conclusion that a strong intramolecular hydrogen bond fixes the conformation of **217b**. Structural calculations on the C-terminal benzyl ester of **217b** also revealed potential H-bond formation.[59, 247] As this tripeptide is the one showing poor catalytic performance, it is suggested that the internal H-bond separates the two functional groups responsible for catalytic activity, thus leading to an inactive catalyst. On the other hand, H-Pro-▲-Pro-OH (**217a**) is highly flexible, allowing for positioning of the functional groups into the desired conformation. It was already shown by *Reiser et al.* that **217a** exists in predominantly two major conformations.[58] At ambient temperature **217a** was shown to exist in a 1:3 *cis/trans* ratio in methanol-d_3, whereas the minor *cis*-amide conformer was proposed to be the catalytically active species. X-ray analysis of peptide **217a** was not possible due to the high intrinsic flexibility (tripeptide **217b** could be crystallized but the obtained crystals were unfortunately not measurable). Moreover, this

would only lead to solid state insights, whereas the solution structure is much more important in this case. Therefore, we attempted to generate molecular models of the tripeptides, which would allow a more detailed perception into the structural preferences of the latter. The molecular modeling software package *Spartan 06* was used for the conformational sampling and energy calculations. Figure **21** presents low energy structures of tripeptides **217a** and **217b** obtained from a conformational search using six rotatable backbone bonds each without distance restraints. The resulting structures (324) were then minimized in energy and sorted afterwards. Due to severe overlap of the NMR signals, precise integration of all nuclear *Overhauser* effect (NOE) cross peaks could not be achieved, however, distinct NOEs were found for all of the proposed conformations and were taken into account in the process of sorting the conformers. Regarding this aspect, it has to be noted that the conformations of tripeptides **217a** and **217b** presented in figure **21** are rather ideal model structures than exact reflections of what actually happens in solution.
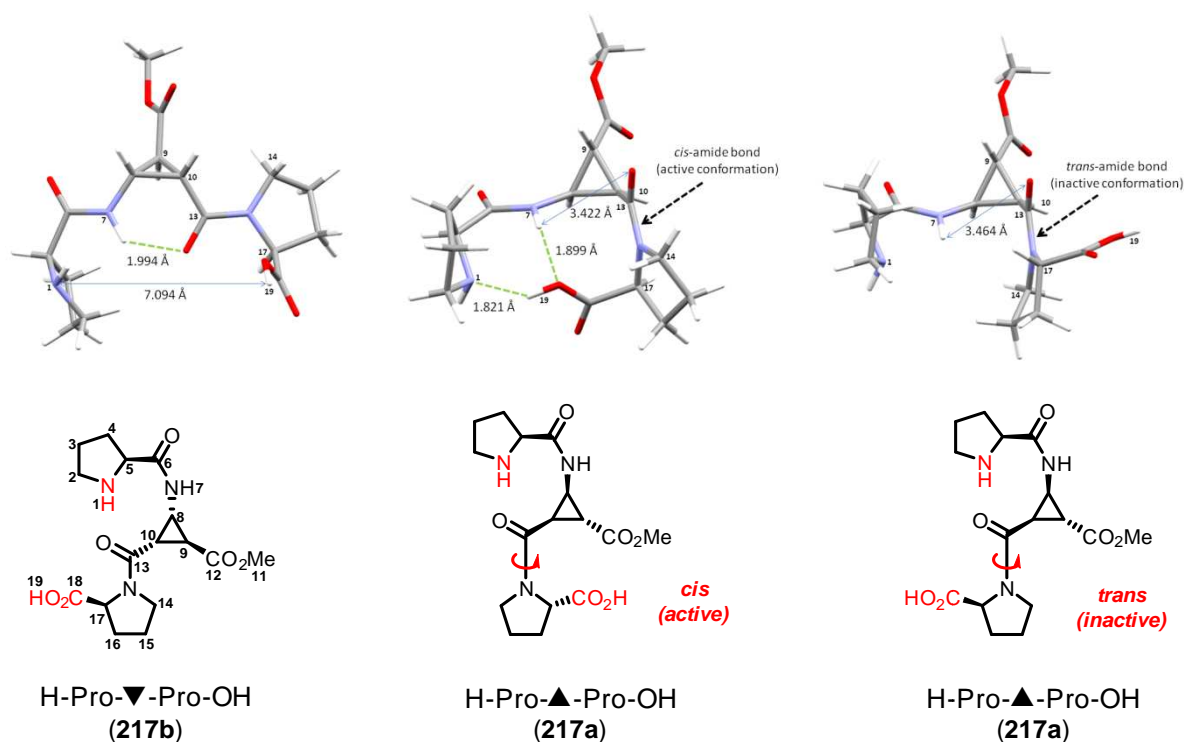
Figure 21. Low energy models of tripeptides **217b** (*left*) and **217a** (*center*, *right*) generated by *Spartan 06*. It is assumed that **217b** is stabilized by a strong intramolecular H-bond (*green*), which separates the two crucial functions (NH[1] and HO[19]) from each other (*left*). In contrast, **217a** exists in predominantly two conformations (*cis* and *trans*), from which only the minor conformation with a *cis*-amide bond would be the catalytically active species (*center*), while the *trans*-conformation has some kind of *resting state character* (in the chemical structures the groups responsible for catalytic activity are highlighted in *red*; *blue* arrows give distances between NH[7]-OC[13], and NH[1]-HO[19] in Å; H-bonds with corresponding distances are indicated in *green*).

The low energy structure of tripeptide **217b** shows a potential hydrogen bond (d = 1.994 Å) between NH^7 and OC^{13}, which has also been predicted by the abovementioned experiments. In such a conformation the two functional groups responsible for efficient catalysis are spatially separated (7.094 Å); a structural feature which would disallow bifunctional organocatalysis, and therefore explain the poor catalytic performance of **217b** (*left part* of figure **21**). In contrast to **217b**, **217a** is suggested to be rather flexible, allowing for rapid changes of conformation. The two major conformations are proposed to be *cis/trans*-isomers of the C-terminal amide bond (OC^{13}-N).[10][248] In both, the *cis*-amide conformation (*center*) and the *trans*-amide conformation (*right*) the distances between NH^7 and OC^{13} are rather large (3.422 Å and 3.464 Å, respectively) and out of plane, thus avoiding a restraining H-bond similar to **217b**. The minor populated *cis*-conformer (*center*) shows close spatial proximity of the catalytically active functional groups with two weak H-bonds arranging them in space (NH^7-CO^{18}: 1.899 Å, HN^1-HO^{19}: 1.821 Å). On the other hand, the *trans*-conformation of **217a** (*right*) represents a kind of *resting state* of the catalyst, but though allows for rapid interconversion of the conformers.
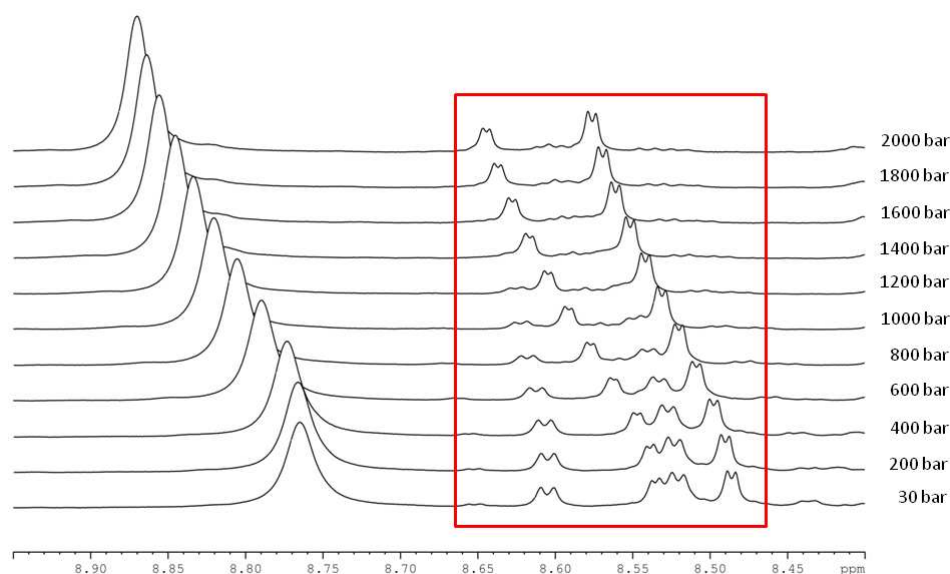
Figure 22. ^{1}H-NMR spectral region of the amide signal of tripeptide **217a** at varying pressures (30-2000 bar). While the amide signal of the major conformer (*left*) only shows shifting and marginal line sharpening upon increasing pressure, the region of minor populated conformational states (*red frame*) reveals distinct changes (800 MHz, CD_3OH, 0.18 M, 298 K).

In order to investigate whether pressure can influence the conformational equilibrium of our catalyst, we investigated the ^{1}H-NMR amide region of H-Pro-▲-Pro-OH (**217a**) under

---

[10] *For the conformations of proline amide bonds see:* ref. [248]

varying pressures (figure **22**). While the amide NH signal for the major conformer (*trans*, *left part of the spectra*) only showed shifting and rather insignificant line sharpening upon increasing pressure, the region of the minor populated conformational states revealed distinct effects (*red frame*). Indeed it seems that some of the signals are completely vanishing at higher pressures. This suggests a substantial effect of pressure on the conformational preferences of such a small peptide, which is remarkable. In order to provide more experimental proof for the proposed mechanism of action, we conducted experiments using tripeptides **217a** and **217b** as catalysts for aldol reactions at ambient- and high-pressure conditions.

4.5 Organocatalysis under high pressure

It is a well-known fact that pressure influences the dissociation of water.[249] As it is also known that water plays a vital role in a plethora of organocatalytic transformations, it seems plausible to apply high pressure for the acceleration of said reactions. Despite of the effect on reactivity, it should also be investigated whether pressure can have an influence on the conformational equilibrium of the peptides, and thus could affect selectivity. Hence, tripeptide catalyst H-Pro-▲-Pro-OH (**217a**) was tested in the model reaction between acetone **223** and *para*-nitrobenzaldehyde **224** under ambient- and high-pressure conditions (table **11**).
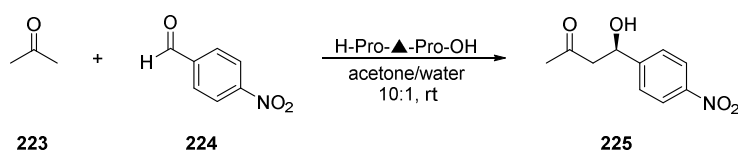
Table 11. Organocatalyzed aldol reactions under ambient- and high-pressure conditions.

| entry[a]	catalyst [mol%]	time [h]	pressure [bar][d]	conversion[e]	yield [%][f]	ee [%][g]
1	-	24	1	40	17	0
2	-	24	4600	14	9	0
3	10	24	1	84	68	69 (*R*)
4	10	16	5200	100	81	65 (*R*)
5	10	4	4800	97	73	67 (*R*)
6[b]	20	24	1	n.d.	89	78 (*R*)
7[b,c]	20	24	1	n.d.	77	6 (*R*)

a) 0.20 mmol (30 mg) **224**, 2 ml acetone/water (10:1 (v/v)); b) taken from ref. [58]; c) H-Pro-▼-Pro-OH, acetone/water (5:1 (v/v)); d) deviations of pressure are due to the experimental setup; e) determined by TLC analysis/isolated starting material; f) isolated yield after column chromatography; g) determined by chiral HPLC (Chiralcel AS-H, *n*-heptane/*i*PrOH = 99:1, flow = 0.5 ml/min, λ_{max} = 254 nm, r_t = 18.97 min (*R*), r_t = 22.38 min (*S*)).

In order to see the potential effects of pressure on selectivity, a benchmark reaction with a moderate degree of enantioselectivity was chosen on purpose. From entries 1 and 2 it can be concluded that uncatalyzed background reactions indeed occur, but to a significantly lower extent at 5 kbar. When comparing entries 3 and 5, it becomes obvious that a pressure of 5 kbar leads to a sixfold increase in reaction rate (reaction time reduced from 24 h to 4 h). However, no significant effects on enantioselectivity were observed. Comparison of entries 6 and 7 reveals that H-Pro-▼-Pro-OH (**217b**) is still an active catalyst (leading to 77% yield), but conveys extremely poor selectivity (entry 7). This result nicely fits our proposed model, where the secondary amine (NH^1) is widely separated from the acid function (OH^{19}), but still is able to catalyze the reaction. It is assumed that the chiral information is transferred by the H-bonding capability of OH^{19} (orienting the transition state), thus explaining the low enantioselectivity value for **217b** (6% *ee*). Although it was stated before that rigidity plays a crucial role in peptide catalyst activity, this example clearly demonstrates that a certain degree of conformational freedom can be essential for efficient catalytic performance.

4.6 Structural investigations of longer α,β-peptide foldamers under high pressure

High pressure is a valuable tool in protein biochemistry as it enables the investigation of folding/unfolding mechanisms of proteins, which are of major concern with regard to diseases like *Altzheimer's* disease, *Parkinson's* disease or amyotrophic lateral sclerosis (ALS).[250] In most cases it is a non-invasive method that allows for tracking of folding intermediates, thus giving insight into conformational preferences of proteins and poly-peptides.[251, 252] In the following, we attempted structural studies of peptide foldamers with HP-NMR and HP-FTIR spectroscopy in order to explore the feasibility of such methods for systems much smaller than proteins.
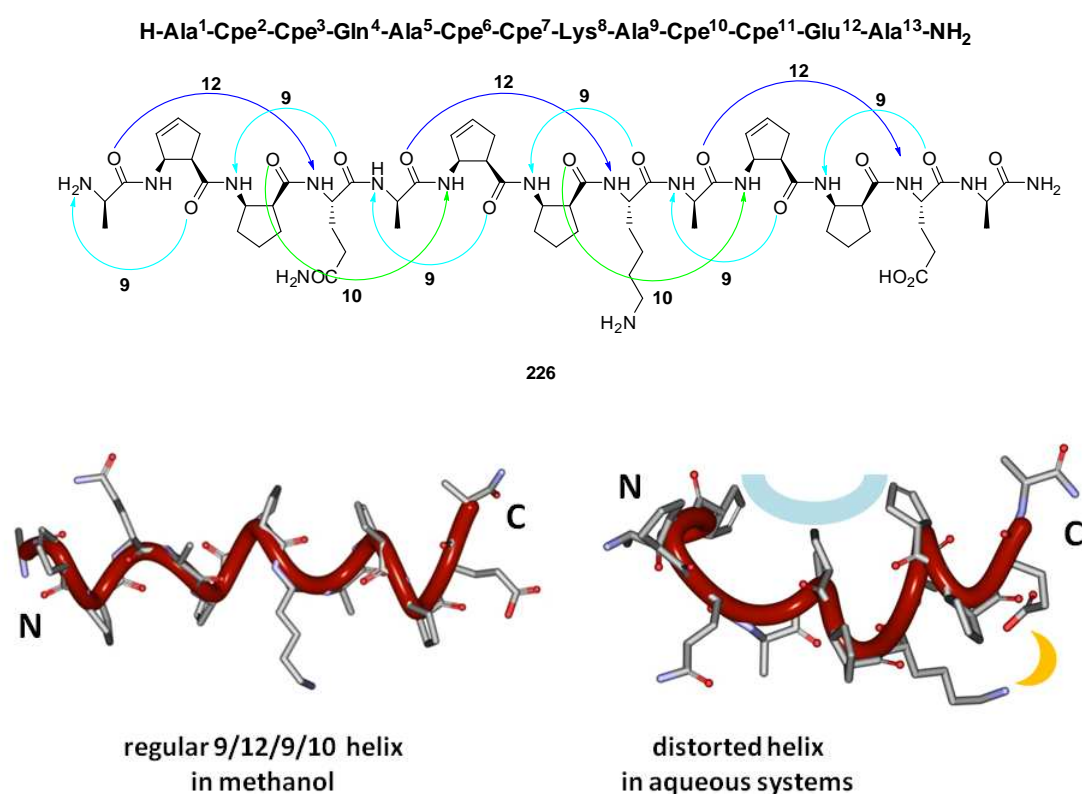

Figure 23. Three-letter coded sequence and chemical structure of 13-residue α/β-peptide foldamer **226**, including H-bonds (Cpe = cispentacin; digits on arrows indicate the number of atoms forming the H-bonded rings; *top*). NMR solution structures of **226** in methanol (*left*) and water (*right*). Foldamer **226** adopts a regular 9/12/9/10 helix in methanol solution. In contrast the helix is distorted to some extent in aqueous media, possibly due to hydropobic interactions and π-stacking between the unsaturated rings (Cpe-2, Cpe-6, Cpe-10) on one face of the helix (*blue*), and formation of a salt-bridge between Lys-8 and Glu-12 on the opposite side (*orange*).

Mixed α/β-peptide foldamers[253, 254] like **226** were designed using the so-called *stereochemical patterning approach* of *Martinek and Fülöp et al.*[255] and were shown to exhibit stable helical structures, even in aqueous media (figure **23**).[256, 257] In order to test

the power of HP-methods for structural studies of relatively short peptidic foldamers, we investigated the behavior of foldamer **226** as a model compound with HP-NMR (up to 2 kbar) and HP-FTIR (up to 6.5 kbar). The results of our experiments are summarized in the following section.

4.6.1 High-pressure NMR experiments of foldamer 226

NMR spectra of 13-residue peptide foldamer **226** were recorded in aqueous buffer at pressures ranging from ambient pressure (30 bar) to 2040 bar. The chemical shifts of the backbone amide signals – which are generally the most meaningful part of peptide or protein NMR spectra in terms of structural studies, as they reflect the backbone conformation – were analyzed (figure **24**).
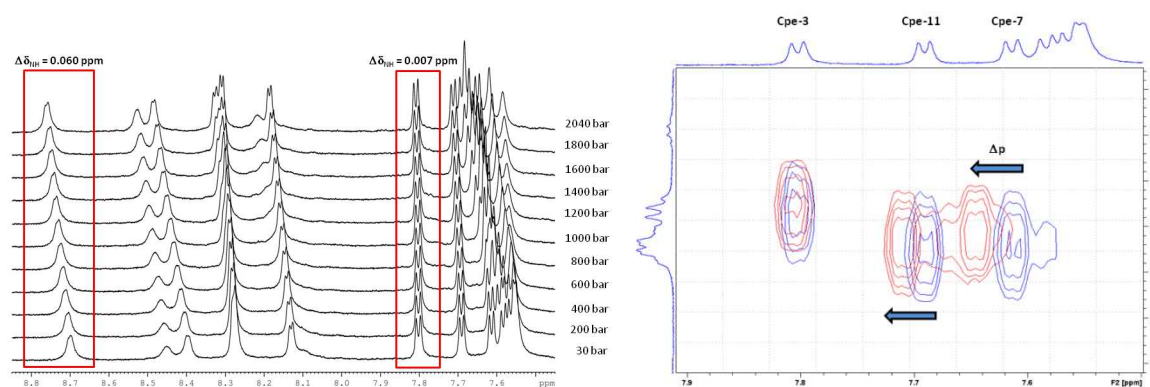

Figure 24. *Left:* ^{1}H-NMR spectral region of the amide signals of foldamer **226** at varying pressures (30-2040 bar). Comparison of the signals for Ala-13 (*left red frame*) and Cpe-3 (*right red frame*) reveals non-uniform shifts of the amide signals, which indicates conformational changes of the helical backbone of the peptide foldamer. *Right:* Overlay of excerpts from NOESY spectra of **226** at 30 bar (blue) and 1830 bar (red). Arrows indicate pressure induced cross-peak shifts. 1D projection represents the 1H-NMR spectra of **226** at 30 bar according to the *blue* crosspeaks. (800 MHz, 20 mM aqueous phosphate buffer pH 7.4, 4 mM, 300 K, 800 ms mixing time).[258]

Obviously, the general trend upon increasing pressure is a low-field shift of most of the amide signals of **226**. However, some of the backbone amide proton signals do not move to a significant extent ($\Delta\delta_{NH}$ = 0.007 ppm for Cpe-3), while others shift quite intensely ($\Delta\delta_{NH}$ = 0.060 ppm for Ala-13). This feature is clear evidence that structural changes in the backbone conformation of the helical peptide occur, rather than solely compression of the helix, which would result in a constant shifting of all amide signals in question. Furthermore, the amide protons of the minor shifting signals show almost no changes of the *J*-coupling constants upon increasing pressure (Cpe-3: $^3J_{HH}$ (30 bar) = 8.49 Hz, $^3J_{HH}$ (2040 bar) = 8.41 Hz; Cpe-11:

[3]J_{HH} (30 bar) = 8.11 Hz, [3]J_{HH} (2040 bar) = 8.24 Hz). Based on the low chemical shift differences and almost constant *J*-coupling values of such signals one can assume that these residues are rather buried in the interior of the helical structure and keep their strong hydrogen bonding character. On the other hand, terminal residues that are not incorporated within a strong hydrogen bonding network (e.g. Ala-13) tend to be more flexible.

4.6.2 High-pressure FTIR experiments of foldamer 226

Infrared (IR) spectroscopy is a well-established technique for studying protein conformations.[259-262] In order to get a deeper insight into the conformational behavior of our model peptide **226**, we conducted HP-FTIR measurements, as it is known that protein secondary structures can be reliably assigned by using such methods.[263] Figure **25** depicts the amide-I band of the FTIR spectra (1600-1700 cm^{-1}) – which is mostly associated with the carbonyl stretching vibration – of foldamer **226** in D_2O under varying external perturbations (e.g. temperature and pressure). An approach for the cautious interpretation of the obtained data is described in the following.
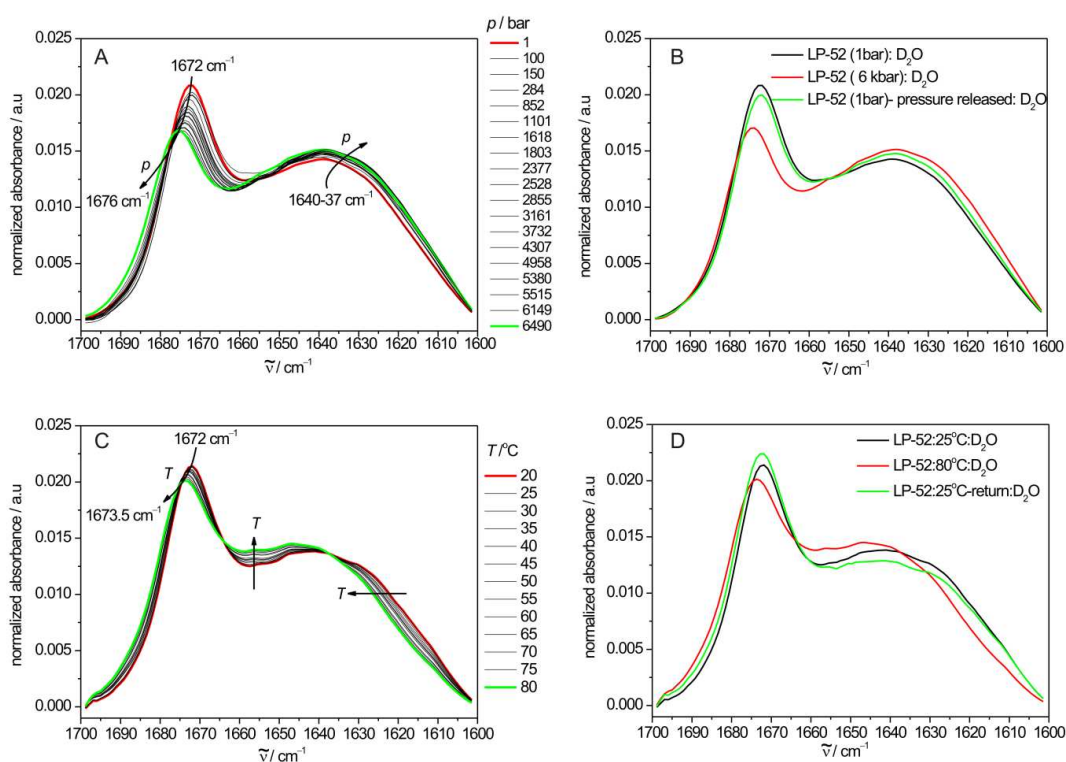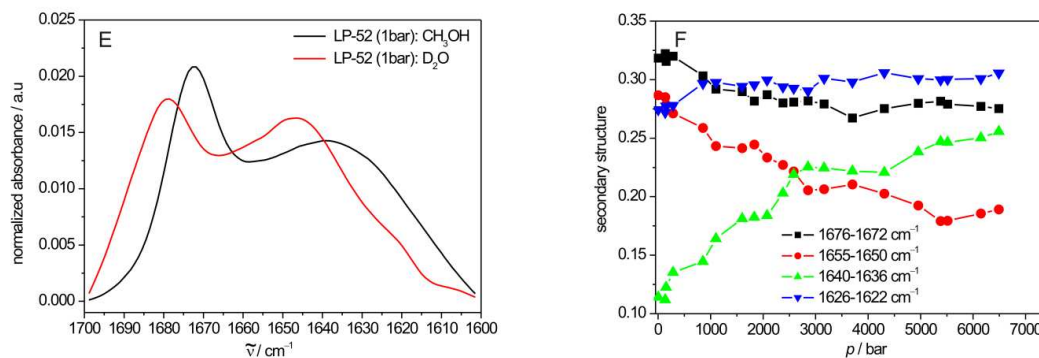
Figure 25. Results from the pressure (**A** and **B**) and temperature (**C** and **D**) dependent FTIR measurements of foldamer **226** in D_2O at 298 K. Structural changes are reversible in regard of pressure (**B**) and temperature (**D**). FTIR spectra of **226** in D_2O and MeOH (**E**), and pressure dependency of secondary structure motifs (**F**; *black* = turn-like structures, *red* = helical structures, *green* = unordered structures, *blue* = usually associated with β-sheets, but in the present case may be assigned to short extended chains connecting the helical segments).

The FTIR amide-I band of **226** at ambient pressure shows a narrow band at around 1672 cm^{-1}, usually associated with turn-like secondary structures (figure **25 A**). The broad band centered at around 1640 cm^{-1} is an overlapping component between unordered motifs (at 1638-45 cm^{-1}) and α-helical structures (1650-55 cm^{-1}). Since the H-bonding pattern in the foldamer is different from that of a traditional α-helix, differences in the wavenumbers are expected. For example, foldamer **226** likely forms 9/12/9/10 membered rings (compared with a 13 membered ring in an α-helix), thus the helical structure formed by **226** is probably tighter and so the wavenumber is expected to be lower (similar to a 3_{10}-helix which exhibits an IR band around 1641±3 cm^{-1}).[262] Upon pressurization, the broadening of the amide-I band suggests a loss of well-defined structural motifs, and shifting of the peak associated with turns to higher wavenumber suggests weakened H-bonding (figure **25 A**). The peak-position dependent quantitative fits of the amide-I band with pressure (figure **25 F**) reveals a reduction in the contribution of the band at 1650 and 1672 cm^{-1} (most likely: the loss of helical folds and turns), and a concomitant increase of the unordered structures (1636-1640 cm^{-1}). Figure **25 B** shows that the changes prompted by pressure are reversible. The temperature-dependent measurements reveal a similar trend for the turn-like structures, but the changes in the helical/unordered region show an opposite behavior (figure **25 C**). Temperature induces a narrowing of the amide band at the low wavenumber side and a minor shift in the peak position. This could again arise due to a different H-bonding pattern at higher temperatures (also indicative of changes in the conformational equilibrium), but the changes are reversible (figure **25 D**). Figure **25 E** shows the amide-I band in methanol is blue shifted compared with the aqueous solution (probably mainly owing to the different solvent composition). Due to

less effective H-donor abilities of methanol, a blue-shift by about 10 cm^{-1} in helical peptides has been reported.[264] In the present case, turn-like and helical structures exhibit shifts by 6 and 9 cm^{-1}, respectively. In addition, a change of solvent from methanol to water causes a hydrophobic-collapse leading to partial loss of helical geometry, also evident by the shape of the amide-I band. These results suggest that the broad band centered at 1640 cm^{-1} most likely reflects the conformational equilibrium between purely helical and partially collapsed conformations, which is changed reversibly by pressure, temperature and solvent.

In conclusion, both, NMR and IR measurements of α/β-peptide foldamer **226** indicate a partial unfolding of the helical conformation upon increasing pressure, which was shown to be of a reversible nature.

4.6.3 Temperature-dependent CD spectroscopy of foldamer 226

Circular dichroism (CD) spectroscopy has been shown to be an invaluable methodology for the analysis of secondary structures of proteins and peptides.[265] Although the characteristic CD signals for regular α-peptides do vary significantly from those of β-peptides or mixed α/β-peptide foldamers, CD has nevertheless been shown to be appropriate for conformational studies of the latter.[266, 267] CD spectroscopy under high-pressure conditions has been realized,[268] but unfortunately, due to limitations in the experimental setup such measurements could not be conducted in the present work. Nevertheless, variable temperature (VT) CD spectroscopy has the potential to reveal insights into the thermal stability of secondary structures and can also indicate changes in secondary structure upon the external stimulus. Furthermore, the obtained data from temperature-dependent CD can directly be compared to those from temperature-dependent FTIR spectroscopy (chapter **B 4.6.2**). The CD spectrum of α/β-peptide foldamer **226** in water shows a strong positive *Cotton* effect at 206 nm (figure **26**), which was assigned to a right-handed helix (confirmed by NMR solution structure and theoretical calculations).[256] In order to investigate the structural behavior of foldamer **226** under thermal 'stress', CD spectra of **226** in water at varying temperatures were collected and analyzed (figure **26**).
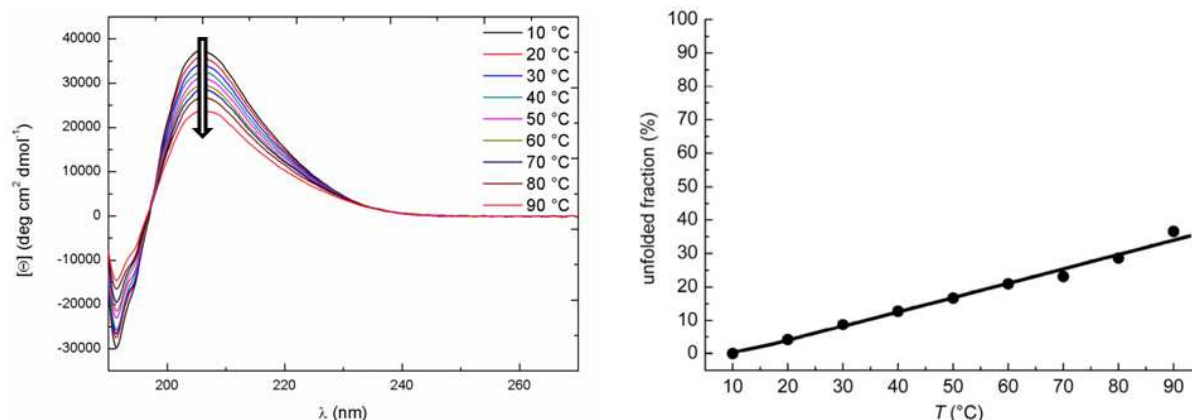
Figure 26. *Left:* Temperature-dependent circular dichroism spectra of peptide foldamer **226** in water at temperatures ranging from 10 °C to 90 °C (arrow indicates the decrease of molar ellipticity of the maximum at 206 nm with increasing temperature). *Right:* Thermal unfolding behavior of **226** based on the temperature-induced variation of the maximum at 206 nm. (Data from ref. [256]. Copyright: Wiley-VCH Verlag GmbH & Co. KGaA. Reproduced with permission).

As expected, the characteristic maximum at 206 nm decreases upon increasing temperature from 10 °C to 90 °C (*left part* in figure **26**). Plotting of the temperature-induced variation of the CD maximum at 206 nm against temperature reveals a linear behavior and gives insight into the thermal unfolding of foldamer **226**. In these experiments, a remarkably high helical stability of **226** with only 35% unfolding at 90 °C was discovered (*right part* of figure **26**). In analogy to the abovementioned structural features of **226** revealed by HP-NMR, HP-IR and VT-IR, the thermal unfolding behavior of foldamer **226** was also shown to be reversible by CD spectroscopy.

C Summary

Cyclopropanated heterocycles have been shown to be invaluable building blocks for the synthesis of a broad variety of natural products and other biologically relevant compounds. The first part of the present thesis describes the enantioselective cyclopropanation of furan and pyrrole derivatives, as well as their further transformations of the derived compounds. Furan-3-carboxylic acid methyl ester **91** was used as starting material for the total synthesis of (-)-Paeonilide **27**, however, only in 83% *ee*, as enantiopure material was not accessible at that time. In the course of this project an enantioselective cyclopropanation reaction of **91** was developed, which leads to cyclopropane **15** in > 99% *ee* and multi-gram quantity (scheme **50**).
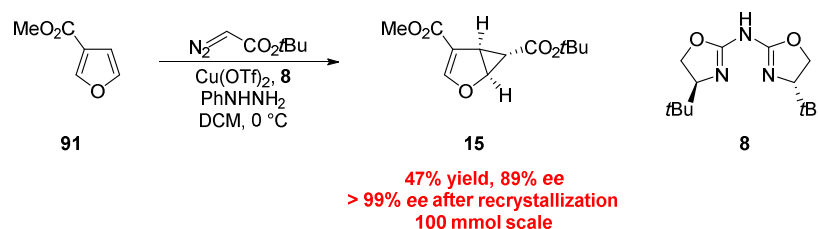
Scheme 50. Enantioselective cyclopropanation of furan-3-carboxylic acid methyl ester **91** on 100 mmol scale.

Key features for the success were the application of azabox ligand **8** as the chiral ligand and the modification of the ratio of catalyst to ligand from 1:1 to 1:2. On the other hand, cyclopropanation products of *N*-Boc-pyrrole **101**, which already have been applied for various synthetic endeavors, could not be accessed by enantioselective cyclopropanation so far. In the present work, a strategy for the enantioselective cyclopropanation of **101** with the use of *tert*-butyl diazoacetate as carbene source and again azabox ligand **8** was developed (scheme **51**).
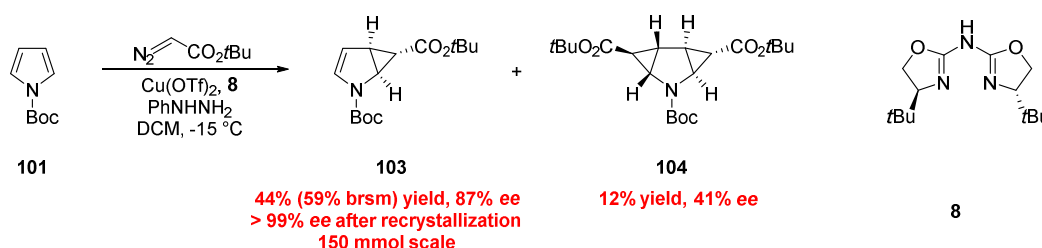
Scheme 51. Enantioselective cyclopropanation of *N*-Boc-pyrrole **101** on 150 mmol scale.

Cyclopropane **103** can be obtained in > 99% *ee* and multi-gram quantity, along with doubly cyclopropanated **104** (max. 41% *ee*). The application of *tert*-butyl diazoacetate and the ligand **8** turned out to be crucial for achieving high enantiomeric excess of the product. In the course of this project *tert*-butyl substituted azabox ligand **8** was identified to be superior to a great variety of other ligands for the asymmetric cylopropanation of both **91** and **101**. Cyclopropane **103** was applied for a short and efficient synthesis of the biologically active GABA analogue (*S*)-(+)-homo-β-proline **109** (scheme **52**).
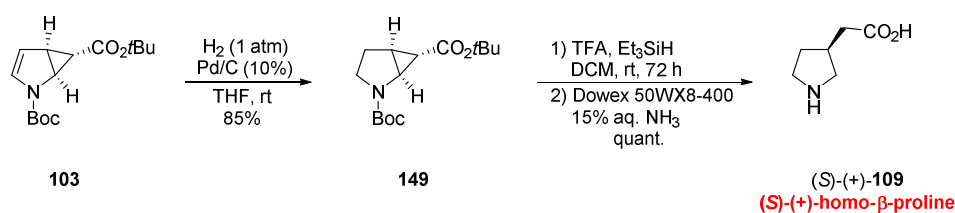
Scheme 52. Synthesis of (*S*)-(+)-homo-β-proline **109** from cyclopropane **103**.

Starting from *N*-Boc-pyrrole **101**, (*S*)-(+)-**109** could be prepared in three steps and 37% yield. However, the occurrence of epimerzation during the acid catalyzed cyclopropane ring opening step prohibited access to enantiomerically pure **109**.

In the second part of the present thesis the structural and conformational behavior of α/β-peptide foldamers were investigated by the application of high-pressure NMR (up to 2 kbar) and FTIR (up to 6.5 kbar) spectroscopic methods. Short tripeptides **217a** and **217b** containing a central cyclopropane amino acid, were analyzed in terms of their catalytic performance related to the application of pressure (figure **27**).
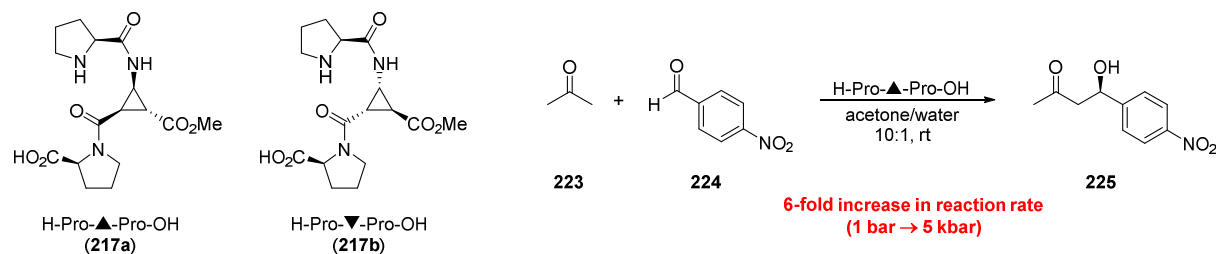
Figure 27. Chemical structures of tripeptide organocatalysts **217a** and **217b** for the intermolecular aldol reaction of acetone **223** and *para*-nitrobenzaldehyde **224**.

The fact that **217a** acts as a highly efficient organocatalyst for intermolecular aldol reactions, while its enantiomer **217b** gives poor results, led us to the investigation of this feature. A plausible model for explaining the discrepancy of catalytic performance of **217a** and **217b** was proposed. While **217b** shows clear indications for a strong internal hydrogen bond that separates the two catalytic functional groups, **217b** shows a significantly higher degree for flexibility that allows it for reaching an optimal conformation for catalysis. Experiments under high-pressure conditions revealed a sixfold increase in reaction rate upon a pressure jump from 1 bar to 5 kbar, but this was rather assigned to the general effect of pressure than to a change of the equilibrium of conformations of **217a**. In addition to short tripeptides **217a** and **217b**, the 13-residue α/β-peptide foldamer **226** was examined under variable pressure and temperature. Conformational studies by NMR, FTIR and CD spectroscopy revealed a partial unfolding of the helical structure of **226** at elevated pressures and temperatures, which was shown to be reversible.

D Zusammenfassung

Cyclopropanierte Heterocylen haben sich als unschätzbare Bausteine für die Synthese einer großen Vielfalt an Naturstoffen und anderen biologisch relevanten Molekülen bewährt. Der erste Teil der vorliegenden Arbeit behandelt die enantioselektive Cyclopropanierung von Furan- und Pyrrolderivaten, sowie die weitere Umsetzung der hierbei erhaltenen Verbindungen. Furan-3-carbonsäuremethylester **91** wurde als Grundlage für die Totalsynthese von (-)-Paeonilid **27** eingesetzt, jedoch nur in 83% *ee*, da enantiomerenreines **15** zum Zeitpunkt der Veröffentlichung noch nicht zugänglich war. Im Laufe dieser Arbeit wurde eine enantioselektive Cyclopropanierungsreaktion von **91** entwickelt, welche Cyclopropan **15** in > 99% *ee* und Multigrammmaßstab liefert (Schema **1**).
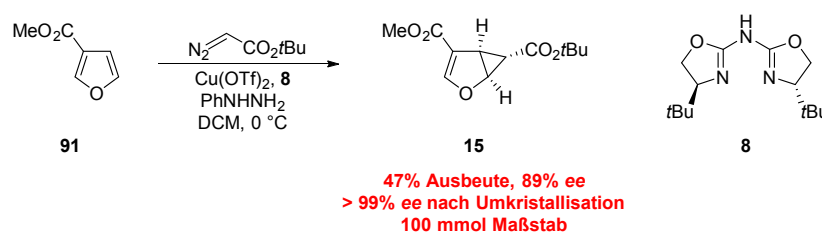
Schema 1. Enantioselektive Cyclopropanierung von Furan-3-carbonsäuremethylester **91** im 100 mmol Maßstab.

Die Kernpunkte für den Erfolg waren der Einsatz von Azabox Ligand **8** als chiralen Liganden, sowie die Veränderung des Verhältnisses von Katalysator zu Ligand von 1:1 zu 1:2. Neben Furanen sind auch die Cyclopropanierungsprodukte von Pyrrolen von Interesse, jedoch konnte bisher keine Möglichkeit zur asymmetrischen Cyclopropanierung von *N*-Boc-Pyrrol **101** gefunden werden. In der vorliegenden Arbeit wurde eine Strategie zur enantioselektiven Cyclopropanierung von **101** unter der Verwendung von *tert*-Butyldiazoester als Carbenquelle und wiederum **8** als chiralem Liganden entwickelt (Schema **2**).
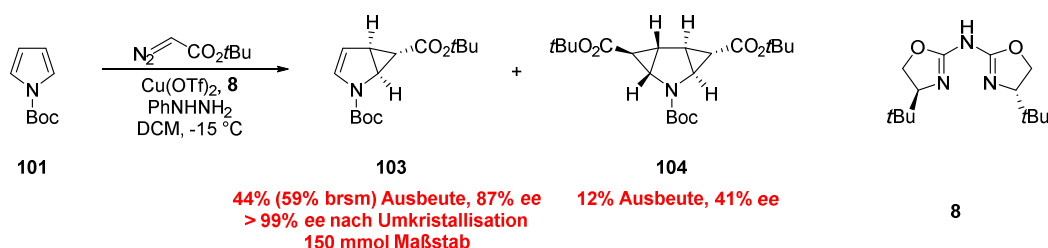
Schema 2. Enantioselektive Cyclopropanierung von *N*-Boc-Pyrrol **101** im 150 mmol Maßstab.

Cyclopropan **103** kann hierbei in > 99% *ee* und Multigrammmaßstab, zusammen mit doppelt cyclopropaniertem **104** (max. 41% *ee*) erhalten werden. An dieser Stelle erwies sich die Kombination von *tert*-Butyldiazoester und Ligand **8** als essentiell, um hohe Enantiomerenüberschüsse des Produktes **103** zu erhalten. Im Laufe dieser Untersuchungen kristallisierte sich der *tert*-Butyl substituierte Azabox Ligand **8** als herausragend für die asymmetrische Cyclopropanierung von **91** und **101** heraus. Desweiteren wurde Cyclopropan **103** für eine kurze und effiziente Synthese des biologisch aktiven GABA Analogons (*S*)-(+)-homo-β-Prolin **109** verwendet (Schema **3**).
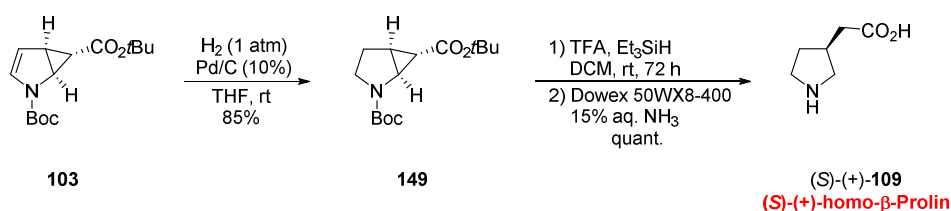
Schema 3. Synthese von (*S*)-(+)-homo-β-Prolin **109** ausgehend von Cyclopropan **103**.

Das Zielmolekül (*S*)-(+)-**109** konnte in nur drei Stufen und 37% Ausbeute ausgehend von *N*-Boc-Pyrrol **101** erhalten werden. Nichtdestotrotz verhinderte das Auftreten von Epimerisierung während der säurekatalysierten Cyclopropanöffnung die vollständig enantiomerenreine Darstellung von **109**.

Im zweiten Teil der vorliegenden Arbeit wurden die strukturellen und konformativen Eigenschaften von gemischten α/β-Peptidfoldameren unter Anwendung von Hochdruck-NMR (bis zu 2 kbar) und Hochdruck-IR (bis zu 6.5 kbar) Spektroskopie untersucht. Kurze Tripeptide mit einem zentralen Cyclopropanbaustein **217a** und **217b** wurden hierbei bezüglich ihrer katalytischen Aktivität unter dem Einfluss von Druck untersucht (Abbildung **27**).
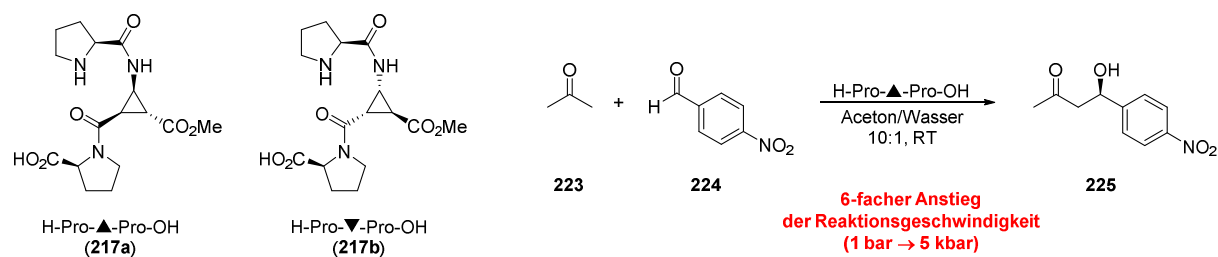
Abbildung 1. Chemische Strukturformeln von Tripeptid-Organokatalysatoren **217a** und **217b** für die intermolekulare Aldolreaktion von Aceton **223** und *para*-Nitrobenzaldehyd **224**.

Die Tatsache, dass **217a** ein hocheffizienter Organokatalysator für intermolekulare Aldolreaktionen ist, während sein Enantiomer **217b** nur mäßigen Erfolg einbringt, wurde als Grundlage für die Untersuchungen dieser Arbeit genommen. Ein plausibles Modell für die Erklärung des unterschiedlichen katalyischen Verhaltens von **217a** und **217b** wurde hierin vorgestellt. Während **217b** klare Anzeichen für eine starke interne Wasserstoffbrücke zeigt, welche die beiden für die Katalyse notwendigen funktionellen Gruppen räumlich separiert, ist sein Isomer **217a** deutlich flexibler und kann dadurch leichter eine ideale Konformation für die Katalyse erreichen. Katalysen unter Hochdruckbedingungen zeigen einen sechsfachen Anstieg der Reaktionsgeschwindigkeit bei einem Druckanstieg von 1 bar nach 5 kbar, was jedoch eher auf den generellen Einfluss des Drucks, als eine Änderung des Konformationsgleichgewichts von **217a** zurückzuführen ist. Zusätzlich zu den kurzen Tripeptiden **217a** und **217b** wurde auch ein längeres α/β-Peptidfoldamer (13 Aminosäurebausteine) unter druck- und temperaturabhängigen Bedingungen untersucht. Konformative Untersuchungen mittels NMR, FTIR und CD Spektroskopie zeigen eine partielle Entfaltung der helikalen Struktur von **226** bei hohen Drücken und Temperaturen, welche aber reversibel ist.

E Experimental part

1 Instruments and general techniques

^{1}H-NMR spectra were recorded on Bruker Avance 300 (300 MHz), Bruker Avance 400 (400 MHz) and Bruker Avance III 600 TCI Cryo (600 MHz). The chemical shifts are reported in δ (ppm) relative to chloroform (CDCl$_3$, 7.26 ppm), methanol-d_3 or methanol-d_4 (CD$_3$OH, 3.34 ppm). The spectra were analyzed by first order, the coupling constants (J) are reported in Hertz (Hz). Characterization of the signals: s = singlet, bs = broad singlet, d = dublet, t = triplet, q = quartet, quin = quintet, m = multiplet, dd = double dublet, ddd = double double dublet, dt = double triplet, dquin = double quintet, po = pseudo octet. Integration is determined as the relative number of atoms.

^{13}C-NMR spectra were recorded on Bruker Avance 300 (75.5 MHz) and Bruker Avance 400 (100.6 MHz). The chemical shifts are reported in δ (ppm) relative to chloroform (CDCl$_3$, 77.0 ppm) or methanol-d_4 (MeOD, 49.0 ppm). ^{13}C-NMR resonance assignment was aided by the use of HSQC, DEPT 135 and DEPT 90 techniques (DEPT = distorsionless enhancement by polarization transfer) to determine the number of hydrogens attached to each carbon atom and is declared as: + = primary or tertiary (CH$_3$, CH, positive DEPT signal), - = secondary (CH$_2$, negative DEPT signal), Cq = quarternary (no DEPT signal) carbon atoms.

High-pressure NMR was performed on Bruker Avance 800 (800 MHz) in the group of Prof. H. R. Kalbitzer in the Institute of Biophysics and Physical Biochemistry at the University of Regensburg. A ceramic cell containing the sample solution was inserted into a titanium autoclave and external pressure was applied via a flexible polyethylene terephthalate (PET) membrane and water as compression fluid. Pressure was generated and maintained via a manually operated piston compressor. For a detailed description of the experimental setup see: [258]

Infrared spectroscopy (IR) in form of ATR-IR spectroscopy was carried out on a Biorad Excalibur FTS 3000 spectrometer, equipped with a Specac Golden Gate Diamond Single Reflection ATR-System. Pressure- and temperature dependent FTIR spectra were collected by

Prof. Roland Winter in the Faculty of Chemistry and Chemical Biology at the TU Dortmund. A diamond anvil cell served as the reaction vessel for the measurements. For a detailed description of the experimental setup see: [269]

Mass spectrometry (MS) was performed in the Central Analytic Department of the University of Regensburg on Finnigan MAT 95, ThermoQuest Finnigan TSQ 7000, Agilent Q-TOF 6540 UHD and Finnigan MAT SSQ 710 A.

Elemental analysis was measured on a Vario EL III or Mikro-Rapid CHN (Heraeus) (Microanalytic section of the University of Regensburg).

Optical rotations were determined in a Perkin Elmer 241 polarimeter at 589 nm wavelength (sodium-*d*-line) in a 1.0 dm measuring cell and the specified solvent.

Lyophilization was carried out with a Christ alpha 2-4 LD equipped with a vacuubrand RZ 6 rotary vane vacuum pump.

X-ray analysis of single crystals was performed in the X-ray crystallographic Department of the University of Regensburg on Agilent Technologies SuperNova, Agilent Technologies Gemini R Ultra or Stoe IPDS I.

High performance liquid chromatography (HPLC). Analytical HPLC was performed on a Varian 920-LC with DAD. Phenomenex Lux Cellulose-1 and 2, Chiralcel OD-H and AS served as chiral stationary phase, and mixtures of *n*-heptane and *i*PrOH were used for elution.

Thin layer chromatography (TLC) was performed on alumina plates coated with silica gel (Merck silica gel 60 F 254, d = 0.2 mm). Visualization was accomplished by UV light (λ = 254 nm or 366 nm), iodine, ninhydrin/acetic acid solution, vanillin/sulfuric acid solution, potassium permanganate solution, *Seebach's Magic Stain*, or *Dragendorff-Munier* reagent.

Circular dichroism spectroscopy (CD) was performed on a JASCO model J-710/720 at temperatures between 10 °C and 90 °C and wavelengths between 280 and 190 nm in water, by using the following parameters: 0.2 nm resolution, 1.0 nm band width, 100 mdeg sensitivity, 0.25 s response, 20 nm/min speed, 5 scans. The length of the cuvette was 1.0 mm. The CD spectrum of the sole solvent was recorded and subtracted from the raw data. The peptide concentration of the samples was 1 mM. The CD intensity is given as mean-residue molar ellipticity (deg cm^2 dmol^{-1}).

Molecular modeling. Molecular mechanical simulations were carried out using the *Wavefunctions Spartan 06* programme. For the conformational searches and energy calculations, the *Tripos Sybyl* force field was used. Six rotatable backbone bonds of tripeptides **217a** and **217b** were used, leading to 324 conformations each that were subsequently minimized in energy for both conformers. The resulting low energy structures were then sorted and analyzed.

Solvents and chemicals. DCM, ethyl acetate and hexanes (petroleum ether, PE (60/40)) were distilled prior to use for column chromatography. Dry solvents were prepared according to standard procedures. Commercially available chemicals were used as received, without further purification. A saturated solution of HCl in ethylacetate was prepared by inserting gaseous HCl (predried wit conc. H_2SO_4) into a cooled solution of dry ethylacetate. The concentration of the solution was determined by titration against NaOH (1 M) with bromothymol blue as indicator to be 4.2 M. The solution was stored under nitrogen atmosphere at -20 °C.

High-pressure reactions up to 5 kbar were performed using a self-made hydraulic high-pressure apparatus from Unipress (Warsaw) using melted polytetrafluororethylene (PTFE) tubes as reaction vessels. A 1:1 (v/v) mixture of decahydronaphthalene (decalin, *cis/trans* mixture) and 2,2,4-trimethylpentane (*iso*-octane) was used as pressurizing medium.

2 Synthesis of compounds

Following compounds were synthesized according to literature known procedures and spectroscopic data matched well with those reported:

4-Methylbenzenesulfonyl azide (tosyl azide),[270] methyl-2-diazoacetate,[271] ethyl-2-diazoacetate,[272] (*S*)-2-amino-3,3-dimethylbutan-1-ol ((*S*)-*tert*-leucinol **70**),[88] (*S*)-2-amino-3-methylbutan-1-ol ((*S*)-valinol),[89] (*S*)-4-isopropyl-4,5-dihydrooxazol-2-amine,[62] (*S*)-4-isopropyloxazolidin-2-one,[63] (*S*)-2-ethoxy-4-isopropyl-4,5-dihydrooxazole **75**,[63] 2-iodoxybenzoic acid (IBX).[273]

Azabox ligands other than **8**, **9**, **60** and **74** were either on stock in the laboratory or were prepared in analogy to the described synthesis of **8** (main part chapter **B 1.1**, scheme **7**), following the improved methodology of ref. [63].

N_2 CO$_2$*t*Bu
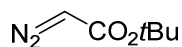
tert-Butyl-2-diazoacetate[274]

n-Pentane (900 ml) was cooled to 0 °C and *tert*-butyl acetoacetate (52.8 ml, 318 mmol, 1.0 equiv), tosyl azide (62.6 g, 318 mmol, 1.0 equiv), and TBAB (2.05 g, 6.46 mmol, 0.02 equiv) were added. The mixture was treated with a precooled solution of NaOH (36 g in 300 ml water, 0.9 mol, 2.8 equiv) over a period of 15 min. Afterwards, the cooling bath was removed and the solution was stirred for 15 h at room temperature. The reaction mixture was then filtered through a plug of Celite to remove precipitates and the filtrate was transferred into a separating funnel. After separation of the phases the aqueous layer was extracted with *n*-pentane (3 x). The combined organic layers were washed with water (2 x) and brine (1 x), dried over Na$_2$SO$_4$ and finally concentrated under reduced pressure (15 °C water bath) to yield the title compound *tert*-butyl-2-diazoacetate (43.3 g, 308 mmol, 96%) as a yellow oil that was diluted with DCM to the required concentration.

^{1}H-NMR (300 MHz, CDCl$_3$): δ_H (ppm) = 1.48 (s, 9 H), 4.61 (s, 1 H).
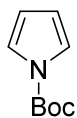
tert-Butyl-1*H*-pyrrole-1-carboxylate (**101**)[241]

N-Boc protected pyrrole **101** was synthesized following a slightly modified procedure of *Grehn et al*. Freshly distilled pyrrole **50** (68.0 g, 1.01 mol, 1.0 equiv) was dissolved in DCM (450 ml) and DMAP (9.9 g, 0.08 mol, 0.08 equiv) was added. Boc$_2$O (246.3 g, 1.13 mol, 1.1 equiv) was adde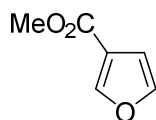d portionwise and the mixture was stirred at room temperature until gas evolution stopped (48 h). The reaction mixture was treated with DEAEA (38 ml, 0.27 mol, 0.3 equiv) and stirred for further 30 min. Afterwards, the reaction mixture was concentrated to half its volume, washed with KHSO$_4$ (1 M, 3 x), NaHCO$_3$ (sat., 1 x), and the organic layer was dried over Na$_2$SO$_4$. After evaporation of the solvent, the crude residue was distilled under reduced pressure to yield **101** (139.6 g, 0.83 mol, 82%) as a colorless liquid.

R$_f$ = 0.60 (PE/EA = 5:1) – **^{1}H-NMR** (300 MHz, CDCl$_3$): δ$_H$ (ppm) = 1.60 (s, 9 H), 6.20-6.23 (m, 2 H), 7.22-7.25 (m, 2 H). – **bp** = 80 °C/8 hPa.

Methyl-furan-3-carboxylate (**15**)[45]

Furan-3-carboxylic acid **88** (10.0 g, 89.2 mmol, 1.0 equiv) was dissolved in MeOH (45 ml) and cooled to 0 °C. H$_2$SO$_4$ (conc., 10 ml) was added dropwise and the solution was stirred overnight at room temperature. The mixture was treated with water and extracted with Et$_2$O (3 x). The combined organic layers were washed with NaHCO$_3$ (sat., 1 x), dried over Na$_2$SO$_4$ and concentrated under reduced pressure. The crude residue was distilled under reduced pressure to yield **15** (7.8 g, 61.7 mmol, 69%) as a colorless liquid.

R$_f$ = 0.69 (PE/EA = 3:1) – **^{1}H-NMR** (300 MHz, CDCl$_3$): δ$_H$ (ppm) = 3.84 (s, 3 H), 6.74 (dd, 1 H, *J* = 1.9 Hz, 0.8 Hz), 7.41-7.43 (m, 1 H), 8.00-8.02 (m, 1 H). – **bp** = 55 °C/8 hPa.
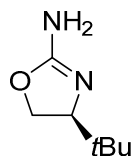
(*S*)-4-(*tert*-Butyl)-4,5-dihydrooxazol-2-amine (**71**)[62]

NaCN (2.57 g, 52.42 mmol, 1.05 equiv) was added portionwise to solution of Br_2 (2.69 ml, 52.42 mmol, 1.05 equiv) in MeOH (40 ml) at 0 °C. To that solution a solution of **70** (5.85 g, 49.92 mmol, 1.0 equiv) in MeOH (80 ml) was added and the mixture was stirred at 0 °C for 1 h. Aqueous ammonia (25% (m/m), 25 ml) was added and the mixture was concentrated in vacuo. The resulting residue was treated with NaOH (20% (m/m), 50 ml) and extracted with EA (4 x, 60 ml). After drying over $MgSO_4$ and filtration, the solvent was evaporated under reduced pressure to give **71** (5.17 g, 36.39 mmol, 73%) as a white solid.

R$_f$ = 0.04 (PE/EA = 2:1) – **^{1}H-NMR** (300 MHz, $CDCl_3$): δ_H (ppm) = 0.87 (s, 9 H), 2.75 (bs, 2 H), 3.74 (dd, 1 H, *J* = 9.3 Hz, 7.1 Hz), 4.07 (dd, 1 H, *J* = 8.3 Hz, 7.1 Hz), 4.22 (dd, 1 H, *J* = 9.2 Hz, 8.3 Hz).
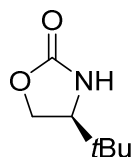
(*S*)-4-(*tert*-Butyl)oxazolidin-2-one (**72**)[63]

Sodium metal (0.58 g, 25.60 mmol, 1.0 equiv) was dissolved in EtOH (37 ml), the solution was treated with aminoalcohol **70** (3.00 g, 25.60 mmol, 1.0 equiv) and diethylcarbonate (3.41 ml, 28.16 mmol, 1.1 equiv), and the mixture was refluxed for 20 h. The solution was then concentrated under reduced pressure, treated with DCM and NH_4Cl (sat.), and extracted with DCM (2 x). After drying over $MgSO_4$ and filtration the solvent was evaporated under reduced pressure to give a white solid that was recrystallized from Et_2O to yield **72** (3.00 g, 20.93 mmol, 82%) as a white solid.

R_f = 0.15 (PE/EA = 2:1) – **¹H-NMR** (300 MHz, CDCl$_3$): δ_H (ppm) = 0.91 (s, 9 H), 3.59 (ddd, 1 H, J = 8.9 Hz, 5.8 Hz, 0.9 Hz), 4.20 (dd, 1 H, J = 9.0 Hz, 5.8 Hz), 4.34-4.41 (m, 1 H), 5.71 (bs, 1 H).
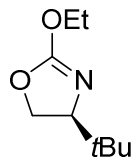
(*S*)-4-(*tert*-Butyl)-2-ethoxy-4,5-dihydrooxazole (**73**)[63]

A solution of oxazolidinone **72** (1.73 g, 12.06 mmol, 1.0 equiv) in dry DCM (15 ml) was cooled to 0 °C and a solution of triethyloxonium tetrafluoroborate (2.75 g, 14.47 mmol, 1.2 equiv) in DCM (9 ml) was added dropwise. The reaction was allowed to warm to room temperature and was stirred for 44 h. The reaction mixture was then poured into an ice-cold solution of Na$_2$CO$_3$ (50 ml) and extracted with DCM (3 x). After drying over Na$_2$SO$_4$ and filtration the solvent was evaporated under reduced pressure to give **73** (1.94 g, 11.33 mmol, 94%) as a pale yellow oil that was used without further purification.

R_f = 0.67 (PE/EA = 2:1) – **¹H-NMR** (300 MHz, CDCl$_3$): δ_H (ppm) = 0.88 (s, 9 H), 1.35 (t, 3 H, J = 7.1 Hz), 3.76 (dd, 1 H, J = 9.4 Hz, 6.7 Hz), 4.18 (dd, 1 H, J = 8.5 Hz, 6.7 Hz), 4.23-4.34 (m, 3 H).
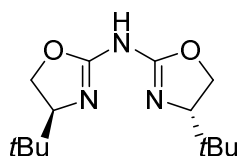
(*S*)-Bis((*S*)-4-(*tert*-butyl)-4,5-dihydrooxazol-2-yl)amine (**8**)[63]

Ethoxyoxazoline **73** (1.94 g, 11.33 mmol, 1.2 equiv) was dissolved in dry toluene (20 ml) and aminooxazoline **71** (1.34 g, 9.44 mmol, 1.0 equiv) was added. After addition of *p*-TSA (163 mg, 0.94 mmol, 0.1 equiv) the reaction mixture was refluxed under nitrogen for 16 h. The crude mixture was concentrated under reduced pressure and purified via flash chromatography (silica, PE/EA = 1:9) to yield **8** (2.27 g, 8.50 mmol, 90%) as a colorless crystalline solid that can be recrystallized from acetone.

R_f = 0.33 (EA) – **^{1}H-NMR** (300 MHz, CDCl$_3$): δ_H (ppm) = 0.86 (s, 18 H), 3.77 (dd, 2 H, J = 9.4 Hz, 6.7 Hz), 4.11 (dd, 2 H, J = 8.8 Hz, 6.6 Hz), 4.21-4.31 (m, 2 H), 8.61 (bs, 1 H). – **^{13}C-NMR** (101 MHz, CDCl$_3$): δ_C (ppm) = 25.3 (+, CH$_3$), 33.6 (Cq), 67.4 (-, CH$_2$), 68.7 (+, CH), 165.9 (Cq).
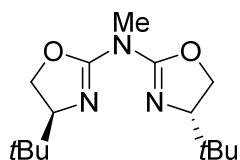
(*S*)-4-(*tert*-Butyl)-*N*-((*S*)-4-(*tert*-butyl)-4,5-dihydrooxazol-2-yl)-*N*-methyl-4,5-dihydrooxazol-2-amine (**9**)[62]

Ligand **8** (300 mg, 1.12 mmol, 1.0 equiv) was dissolved in dry THF (10 ml) and cooled to -78 °C. *n*BuLi (1.6 M solution in *n*-hexane; 769 µl, 1.23 mmol, 1.1 equiv) was added slowly and the solution was stirred for 20 min at -78 °C, before MeI (351 µl, 5.61 mmol, 5.0 equiv) was added and the reaction was stirred in the defrosting cooling bath overnight (17 h). Volatiles were removed in vacuo and the residue was treated with DCM and NaHCO$_3$ (sat.). After phase separation the aqueous layer was extracted with DCM (3 x) and the organic layer was dried over MgSO$_4$. Evaporation of the solvent yielded pure **9** (269 mg, 0.96 mmol, 85%) as a white solid.

R_f = 0.18 (PE/EA = 1:2) – **^{1}H-NMR** (300 MHz, CDCl$_3$): δ_H (ppm) = 0.88 (s, 18 H), 3.41 (s, 3 H), 3.79 (dd, 2 H, J = 9.5 Hz, 6.7 Hz), 4.23 (dd, 2 H, J = 8.5 Hz, 6.7 Hz), 4.34 (dd, 2 H, J = 9.4 Hz, 8.6 Hz). – **^{13}C-NMR** (101 MHz, CDCl$_3$): δ_C (ppm) = 25.5 (+, CH$_3$), 34.0 (Cq), 37.4 (+, CH$_3$), 70.3 (-, CH$_2$), 73.2 (+, CH), 157.8 (Cq).
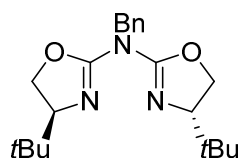
(S)-N-Benzyl-4-(tert-butyl)-N-((S)-4-(tert-butyl)-4,5-dihydrooxazol-2-yl)-4,5-dihydrooxazol-2-amine (**74**)[11]

Ligand **8** (276 mg, 1.03 mmol, 1.0 equiv) was dissolved in dry THF (10 ml) and cooled to -78 °C. *n*BuLi (1.6 M solution in *n*-hexane; 644 µl, 1.03 mmol, 1.0 equiv) was added slowly and the solution was stirred for 20 min at -78 °C, before BnBr (122 µl, 1.03 mmol, 1.0 equiv) was added and the reaction was stirred in the defrosting cooling bath overnight (20 h). Volatiles were removed in vacuo and the residue was treated with DCM and $NaHCO_3$ (sat.). After phase separation the aqueous layer was extracted with DCM (3 x) and the organic layer was dried over $MgSO_4$. Evaporation of the solvent yielded pure **74** (357 mg, 1.00 mmol, 97%) as a white solid.

^{1}H-NMR (300 MHz, $CDCl_3$): δ_H (ppm) = 0.73 (s, 18 H), 3.74 (dd, 2 H, J = 9.5 Hz, 6.6 Hz), 4.15 (dd, 2 H, J = 8.5 Hz, 6.5 Hz), 4.24-4.29 (m, 2 H), 4.91 (d, 1 H, J = 15.0 Hz), 5.10 (d, 1 H, J = 15.0 Hz), 7.12-7.27 (m, 3 H), 7.35-7.40 (m, 2 H). – **^{13}C-NMR** (101 MHz, $CDCl_3$): δ_C (ppm) = 25.4 (+, CH_3), 34.0 (Cq), 53.2 (-, CH_2), 70.1 (-, CH_2), 73.4 (+, CH), 127.1 (+, CH), 128.1 (+, CH), 137.8 (Cq), 157.2 (Cq).
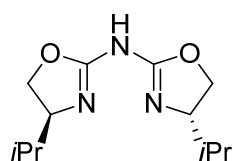
(S)-Bis((S)-4-*iso*-propyl-4,5-dihydrooxazol-2-yl)amine (**60**)

Ethoxyoxazoline **75** (297 mg, 1.89 mmol, 2.0 equiv) was dissolved in dry MeOH (5 mL) under a nitrogen atmosphere. A solution of gaseous NH_3 in MeOH (7 M, 0.14 ml, 0.95 mmol, 1.0 equiv) was added slowly and the reaction mixture was heated to 80 °C for 24 h. The reaction mixture was allowed to cool to ambient temperature and was then extracted with

---

[11] Ligand **74** was prepared in analogy to **9**, with benzyl bromide as alkylating agent. So far, different methods have been employed for the synthesis of **74** in literature.

DCM (3 x). The organic layers were dried over Na_2SO_4, filtered and the solvent was evaporated under reduced pressure. The crude mixture was purified via flash chromatography (silica, EA) to yield azabox **60** (36 mg, 0.15 mmol, 16%) as a colorless crystalline solid.

R$_f$ = 0.35 (EA) – **^{1}H-NMR** (300 MHz, CDCl$_3$): δ$_H$ (ppm) = 0.88 (d, 6 H, J = 6.8 Hz), 0.96 (d, 6 H, J = 6.7 Hz), 1.70 (po, 2 H, J = 6.7 Hz), 3.75-3.85 (m, 2 H), 4.03 (dd, 2 H, J = 8.5 Hz, 7.1 Hz), 4.32-4.51 (m, 2 H), 8.47 (bs, 1 H). – **^{13}C-NMR** (75 MHz, CDCl$_3$): δ$_C$ (ppm) = 18.1 (+, CH$_3$), 18.7 (+, CH$_3$), 33.0 (+, CH), 65.4 (+, CH), 69.4 (-, CH$_2$), 165.8 (Cq).
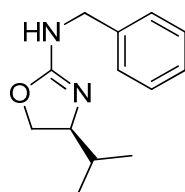
(*S*)-*N*-Benzyl-4-*iso*-propyl-4,5-dihydrooxazol-2-amine (**82**)

To a solution of **75** (300 mg, 1.89 mmol, 2.0 equiv) in dry toluene *p*-TSA (16 mg, 0.09 mmol, 0.1 equiv) and *N*-benzylamine (103 µl, 0.95 mmol, 1.0 equiv) were added and the mixture was heated to reflux for 1.5 h. The solvent was evaporated and the crude mixture was purified via flash chromatography (silica, EA) to yield **82** (174 mg, 0.80 mmol, 84%) as colorless crystals.

R$_f$ = 0.17 (PE/EA = 1:1) – **^{1}H-NMR** (300 MHz, CDCl$_3$): δ$_H$ (ppm) = 0.79 (d, 3 H, J = 6.7 Hz), 0.87 (d, 3 H, J = 6.7 Hz), 1.62 (po, 1 H, J = 6.7 Hz), 3.68-3.78 (m, 1 H), 3.89 (dd, 1 H, J = 7.9 Hz, 6.8 Hz), 4.17 (dd, 1 H, J = 8.7 Hz, 8.1 Hz), 4.29 (d, 1 H, J = 14.8 Hz), 4.36 (d, 1 H, J = 14.8 Hz), 4.90 (bs, 1 H), 7.16-7.33 (m, 5 H). – **^{13}C-NMR** (101 MHz, CDCl$_3$): δ$_C$ (ppm) = 17.8 (+, CH$_3$), 18.9 (+, CH$_3$), 33.2 (+, CH), 47.0 (-, CH$_2$), 70.0 (+, CH), 70.4 (-, CH$_2$), 127.2 (+, CH), 127.4 (+, CH), 128.5 (+, CH), 139.1 (Cq), 160.5 (Cq). – **mp** = 95 °C. – **IR** (neat): ṽ (cm^{-1}) = 3230, 3027, 2954, 2879, 1643, 1552, 1494, 1454, 1348, 1286, 1242, 1113, 1078, 1027, 974, 935, 729, 694, 585, 458. – [α]$_D^{20}$ = -38.3 (*c* = 1, DCM). – **LRMS** (ESI): *m/z* = 219.1 [M+H]$^+$. – **HRMS** (ESI): *m/z* = 219.1493 [M+H]$^+$; calc. for [C$_{13}$H$_{19}$N$_2$O]$^+$ = 219.1492.

General procedure for small scale cyclopropanations of furan-3-carboxylic acid methyl ester 91 (GP-1):

Under nitrogen atmosphere a flame dried flask was charged with Cu(OTf)$_2$ (14.3 mg, 0.04 mmol, 0.01 equiv) and ligand (0.09 mmol, 0.022 equiv) in dry DCM (1 ml) and stirred for 30 minutes at room temperature. In a second flask under nitrogen atmosphere a solution of 3-methyl furoate **91** (500 mg, 3.97 mmol, 1.0 equiv) in dry DCM (2 ml) was prepared. This flask was cooled to the specified temperature and the solution of flask one was added in one portion through a syringe filter. A 5% (v/v) solution of phenylhydrazine in DCM (78 µl, 0.04 mmol, 0.01 equiv) was added to the reaction mixture. *tert*-Butyldiazoacetate (solution in DCM; 1.5 equiv) was added by syringe pump. The mixture was stirred overnight, filtered through basic alumina and washed with DCM (200 ml). The solvent was evaporated in vacuo and the crude product was purified by flash chromatography (silica, PE/EA = 15:1) to provide **15** as a white solid that was recrystallized from *n*-pentane or *n*-heptane.

Cyclopropanation reactions on larger scale were performed according to **GP-1** with the exception that an electronically controlled dropping system was applied for the addition of larger amounts of the diazo compound, and PhNHNH$_2$ was added in pure form.
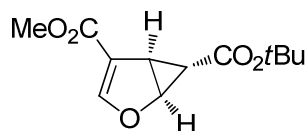
 (1*S*,5*R*,6*S*)-6-*tert*-Butyl-4-methyl-2-oxabicyclo[3.1.0]hex-3-ene-4,6-dicarboxylate ((*S*,*R*,*S*)-(-)-**15**)

According to **GP-1 91** (12.91 g, 102.37 mmol, 1.0 equiv) was cyclopropanated with *tert*-butyldiazoacetate (171 g, 12.8 wt%, 1.5 equiv), Cu(OTf)$_2$ (370 mg, 1.02 mmol, 0.01 equiv), ligand **8** (602 mg, 2.25 mmol, 0.022 equiv) and neat PhNHNH$_2$ (101 µl, 1.02 mmol, 0.01 equiv) in dry DCM (75 ml) to yield **15** (11.56 g, 448.13 mmol, 47%) as white solid.

R$_f$ = 0.30 (PE/EA = 15:1) – **^{1}H-NMR** (300 MHz, CDCl$_3$): δ_H (ppm) = 1.00-1.04 (m, 1 H), 1.42 (s, 9 H), 3.00 (dd, 1 H, *J* = 5.6 Hz, 2.9 Hz), 3.73 (s, 3 H), 4.90-4.94 (m, 1 H), 7.16 (s, 1 H). – **^{13}C-NMR** (101 MHz, CDCl$_3$): δ_C (ppm) = 22.5 (+, CH), 28.1 (+, CH$_3$), 29.1, (+, CH), 51.5 (+, CH$_3$), 68.9 (+, CH), 81.4 (Cq), 115.8 (Cq), 156.4 (+, CH), 164.2 (Cq), 170.8 (Cq). –

mp = 76 °C (*Lit.:* 72 °C) – **IR** (neat): ṽ (cm^{-1}) = 3109, 3062, 2976, 1699, 1598, 1444, 1367, 1323, 1269, 1158, 1097, 1044, 974, 830, 792, 760, 720, 663, 558, 509, 468, 425. – $[\alpha]_D^{20}$ = **-27.2** (*c* = 1, DCM, > 99% *ee*) (*Lit.:* -20.5 (*c* = 1, DCM, 83% *ee*)[45]). – **HPLC analysis** (Phenomenex Lux Cellulose-2, *n*-heptane/*i*PrOH 99:1, 1.0 ml/min, 254 nm): t_r = 13.81 min, t_r = 19.50 min; > 99% *ee*. – **LRMS** (ESI): *m/z* = 185.0 [M+H-C$_4$H$_8$]$^+$, 241.1 [M+H]$^+$, 258.1 [M+NH$_4$]$^+$, 263.1 [M+Na]$^+$. – **HRMS** (ESI): *m/z* = 241.1074 [M+H]$^+$; calc. for [C$_{12}$H$_{17}$O$_5$]$^+$ = 241.1071.

General procedure for small scale cyclopropanations of *N*-Boc-pyrrole 101 (GP-2):

Under nitrogen atmosphere a flame dried flask was charged with Cu(OTf)$_2$ (10.8 mg, 0.03 mmol, 0.01 equiv) and ligand (0.06 mmol, 0.022 equiv) in dry DCM (1 ml) and stirred for 30 minutes at room temperature. In a second flask under nitrogen atmosphere a solution of *N*-Boc-pyrrole **101** (500 mg, 2.99 mmol, 1.0 equiv) in dry DCM (2 ml) was prepared. This flask was cooled to the specified temperature and the solution of flask one was added in one portion through a syringe filter. A 5% (v/v) solution of phenylhydrazine in DCM (59 µl, 0.03 mmol, 0.01 equiv) was added to the reaction mixture. *tert*-Butyldiazoacetate (solution in DCM; 1.5 equiv) was added by syringe pump. The mixture was stirred overnight, filtered through basic alumina and washed with DCM (200 ml). The solvent was evaporated in vacuo and the crude product was purified by flash chromatography (silica, PE/EA = 50:1) to provide **103** as a white solid that was recrystallized from PE.

Cyclopropanation reactions on larger scale were performed according to **GP-2** with the exception that an electronically controlled dropping system was applied for the addition of larger amounts of the diazo compound, and PhNHNH$_2$ was added in pure form.
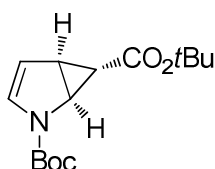
(1*S*,5*S*,6*S*)-di-*tert*-Butyl-2-azabicyclo[3.1.0]hex-3-ene-2,6-dicarboxylate ((*S*,*S*,*S*)-(-)-**103**)

According to **GP-2 101** (25.20 g, 150.60 mmol, 1.0 equiv) was cyclopropanated with *tert*-butyldiazoacetate (32.0 g, 11.1 wt%, 1.5 equiv), Cu(OTf)$_2$ (543 mg, 1.51 mmol, 0.01 equiv), ligand **8** (885 mg, 3.31 mmol, 0.022 equiv) and neat PhNHNH$_2$ (148 μl, 1.51 mmol, 0.01 equiv) in dry DCM (30 ml) at -15 °C to yield **103** (18.64 g, 66.26 mmol, 44%) as white solid. In addition, starting material **101** (3.78 g, 22.59 mmol, 15%) could be reisolated.

R$_f$ = 0.45 (PE/EA = 10:1) – **^{1}H-NMR** (300 MHz, CDCl$_3$): δ$_H$ (ppm) = 0.87-0.88 (m, 1 H), 1.41 (s, 9 H, CH_3), 1.47 (s, 9 H, CH_3), 2.62-2.75 (m, 1 H), 4.12-4.40 (m, 1 H), 5.24-5.40 (m, 1 H), 6.32-6.58 (m, 1 H). – **^{13}C-NMR** (101 MHz, CDCl$_3$): δ$_C$ (ppm) = 23.9 (+, CH), 28.1 (+, CH$_3$), 28.2 (+, CH$_3$), 30.6 + 31.6 (+, CH), 43.7 + 44.0 (+, CH), 80.6 (Cq), 81.5 (Cq), 110.0 (+, CH), 129.4 + 129.6 (+, CH), 151.0 + 151.3 (Cq, CO), 172.0 +172.3 (Cq, CO). Signal doubling due to rotamers. – **mp** = 77-79 °C – **IR** (neat): ṽ (cm^{-1}) = 2978, 2934, 1703, 1590, 1454, 1391, 1367, 1346, 1292, 1248, 1135, 1018, 930, 866, 831, 759, 721, 547, 468. – $[α]_D^{20}$ = -253.0 (*c* = 1, DCM, > 99% *ee*) – **Elemental analysis** calcd. (%) for C$_{15}$H$_{23}$NO$_4$ (281.16): C 64.03, H 8.24, N 4.98, found: C 64.03, H 8.22, N 4.73. – **HPLC analysis** (Phenomenex Lux Cellulose-2, *n*-heptane/*i*PrOH 98:2, 0.5 ml/min, 254 nm): t$_r$ = **11.25 min**, t$_r$ = 19.86 min; > 99% *ee*. – **LRMS** (ESI): *m/z* = 282.2 [M+H]$^+$, 304.2 [M+Na]$^+$. – **HRMS** (ESI): *m/z* = 282.1704 [M+H]$^+$; calc. for [C$_{15}$H$_{24}$NO$_4$]$^+$ = 282.1700.
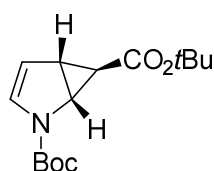
(1*R*,5*R*,6*R*)-di-*tert*-Butyl-2-azabicyclo[3.1.0]hex-3-ene-2,6-dicarboxylate ((*R,R,R*)-(+)-**103**)

Compound (*R,R,R*)-(+)-**103** was prepared according to **GP-2** with (*ent*)-**6**, **61** or **68** as chiral ligand. Enantiopure material was obtained upon recrystallized from PE. Spectroscopic data were identical to those for its enantiomer (*S,S,S*)-(-)-**103**. – $[α]_D^{20}$ = +246.5 (*c* = 1, DCM, > 99% *ee*) – **HPLC analysis** (Phenomenex Lux Cellulose-2, *n*-heptane/*i*PrOH 98:2, 0.5 ml/min, 254 nm): t$_r$ = 11.25 min, t$_r$ = **19.86 min**; > 99% *ee*.
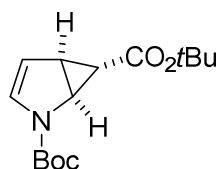
di-*tert*-Butyl-2-azabicyclo[3.1.0]hex-3-ene-2,6-dicarboxylate ((*rac*)-(±)-**103**)

Racemic (±)-**103** was prepared according to **GP-2** with the exception that no ligand was used for the cyclopropanation reaction. Spectroscopic data were identical to those of its enantiomers (*S,S,S*)-(-)-**103** and (*R,R,R*)-(+)-**103**. – **HPLC analysis** (Phenomenex Lux Cellulose-2, *n*-heptane/*i*PrOH 98:2, 0.5 ml/min, 254 nm): t_r = 11.25 min, t_r = 19.86 min.
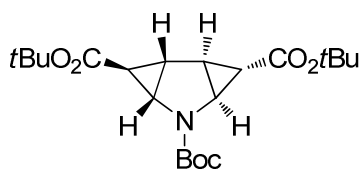
(1*S*,2*S*,3*S*,4*S*,6*S*,7*S*)-tri-*tert*-Butyl-5-azatricyclo[4.1.0.0^{2,4}]heptane-3,5,7-tricarboxylate (**104**)

Doubly cyclopropanated **104** was obtained as a side product of **103**. After purification via flash chromatography (silica, PE/EA = 50:1), **104** was recrystallized from EA to obtain fine white needles (6.86 g, 17.34 mmol, 12%, 41% *ee*).

R$_f$ = 0.71 (PE/EA = 5:1) – **^{1}H-NMR** (300 MHz, CDCl$_3$): δ_H (ppm) = 1.42 (bs, 18 H), 1.47 (s, 9 H), 1.67 (dd, *J* = 3.5 Hz, 1.8 Hz, 2 H), 2.19-2.36 (m, 2 H), 3.24 (d, *J* = 5.9 Hz, 1 H), 3.49 (d, *J* = 5.9 Hz, 1 H). – **^{13}C-NMR** (101 MHz, CDCl$_3$): δ_C (ppm) = 27.4 (+), 28.1 (+), 28.4 (+), 28.9 (+), 42.1 (+), 80.8 (Cq), 81.1 (Cq), 154.7 (Cq), 169.6 (Cq), 169.9 (Cq). – **mp** = 175 °C – **IR** (neat): $\tilde{v}$ (cm^{-1}) = 2984, 2936, 1692, 1397, 1369, 1329, 1299, 1252, 1148, 1125, 1043, 841, 763, 734, 707, 553, 460. – **Elemental analysis** calcd. (%) for C$_{21}$H$_{33}$NO$_6$ (395.23): C 63.78, H 8.41, N 3.54, found C 63.81, H 8.19, N 3.49. – $[\alpha]_D^{20}$ = +43.2 (*c* = 1, DCM, 41% *ee*). – **HPLC analysis** (Phenomenex Lux Cellulose-2, *n*-heptane/*i*PrOH 98:2, 0.5 ml/min, 215 nm): t_r = 27.46 min, t_r = 36.10 min. – **LRMS** (ESI): *m/z* = 362.2 [M+Na-C$_4$H$_8$]$^+$, 396.2 [M+H]$^+$, 418.2 [M+Na]$^+$, 791.5 [2M+H]$^+$, 813.5 [2M+Na]$^+$. – **HRMS** (ESI): *m/z* = 396.2381 [M+H]$^+$; calc. for [C$_{21}$H$_{34}$NO$_6$]$^+$ = 396.2381.
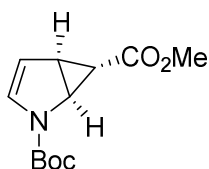
2-(*tert*-Butyl)-6-methyl-(1*S*,5*S*,6*S*)-2-azabicyclo[3.1.0]hex-3-ene-2,6-dicarboxylate (**18**)[17]

Method A: Following **GP-2** *N*-Boc-pyrrole (500 mg, 2.99 mmol, 1.0 equiv) was cyclopropanated using methyl diazoacetate and ligand **8**. After purification via flash chromatography (silica, PE/EA = 10:1) **18** (250 mg, 1.05 mmol, 35%) was obtained as a white solid.

Method B: To a solution of (*S,S,S*)-(-)-**103** (1.05 g, 3.73 mmol, 1.0 equiv) in dry MeOH (50 ml) a solution of freshly prepared NaOMe in MeOH (2 M, 2.13 ml, 4.47 mmol, 1.2 equiv) was added and the reaction mixture was refluxed under nitrogen for 6 h. The solvent was removed under reduced pressure and the crude mixture was purified via flash chromatography (silica, PE/EA = 15:1) to yield **18** (413 mg, 1.73 mmol, 46%) as a white solid, along with reisolated starting material **103** (99 mg, 0.35 mmol, 9%).

R$_f$ = 0.36 (PE/EA = 10:1) – **^{1}H-NMR** (300 MHz, CDCl$_3$): δ_H (ppm) = 0.93-1.01 (m, 1 H), 1.49-1.53 (m, 9 H), 2.76-2.85 (m, 1 H), 3.63-3.74 (m, 3 H), 4.24-4.50 (m, 1 H), 5.30-5.45 (m, 1 H), 6.39-6.66 (m, 1 H). – **^{13}C-NMR** (101 MHz, CDCl$_3$): δ_C (ppm) = 22.8 + 22.9 (+, CH), 28.2 (+, CH$_3$), 31.0 + 32.3 (+, CH), 44.2 + 44.3 (+, CH), 51.8 (+, CH$_3$), 81.7 (Cq), 109.9 (+, CH), 129.7 + 129.9 (+, CH), 151.0 + 151.3 (Cq), 173.3 + 173.6 (Cq). Signal doubling due to rotamers. – **HPLC analysis** (Phenomenex Lux Cellulose-1, *n*-heptane/*i*PrOH = 99:1, 1.0 ml/min, 240 nm): t$_r$ = **6.20 min**, t$_r$ = 10.15; 55% *ee*.
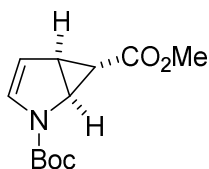
2-(*tert*-Butyl)-6-methyl-2-azabicyclo[3.1.0]hex-3-ene-2,6-dicarboxylate ((*rac*)-(±)-**18**)[50]

Racemic (±)-**18** was prepared according to **GP-2** with methyl diazoacetate (653 g, 5.5 wt%, 1.2 equiv), **101** (50.0 g, 299.0 mmol, 1.0 equiv), Cu(OTf)$_2$ (2.16 g, 5.98 mmol, 0.02 equiv) and neat PhNHNH$_2$ (0.59 ml, 5.98 mmol, 0.02 equiv) in dry DCM (100 ml) at room

temperature to yield (±)-**18** (32.2 g, 135.6 mmol, 45%) as white solid. No ligand was used for the cyclopropanation reaction. Spectroscopic data were identical to those of its enantiomer (*S,S,S*)-(-)-**18**. – **HPLC analysis** (Phenomenex Lux Cellulose-1, *n*-heptane/*i*PrOH = 99:1, 1.0 ml/min, 240 nm): t_r = 6.20 min, t_r = 10.15.
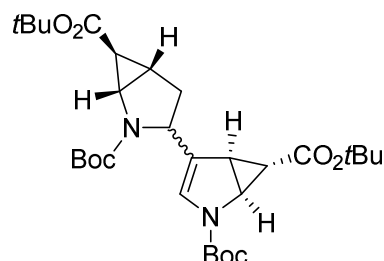
(1*S*,5*R*,6*S*)-di-*tert*-Butyl-4-((1*S*,5*S*,6*S*)-2,6-bis(*tert*-butoxycarbonyl)-2-azabicyclo[3.1.0]hexan-3-yl)-2-azabicyclo[3.1.0]hex-3-ene-2,6-dicarboxylate (**151**)

103 (209.5 mg, 0.75 mmol, 1.0 equiv) was dissolved in DCM (2 ml) at room temperature and TFA (68 μl, 0.89 mmol, 1.2 equiv) was added. The mixture was stirred for 3 h until starting material vanished completely (TLC control). Volatiles were removed in vacuo and the crude mixture was purified via flash chromatography (silica, PE/EA = 10:1) to afford **151** as a white solid (115.6 mg, 0.21 mmol, 55%, mixture of 2 diastereoisomers; *dr* ~ 3:1).

R$_f$ = 0.44 + 0.37 (PE/EA = 5:1) – **^{1}H-NMR** (300 MHz, CDCl$_3$): δ_H (ppm) = 0.92-1.01 (m, 1 H), 1.36-1.50 (m, 36 H), 1.50-1.55 (m, 1 H), 2.05-2.34 (m, 3 H), 2.57-2.71 (m, 1 H), 3.58-3.74 (m, 1 H), 4.09-4.38 (m, 2 H), 6.18-6.42 (m, 1 H). – **^{13}C-NMR** (101 MHz, CDCl$_3$): δ_C (ppm) = 23.3 (+, CH), 24.5 (+, CH), 28.1 (+, CH$_3$), 28.2 (+, CH$_3$), 28.2 (+, CH$_3$), 28.3 (+, CH$_3$), 29.0 (+, CH), 30.2 (+, CH), 33.2 (-, CH$_2$), 43.3 + 43.9 (+, CH), 45.3 (+, CH), 56.9 + 57.2 (+, CH), 80.2 (Cq), 80.7 (Cq), 80.8 (Cq), 81.5 (Cq), 124.3 (+, CH), 124.5 + 124.7 + 125.2 (Cq), 151.0 + 151.2 (Cq), 155.0 (Cq), 169.9 (Cq), 172.2 + 172.5 (Cq). Signal doubling due to rotamers. – **IR** (neat): $\tilde{v}$ (cm^{-1}) = 2977, 2934, 1702, 1635, 1477, 1457, 1407, 1391, 1366, 1301, 1255, 1144, 1121, 1024, 948, 837, 752, 667, 623, 545, 464. – $[\alpha]_D^{20}$ = -99.2 (*c* = 1, DCM) – **LRMS** (ESI): *m/z* = 563.3 [M+H]$^+$, 580.4 [M+NH$_4$]$^+$, 585.3 [M+Na]$^+$, 1147.6 [2M+Na]$^+$. – **HRMS** (ESI): *m/z* = 563.3328 [M+H]$^+$; calc. for [C$_{30}$H$_{47}$N$_2$O$_8$]$^+$ = 563.3327.
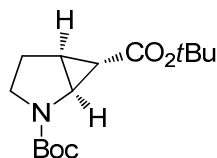
(1*S*,5*S*,6*S*)-di-*tert*-Butyl-2-azabicyclo[3.1.0]hexane-2,6-dicarboxylate (**149**)

Method A: In a Schlenk flask **103** (143.5 mg, 0.51 mmol, 1.0 equiv) was dissolved in THF (6 ml) and Pd/C (10 wt%) was added. A balloon with hydrogen (1 atm) was attached and the atmosphere in the flask was flushed twice with hydrogen gas. The mixture was stirred under a hydrogen atmosphere at ambient temperature for 1.5 h. After completion the crude mixture was filtered through a plug of celite and concentrated in vacuo. The crude product was purified via flash chromatography (silica, PE/EA = 15:1) to afford **149** (122.5 mg, 0.43 mmol, 85%) as a white solid that can be recrystallized from PE.

Method B: To a solution of **103** (167.6 mg, 0.60 mmol, 1.0 equiv) in DCM Et$_3$SiH (0.48 ml, 2.98 mmol, 5.0 equiv) and TFA (92 µl, 1.19 mmol, 2.0 equiv) were added and the solution was stirred at ambient temperature for 6 h. After completion the volatiles were removed in vacuo and the crude mixture was purified via flash chromatography (silica, PE/EA = 15:1) to afford **149** (55.0 mg, 0.19 mmol, 33%) as a white solid.

R$_f$ = 0.23 (PE/EA = 10:1) – **^{1}H-NMR** (300 MHz, CDCl$_3$): δ$_H$ (ppm) = 1.41 (s, 9 H, CH$_3$), 1.44 (s, 9 H, CH$_3$), 1.61 (dd, *J* = 3.7 Hz, 1.6 Hz, 1 H), 1.94-2.24 (m, 3 H), 2.79-3.01 (m, 1 H), 3.49-3.95 (m, 2 H). – **^{13}C-NMR** (101 MHz, CDCl$_3$): δ$_C$ (ppm) = 24.7 (+, CH), 25.9 (-, CH$_2$, 4), 26.9 (+, CH), 28.1 (+, CH$_3$), 28.4 (+, CH$_3$), 43.9 (-, CH$_2$), 44.1 (+, CH), 79.9 (Cq), 80.6 (Cq), 154.6 (Cq), 170.3 (Cq). – **mp** = 62 °C – **IR** (neat): ṽ (cm^{-1}) = 2970, 2935, 1689, 1388, 1364, 1322, 1287, 1257, 1150, 1121, 1049, 1019, 911, 877, 846, 768, 717, 552, 466. – [α]$_D^{20}$ = -10.3 (*c* = 1, DCM, > 99% *ee*). – **Elemental analysis** calcd. (%) for C$_{15}$H$_{25}$NO$_4$ (283.18): C 63.58, H 8.89, N 4.94, found: C 63.90, H 8.69, N 4.87. – **HPLC analysis** (Phenomenex Lux Cellulose-2, *n*-heptane/*i*PrOH 70:30, 0.5 ml/min, 215 nm): t$_r$ = 6.95 min, t$_r$ = 10.79 min. – **LRMS** (ESI): *m/z* = 284.2 [M+H]$^+$, 301.2 [M+NH$_4$]$^+$, 306.2 [M+Na]$^+$, 589.3 [2M+Na]$^+$. – **HRMS** (ESI): *m/z* = 284.1857 [M+H]$^+$; calc. for [C$_{15}$H$_{26}$NO$_4$]$^+$ = 284.1856.
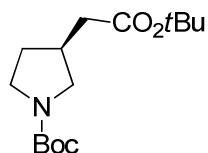
(*S*)-*tert*-Butyl-3-(2-(*tert*-butoxy)-2-oxoethyl)pyrrolidine-1-carboxylate (**150**)

Method A: To a solution of **103** (167.6 mg, 0.60 mmol, 1.0 equiv) in DCM Et$_3$SiH (0.48 ml, 2.98 mmol, 5.0 equiv) and TFA (92 µl, 1.19 mmol, 2.0 equiv) were added and the solution was stirred at ambient temperature for 6 h. After completion the volatiles were removed in vacuo and the crude mixture was purified via flash chromatography (silica, PE/EA = 10:1) to afford **150** (38.4 mg, 0.14 mmol, 23%) as a colorless crystalline solid.

Method B: To a solution of hydrogenation product **149** (65.3 mg, 0.23 mmol, 1.0 equiv) in DCM Et$_3$SiH (0.11 ml, 0.69 mmol, 3.0 equiv) and TFA (35 µl, 0.46 mmol, 2.0 equiv) were added and the solution was stirred at ambient temperature for 65 h. Volatiles were removed in vacuo and the crude mixture was purified via flash chromatography (silica, PE/EA = 10:1) to afford **150** (32.5 mg, 0.11 mmol, 50%) as a colorless crystalline solid.

R$_f$ = 0.14 (PE/EA = 10:1) – **^{1}H-NMR** (300 MHz, CDCl$_3$): δ_H (ppm) = 1.39-1.46 (m, 18 H, CH$_3$), 1.47-1.60 (m, 1 H), 1.95-2.10 (m, 1 H), 2.18-2.37 (m, 2 H), 2.50 (sept, 1 H, *J* = 7.6 Hz), 2.82-2.99 (m, 1 H), 3.17-3.33 (m, 1 H), 3.33-3.63 (m, 2 H). – **^{13}C-NMR** (101 MHz, CDCl$_3$): δ_C (ppm) = 28.1 (+, CH$_3$), 28.5 (+, CH$_3$), 30.8 (-, CH$_2$), 31.5 (-, CH$_2$), 34.7 (+, CH), 35.5 (+, CH), 39.0 (-, CH$_2$), 45.0 (-, CH$_2$), 45.4 (-, CH$_2$), 50.8 (-, CH$_2$), 51.2 (-, CH$_2$), 79.1 (Cq), 80.6 (Cq), 154.5 (Cq), 171.5 (Cq), 171.6 (Cq). (Signal doubling due to rotamers). – **mp** = 54-56 °C – **IR** (neat): $\tilde{v}$ (cm^{-1}) = 2975, 2930, 2878, 1722, 1685, 1457, 1406, 1365, 1307, 1253, 1219, 1149, 1062, 942, 884, 842, 772, 581, 548, 463. – $[\alpha]_D^{20}$ = +18.6 (*c* = 1, DCM). – **HPLC analysis** (Phenomenex Lux Cellulose-1, *n*-heptane/*i*PrOH 99:1, 0.5 ml/min, 200 nm): t$_r$ = 17.03 min, t$_r$ = 19.25 min. – **LRMS** (ESI): *m/z* = 286.2 [M+H]$^+$, 308.2 [M+Na]$^+$, 553.4 [2M+Na]$^+$. – **HRMS** (ESI): *m/z* = 286.2013 [M+H]$^+$; calc. for [C$_{15}$H$_{28}$NO$_4$]$^+$ = 286.2013.
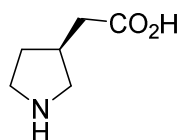
(*S*)-2-(Pyrrolidin-3-yl)acetic acid ((*S*)-(+)-**109**)

Cyclopropane **149** (103.5 mg, 0.37 mmol, 1.0 equiv) was dissolved in dry DCM (5 ml) and Et$_3$SiH (0.23 ml, 1.46 mmol, 4.0 equiv) and TFA (56 µl, 0.73 mmol, 2.0 equiv) were added. The reaction mixture was stirred at room temperature for 24 h. Then more TFA (112 µl, 1.46 mmol, 4.0 equiv) was added and the mixture stirred for another 48 h. After completion of the reaction (TLC) the volatiles were removed in vacuo to yield **109** as TFA salt. For removal of the counterion **109** was loaded onto a column with Dowex 50WX8-400 (preactivated with 0.1 M HCl). The resin was washed with water and finally eluted with 15% NH$_3$ (aq.). The fractions were then concentrated under reduced pressure and lyophilized to yield **109** (47.4 mg, 0.37 mmol, quant.) as a slightly beige-colored amorphous solid.

^{1}H-NMR (300 MHz, D$_2$O): δ_H (ppm) = 1.47-1.65 (m, 1 H), 2.05-2.21 (m, 1 H), 2.43 (d, 1 H, J = 5.6 Hz), 2.45 (d, 1 H, J = 3.8 Hz), 2.47-2.68 (m, 1 H), 2.82 (dd, 1 H, J = 11.3 Hz, 8.9 Hz), 3.07-3.23 (m, 1 H), 3.23-3.34 (m, 1 H), 3.43 (dd, 1 H, J = 11.7 Hz, 7.4 Hz). – **^{13}C-NMR** (101 MHz, D$_2$O): δ_C (ppm) = 29.5 (-, CH$_2$), 33.7 (+, CH), 36.4 (-, CH$_2$), 45.1 (-, CH$_2$), 49.5 (-, CH$_2$), 176.4 (Cq). – **[α]$_D^{20}$** = +7.7 (*c* = 1, H$_2$O; *Lit.:* +9.6 (*c* = 1, H$_2$O)[114]). – **LRMS** (ESI): *m/z* = 130.1 [M+H]$^+$. – **HRMS** (ESI): *m/z* = 130.0866 [M+H]$^+$; calc. for [C$_6$H$_{12}$NO$_2$]$^+$ = 130.0863.
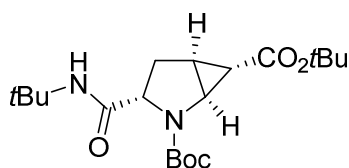
(1*S*,3*S*,5*S*,6*S*)-di-*tert*-Butyl-3-(*tert*-butylcarbamoyl)-2-azabicyclo[3.1.0]hexane-2,6-dicarboxylate (**165a major**)
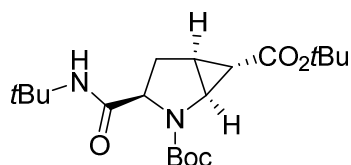
(1*S*,3*R*,5*S*,6*S*)-di-*tert*-Butyl-3-(*tert*-butylcarbamoyl)-2-azabicyclo[3.1.0]hexane-2,6-dicarboxylate (**165b minor**)

To a solution of **103** (193.6 mg, 0.69 mmol, 1.0 equiv) in DCM (40 ml) *tert*-butyl-isocyanide (0.78 ml, 6.88 mmol, 10.0 equiv) and TFA (0.22 ml, 2.75 mmol, 4.0 equiv) were added and solution was stirred at ambient temperature for 5 d. After completion of the reaction volatiles were removed in vacuo and the crude mixture was purified via flash chromatography (silica, PE/EA = 5:1) to yield diastereoisomers **165a** (133.1 mg, 0.35 mmol, 51%) and **165b** (46.9 mg, 0.12 mmol, 18%) as white solid compounds.

165a (major): R$_f$ = 0.36 (PE/EA = 5:1) – **^{1}H-NMR** (300 MHz, CDCl$_3$): δ_H (ppm) = 0.74-0.94 (m, 1 H), 1.33 (s, 9 H), 1.42 (s, 9 H), 1.46 (s, 9 H), 2.07-2.18 (m, 1 H), 2.24-2.43 (m, 1 H), 2.43-2.67 (m, 1 H), 3.54-3.68 (m, 1 H), 3.80-3.96 (m, 1 H), 6.26 (bs, 1 H). – **^{13}C-NMR** (151 MHz, CDCl$_3$): δ_C (ppm) = 25.1 (+, CH), 28.1 (+, CH$_3$), 28.2 (+, CH$_3$), 28.6 (+, CH$_3$), 29.6 (-, CH$_2$), 31.7 (+, CH), 45.5 (+, CH), 50.9 (Cq), 62.9 (+, CH), 80.8 (Cq), 81.4 (Cq), 156.3 (Cq), 169.6 (Cq), 170.2 (Cq). – **mp** = 139 °C – **IR** (neat): ṽ (cm^{-1}) = 3347, 3312, 2975, 2933, 2033, 1719, 1698, 1677, 1655, 1550, 1479, 1455, 1392, 1365, 1310, 1278, 1257, 1224, 1148, 1125, 1019, 985, 961, 913, 857, 842, 796, 758, 663, 644, 616, 561, 486, 466, 408. – **[α]$_D^{20}$** = -47.2 (*c* = 1, DCM) – **LRMS** (ESI): *m/z* = 327.2 [M+H-C$_4$H$_8$]$^+$, 383.3 [M+H]$^+$, 405.2 [M+Na]$^+$. – **HRMS** (ESI): *m/z* = 383.2542 [M+H]$^+$; calc. for [C$_{20}$H$_{35}$N$_2$O$_5$]$^+$ = 383.2540.

165b (minor): R$_f$ = 0.50 (PE/EA = 5:1) – **^{1}H-NMR** (400 MHz, CDCl$_3$, 223 K): δ_H (ppm) = 1.26 (s, 9 H), 1.39 (s, 9 H), 1.47 (s, 9 H), 1.69 (dd, 1 H, *J* = 3.6 Hz, 1.6 Hz), 1.95-2.04 (m, 1 H), 2.12-2.22 (m, 1 H), 2.64 (dd, 1 H, *J* = 13.5 Hz, 1.8 Hz), 3.81 (dd, 1 H, *J* = 6.6 Hz, 1.6 Hz), 4.45 (dd, 1 H, *J* = 10.5 Hz, 1.6 Hz), 7.05 (s, 1 H, N*H*). – **^{13}C-NMR** (101 MHz, CDCl$_3$, 223 K): δ_C (ppm) = 24.7 (+, CH), 26.1 (-, CH$_2$), 27.4 (+, CH), 27.9 (+, CH$_3$), 28.0 (+, CH$_3$), 28.2 (+, CH$_3$), 44.2 (+, CH), 50.8 (Cq), 59.3 (+, CH), 80.9 (Cq), 81.5 (Cq), 154.9 (Cq), 170.7 (Cq), 171.2 (Cq). (Signal doubling due to rotamers; peaks of major rotamer given only). – **mp** = 152 °C – **IR** (neat): ṽ (cm^{-1}) = 3316, 2972, 2936, 1698, 1657, 1549, 1455, 1396, 1365, 1328, 1261, 1223, 1147, 1029, 1001, 842, 765, 728, 559. – **[α]$_D^{20}$** = +42.6 (*c* = 1, DCM). – **LRMS**

(ESI): m/z = 327.2 [M+H-C$_4$H$_8$]$^+$, 383.3 [M+H]$^+$, 405.2 [M+Na]$^+$. – **HRMS** (ESI): m/z = 383.2539 [M+H]$^+$; calc. for [C$_{20}$H$_{35}$N$_2$O$_5$]$^+$ = 383.2540.
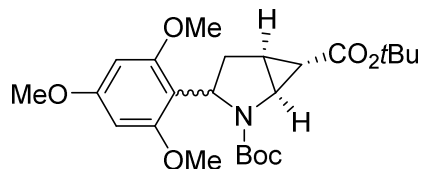
di-*tert*-Butyl-(1*S*,5*S*,6*S*)-3-(2,4,6-trimethoxyphenyl)-2-azabicyclo[3.1.0]hexane-2,6-dicarboxylate (**172**)

To a solution of **103** (152.8 mg, 0.54 mmol, 1.0 equiv) and 1,3,5-trimethoxybenzene (109.6 mg, 0.65 mmol, 1.2 equiv) in dry DCM TFA (50 µl, 0.65 mmol, 1.2 equiv) was added and the reaction mixture was stirred for one hour at room temperature. Volatiles were removed in vacuo and the crude mixture was purified via flash chromatography (silica, PE/EA = 5:1) to yield **172** (32.7 mg, 0.07 mmol, 13%) as a pale yellow oil.

R$_f$ = 0.23 (PE/EA = 5:1) – **^{1}H-NMR** (400 MHz, CDCl$_3$): δ_H (ppm) = 0.81-0.94 (m, 1 H), 1.02-1.31 (m, 9 H), 1.43 (s, 9 H), 2.09-2.31 (m, 2 H), 2.39 (dd, 1 H, J = 12.8 Hz, 9.8 Hz), 3.72-3.83 (m, 9.4 H), 3.85-4.00 (m, 0.6 H), 4.94-5.31 (m, 1 H), 6.03-6.11 (m, 2 H). – **^{13}C-NMR** (101 MHz, CDCl$_3$): δ_C (ppm) = 25.3 (+, CH), 28.2 (+, CH$_3$), 30.7 (+, CH), 34.9 (-, CH$_2$), 46.1 (+, CH), 52.8 (+, CH), 55.3 (+, CH$_3$), 55.6 (+, CH$_3$), 79.1 (Cq), 80.2 (Cq), 90.5 (+, CH), 112.5 (Cq), 154.9 (Cq), 158.6 (Cq), 160.1 (Cq), 170.8 (Cq). – **IR** (neat): $\tilde{v}$ (cm^{-1}) = 2972, 2935, 2843, 1689, 1593, 1497, 1458, 1401, 1370, 1321, 1252, 1228, 1201, 1147, 1119, 1060, 1041, 978, 961, 951, 931, 918, 879, 845, 812, 754, 666. – $[\alpha]_D^{20}$ = +23.5 (c = 1, CHCl$_3$). – **LRMS** (ESI): m/z = 450.2 [M+H]$^+$, 472.2 [M+Na]$^+$, 921.5 [2M+Na]$^+$. – **HRMS** (ESI): m/z = 450.2493 [M+H]$^+$; calc. for [C$_{20}$H$_{35}$N$_2$O$_5$]$^+$ = 450.2486.
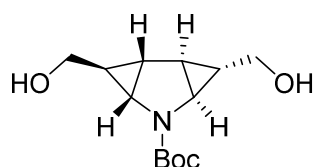
(1*S*,2*S*,3*S*,4*S*,6*S*,7*S*)-*tert*-Butyl-3,7-bis(hydroxymethyl)-5-azatricyclo[4.1.0.02,4]heptane-5-carboxylate (**178**)[205]

To a suspension of LAH (285 mg, 10.14 mmol, 2.0 equiv) in dry THF (65 ml) **104** (2.01 g, 5.07 mmol, 1.0 equiv) was added portion wise at 0 °C and the solution was stirred for 22 h in the defrosting ice bath. After complete consumption of the starting material the reaction was quenched by the addition of EA and NH$_4$Cl (sat.) solution. The aqueous layer was extracted with EA and the organic layers combined and dried over Na$_2$SO$_4$. After evaporation of the solvent the crude mixture was purified by a short silica column (100% EA → 100% MeOH; hereby dissolved silica was filtered from the product from a CHCl$_3$ solution) to yield **178** as a white solid[12] (1.22 g, 4.79 mmol, 95%).

R$_f$ = 0.14 (EA) – **1H-NMR** (300 MHz, CDCl$_3$): δ$_H$ (ppm) = 1.17-1.30 (m, 2 H), 1.42 (s, 9 H, Boc), 1.59 (dd, 1 H, *J* = 6.4 Hz, 3.7 Hz), 1.69 (dd, 1 H, *J* = 6.4 Hz, 3.7 Hz), 2.78 (d, 1 H, *J* = 6.3 Hz), 2.87 (d, 1 H, *J* = 6.3 Hz), 3.15 (dd, 1 H, *J* = 11.6 Hz, 8.4 Hz), 3.25 (dd, 1 H, *J* = 11.4 Hz, 7.7 Hz), 3.33-3.56 (m, 3 H), 4.24 (bs, 1 H, OH). – **13C-NMR** (101 MHz, CDCl$_3$): δ$_C$ (ppm) = 23.9 (+, CH), 25.4 (+, CH), 28.5 (+, CH$_3$), 29.3 + 29.5 (+, CH), 39.2 + 39.8 (+, CH), 61.9 + 62.0 (-, CH$_2$), 80.3 (Cq), 155.9 (Cq). – **mp** = 78 °C – **LRMS** (ESI): *m/z* = 256.2 [M+H]$^+$, 278.1 [M+Na]$^+$, 511.3 [2M+H]$^+$, 533.3 [2M+Na]$^+$. – **HRMS** (ESI): *m/z* = 256.1536 [M+H]$^+$; calc. for [C$_{13}$H$_{22}$NO$_4$]$^+$ = 256.1543.
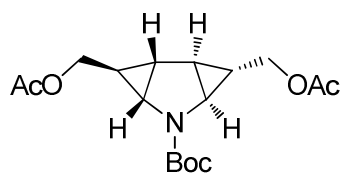
((1*S*,2*S*,3*S*,4*S*,6*S*,7*S*)-5-(*tert*-Butoxycarbonyl)-5-azatricyclo[4.1.0.02,4]heptane-3,7-diyl)bis(methylene) diacetate (**187**)

---

[12] Reported as colorless foam (no mp given).

Diol **178** (77.4 mg, 0.30 mmol, 1.0 equiv) was dissolved in DCM (5 ml) and cooled to 0 °C. DMAP (7 mg, 0.06 mmol, 0.2 equiv), Ac$_2$O (172 μl, 1.82 mmol, 6.0 equiv) and NEt$_3$ (252 μl, 1.82 mmol, 6.0 equiv) were added and the reaction mixture was stirred for 15 min at 0 °C. After quenching the reaction mixture with sat. NH$_4$Cl solution, the aqueous layer was extracted with DCM (4 x). Finally, the combined organic layers were washed with sat. NaHCO$_3$ (1 x) and brine (1 x) and dried over Na$_2$SO$_4$. After evaporation of the solvent the crude product was purified by flash chromatography (silica, PE/EA = 5:1 → 100% EA) to yield **187** (93.6 mg, 0.28 mmol, 91%) as a colorless oil that crystallizes slowly.

R$_f$ = 0.16 (PE/EA = 5:1) – **^{1}H-NMR** (300 MHz, CDCl$_3$): δ$_H$ (ppm) = 1.22-1.34 (m, 2 H), 1.42 (s, 9 H, C*H*$_3$, Boc), 1.65-1.74 (m, 2 H), 2.01 (s, 6 H, C*H*$_3$), 2.83 (d, 1 H, J = 6.4 Hz), 3.03 (d, 1 H, J = 6.43 Hz), 3.70 (dd, 1 H, J = 11.7 Hz, 8.3 Hz), 3.81 (dd, 1 H, J = 7.7 Hz, 2.4 Hz), 3.97 (dd, 1 H, J = 11.8 Hz, 6.5 Hz). – **^{13}C-NMR** (101 MHz, CDCl$_3$): δ$_C$ (ppm) = 21.0 (+, CH$_3$), 24.3 (+, CH), 25.4 + 25.7 (+, CH), 26.0 (+, CH), 28.4 (+, CH$_3$), 39.3 (+, CH), 63.8 + 63.9 (-, CH$_2$), 79.9 (Cq), 155.2 (Cq), 171.0 + 171.1 (Cq). – **IR** (neat): ṽ (cm^{-1}) = 2976, 1737, 1695, 1435, 1393, 1365, 1328, 1226, 1176, 1123, 1030, 972, 851, 763, 632, 539, 497, 462, 399. – **LRMS** (ESI): m/z = 284.1 [M+H-C$_4$H$_8$]$^+$, 340.2 [M+H]$^+$, 362.2 [M+Na]$^+$, 701.3 [2M+Na]$^+$. – **HRMS** (ESI): m/z = 340.1754 [M+H]$^+$; calc. for [C$_{17}$H$_{26}$NO$_6$]$^+$ = 340.1755.
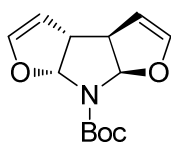
(3a*R*,3b*R*,6a*R*,7a*R*)-*tert*-Butyl-6a,7a-dihydro-3a*H*-difuro[2,3-b:3',2'-d]pyrrole-7(3b*H*)-carboxylate (**179**)[205]

Diol **178** (476 mg, 1.87 mmol, 1.0 equiv) was dissolved in DMSO (32 ml) and IBX (1.15 g, 4.10 mmol, 2.2 equiv) was added. The reaction mixture was stirred at room temperature for 64 h until the starting material vanished completely (TLC control). The mixture was treated with water and extracted with EA (5 x). The combined organic layers were washed with water and dried over Na$_2$SO$_4$. After evaporation of the solvent the crude product was purified by flash chromatography (silica, PE/EA = 7:1) to yield **179** (242 mg, 0.96 mmol, 52%) as a colorless oil.

$\mathbf{R}_f$ = 0.38 (PE/EA = 5:1) – **^{1}H-NMR** (300 MHz, CDCl$_3$): δ_H (ppm) = 1.48 (s, 9 H, CH$_3$), 3.43 (d, 2 H, J = 6.6 Hz), 4.85-4.89 (m, 2 H), 5.95-6.16 (m, 2 H), 6.21 (bs, 2 H). – **^{13}C-NMR** (101 MHz, CDCl$_3$): δ_C (ppm) = 28.2 (+, CH$_3$), 51.3 + 51.4 (+, CH), 81.2 (Cq), 92.4 (+, CH), 102.9 (+, CH), 144.6 + 144.7 (+, CH), 153.3 (Cq). – **LRMS** (ESI): m/z = 196.1 [M+H-C$_4$H$_8$]$^+$, 252.1 [M+H]$^+$, 274.1 [M+Na]$^+$, 525.2 [2M+Na]$^+$. – **HRMS** (ESI): m/z = 252.1237 [M+H]$^+$; calc. for [C$_{13}$H$_{18}$NO$_4$]$^+$ = 252.1230.
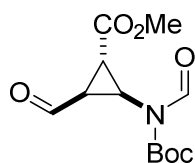
Methyl-2-(*N*-(*tert*-butoxycarbonyl)formamido)-3-formylcyclopropane-1-carboxylate ((±)-**218**)[275]

Cyclopropane (±)-**18** (402 mg, 1.68 mmol, 1.0 equiv) was dissolved in DCM (45 ml) and cooled to -78 °C. Then ozone was bubbled through the solution until a characteristic blue color persisted (~ 15 min). After completion, oxygen was bubbled through the solution to displace excess ozone until the blue color vanished (~ 10 min). The gas inlet was removed, DMS (0.61 ml, 8.40 mmol, 5.0 equiv) was added and the solution was stirred overnight in the defrosting cooling bath. The reaction mixture was then concentrated under reduced pressure and purified via flash chromatography (silica, PE/EA = 3:1) to yield (±)-**218** (440 mg, 1.62 mmol, 97%) as a colorless oil that slowly crystallized in the freezer.

$\mathbf{R}_f$ = 0.35 (PE/EA = 3:1) – **^{1}H-NMR** (300 MHz, CDCl$_3$): δ_H (ppm) = 1.52 (s, 9 H, CH$_3$), 2.75 (dd, 1 H, J = 5.9 Hz, 4.8 Hz), 2.92-2.99 (m, 1 H), 3.21 (dd, 1 H, J = 8.0 Hz, 4.8 Hz), 3.75 (s, 3 H, CH$_3$), 9.07 (s, 1 H), 9.54 (d, 1 H, J = 2.4 Hz).
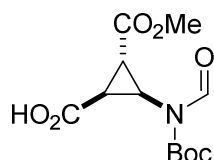
2-(*N*-(*tert*-Butoxycarbonyl)formamido)-3-(methoxycarbonyl)cyclopropane-1-carboxylic acid ((±)-**219**)[275]

Cyclopropane (±)-**218** (440 mg, 1.62 mmol, 1.0 equiv) was dissolved in MeCN (5 ml) and cooled to 0 °C. After that KH_2PO_4 (132 mg, 0.97 mmol, 0.6 equiv) in water (1 ml), H_2O_2 (0.16 ml, 5.35 mmol, 3.3 equiv) and $NaClO_2$ (322 mg, 3.56 mmol, 2.2 equiv) in water (3 ml) were added and the reaction mixture was stirred for 2.5 h at 0 °C until gas evolution ceased. Then Na_2SO_3 (0.8 equiv) was added and the solution was stirred for one additional hour at 0 °C. The reaction mixture was then acidified with 1 M KHSO4 (pH 1-2), the phases were separated and the aqueous layer was extracted with EA (5 x). The combined organic layers were dried over Na_2SO_4, filtered and concentrated in vacuo to yield (±)-**219** (467 mg, 1.63 mmol, quant.) as a white solid.

R$_f$ = 0.11 (PE/EA = 2:1) – **¹H-NMR** (300 MHz, $CDCl_3$): δ_H (ppm) = 1.52 (s, 9 H, CH_3), 2.56-2.68 (m, 2 H), 3.22 (dd, 1 H, *J* = 7.7 Hz, 5.1 Hz), 3.77 (s, 3 H, CH_3), 7.86 (bs, 1 H), 9.13 (s, 1 H).
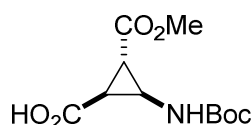
2-((*tert*-Butoxycarbonyl)amino)-3-(methoxycarbonyl)cyclopropane-1-carboxylic acid ((±)-**33**)[275]

Cyclopropane (±)-**219** (467 mg, 1.63 mmol, 1.0 equiv) was dissolved in MeCN (5 ml), DEAEA (0.47 ml, 3.34 mmol, 2.05 equiv) was added and the reaction mixture was stirred at room temperature for 28 h. The mixture was concentrated under reduced pressure, EA was added and the pH of the solution was adjusted to pH 2 with 1 M $KHSO_4$. The aqueous layer was extracted with EA (4 x) and the combined organic layers were dried over Na_2SO_4, filtered and concentrated in vacuo to yield (±)-**33** (348 mg, 1.34 mmol, 82%) as a white solid.

^{1}H-NMR (300 MHz, CDCl$_3$): δ_H (ppm) = 1.46 (s, 9 H, CH$_3$), 2.22-2.57 (m, 2 H), 3.62-3.99 (m, 4 H), 5.45 + 6.54 (bs, 1 H).
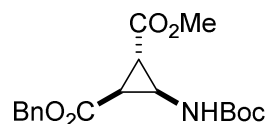
1-Benzyl-2-methyl-3-((*tert*-butoxycarbonyl)amino)cyclopropane-1,2-dicarboxylate (($\pm$)-**220**)[275]

Cyclopropane ($\pm$)-**33** (348 mg, 1.34 mmol, 1.0 equiv) was dissolved in DMF (5 ml), NaHCO$_3$ (225 mg, 2.68 mmol, 2.0 equiv) and BnBr (175 µl, 1.47 mmol, 1.1 equiv) were added and the mixture was stirred at room temperature for 48 h. EA (10 ml) and water (10 ml) were added, the phases separated and the aqueous layer was extracted with EA (4 x). The combined organic layers were washed with water (2 x), dried over Na$_2$SO$_4$, filtered and concentrated in vacuo. Flash chromatography (silica, PE/EA = 5:1) yielded pure ($\pm$)-**220** (429 mg, 1.23 mmol, 92%) as a white solid.

R$_f$ = 0.27 (PE/EA = 5:1) – **^{1}H-NMR** (300 MHz, CDCl$_3$): δ_H (ppm) = 1.44 (s, 9 H, CH$_3$), 2.24-2.31 (m, 1 H), 2.52 (dd, 1 H, J = 8.3 Hz, 5.2 Hz), 3.69 (s, 3 H, CH$_3$), 3.76-3.95 (m, 1 H), 5.12 (d, 1 H, J = 12.2 Hz), 5.21 (d, 1 H, J = 12.2 Hz), 5.53 (bs, 1 H), 7.30-7.42 (m, 5 H).
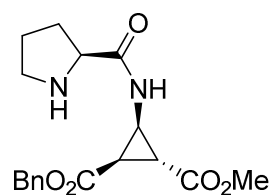
1-Benzyl-2-methyl-(1*R*,2*R*,3*S*)-3-((*S*)-pyrrolidine-2-carboxamido)cyclopropane-1,2-dicarboxylate (**221a**)
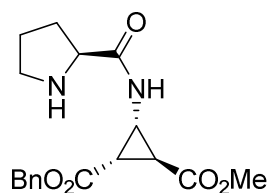
1-Benzyl-2-methyl-(1*S*,2*S*,3*R*)-3-((*S*)-pyrrolidine-2-carboxamido)cyclopropane-1,2-dicarboxylate (**221b**)

Racemic β-ACC (±)-**220** (4.38 g, 12.54 mmol, 1.0 equiv) was dissolved in dry EA (10 ml) and cooled to 0 °C. A solution of HCl in EA (4.2 M, 45 ml) was added and the reaction mixture was stirred at 0 °C until starting material was fully consumed (4 h; TLC analysis). Volatiles were removed in vacuo and the resulting white (pinkish) residue was treated with a premixed solution of *N*-Boc-*L*-proline (3.37 g, 15.68 mmol, 1.25 equiv) and EDC•HCl (3.00 g, 15.68 mmol, 1.25 equiv) in DCM. Finally, triethylamine (2.17 ml, 15.68 mmol, 1.25 equiv) was added and the reaction was stirred at room temperature overnight (17 h). The crude reaction mixture treated with water (50 ml), the pH was adjusted to pH 3 by the addition of 1M $KHSO_4$ and the aqueous layer was extracted with DCM (4 x). The combined organic layers were then washed with $NaHCO_3$ (sat. 1 x) and brine (1 x), dried over Na_2SO_4, filtered and concentrated in vacuo. The crude was purified via flash chromatography (silica, PE/EA = 2:1) to yield a mixture of two *N*-Boc protected diastereomeric dipeptides Boc-Pro-▲/▼-OBn (4.13 g, 9.24 mmol, 74%) as a white foam. The mixture of diastereomers Boc-Pro-▲/▼-OBn (4.70 g, 10.53, mmol, 1.0 equiv) was deprotected with a solution of HCl in EA (4.2 M, 50 ml) at 0 °C and the two diastereomers were separated via flash chromatography (silica, DCM/MeOH = 15:1) to yield **221a** (1.57 g, 4.54 mmol, 43%) and **221b** (1.21 g, 3.49 mmol, 33%).

221a (major): R$_f$ = 0.49 (DCM/MeOH = 9:1) – **^{1}H-NMR** (300 MHz, CDCl$_3$): δ$_H$ (ppm) = 1.50-1.69 (m, 2 H), 1.73-1.91 (m, 1 H), 1.94-2.08 (m, 2 H), 2.26-2.34 (m, 1 H), 2.45-2.54 (m, 1 H), 2.71-2.96 (m, 2 H), 3.53-3.68 (m, 4 H), 3.94-4.08 (m, 1 H), 5.00-5.17 (m, 2 H), 7.23-7.33 (m, 5 H), 8.36 (d, 1 H, *J* = 8.4 Hz).

221b (minor): R$_f$ = 0.29 (DCM/MeOH = 9:1) – **^{1}H-NMR** (300 MHz, CDCl$_3$): δ$_H$ (ppm) = 1.44-1.64 (m, 2 H), 1.69-1.83 (m, 1 H), 1.93-2.10 (m, 2 H), 2.30-2.36 (m, 1 H), 2.48-2.55 (m, 1 H), 2.65-2.67 (m, 1 H), 2.84-2.96 (m, 1 H), 3.60-3.71 (m, 4 H), 3.94-4.03 (m, 1 H), 5.04-5.15 (m, 2 H), 7.25-7.34 (m, 5 H), 8.41 (d, 1 H, *J* = 8.2 Hz).
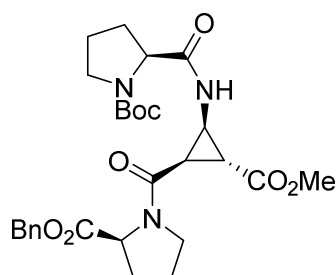
tert-Butyl-(*S*)-2-(((1*R*,2*R*,3*R*)-2-((*S*)-2-((benzyloxy)carbonyl)pyrrolidine-1-carbonyl)-3-(methoxycarbonyl)cyclopropyl)carbamoyl)pyrrolidine-1-carboxylate (**222a**)

Dipeptide **221a** (271 mg, 0.78 mmol, 1.0 equiv) and Boc$_2$O (179 mg, 0.82 mmol, 1.05 equiv) were dissolved in dry DCM (5 ml). A solution of DMAP (10 mg, 0.08 mmol, 0.1 equiv) and NEt$_3$ (81 µl, 0.59 mmol, 0.75 equiv) in dry DCM (5 ml) was added dropwise, and the reaction mixture was stirred at room temperature for 16 h. The reaction was quenched with water and then acidified with 1 M KHSO$_4$ (pH 2-3). After extraction with DCM (3 x), the combined organic layers were washed with brine (1 x), dried over Na$_2$SO$_4$, filtered and concentrated in vacuo to yield the *N*-Boc protected dipeptide Boc-Pro-▲-OBn (328 mg, 0.73 mmol, 94%). The protected dipeptide Boc-Pro-▲-OBn (1.78 g, 3.98 mmol, 1.0 equiv) was dissolved in MeOH (50 ml), Pd/C (10%) was added and a balloon of hydrogen gas (1 atm) was mounted to the flask. The atmosphere was flushed with hydrogen gas to remove air and the mixture was stirred at room temperature for 5 h. After filtration of the reaction mixture through a plug of Celite and washing with MeOH, the solvent was removed in vacuo to yield the free acid Boc-Pro-▲-OH (1.44 g, quant.). Boc-Pro-▲-OH (284 mg, 0.76 mmol, 1.0 equiv) and EDC•HCl (153 mg, 0.80 mmol, 1.05 equiv) were dissolved in dry DCM (12 ml) and stirred for 30 min at room temperature. H-Pro-OBn•HCl (221 mg, 0.91 mmol, 1.2 equiv) and NEt$_3$ (127 µl, 0.91 mmol, 1.2 equiv) were added and the reaction mixture was stirred for 48 h. Water (10 ml) and DCM (10 ml) were added and the pH was adjusted to pH 4 with 1 M KHSO$_4$. The organic layer was then washed with NaHCO$_3$ (sat. 1 x) and brine (1 x), dried over Na$_2$SO$_4$, filtered and concentrated in vacuo. The crude mixture was purified via flash chromatography (silica, DCM/MeOH = 49:1) to yield **222a** (255 mg, 0.47 mmol, 62%) as a colorless foam.

R$_f$ = 0.36 (DCM/MeOH = 19:1) – **^{1}H-NMR** (300 MHz, CDCl$_3$): δ$_H$ (ppm) = 1.43 (s, 9 H), 1.74-2.29 (m, 8 H), 2.29-2.42 (m, 1 H), 2.49-2.71 (m, 1 H), 3.22-3.59 (m, 2 H), 3.59-3.90 (m, 5 H), 4.01-4.35 (m, 2 H), 4.41-4.63 (m, 1 H), 5.04-5.29 (m, 2 H), 7.28-7.83 (m, 6 H).
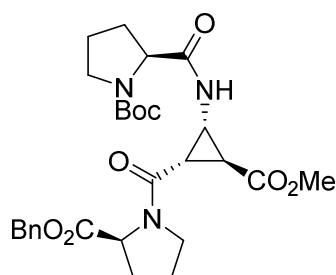
tert-Butyl-(*S*)-2-(((1*S*,2*S*,3*S*)-2-((*S*)-2-((benzyloxy)carbonyl)pyrrolidine-1-carbonyl)-3-(methoxycarbonyl)cyclopropyl)carbamoyl)pyrrolidine-1-carboxylate (**222b**)

Dipeptide **221b** (1.21 g, 3.49 mmol, 1.0 equiv) and Boc$_2$O (800 mg, 3.67 mmol, 1.05 equiv) were dissolved in dry DCM (20 ml). A solution of DMAP (43 mg, 0.35 mmol, 0.1 equiv) and NEt$_3$ (0.36 ml, 2.62 mmol, 0.75 equiv) in dry DCM (20 ml) was added dropwise, and the reaction mixture was stirred at room temperature for 24 h. The reaction was quenched with water and then acidified with 1 M KHSO$_4$ (pH 2-3). After extraction with DCM (3 x), the combined organic layers were washed with brine (1 x), dried over Na$_2$SO$_4$, filtered and concentrated in vacuo to yield the *N*-Boc protected dipeptide Boc-Pro-▼-OBn (1.49 g, 3.33 mmol, 95%). The protected dipeptide Boc-Pro-▼-OBn (570 mg, 1.28 mmol, 1.0 equiv) was dissolved in MeOH (15 ml), Pd/C (10%) was added and a balloon of hydrogen gas (1 atm) was mounted to the flask. The atmosphere was flushed with hydrogen gas to remove air and the mixture was stirred at room temperature for 1 h. After filtration of the reaction mixture through a plug of Celite and washing with MeOH, the solvent was removed in vacuo to yield the free acid Boc-Pro-▼-OH (485 mg, quant.). Boc-Pro-▼-OH (458 mg, 1.28 mmol, 1.0 equiv) and EDC•HCl (257 mg, 1.34 mmol, 1.05 equiv) were dissolved in dry DCM (20 ml) and stirred for 30 min at room temperature. H-Pro-OBn•HCl (370 mg, 1.53 mmol, 1.2 equiv) and NEt$_3$ (212 µl, 1.53 mmol, 1.2 equiv) were added and the reaction mixture was stirred for 48 h. Water (10 ml) and DCM (10 ml) were added and the pH was adjusted to pH 4 with 1 M KHSO$_4$. The organic layer was then washed with NaHCO$_3$ (sat. 1 x) and brine (1 x), dried over Na$_2$SO$_4$, filtered and concentrated in vacuo. The crude mixture was purified via flash chromatography (silica, DCM/MeOH = 49:1) to yield **222b** (395 mg, 0.73 mmol, 57%) as a colorless foam.

R$_f$ = 0.32 (DCM/MeOH = 19:1) – **^{1}H-NMR** (300 MHz, CDCl$_3$): δ$_H$ (ppm) = 1.45 (s, 9 H), 1.73-1.93 (m, 3 H), 1.93-2.25 (m, 5 H), 2.28-2.39 (m, 1 H), 2.49-2.65 (m, 1 H), 3.18-3.55 (m,

2 H), 3.56-3.76 (m, 4 H), 3.78-3.95 (m, 1 H), 4.04-4.34 (m, 2 H), 4.46-4.58 (m, 1 H), 5.03-5.26 (m, 2 H), 7.28-7.61 (m, 6 H).
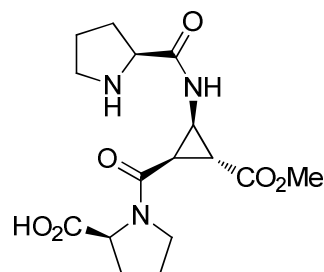
(*S*)-1-((1*R*,2*R*,3*R*)-2-(Methoxycarbonyl)-3-((*S*)-pyrrolidine-2-carboxamido)cyclopropanecarbonyl)pyrrolidine-2-carboxylic acid (**217a**)[58, 240]

Orthogonally protected tripeptide **222a** (154 mg, 0.28 mmol, 1.0 equiv) was deprotected with a solution of HCl in EA (4.2 M, 4 ml) at 0 °C for 1.5 h. The volatiles were removed in vacuo and the residue was treated with water (5 ml) and extracted with Et_2O (2 x). The pH of the aqueous layer was adjusted to pH 9 by the use of $NaHCO_3$ (sat.) and then extracted with DCM (4 x). The combined organic layers were dried over Na_2SO_4, filtered and concentrated in vacuo to yield H-Pro-▲-Pro-OBn (116 mg, 0.26 mmol, 93%) as white foam. H-Pro-▲-Pro-OBn (116 mg, 0.26 mmol, 1.0 equiv) was dissolved in MeOH (5 ml), Pd/C (10%) was added and a balloon of hydrogen gas (1 atm) was mounted to the flask. The atmosphere was flushed with hydrogen gas to remove air and the mixture was stirred at room temperature for 1 h. After filtration of the reaction mixture through a plug of Celite and washing with MeOH, the solvent was removed in vacuo to yield **217a** (106 mg, quant.) as white amorphous solid.

R$_f$ = 0.04 (DCM/MeOH = 4:1) – **^{1}H-NMR** (300 MHz, MeOD): δ_H (ppm) = 1.75-2.13 (m, 6 H), 2.13-2.43 (m, 2 H), 2.43-2.72 (m, 2 H), 3.36-3.46 (m, 1 H), 3.53 (dd, 1 H, *J* = 7.9 Hz, 4.5 Hz), 3.55-3.66 (m, 1 H), 3.63-4.01 (m, 5 H), 4.19-4.68 (m, 2 H). – **^{13}C-NMR** (101 MHz, MeOD): δ_C (ppm) = 25.0 (-, CH_2), 25.4 (-, CH_2), 26.7 (+, CH), 28.0 (+, CH), 28.7 (+, CH), 30.9 (+, CH), 31.0 (-, CH_2), 31.2 (-, CH_2), 36.1 (+, CH), 36.6 (+, CH), 47.6 (-, CH_2), 49.1 (-, CH_2), 53.1 (+, CH_3), 60.8 (+, CH), 62.2 (+, CH), 167.7 (Cq, CO), 171.1 (Cq, CO), 171.4 (Cq, CO, minor), 172.1 (Cq, CO, minor), 172.3 (Cq, CO), 175.8 (Cq, COOH). (signal doubling due to rotamers).
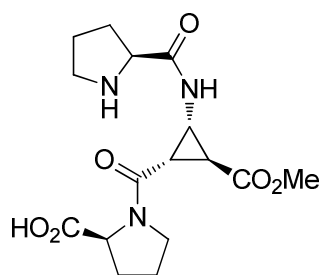
(*S*)-1-((1*S*,2*S*,3*S*)-2-(Methoxycarbonyl)-3-((*S*)-pyrrolidine-2-carboxamido)cyclopropanecarbonyl)pyrrolidine-2-carboxylic acid (**217b**)[58, 240]

Orthogonally protected tripeptide **222b** (322 mg, 0.59 mmol, 1.0 equiv) was deprotected with a solution of HCl in EA (4.2 M, 10 ml) at 0 °C for 3 h. The volatiles were removed in vacuo and the residue was treated with water (10 ml) and extracted with Et$_2$O (1 x). The pH of the aqueous layer was adjusted to pH 8-9 by the use of NaHCO$_3$ (sat.) and then extracted with DCM (4 x). The combined organic layers were dried over Na$_2$SO$_4$, filtered and concentrated in vacuo to yield H-Pro-▼-Pro-OBn (259 mg, 0.58 mmol, 99%) as white foam. H-Pro-▼-Pro-OBn (259 mg, 0.58 mmol, 1.0 equiv) was dissolved in MeOH (10 ml), Pd/C (10%) was added and a balloon of hydrogen gas (1 atm) was mounted to the flask. The atmosphere was flushed with hydrogen gas to remove air and the mixture was stirred at room temperature for 1.5 h. After filtration of the reaction mixture through a plug of Celite and washing with MeOH, the solvent was removed in vacuo to yield **217b** (223 mg, quant.) as white amorphous solid.

R$_f$ = 0.07 (DCM/MeOH = 4:1) – **^{1}H-NMR** (300 MHz, MeOD): δ_H (ppm) = 1.82-1.94 (m, 1 H), 1.94-2.10 (m, 6 H), 2.31-2.42 (m, 1 H), 2.62 (dd, 1 H, *J* = 5.2 Hz, 4.3 Hz), 2.71 (dd, 1 H, *J* = 8.2 Hz, 5.3 Hz), 3.32-3.42 (m, 2 H), 3.65-3.71 (m, 2 H), 3.72 (s, 3 H), 3.92-4.02 (m, 1 H), 4.18 (dd, 1 H, *J* = 8.6 Hz, 6.9 Hz), 4.36 (dd, 1 H, *J* = 8.4 Hz, 2.3 Hz). – **^{13}C-NMR** (101 MHz, MeOD): δ_C (ppm) = 25.2 (-, CH$_2$), 25.3 (-, CH$_2$), 25.9 (+, CH), 30.6 (-, CH$_2$), 30.7 (-, CH$_2$), 31.0 (+, CH), 36.1 (+, CH), 47.5 (-, CH$_2$), 48.5 (-, CH$_2$), 52.9 (+, CH$_3$), 61.2 (+, CH), 61.8 (+, CH), 166.2 (Cq), 171.6 (Cq), 172.4 (Cq), 177.2 (Cq). (signal doubling due to rotamers).

General procedure for organocatalyic aldol reactions under ambient- and high-pressure conditions:
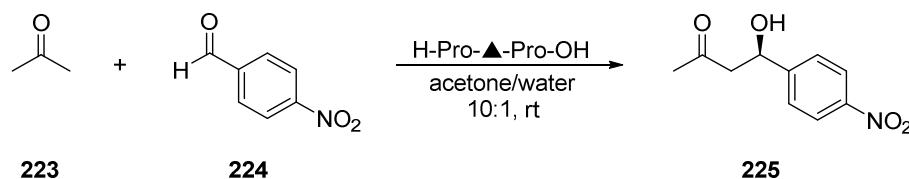
To a solution of *para*-nitrobenzaldehyde **224** (30.2 mg, 0.2 mmol, 1.0 equiv) in 2 ml of acetone/water (10:1 (v/v)) catalyst **217a** (7.1 mg, 0.02 mmol, 0.1 equiv) was added and the solution was stirred for the indicated time at room temperature. Acetone was removed in vacuo and the residue was treated with EA (5 ml) and water (2 ml). After separation of the phases the organic layer was washed with water (1 ml), dried over Na_2SO_4, filtered and evaporated under reduced pressure. The aqueous layer was washed with diethylether (2 ml) and then lyophilized in order to recover the catalyst. On the other hand, the crude reaction mixture was purified via flash chromatography (silica, PE/EA = 2:1) and the product was analyzed by chiral HPLC.

For reactions under high pressure the prepared reaction mixture was transferred into a PTFE tube that was subsequently sealed by melting the tube and then incorporated into the high-pressure apparatus. Pressure was generated and maintained for the indicated time period without agitation of the reaction mixture.
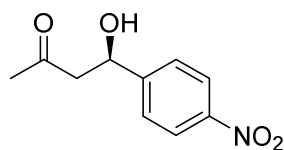
(*R*)-4-Hydroxy-4-(4-nitrophenyl)butan-2-one (**225**)[58]

R$_f$ = 0.17 (PE/EA = 2:1) – **^{1}H-NMR** (300 MHz, CDCl$_3$): δ$_H$ (ppm) = 2.22 (s, 3 H), 2.82-2.87 (m, 2 H), 3.60 (bs, 1 H), 5.26 (dd, 1 H, *J* = 7.4 Hz, 4.9 Hz), 7.49-7.57 (m, 2 H), 8.16-8.23 (m, 2 H). – **HPLC analysis** (Chiralcel AS-H, *n*-heptane/*i*PrOH 99:1, 0.5 ml/min, 254 nm) t$_r$ = 18.97 min (*R*), t$_r$ = 22.38 min (*S*).
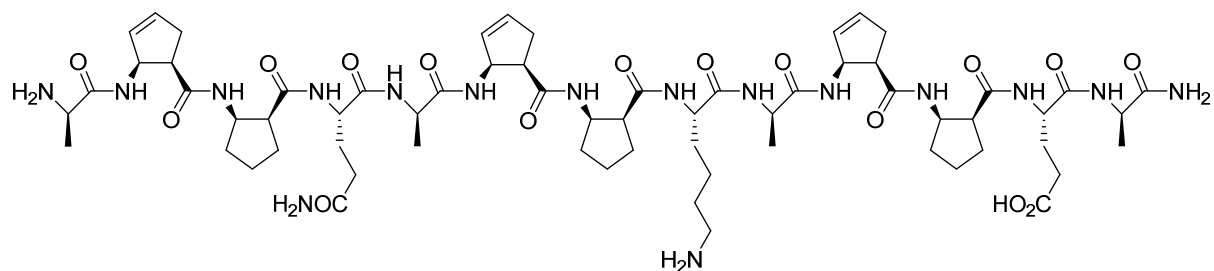
(*S*)-5-(((*R*)-1-Amino-1-oxopropan-2-yl)amino)-4-((1*S*,2*R*)-2-((1*R*,2*S*)-2-((*R*)-2-((*S*)-6-amino-2-((1*S*,2*R*)-2-((1*R*,2*S*)-2-((*R*)-2-((*S*)-5-amino-2-((1*S*,2*R*)-2-((1*R*,2*S*)-2-((*R*)-2-aminopropanamido)cyclopent-3-ene-1-carboxamido)cyclopentane-1-carboxamido)-5-oxopentanamido)propanamido)cyclopent-3-ene-1-carboxamido)cyclopentane-1-carboxamido)hexanamido)propanamido)cyclopent-3-ene-1-carboxamido)cyclopentane-1-carboxamido)-5-oxopentanoic acid (**226**)[256]

Foldamer **226** was obtained from solid phase synthesis on TentaGel R RAM resin via Fmoc/*t*Bu strategy. For synthesis and purification details as well as spectroscopic data of **226** see refs. [256, 257].

F References

1. Müller, E., et al., *Homologation of 5-ring aromatic compounds with diazomethane.* Tetrahedron Lett., 1963(Copyright (C) 2014 American Chemical Society (ACS). All Rights Reserved.): p. 1047-9.

2. Schenck, G. O., Steinmetz, R., *Photochemical formations and rearrangements of thiopheno- and furanocyclopropanecarboxylic acid esters. cis,trans-Muconaldehydic acid esters by valence isomerization of 2-oxabicyclo[3.1.0]hex-3-ene-6-carboxylic acid esters.* Justus Liebigs Ann. Chem., 1963. **668**(Copyright (C) 2014 American Chemical Society (ACS). All Rights Reserved.): p. 19-30.

3. Schenck, G. O., Steinmetz, R., *Radiation chemical reactions with ethyl diazoacetate.* Angew. Chem., 1958. **70**(Copyright (C) 2014 American Chemical Society (ACS). All Rights Reserved.): p. 504-5.

4. Wenkert, E., et al., *Polyene synthesis. Ready construction of retinol-carotene fragments, (±)-6(E)-LTB3 leukotrienes, and corticrocin.* J. Org. Chem., 1990. **55**(Copyright (C) 2014 American Chemical Society (ACS). All Rights Reserved.): p. 6203-14.

5. Wenkert, E., Khatuya, H., Klein, P. S., *Reactions of Et diazoacetate with β-methylfurans.* Tetrahedron Lett., 1999. **40**(Copyright (C) 2014 American Chemical Society (ACS). All Rights Reserved.): p. 5171-5174.

6. Wenkert, E., Khatuya, H., *The effect of substituents of α-alkyl side chains on furan-diazo ester interactions.* Tetrahedron Lett., 1999. **40**(Copyright (C) 2014 American Chemical Society (ACS). All Rights Reserved.): p. 5439-5442.

7. Fowler, F. W., *Cycloadditions of N-Methoxycarbonyl-2,3-homopyrrole.* Angewandte Chemie International Edition in English, 1971. **10**(2): p. 135-136.

8. Fowler, F. W., *Synthesis and Thermolysis of N-Methoxycarbonyl-2,3-homopyrrole.* Angewandte Chemie International Edition in English, 1971. **10**(2): p. 135-135.

9. Tanny, S. R., Grossman, J., Fowler, F. W., *Synthesis and thermal rearrangement of the 2-azabicyclo[3.1.0]hex-3-ene ring system.* J. Amer. Chem. Soc., 1972. **94**(Copyright (C) 2014 American Chemical Society (ACS). All Rights Reserved.): p. 6495-501.

10. Caballero, A., et al., *Copper-Catalyzed Addition of Ethyl Diazoacetate to Furans: An Alternative to Dirhodium(II) Tetraacetate.* The Journal of Organic Chemistry, 2005. **70**(15): p. 6101-6104.

11. Perez, J., et al., *Synthesis of new copper(I) complexes with tris(2-pyridyl) ligands. Applications to carbene and nitrene transfer reactions.* Dalton Trans., 2009(Copyright (C) 2014 American Chemical Society (ACS). All Rights Reserved.): p. 375-382.

12. Davies, H. M. L., Hedley, S. J., *Intermolecular reactions of electron-rich heterocycles with copper and rhodium carbenoids.* Chemical Society Reviews, 2007. **36**(7): p. 1109-1119.

13. Böhm, C., et al., *A New Strategy for the Stereoselective Synthesis of 1,2,3-Trisubstituted Cyclopropanes.* European Journal of Organic Chemistry, 2000. **2000**(16): p. 2955-2965.

14. Schinnerl, M., et al., *New bis(oxazoline) ligands with secondary binding sites for the asymmetric cyclopropanation of furans.* Tetrahedron: Asymmetry, 2003. **14**(7): p. 765-771.

15. Jezek, E., et al., *Radical Cyclizations as Key Step for the Stereoselective Synthesis of Bi- and Tricyclic Sesquiterpene Lactones.* Synlett, 2005. **2005**(06): p. 0915-0918.

16. Hedley, S. J., et al., *Investigation into Factors Influencing Stereoselectivity in the Reactions of Heterocycles with Donor–Acceptor-Substituted Rhodium Carbenoids.* The Journal of Organic Chemistry, 2006. **71**(14): p. 5349-5356.

17. Beumer, R., et al., *The Synthesis of Diastereo- and Enantiomerically Pure β-Aminocyclopropanecarboxylic Acids.* The Journal of Organic Chemistry, 2000. **65**(26): p. 8960-8969.

18. Gheorghe, A., Schulte, M., Reiser, O., *Synthesis of Functionalized Pyrrolidin-2-ones and (S)-Vigabatrin from Pyrrole.* The Journal of Organic Chemistry, 2006. **71**(5): p. 2173-2176.

19. Klärner, F. G., Schröer, D., *1,5-Electrocyclization in homofuran, homopyrrole, and homothiophene.* Angew. Chem., 1987. **99**(Copyright (C) 2014 American Chemical Society (ACS). All Rights Reserved.): p. 1295-7.

20. Klärner, F.G., Schröer, D., *Organic reactions at high pressure: the mechanism of the homo-Diels-Alder reaction of homofuran (2-oxabicyclo[3.1.0]hex-3-ene).* Chem. Ber., 1989. **122**(Copyright (C) 2014 American Chemical Society (ACS). All Rights Reserved.): p. 179-85.

21. Klärner, F. G., et al., *Effect of the benzene ring on 1,5-electrocyclizations: synthesis and thermolysis of optically active benzohomofuran, benzohomothiophene, N-carbomethoxyhomoindole, benzohomophosphole and homoindene.* Tetrahedron: Asymmetry, 1993. **4**(Copyright (C) 2014 American Chemical Society (ACS). All Rights Reserved.): p. 479-90.

22. Golz, T., Hammes, S., Klärner, F. G., *Reactivity of σ-bishomoaromatic heterocycles: electrocyclic reactions and cycloadditions of syn- and anti-bishomofuran and -bishomothiophene.* Chem. Ber., 1993. **126**(Copyright (C) 2014 American Chemical Society (ACS). All Rights Reserved.): p. 485-98.

23. Cai, P.-J., et al., *Homopyrrole and homofuran as masked 1,5-dipoles in metal-free (5+2) cycloadditions with dienophiles: a DFT study.* Tetrahedron, 2013. **69**(Copyright (C) 2014 American Chemical Society (ACS). All Rights Reserved.): p. 7854-7860.

24. Herges, R., Ugi, I., *Synthesis of seven-membered rings by [(σ2 + π2) + π2] cycloaddition on homodienes.* Angew. Chem., 1985. **97**(Copyright (C) 2014 American Chemical Society (ACS). All Rights Reserved.): p. 596-7.

25. Tanny, S. R., Fowler, F. W., *Cycloaddition reactions of the 2-azabicyclo[3.1.0]hex-3-ene ring system.* J. Org. Chem., 1974. **39**(Copyright (C) 2014 American Chemical Society (ACS). All Rights Reserved.): p. 2715-8.

26. Leblanc, Y., et al., *[4 + 2] Cycloaddition reaction of dibenzyl azodicarboxylate and glycals.* J. Am. Chem. Soc., 1989. **111**(Copyright (C) 2014 American Chemical Society (ACS). All Rights Reserved.): p. 2995-3000.

27. Leblanc, Y., et al., *The total synthesis of 12-HETE (12-hydroxyeicosatetraenoic acid) and 12,20-diHETE.* J. Org. Chem., 1986. **51**(Copyright (C) 2014 American Chemical Society (ACS). All Rights Reserved.): p. 789-93.

28. Wenkert, E., et al., *Methyl β-(2-methyl-5-oxocyclopentenylpropionate and ethyl 3-methyl-6-oxohepta-2,4-dienoate.* Synth. Commun., 1981. **11**(Copyright (C) 2014 American Chemical Society (ACS). All Rights Reserved.): p. 533-43.

29. Monn, J. A., et al., *Synthesis, Pharmacological Characterization, and Molecular Modeling of Heterobicyclic Amino Acids Related to (+)-2-Aminobicyclo[3.1.0]hexane-2,6-dicarboxylic Acid (LY354740): Identification of Two New Potent, Selective, and Systemically Active Agonists for Group II Metabotropic Glutamate Receptors.* J. Med. Chem., 1999. **42**(Copyright (C) 2014 American Chemical Society (ACS). All Rights Reserved.): p. 1027-1040.

30. Barrett, J. E., *mGluR2-Positive Allosteric Modulators: Therapeutic Potential for Treating Cocaine Abuse?* Neuropsychopharmacology, 2010. **35**(Copyright (C) 2014 American Chemical Society (ACS). All Rights Reserved.): p. 2007-2008.

31. Böhm, C., Reiser, O., *Enantioselective Synthesis of (−)-Roccellaric Acid.* Organic Letters, 2001. **3**(9): p. 1315-1318.

32. Nosse, B., et al., *Facile Asymmetric Synthesis of the Core Nuclei of Xanthanolides, Guaianolides, and Eudesmanolides.* Organic Letters, 2003. **5**(6): p. 941-944.

33. Bandichhor, R., Nosse, B., Reiser, O., *Paraconic acids - the natural products from Lichen symbiont.* Top. Curr. Chem., 2005. **243**(Copyright (C) 2014 American Chemical Society (ACS). All Rights Reserved.): p. 43-72.

34. Seitz, M., Reiser, O. *Synthetic approaches towards structurally diverse γ-butyrolactone natural-product-like compounds.* Current Opinion in Chemical Biology, 2005. **9**(3): p. 285-292.

35. Schanderl, M., et al., *Stereoselective rearrangement of guaianolides to tricyclic [small delta]-valerolactones.* Organic & Biomolecular Chemistry, 2011. **9**(7): p. 2543-2547.

36. Macabeo, A. P. G., Kreuzer, A., Reiser, O., *Stereoselective routes to aryl substituted γ-butyrolactones and their application towards the synthesis of highly oxidised furanocembranoids.* Org. Biomol. Chem., 2011. **9**(Copyright (C) 2014 American Chemical Society (ACS). All Rights Reserved.): p. 3146-3150.

37. Macabeo, A. P. G., Lehmann, C. W., Reiser, O., *Diastereoselective Synthesis of Enantiopure γ-Butenolide-butyrolactones towards Pseudopterogorgia Lactone Furanocembranoid Substructures.* Synlett, 2012. **23**(Copyright (C) 2014 American Chemical Society (ACS). All Rights Reserved.): p. 2909-2912.

38. Mengel, A., Reiser, O., *Around and beyond Cram's Rule.* Chem. Rev. (Washington, D. C.), 1999. **99**(Copyright (C) 2014 American Chemical Society (ACS). All Rights Reserved.): p. 1191-1223.

39. Chhor, R. B., et al., *Enantioselective Synthesis of Paraconic Acids.* Chemistry − A European Journal, 2003. **9**(1): p. 260-270.

40. Kalidindi, S., et al., *Enantioselective Synthesis of Arglabin.* Angewandte Chemie International Edition, 2007. **46**(33): p. 6361-6363.

41. Kreuzer, A., et al., *Asymmetric Synthesis of Both Enantiomers of Arteludovicinolide A.* Organic Letters, 2013. **15**(13): p. 3420-3423.

42. Kim, C., et al., *Synthesis of fused tetrahydrofuran-γ-lactone motifs via one-pot ring expansion of cyclopropane rings.* Synth. Commun., 2004. **34**(Copyright (C) 2014 American Chemical Society (ACS). All Rights Reserved.): p. 1951-1965.

43. Haveli, S. D., et al., *Efficient Synthesis of Fused Perhydrofuro[2,3-b]pyrans (and Furans) by Ring Opening of 1,2-Cyclopropanated Sugar Derivatives.* Org. Lett., 2007. **9**(Copyright (C) 2014 American Chemical Society (ACS). All Rights Reserved.): p. 1331-1334.

44. Weisser, R., Yue, W., Reiser, O., *Enantioselective Synthesis of Furo[2,3-b]furans, a Spongiane Diterpenoid Substructure.* Org. Lett., 2005. **7**(Copyright (C) 2014 American Chemical Society (ACS). All Rights Reserved.): p. 5353-5356.

45. Harrar, K., Reiser, O., *Enantioselective synthesis of (-)-paeonilide.* Chemical Communications, 2012. **48**(28): p. 3457-3459.

46. Brady, T. P., et al., *Norrisolide: Total synthesis and related studies.* Chem. - Eur. J., 2005. **11**(Copyright (C) 2014 American Chemical Society (ACS). All Rights Reserved.): p. 7175-7190.

47. Bodensteiner, J., et al., *Synthesis and pharmacological characterization of new tetrahydrofuran based compounds as conformationally constrained histamine receptor ligands.* Organic & Biomolecular Chemistry, 2013. **11**(24): p. 4040-4055.

48. Gnad, F., Reiser, O., *Synthesis and Applications of β-Aminocarboxylic Acids Containing a Cyclopropane Ring.* Chem. Rev. (Washington, DC, U. S.), 2003. **103**(Copyright (C) 2014 American Chemical Society (ACS). All Rights Reserved.): p. 1603-1623.

49. Bubert, C., et al., *A new approach to β- and γ-amino esters and amino aldehydes by regioselective ozonolysis of 2,3-dihydropyrroles and 1,2,3,4-tetrahydropyridines.* Synlett, 1994(Copyright (C) 2014 American Chemical Society (ACS). All Rights Reserved.): p. 675-7.

50. Bubert, C., Cabrele, C., Reiser, O., *Novel strategies for the synthesis of peptides containing cis- or trans-β-aminocyclopropanecarboxylic acids.* Synlett, 1997(Copyright (C) 2014 American Chemical Society (ACS). All Rights Reserved.): p. 827-829.

51.   Beumer, R., Reiser, O., *β-Aminocyclopropanecarboxylic acids with α-amino acid side chain functionality.* Tetrahedron, 2001. **57**(Copyright (C) 2014 American Chemical Society (ACS). All Rights Reserved.): p. 6497-6503.

52.   Gnad, F., Poleschak, M., Reiser, O., *Stereoselective synthesis of novel conformationally restricted β- and γ-amino acids.* Tetrahedron Letters, 2004. **45**(22): p. 4277-4280.

53.   De Pol, S., et al., *Surprisingly stable helical conformations in α/β-peptides by incorporation of cis-β-aminocyclopropane carboxylic acids.* Angew. Chem., Int. Ed., 2004. **43**(Copyright (C) 2014 American Chemical Society (ACS). All Rights Reserved.): p. 511-514.

54.   Koglin, N., et al., *Analogues of neuropeptides Y containing β-aminocyclopropane carboxylic acids are the shortest linear peptides that are selective for the Y1 receptor.* Angew. Chem., Int. Ed., 2003. **42**(Copyright (C) 2014 American Chemical Society (ACS). All Rights Reserved.): p. 202-205.

55.   Lang, M., et al., *Structural properties of orexins for activation of their receptors.* Journal of Peptide Science, 2006. **12**(4): p. 258-266.

56.   Lang, M., et al., *Identification of the Key Residue of Calcitonin Gene Related Peptide (CGRP) 27-37 to Obtain Antagonists with Picomolar Affinity at the CGRP Receptor.* J. Med. Chem., 2006. **49**(Copyright (C) 2014 American Chemical Society (ACS). All Rights Reserved.): p. 616-624.

57.   Urman, S., et al., *The Constrained Amino Acid β-Acc Confers Potency and Selectivity to Integrin Ligands.* Angewandte Chemie International Edition, 2007. **46**(21): p. 3976-3978.

58.   D'Elia, V., Zwicknagl, H., Reiser, O., *Short α/β-peptides as catalysts for intra- and intermolecular aldol reactions.* J. Org. Chem., 2008. **73**(Copyright (C) 2014 American Chemical Society (ACS). All Rights Reserved.): p. 3262-3265.

59.   Schmid, M. B., et al., *Residual dipolar couplings in short peptidic foldamers: combined analyses of backbone and side-chain conformations and evaluation of structure coordinates of rigid unnatural amino acids.* ChemBioChem, 2009. **10**(Copyright (C) 2014 American Chemical Society (ACS). All Rights Reserved.): p. 440-444.

60.   Roy, S., Reiser, O., *A Catalytic Multicomponent Approach for the Stereoselective Synthesis of cis-4,5-Disubstituted Pyrrolidinones and Tetrahydro-3H-pyrrolo[3,2-c]quinolines.* Angewandte Chemie International Edition, 2012. **51**(19): p. 4722-4725.

61.   Andrey, O., et al., *Free-radical functionalization of vinylcyclopropanes.* Tetrahedron, 2003. **59**(Copyright (C) 2014 American Chemical Society (ACS). All Rights Reserved.): p. 8543-8550.

62.   Glos, M., Reiser, O., *Aza-bis(oxazolines): New Chiral Ligands for Asymmetric Catalysis†.* Organic Letters, 2000. **2**(14): p. 2045-2048.

63.   Werner, H., et al., *Improved Synthesis of Aza-bis(oxazoline) Ligands.* The Journal of Organic Chemistry, 2003. **68**(26): p. 10166-10168.

64.   Gissibl, A., Finn, M. G., Reiser, O., *Cu(II)-aza(bisoxazoline)-catalyzed asymmetric benzoylations.* Org Lett, 2005. **7**(12): p. 2325-8.

65.   Geiger, C., Kreitmeier, P., Reiser, O., *Cobalt(II)-Azabis(oxazoline)-Catalyzed Conjugate Reduction of α,β-Unsaturated Carbonyl Compounds.* Advanced Synthesis & Catalysis, 2005. **347**(2-3): p. 249-254.

66.   Rasappan, R., et al., *Highly Enantioselective Michael Additions of Indole to Benzylidene Malonate Using Simple Bis(oxazoline) Ligands: Importance of Metal/Ligand Ratio.* Organic Letters, 2006. **8**(26): p. 6099-6102.

67.   Fritschi, H., et al., *Semicorrin Metal Complexes as Enantioselective Catalysts. Part 1. Synthesis of chiral semicorrin ligands and general concepts.* Helvetica Chimica Acta, 1988. **71**(6): p. 1541-1552.

68.   Fritschi, H., Leutenegger, U., Pfaltz, A., *Semicorrin metal complexes as enantioselective catalysts. Part 2. Enantioselective cyclopropane formation from olefins with diazo compounds*

catalyzed by chiral (semicorrinato)copper complexes. Helvetica Chimica Acta, 1988. **71**(6): p. 1553-1565.

69. Fritschi, H., Leutenegger, U., Pfaltz, A., *Chiral Copper-Semicorrin Complexes as Enantioselective Catalysts for the Cyclopropanation of Olefins by Diazo Compounds.* Angewandte Chemie International Edition in English, 1986. **25**(11): p. 1005-1006.

70. Leutenegger, U., et al., *5-aza-semicorrins: A new class of bidentate nitrogen ligands for enantioselective catalysis.* Tetrahedron, 1992. **48**(11): p. 2143-2156.

71. Lowenthal, R. E., Masamune, S. *Asymmetric copper-catalyzed cyclopropanation of trisubstituted and unsymmetrical cis-1,2-disubstituted olefins: modified bis-oxazoline ligands.* Tetrahedron Letters, 1991. **32**(50): p. 7373-7376.

72. Lowenthal, R. E., Abiko, A., Masamune, S., *Asymmetric catalytic cyclopropanation of olefins: bis-oxazoline copper complexes.* Tetrahedron Letters, 1990. **31**(42): p. 6005-6008.

73. Evans, D. A., et al., *Bis(oxazolines) as chiral ligands in metal-catalyzed asymmetric reactions. Catalytic, asymmetric cyclopropanation of olefins.* Journal of the American Chemical Society, 1991. **113**(2): p. 726-728.

74. Evans, D. A., Woerpel, K. A., Scott, M. J. *„Bis(oxazoline)" als Liganden für sich selbst organisierende, chirale Koordinationspolymere; Struktur eines Kupfer(I)-Katalysators für die enantioselektive Cyclopropanierung von Olefinen.* Angewandte Chemie, 1992. **104**(4): p. 439-441.

75. Desimoni, G., Faita, G., Jørgensen, K. A., *Update 1 of: C2-Symmetric Chiral Bis(oxazoline) Ligands in Asymmetric Catalysis.* Chem. Rev. (Washington, DC, U. S.), 2011. **111**(Copyright (C) 2014 American Chemical Society (ACS). All Rights Reserved.): p. PR284-PR437.

76. Fraile, J. M., et al., *Multipurpose box- and azabox-Based Immobilized Chiral Catalysts.* Advanced Synthesis & Catalysis, 2006. **348**(12-13): p. 1680-1688.

77. Werner, H., et al., *Synthesis of Polymer Bound Azabis(oxazoline) Ligands and their Application in Asymmetric Cyclopropanations.* Advanced Synthesis & Catalysis, 2006. **348**(1-2): p. 125-132.

78. Gissibl, A., et al., *Synthesis and Application of Phosphorus Dendrimer Immobilized Azabis(oxazolines).* Organic Letters, 2007. **9**(15): p. 2895-2898.

79. Schätz, A., Hager, M., Reiser, O., *Cu(II)-Azabis(oxazoline)-Complexes Immobilized on Superparamagnetic Magnetite@Silica-Nanoparticles: A Highly Selective and Recyclable Catalyst for the Kinetic Resolution of 1,2-Diols.* Advanced Functional Materials, 2009. **19**(13): p. 2109-2115.

80. Paluti, C. C., Gawalt, E. S., *Immobilized aza-bis(oxazoline) copper catalysts on alkanethiol self-assembled monolayers on gold: Selectivity dependence on surface electronic environments.* Journal of Catalysis, 2010. **275**(1): p. 149-157.

81. Zhou, J., Tang, Y., *The development and application of chiral trisoxazolines in asymmetric catalysis and molecular recognition.* Chemical Society Reviews, 2005. **34**(8): p. 664-676.

82. Gade, L. H., Bellemin-Laponnaz, S., *Exploiting Threefold Symmetry in Asymmetric Catalysis: The Case of Tris(oxazolinyl)ethanes ("Trisox").* Chemistry – A European Journal, 2008. **14**(14): p. 4142-4152.

83. Brunner, H., Obermann, U., *Asymmetrische Katalysen, 45. Enantioselektive Hydrosilylierung von Ketonen mit [Rh(COD)Cl]2/Pyridinyloxazolin-Katalysatoren.* Chemische Berichte, 1989. **122**(3): p. 499-507.

84. Brunner, H., Obermann, U., Wimmer, P., *Asymmetric catalysis. 44. Enantioselective monophenylation of diols with cupric acetate/pyridinyloxazoline catalysts.* Organometallics, 1989. **8**(3): p. 821-826.

85. Gissibl, A., *Synthese und Immobilisierung neuer Azabis(oxazolin)liganden und deren Anwendung in der asymmetrischen Katalyse.* Dissertation, 2006.

86.   Fraile, J. M., et al., *C1-Symmetric Versus C2-Symmetric Ligands in Enantioselective Copper–Bis(oxazoline)-Catalyzed Cyclopropanation Reactions.* Chemistry – A European Journal, 2007. **13**(31): p. 8830-8839.

87.   Hager, M., *Synthesis and Applications of Azabis(oxazoline)-Ligands.* Dissertation, 2010.

88.   McKennon, M. J., et al., *A convenient reduction of amino acids and their derivatives.* The Journal of Organic Chemistry, 1993. **58**(13): p. 3568-3571.

89.   Abiko, A., Masamune, S., *An improved, convenient procedure for reduction of amino acids to aminoalcohols: Use of $NaBH_4$-H_2SO_4.* Tetrahedron Letters, 1992. **33**(38): p. 5517-5518.

90.   Poos, G. I., et al., *2-amino-5-Aryl-2-oxazolines. Potent New Anorectic Agents.* Journal of Medicinal Chemistry, 1963. **6**(3): p. 266-272.

91.   Wittekind, R. R., Rosenau, J. D., Poos, G. I., *Ring Cleavage Reactions of trans-2-Amino-3a,4,5,6,7,7a-hexahydrobenzoxazole.* The Journal of Organic Chemistry, 1961. **26**(2): p. 444-446.

92.   Newhall, W. F., et al., *Hydroxycarbamonitriles from the Reaction of Amino Alcohols with Cyanogen Bromide1.* The Journal of Organic Chemistry, 1964. **29**(7): p. 1809-1812.

93.   Meerwein, H., et al., J. Prakt. Chem. (Weinheim, Ger.), 1937. **147**(2): p. 257.

94.   Meerwein, H., *Triethyloxonium Fluoborate.* Organic Synthesis, 1966. **46**: p. 113.

95.   Granik, V. G., Pyatin, B. M., Glushkov, R. G., *Chemistry of trialkyloxonium fluoroborates.* Usp. Khim., 1971. **40**(Copyright (C) 2014 American Chemical Society (ACS). All Rights Reserved.): p. 1593-620.

96.   Gawley, R. E., Rein, K., Chemburkar, S., *Acyclic stereoselection in the alkylation of chiral dipole-stabilized organolithiums: a self-immolative chirality transfer process for the synthesis of primary amines.* The Journal of Organic Chemistry, 1989. **54**(13): p. 3002-3004.

97.   Sam, J., Plampin, J. N., *Benzoxazoles: Potent skeletal muscle relaxants.* Journal of Pharmaceutical Sciences, 1964. **53**(5): p. 538-544.

98.   César, V., Bellemin-Laponnaz, S., Gade, L. H., *Direct Coupling of Oxazolines and N-Heterocyclic Carbenes: A Modular Approach to a New Class of C–N Donor Ligands for Homogeneous Catalysis.* Organometallics, 2002. **21**(24): p. 5204-5208.

99.   Meyers, A. I., Novachek, K. A., *Pd-Mediated cross-coupling of aryl, alkenyl, and alkynyl stannanes with chiral 2-bromo oxazolines.* Tetrahedron Letters, 1996. **37**(11): p. 1747-1748.

100.   Foltz, C., et al., *Thermal Rearrangement of 2-Bromooxazolines to 2-Bromoisocyanates.* Organic Letters, 2007. **10**(2): p. 305-308.

101.   Gade, L. H., César, V., Bellemin-Laponnaz, S., *A Modular Assembly of Chiral Oxazolinylcarbene–Rhodium Complexes: Efficient Phosphane-Free Catalysts for the Asymmetric Hydrosilylation of Dialkyl Ketones.* Angewandte Chemie International Edition, 2004. **43**(8): p. 1014-1017.

102.   Wenkert, E., et al., *Polyene synthesis. Ready construction of retinol-carotene fragments, (±)-6(E)-LTB₃ leukotrienes, and corticrocin.* The Journal of Organic Chemistry, 1990. **55**(25): p. 6203-6214.

103.   Wenkert, E., Khatuya, H., *Facile Synthesis of Furan-3,4-diacetates.* Helvetica Chimica Acta, 1998. **81**(12): p. 2370-2374.

104.   Schätz, A., et al., *Dependence of Enantioselectivity on the Ligand/Metal Ratio in the Asymmetric Michael Addition of Indole to Benzylidene Malonates: Electronic Influence of Substrates.* Chemistry – A European Journal, 2008. **14**(24): p. 7259-7265.

105.   Glos, M., *Synthese von Oxazolinen als Bausteine für chirale Liganden.* Dissertation, 2000.

106.   Poleschak, M., *Entwicklung neuer, planar-chiraler Ferrocenkatalysatoren sowie Synthese und Untersuchung von Oligopeptiden aus b-Aminocyclopropancarbonsäuren.* Dissertation, 2002.

107.   Schulte, M., et al., *Enantiomer separation of 2,6-disubstituted 2-azabicyclo[3.1.0]hex-3-enes*, 2000, Merck Patent G.m.b.H., Germany . p. 10 pp.

108.   Hu, W., Timmons, D. J., Doyle, M. P., *In Search of High Stereocontrol for the Construction of cis-Disubstituted Cyclopropane Compounds. Total Synthesis of a Cyclopropane-Configured Urea-PETT Analogue That Is a HIV-1 Reverse Transcriptase Inhibitor.* Organic Letters, 2002. **4**(6): p. 901-904.

109.   Smith, A. B., et al., *Complestatin synthetic studies: the effect of the amino acid configuration on peptide backbone conformation in the common western BCD macrocycle.* Bioorg. Med. Chem. Lett., 2004. **14**(Copyright (C) 2014 American Chemical Society (ACS). All Rights Reserved.): p. 1697-1702.

110.   Hu, D. X., Grice, P., Ley, S. V., *Rotamers or Diastereomers? An Overlooked NMR Solution.* J. Org. Chem., 2012. **77**(Copyright (C) 2014 American Chemical Society (ACS). All Rights Reserved.): p. 5198-5202.

111.   Al-Horani, R. A., Desai, U. R., *Electronically rich N-substituted tetrahydroisoquinoline 3-carboxylic acid esters: concise synthesis and conformational studies.* Tetrahedron, 2012. **68**(Copyright (C) 2014 American Chemical Society (ACS). All Rights Reserved.): p. 2027-2040.

112.   Fox, D. J., Pedersen, D. S., Warren, S., *Asymmetric synthesis of orthogonally protected trans-cyclopropane [gamma]-amino acids via intramolecular ring closure.* Organic & Biomolecular Chemistry, 2006. **4**(16): p. 3113-3116.

113.   Fahn, S., *Regional distribution studies of GABA and other putative neurotransmitters and their enzymes enzymes, in GABA in Nervous System Function (ROBERTS E ., CHASE T. N. & TOWER D. B., eds.) pp. 169-186. Raven Press, New York.* 1976.

114.   Nielsen, L., Brehm, L., Krogsgaard-Larsen, P., *GABA agonists and uptake inhibitors. Synthesis, absolute stereochemistry, and enantioselectivity of (R)-(-)- and (S)-(+)-homo-.beta.-proline.* Journal of Medicinal Chemistry, 1990. **33**(1): p. 71-77.

115.   Bowery, N. G., Smart, T. G., *GABA and glycine as neurotransmitters: a brief history.* Br. J. Pharmacol., 2006. **147**(Copyright (C) 2014 American Chemical Society (ACS). All Rights Reserved.): p. S109-S119.

116.   Roth, F. C., Draguhn, A., *GABA metabolism and transport: effects on synaptic efficacy.* Neural Plast., 2012(Copyright (C) 2014 American Chemical Society (ACS). All Rights Reserved.): p. 805830, 12 pp.

117.   Andersen, K. E., et al., *Synthesis of Novel γ-Aminobutyric Acid (GABA) Uptake Inhibitors. 5.1 Preparation and Structure–Activity Studies of Tricyclic Analogues of Known GABA Uptake Inhibitors.* Journal of Medicinal Chemistry, 2001. **44**(13): p. 2152-2163.

118.   Thorbek, P., Hjeds, H., Schaumburg, K., *Syntheses and proton NMR spectroscopic investigations of some pyrrolidinecarboxylic acids designed as potential glial GABA uptake inhibitors.* Acta Chem. Scand., Ser. B, 1981. **B35**(Copyright (C) 2014 American Chemical Society (ACS). All Rights Reserved.): p. 473-9.

119.   Larsson, O. M., et al., *Effect of homo-β-proline and other heterocyclic GABA analogs on GABA uptake in neurons and astroglial cells and on GABA receptor binding.* J. Neurochem., 1981. **37**(Copyright (C) 2014 American Chemical Society (ACS). All Rights Reserved.): p. 1509-16.

120.   Falch, E., et al., *GABA-mimetic activity and effects on diazepam binding of aminosulphonic acids structurally related to piperidine-4-sulphonic acid.* J Neurochem, 1985. **44**(Copyright (C) 2014 U.S. National Library of Medicine.): p. 68-75.

121.   Krogsgaard-Larsen, P., et al., *GABA uptake inhibitors: relevance to antiepileptic drug research.* Epilepsy Res, 1987. **1**(Copyright (C) 2014 U.S. National Library of Medicine.): p. 77-93.

122.   Crites, G. J., Malizia, L. A., Tunnicliff, G., *Action of 4-amino-2-fluorobutanoic acid and other structural analogues on gamma-aminobutyric acid transport by channel catfish brain.* J. Basic Clin. Physiol. Pharmacol., 2002. **13**(Copyright (C) 2014 American Chemical Society (ACS). All Rights Reserved.): p. 179-192.

123. Olsen, R. W., Sieghart, W., *International Union of Pharmacology. LXX. Subtypes of γ-Aminobutyric AcidA Receptors: Classification on the Basis of Subunit Composition, Pharmacology, and Function. Update.* Pharmacological Reviews, 2008. **60**(3): p. 243-260.

124. Gálvez-Ruano, E., et al., *Superimposition-based protocol as a tool for determining bioactive conformations: II. Application to the GABAA receptor.* Journal of Molecular Graphics and Modelling, 2001. **20**(2): p. 183-197.

125. Bodor, N., Brewster, M. E., *Problems of delivery of drugs to the brain.* Pharmacol. Ther., 1983. **19**(Copyright (C) 2014 American Chemical Society (ACS). All Rights Reserved.): p. 337-86.

126. Krogsgaard-Larsen, P., et al. *GABA uptake inhibitors as experimental tools and potential drugs in epilepsy research*. 1981. Raven.

127. Yunger, L. M., et al., *Novel inhibitors of gamma-aminobutyric acid (GABA) uptake: anticonvulsant actions in rats and mice.* Journal of Pharmacology and Experimental Therapeutics, 1984. **228**(1): p. 109-115.

128. Ali, F. E., et al., *Orally Active and Potent Inhibitors of γ-Aminobutyric Acid Uptake.* Journal of Medicinal Chemistry, 1985. **28**(5): p. 653-660.

129. Bondinell, W.E., J.J. Lafferty, and C.L. Zirkle, *N-Substituted pyrrolidineacetic acids and their esters*, 1985, Smithkline Beckman Corp., USA . p. 7 pp.

130. Bondinell, W. E., Underwood, D.C., Kotzer, C. J., *Use of GABA uptake inhibitors as antitussive agents*, 1997, Smithkline Beecham Corporation, USA; p. 12 pp.

131. Bonanno, G., Raiteri, M., *Coexistence of carriers for dopamine and GABA uptake on a same nerve terminal in the rat brain.* British Journal of Pharmacology, 1987. **91**(1): p. 237-243.

132. Crawford, M. L. A., Carswell, H., Young, J. M., *γ-Aminobutyric acid inhibition of histamine-induced inositol phosphate formation in guinea-pig cerebellum: comparison with guinea-pig and rat cerebral cortex.* British Journal of Pharmacology, 1990. **100**(4): p. 867-873.

133. Antonsson, T., et al., *Pyridine compounds and their use as P2Y12 antagonists and their preparation, pharmaceutical compositions and use in the treatment of platelet aggregation disorders*, 2008, AstraZeneca AB, Swed. . p. 100 pp.

134. Harris, K. J., et al., *Preparation of phenylethylaminopyrimidine derivatives for use as prostaglandin D2 receptor antagonists*, 2011, Aventis Pharmaceuticals Inc., USA . p. 61pp.

135. Fink, B. E., et al., *Preparation of substituted imidazopyridazines as kinase inhibitors*, 2009, Bristol-Myers Squibb Company, USA . p. 433 pp.

136. Bylock, L. A., *Preparation benzodioxanes and their use in combination with other actives for inhibiting leukotriene production*, 2013, Boehringer Ingelheim International GmbH, Germany . p. 210pp.

137. Brunette, S. R., et al., *Preparation benzodioxanes and their use in combination with other actives for inhibiting leukotriene production*, 2013, Boehringer Ingelheim International GmbH, Germany . p. 199pp.

138. Stathakis, C. I., Yioti, E. G., Gallos, J. K., *Total Syntheses of (–)-α-Kainic Acid.* European Journal of Organic Chemistry, 2012. **2012**(25): p. 4661-4673.

139. Clayden, J., Read, B., Hebditch, K. R., *Chemistry of domoic acid, isodomoic acids, and their analogues.* Tetrahedron, 2005. **61**(24): p. 5713-5724.

140. Parsons, A. F., *Recent developments in kainoid amino acid chemistry.* Tetrahedron, 1996. **52**(12): p. 4149-4174.

141. Meda, M., et al., *STRUCTURES OF ISODOMOIC ACIDS A, B AND C, NOVEL INSECTICIDAL AMINO ACIDS FROM THE RED ALGA CHONDRIA ARMATA.* CHEMICAL & PHARMACEUTICAL BULLETIN, 1986. **34**(11): p. 4892-4895.

142. Maeda, M., et al., *Insecticidal and neuromuscular activities of domoic acid and its related compounds.* Nippon Noyaku Gakkaishi, 1984. **9**(Copyright (C) 2014 American Chemical Society (ACS). All Rights Reserved.): p. 27-32.

143.   Takemoto, T., Daigo, K., *Constituents of Chondria armata.* CHEMICAL & PHARMACEUTICAL BULLETIN, 1958. **6**(5): p. 578b-580.

144.   Daigo, K., *Constituents of Chondria armata. I. Detection of anthelmintic constituents.* Yakugaku Zasshi, 1959. **79**(Copyright (C) 2014 American Chemical Society (ACS). All Rights Reserved.): p. 350-3.

145.   Husinec, S., et al., *Some approaches to the synthesis of kainic acid.* Journal of the Chemical Society, Perkin Transactions 1, 1984(0): p. 2517-2522.

146.   Nitta, I., Watase, H., Tomiie, W., *Structure of kainic acid and its isomer, allokainic acid.* Nature (London, U. K.), 1958. **181**(Copyright (C) 2014 American Chemical Society (ACS). All Rights Reserved.): p. 761-2.

147.   McGeer, P. L., McGeer, E. G., Hattori, T., *Kainic acid as a tool in neurobiology*. 1978. Raven.

148.   Simon, R.P. and Editor, *Excitatory Amino Acids. [In: FIDIA Res. Found. Symp. Ser., 1992; 9]*1992: Thieme. 292 pp.

149.   Wheal, H. V., Thomson, A. M., and Editors, *Excitatory Amino Acids and Synaptic Transmission*1991: Academic (London). 482 pp.

150.   Watkins, J. C., Krogsgaard-Larsen, P., Honore, T., *Structure-activity relationships in the development of excitatory amino acid receptor agonists and competitive antagonists.* Trends Pharmacol Sci, 1990. **11**(Copyright (C) 2014 U.S. National Library of Medicine.): p. 25-33.

151.   Tasker, R. A. R. *Domoic acid.* 2002. Imperial College Press.

152.   Coldham, I., Hufton, R., *Synthesis of 3-alkylpyrrolidines by anionic cyclization.* Tetrahedron, 1996. **52**(38): p. 12541-12552.

153.   Cardillo, B., et al., *Cyclization of a Chiral N-Crotyl Methoxycarbonylacetamide Mediated by Mn(III). An Easy Entry to (R)-3-Pyrrolidineacetic Acid.* Synlett, 1995. **1995**(11): p. 1159-1160.

154.   Galeazzi, R., Mobbili, G., Orena, M., *A convenient approach to diastereomerically pure 1,3,4-trisubstituted pyrrolidin-2-ones by intramolecular cyclisation of N-(2-alken-1-yl)amides mediated by Mn(III). An entry to both (R)- and (S)-3-pyrrolidineacetic acid.* Tetrahedron, 1996. **52**(3): p. 1069-1084.

155.   Galeazzi, R., et al., *Diastereomerically pure pyrrolidin-2-ones by intramolecular Michael reaction. Synthesis of both (S)- and (R)-3-pyrrolidineacetic acid.* Tetrahedron: Asymmetry, 1996. **7**(1): p. 79-88.

156.   Ramsamy, K., Olsen, R. K., Emery, T., *Synthesis of N-t-Boc-L-α-aminoadipic acid 1-t-butyl 6-ethyl ester from L-aspartic acid: a new route to L-α-aminoadipic acid.* Synthesis, 1982(Copyright (C) 2014 American Chemical Society (ACS). All Rights Reserved.): p. 42-3.

157.   Eustache, J., et al., *Conformationally constrained no synthase inhibitors: Rigid analogs of L-N-iminoethylornithine.* Bioorganic & Medicinal Chemistry Letters, 1998. **8**(21): p. 2961-2966.

158.   Thomas, C., Orecher, F., Gmeiner, P., *A Practical Ex-Chiral-Pool Synthesis of β-Proline and Homo-β-Proline.* Synthesis, 1998. **1998**(10): p. 1491-1496.

159.   Felluga, F., et al., *A convenient chemoenzymatic synthesis of (R)-(−) and (S)-(+)-homo-β-proline.* Tetrahedron: Asymmetry, 2004. **15**(20): p. 3323-3327.

160.   Ye, W., et al., *Chiral Bicyclic Guanidine as a Versatile Brønsted Base Catalyst for the Enantioselective Michael Reactions of Dithiomalonates and β-Keto Thioesters.* Advanced Synthesis & Catalysis, 2007. **349**(16): p. 2454-2458.

161.   Parnes, Z. N., Kalinkin, M. I., *Ionic hydrogenation of organic compounds (review).* Pharmaceutical Chemistry Journal, 1979. **13**(8): p. 846-852.

162.   Bullock, R. M., *Catalytic Ionic Hydrogenations.* Chemistry – A European Journal, 2004. **10**(10): p. 2366-2374.

163.   Lebrun, S., et al., *Asymmetric synthesis of 5-arylmethylpyrrolidin-2-ones and 2-arylmethylpyrrolidines.* Tetrahedron: Asymmetry, 2003. **14**(17): p. 2625-2632.

164.   de Carné-Carnavalet, B., et al., *A Sonogashira Cross-Coupling/5-exo-dig Cyclization/Ionic Hydrogenation Sequence: Synthesis of 4-Substituted 3-Azabicyclo[3.1.0]hexan-2-ones from 2-*

Iodocyclopropanecarboxamides. The Journal of Organic Chemistry, 2013. **78**(11): p. 5794-5799.

165.   Yu, M., Pagenkopf, B. L., *Recent advances in donor–acceptor (DA) cyclopropanes.* Tetrahedron, 2005. **61**(2): p. 321-347.

166.   Carson, C. A., Kerr, M. A., *Heterocycles from cyclopropanes: applications in natural product synthesis.* Chemical Society Reviews, 2009. **38**(11): p. 3051-3060.

167.   Tang, P., Qin, Y., *Recent Applications of Cyclopropane-Based Strategies to Natural Product Synthesis.* Synthesis, 2012. **44**(19): p. 2969-2984.

168.   Greene, T. W., Wuts, P. G. M., *Protective Groups in Organic Synthesis. 2nd Ed* 1991: John Wiley and Sons, Inc. 473 pp.

169.   Matsubara, R., Kobayashi, S., *Enamides and Enecarbamates as Nucleophiles in Stereoselective C–C and C–N Bond-Forming Reactions.* Accounts of Chemical Research, 2008. **41**(2): p. 292-301.

170.   Carbery, D. R., *Enamides: valuable organic substrates.* Organic & Biomolecular Chemistry, 2008. **6**(19): p. 3455-3460.

171.   Poittevin, C., et al., *Free-Radical Carbo-alkenylation of Enamides and Ene-carbamates.* Organic Letters, 2013. **15**(11): p. 2814-2817.

172.   Franklin, A. S., et al., *Application of the Tethered Biginelli Reaction for Enantioselective Synthesis of Batzelladine Alkaloids. Absolute Configuration of the Tricyclic Guanidine Portion of Batzelladine B.* The Journal of Organic Chemistry, 1999. **64**(5): p. 1512-1519.

173.   Cohen, F., Overman, L. E., *Enantioselective Total Synthesis of Batzelladine F: Structural Revision and Stereochemical Definition.* Journal of the American Chemical Society, 2001. **123**(43): p. 10782-10783.

174.   Pini, D., et al., *Addition of diethylzinc to aryl aldehydes catalyzed by (1S,3S)-N,N1-bis[benzyl]-1,3-diphenyl-1,3-propanediamine and its dilithium salt: a mechanistic rationale investigation.* Tetrahedron, 1993. **49**(42): p. 9613-9624.

175.   Ogino, K., et al., *cis-Diamines as active catalysts for the decarboxylation of oxalacetate.* Journal of the Chemical Society, Perkin Transactions 2, 1996(5): p. 979-984.

176.   Mayans, E., et al., *Diastereodivergent Synthesis of Chiral vic-Disubstituted-Cyclobutane Scaffolds: 1,3-Amino Alcohol and 1,3-Diamine Derivatives – Preliminary Use in Organocatalysis.* European Journal of Organic Chemistry, 2013. **2013**(8): p. 1425-1433.

177.   Kung, H. F., et al., *New brain perfusion imaging agents based on technetium-99m bis(aminoethanethiol) complexes: stereoisomers and biodistribution.* Journal of Medicinal Chemistry, 1989. **32**(2): p. 433-437.

178.   Vickery, K., et al., *Preparation, characterization, cytotoxicity, and mutagenicity of a pair of enantiomeric platinum(II) complexes with the potential to bind enantioselectively to DNA.* Journal of Medicinal Chemistry, 1993. **36**(23): p. 3663-3668.

179.   Kammermeier, T., Wiegrebe, W., *1,3-Diphenylpropane-1,3-diamines, VI: DNA-Interaction, Estrogen Receptor Affinity, and Cytostatic Activity of 1,3-Diphenylpropane-1,3-diamine-Pt(II) Complexes.* Archiv der Pharmazie, 1995. **328**(5): p. 409-415.

180.   Cannarasa, M. J., Chem. Ind. (London), 1996: p. 374.

181.   Bergeron, R. J., et al., *A Comparison of Structure–Activity Relationships between Spermidine and Spermine Analogue Antineoplastics.* Journal of Medicinal Chemistry, 1997. **40**(10): p. 1475-1494.

182.   Chand, P., et al., *Systematic Structure-Based Design and Stereoselective Synthesis of Novel Multisubstituted Cyclopentane Derivatives with Potent Antiinfluenza Activity.* Journal of Medicinal Chemistry, 2001. **44**(25): p. 4379-4392.

183.   Nonn, M., et al., *Synthesis of highly functionalized β-aminocyclopentanecarboxylate stereoisomers by reductive ring opening reaction of isoxazolines.* Beilstein J. Org. Chem.,

2012. **8**(Copyright (C) 2014 American Chemical Society (ACS). All Rights Reserved.): p. 100-106, No. 10.

184. Constantinou-Kokotou, V., Kokotos, G., *Synthesis of 1,3-diamines.* Org. Prep. Proced. Int., 1994. **26**(Copyright (C) 2014 American Chemical Society (ACS). All Rights Reserved.): p. 599-602.

185. Zhao, C.-H., et al., *Asymmetric Mannich-Type Reaction of a Chiral N-(tert-Butylsulfinyl) Ketimine with Imines: Application to the Synthesis of Chiral 1,3-Diamines.* European Journal of Organic Chemistry, 2006. **2006**(13): p. 2977-2986.

186. Vesely, J., et al., *Enantioselective organocatalytic conjugate addition of amines to α,β-unsaturated aldehydes: one-pot asymmetric synthesis of β-amino acids and 1,3-diamines.* Tetrahedron Letters, 2007. **48**(12): p. 2193-2198.

187. Kurokawa, T., Kim, M., Du Bois, J., *Synthesis of 1,3-Diamines Through Rhodium-Catalyzed CH Insertion.* Angewandte Chemie International Edition, 2009. **48**(15): p. 2777-2779.

188. Merla, B., Risch, N., *Efficient Synthesis of Diastereomerically Pure 1,3-Diamines.* Synthesis, 2002. **2002**(10): p. 1365-1372.

189. Yunger, L., Moonsammy, G., Rush, J., *Kinetic analysis of the accumulation of γ-aminobutyric acid by particulate fractions of rat brain.* Neurochemical Research, 1983. **8**(6): p. 757-769.

190. Dömling, A., Ugi, I., *Multicomponent Reactions with Isocyanides.* Angewandte Chemie International Edition, 2000. **39**(18): p. 3168-3210.

191. Nenajdenko, V. G., Gulevich, A. V., Balenkova, E. S., *The Ugi reaction with 2-substituted cyclic imines. Synthesis of substituted proline and homoproline derivatives.* Tetrahedron, 2006. **62**(25): p. 5922-5930.

192. Ugi, I. and Editor, *Isonitrile Chemistry* 1971: Academic. 278 pp.

193. Verzele, D., Goeman, J. L., Madder, A., *LC-(TIC/EIC)-MS as tool in the analysis of diastereomeric 3,12-diamino-analogs of deoxycholic acid.* ARKIVOC (Gainesville, FL, U. S.), 2007(Copyright (C) 2014 American Chemical Society (ACS). All Rights Reserved.): p. 325-336.

194. Le Merrer, Y., et al., *Synthesis of azasugars as potent inhibitors of glycosidases.* Bioorganic & Medicinal Chemistry, 1997. **5**(3): p. 519-533.

195. Bertelsen, S., et al., *Organocatalytic asymmetric [small alpha]-bromination of aldehydes and ketones.* Chemical Communications, 2005(38): p. 4821-4823.

196. Glawar, A. F. G., et al., *3-Hydroxyazetidine Carboxylic Acids: Non-Proteinogenic Amino Acids for Medicinal Chemists.* ChemMedChem, 2013. **8**(4): p. 658-666.

197. Davoren, J. E., et al., *Remarkable [3+2] Annulations of Electron-Rich Olefins with Unstabilized Azomethine Ylides.* Synlett, 2010. **2010**(EFirst): p. 2490-2492.

198. Babij, N. R., Wolfe, J. P., *Desymmetrization of meso-2,5-Diallylpyrrolidinyl Ureas through Asymmetric Palladium-Catalyzed Carboamination: Stereocontrolled Synthesis of Bicyclic Ureas.* Angew. Chem., Int. Ed., 2013. **52**(Copyright (C) 2014 American Chemical Society (ACS). All Rights Reserved.): p. 9247-9250.

199. Reissig, H.-U., Zimmer, R., *Donor–Acceptor-Substituted Cyclopropane Derivatives and Their Application in Organic Synthesis†.* Chemical Reviews, 2003. **103**(4): p. 1151-1196.

200. De Simone, F., Waser, J., *Cyclization and Cycloaddition Reactions of Cyclopropyl Carbonyls and Imines.* Synthesis, 2009. **2009**(EFirst): p. 3353-3374.

201. Blum, A., et al., *Structure-Guided Design of C2-Symmetric HIV-1 Protease Inhibitors Based on a Pyrrolidine Scaffold†.* Journal of Medicinal Chemistry, 2008. **51**(7): p. 2078-2087.

202. Schneider, T. F., et al., *anti-Oligoannelated THF Moieties: Synthesis via Push–Pull-Substituted Cyclopropanes‡.* Organic Letters, 2009. **11**(11): p. 2317-2320.

203. Schneider, T. F., et al., *From Furan to Molecular Stairs: Syntheses, Structural Properties, and Theoretical Investigations of Oligocyclic Oligoacetals.* Chemistry – A European Journal, 2010. **16**(37): p. 11276-11288.

204. Duschek, A., Kirsch, S. F., *2-Iodoxybenzoic Acid—A Simple Oxidant with a Dazzling Array of Potential Applications.* Angewandte Chemie International Edition, 2011. **50**(7): p. 1524-1552.

205. Kaschel, J., et al., *Rearrangements of Furan-, Thiophene- and N-Boc-Pyrrole-Derived Donor-Acceptor Cyclopropanes: Scope and Limitations.* European Journal of Organic Chemistry, 2013. **2013**(21): p. 4539-4551.

206. Pietruszka, J., et al., *Kinetic Enzymatic Resolution of Cyclopropane Derivatives.* Advanced Synthesis & Catalysis, 2003. **345**(12): p. 1273-1286.

207. Willstätter, R., Bruce, J., *Zur Kenntnis der Cyclobutanreihe.* Berichte der deutschen chemischen Gesellschaft, 1907. **40**(4): p. 3979-3999.

208. de Meijere, A., et al., *Spirocyclopropanated Bicyclopropylidenes: Straightforward Preparation, Physical Properties, and Chemical Transformations.* Chemistry – A European Journal, 2001. **7**(18): p. 4021-4034.

209. Adams, J., Belley, M., *Formation of reactive tricyclic intermediates via the intramolecular cyclopropanation of dihydropyrans. Synthesis of eucalyptol.* Tetrahedron Letters, 1986. **27**(19): p. 2075-2078.

210. de Meijere, A., *Bonding Properties of Cyclopropane and Their Chemical Consequences.* Angewandte Chemie International Edition in English, 1979. **18**(11): p. 809-826.

211. Dalko, P. I., Moisan, L., *Enantioselective Organocatalysis.* Angewandte Chemie International Edition, 2001. **40**(20): p. 3726-3748.

212. Dalko, P. I., Moisan, L., *In the Golden Age of Organocatalysis.* Angew. Chem., Int. Ed., 2004. **43**(Copyright (C) 2014 American Chemical Society (ACS). All Rights Reserved.): p. 5138-5175.

213. Schreiner, P. R., *Metal-free organocatalysis through explicit hydrogen bonding interactions.* Chemical Society Reviews, 2003. **32**(5): p. 289-296.

214. Enders, D., Balensiefer, T., *Nucleophilic Carbenes in Asymmetric Organocatalysis.* Acc. Chem. Res., 2004. **37**(Copyright (C) 2014 American Chemical Society (ACS). All Rights Reserved.): p. 534-541.

215. Enders, D., Niemeier, O., Henseler, A., *Organocatalysis by N-Heterocyclic Carbenes.* Chem. Rev. (Washington, DC, U. S.), 2007. **107**(Copyright (C) 2014 American Chemical Society (ACS). All Rights Reserved.): p. 5606-5655.

216. Salem, R. B., Jenner, G., *Comparative Activation Modes in Organic Chemistry. Pressure vs Hydrophobic Effects.* THE REVIEW OF HIGH PRESSURE SCIENCE AND TECHNOLOGY, 1998. **7**: p. 1268-1270.

217. Jenner, G., *Comparative activation modes in organic synthesis. The specific role of high pressure.* Tetrahedron, 2002. **58**(Copyright (C) 2014 American Chemical Society (ACS). All Rights Reserved.): p. 5185-5202.

218. Asano, T., Le, N. W. J., *Activation and reaction volumes in solution.* Chem. Rev., 1978. **78**(Copyright (C) 2014 American Chemical Society (ACS). All Rights Reserved.): p. 407-89.

219. Van Eldik, R., Asano, T., Le, N. W. J., *Activation and reaction volumes in solution. 2.* Chem. Rev., 1989. **89**(Copyright (C) 2014 American Chemical Society (ACS). All Rights Reserved.): p. 549-688.

220. Reiser, O., *Catalysis and high pressure - a useful liaison?!* Top. Catal., 1998. **5**(Copyright (C) 2014 American Chemical Society (ACS). All Rights Reserved.): p. 105-112.

221. Klarner, F.-G., Wurche, F., *The effect of pressure on organic reactions.* J. Prakt. Chem. (Weinheim, Ger.), 2000. **342**(Copyright (C) 2014 American Chemical Society (ACS). All Rights Reserved.): p. 609-636.

222. van Berkom, L. W. A., Kuster, G. J. T., Scheeren, H. W., *High pressure: A promising tool for multicomponent reactions.* Mol. Diversity, 2003. **6**(Copyright (C) 2014 American Chemical Society (ACS). All Rights Reserved.): p. 271-282.

223. Matsumoto, K., Hamana, H., Iida, H., *Compendium of cycloaddition reactions under high pressure.* Helv. Chim. Acta, 2005. **88**(Copyright (C) 2014 American Chemical Society (ACS). All Rights Reserved.): p. 2033-2234.

224. Schettino, V., et al., *Chemical reactions at very high pressure.* Adv. Chem. Phys., 2005. **131**(Copyright (C) 2014 American Chemical Society (ACS). All Rights Reserved.): p. 105-242.

225. Schettino, V., Bini, R., *Constraining molecules at the closest approach: chemistry at high pressure.* Chem. Soc. Rev., 2007. **36**(Copyright (C) 2014 American Chemical Society (ACS). All Rights Reserved.): p. 869-880.

226. Benito-Lopez, F., et al., *High pressure in organic chemistry on the way to miniaturization.* Tetrahedron, 2008. **64**(Copyright (C) 2014 American Chemical Society (ACS). All Rights Reserved.): p. 10023-10040.

227. Toma, S., Sebesta, R., Meciarova, M., *Organocatalytic reactions under unusual conditions.* Curr. Org. Chem., 2011. **15**(Copyright (C) 2014 American Chemical Society (ACS). All Rights Reserved.): p. 2257-2281.

228. Hayashi, Y., Nishimura, K., *Application of high pressure induced by water-freezing to the Michael reaction of alcohols with α,β-enones.* Chem. Lett., 2002(Copyright (C) 2014 American Chemical Society (ACS). All Rights Reserved.): p. 296-298.

229. Hayashi, Y., et al., *The Baylis-Hillman reaction under high pressure induced by water-freezing.* Tetrahedron Lett., 2002. **43**(Copyright (C) 2014 American Chemical Society (ACS). All Rights Reserved.): p. 8683-8686.

230. Hayashi, Y., et al., *Application of High Pressure Induced by Water-Freezing to the Direct Catalytic Asymmetric Three-Component List-Barbas-Mannich Reaction.* J. Am. Chem. Soc., 2003. **125**(Copyright (C) 2014 American Chemical Society (ACS). All Rights Reserved.): p. 11208-11209.

231. Hayashi, Y., et al., *Application of high pressure, induced by water freezing, to the direct asymmetric aldol reaction.* Tetrahedron Lett., 2004. **45**(Copyright (C) 2014 American Chemical Society (ACS). All Rights Reserved.): p. 4353-4356.

232. Kaneda, M., et al., *Pressure control of enantiodifferentiating polar addition of 1,1-diphenylpropene sensitized by chiral naphthalenecarboxylates.* Org. Biomol. Chem., 2004. **2**(Copyright (C) 2014 American Chemical Society (ACS). All Rights Reserved.): p. 1295-1303.

233. Ayitou, A. J. L., et al., *Enantiospecific Photochemical Transformations under Elevated Pressure.* Chem. - Eur. J., 2013. **19**(Copyright (C) 2014 American Chemical Society (ACS). All Rights Reserved.): p. 4327-4334.

234. Kwiatkowski, P., Dudzinski, K., Lyzwa, D., *Effect of High Pressure on the Organocatalytic Asymmetric Michael Reaction: Highly Enantioselective Synthesis of γ-Nitroketones with Quaternary Stereogenic Centers.* Org. Lett., 2011. **13**(Copyright (C) 2014 American Chemical Society (ACS). All Rights Reserved.): p. 3624-3627.

235. Lyzwa, D., Dudzinski, K., Kwiatkowski, P., *High-Pressure Accelerated Asymmetric Organocatalytic Friedel-Crafts Alkylation of Indoles with Enones: Application to Quaternary Stereogenic Centers Construction.* Org. Lett., 2012. **14**(Copyright (C) 2014 American Chemical Society (ACS). All Rights Reserved.): p. 1540-1543.

236. Miller, S. J., *In Search of Peptide-Based Catalysts for Asymmetric Organic Synthesis.* Accounts of Chemical Research, 2004. **37**(8): p. 601-610.

237. Colby, D. E. A., et al., *Asymmetric Catalysis Mediated by Synthetic Peptides.* Chem. Rev. (Washington, DC, U. S.), 2007. **107**(Copyright (C) 2014 American Chemical Society (ACS). All Rights Reserved.): p. 5759-5812.

238. Revell, J. D., Wennemers, H., *Peptidic catalysts developed by combinatorial screening methods.* Curr. Opin. Chem. Biol., 2007. **11**(Copyright (C) 2014 American Chemical Society (ACS). All Rights Reserved.): p. 269-278.

239. Wennemers, H., *Asymmetric catalysis with peptides.* Chem. Commun. (Cambridge, U. K.), 2011. **47**(Copyright (C) 2014 American Chemical Society (ACS). All Rights Reserved.): p. 12036-12041.

240. D'Elia, V., *Synthesis, characterization and application of a/b-oligopeptides as bifunctional organocatalysts for the aldol reaction.* Dissertation, 2009.

241. Grehn, L., Ragnarsson, U., *A Convenient Method for the Preparation of 1-(tert-Butyloxycarbonyl) pyrroles.* Angewandte Chemie International Edition in English, 1984. **23**(4): p. 296-301.

242. Dalcanale, E., Montanari, F., *Selective oxidation of aldehydes to carboxylic acids with sodium chlorite-hydrogen peroxide.* The Journal of Organic Chemistry, 1986. **51**(4): p. 567-569.

243. Raach, A., Reiser, O., *Sodium chlorite-hydrogen peroxide, a mild and selective reagent for the oxidation of aldehydes to carboxylic acids.* J. Prakt. Chem. (Weinheim, Ger.), 2000. **342**(Copyright (C) 2014 American Chemical Society (ACS). All Rights Reserved.): p. 605-608.

244. Voigt, J., Noltemeyer, M., Reiser, O., *An efficient synthesis of conformationally restricted peptides containing β-aminocyclopropanecarboxylic acids.* Synlett, 1997(Copyright (C) 2014 American Chemical Society (ACS). All Rights Reserved.): p. 202-204.

245. Zorn, C., et al., *Deprotection of N-Alloc amines by Pd(0)/DABCO-an efficient method for in situ peptide coupling of labile amino acids.* Tetrahedron Lett., 2001. **42**(Copyright (C) 2014 American Chemical Society (ACS). All Rights Reserved.): p. 7049-7053.

246. Andersen, N. H., et al., *Extracting Information from the Temperature Gradients of Polypeptide NH Chemical Shifts. 1. The Importance of Conformational Averaging.* Journal of the American Chemical Society, 1997. **119**(36): p. 8547-8561.

247. Fleischmann, M., *NMR Investigations on Catalysts and Conformations in Organo- and Photocatalytic Reactions, and Characterization of Electrolytes and Supramolecular Switchable Container Molecules.* Dissertation, 2011.

248. Fischer, G., *Chemical aspects of peptide bond isomerisation.* Chem. Soc. Rev., 2000. **29**(Copyright (C) 2014 American Chemical Society (ACS). All Rights Reserved.): p. 119-127.

249. Bandura, A. V., Lvov, S. N., *The Ionization Constant of Water over Wide Ranges of Temperature and Density.* J. Phys. Chem. Ref. Data, 2006. **35**(Copyright (C) 2014 American Chemical Society (ACS). All Rights Reserved.): p. 15-30.

250. Walker, L., LeVine, H., *The cerebral proteopathies.* Molecular Neurobiology, 2000. **21**(1-2): p. 83-95.

251. Akasaka, K., *Probing Conformational Fluctuation of Proteins by Pressure Perturbation.* Chemical Reviews, 2006. **106**(5): p. 1814-1835.

252. Matthews, B. W., *Proteins under pressure.* Proceedings of the National Academy of Sciences, 2012. **109**(18): p. 6792-6793.

253. Pilsl, L. K. A., Reiser, O., *α/β-Peptide foldamers: state of the art.* Amino Acids, 2011. **41**(Copyright (C) 2014 American Chemical Society (ACS). All Rights Reserved.): p. 709-718.

254. Martinek, T. A., Fülöp, F., *Peptidic foldamers: ramping up diversity.* Chem. Soc. Rev., 2012. **41**(Copyright (C) 2014 American Chemical Society (ACS). All Rights Reserved.): p. 687-702.

255. Mándity, I. M., et al., *Design of Peptidic Foldamer Helices: A Stereochemical Patterning Approach.* Angewandte Chemie International Edition, 2009. **48**(12): p. 2171-2175.

256. Berlicki, Ł., et al., *Unique α,β- and α,α,β,β-peptide foldamers based on cis-β-aminocyclopentanecarboxylic acid.* Angew. Chem., Int. Ed., 2012. **51**(Copyright (C) 2014 American Chemical Society (ACS). All Rights Reserved.): p. 2208-2212, S2208/1-S2208/29.

257. Pilsl, L., *Synthesis of unnatural amino acids - towards foldamers.* Master Thesis, 2010.

258. Köhler, J., et al., *Pressure dependence of 15N chemical shifts in model peptides Ac-Gly-Gly-X-Ala-NH2.* Materials, 2012. **5**(Copyright (C) 2014 American Chemical Society (ACS). All Rights Reserved.): p. 1774-1786.

259. Manas, E. S., et al., *Infrared Spectra of Amide Groups in α-Helical Proteins: Evidence for Hydrogen Bonding between Helices and Water.* J. Am. Chem. Soc., 2000. **122**(Copyright (C) 2014 American Chemical Society (ACS). All Rights Reserved.): p. 9883-9890.

260. Kubelka, J., Huang, R., Keiderling, T. A., *Solvent Effects on IR and VCD Spectra of Helical Peptides: DFT-Based Static Spectral Simulations with Explicit Water.* J. Phys. Chem. B, 2005. **109**(Copyright (C) 2014 American Chemical Society (ACS). All Rights Reserved.): p. 8231-8243.

261. Turner, D. R., Kubelka, J., *Infrared and Vibrational CD Spectra of Partially Solvated α-Helices: DFT-Based Simulations with Explicit Solvent.* J. Phys. Chem. B, 2007. **111**(Copyright (C) 2014 American Chemical Society (ACS). All Rights Reserved.): p. 1834-1845.

262. Kong, J., Yu, S., *Fourier transform infrared spectroscopic analysis of protein secondary structures.* Acta Biochim. Biophys. Sin., 2007. **39**(Copyright (C) 2014 American Chemical Society (ACS). All Rights Reserved.): p. 549-559.

263. Byler, D. M., Susi, H., *Examination of the secondary structure of proteins by deconvolved FTIR spectra.* Biopolymers, 1986. **25**(Copyright (C) 2014 American Chemical Society (ACS). All Rights Reserved.): p. 469-87.

264. Paschek, D., et al., *The solvent-dependent shift of the amide I band of a fully solvated peptide as a local probe for the solvent composition in the peptide/solvent interface.* Chemphyschem, 2008. **9**(Copyright (C) 2014 U.S. National Library of Medicine.): p. 2742-50.

265. Johnson, W. C., *Protein secondary structure and circular dichroism: A practical guide.* Proteins: Structure, Function, and Bioinformatics, 1990. **7**(3): p. 205-214.

266. Arvidsson, P. I., Frackenpohl, J., Seebach, D., *Syntheses and CD-Spectroscopic Investigations of Longer-Chain β-Peptides: Preparation by Solid-Phase Couplings of Single Amino Acids, Dipeptides, and Tripeptides.* Helvetica Chimica Acta, 2003. **86**(5): p. 1522-1553.

267. Price, J. L., Horne, W. S., Gellman, S. H., *Structural Consequences of β-Amino Acid Preorganization in a Self-Assembling α/β-Peptide: Fundamental Studies of Foldameric Helix Bundles.* Journal of the American Chemical Society, 2010. **132**(35): p. 12378-12387.

268. Hayashi, R., et al., *Circular dichroism under high pressure*, in *Progress in Biotechnology*, H. Rikimaru, Editor 2002, Elsevier. p. 583-590.

269. Grobelny, S., et al., *Conformational changes upon high pressure induced hydration of poly(N-isopropylacrylamide) microgels.* Soft Matter, 2013. **9**(25): p. 5862-5866.

270. Regitz, M., Hocker, J., Liedhegener, A., *t-Butyl Diazoacetate.* Org Synth, 1968. **48**: p. 36.

271. Sanda, F., Komiya, T., Endo, T., *Radical polyaddition-isomerization of bifunctional vinylcyclopropanes with dithiols.* Macromolecular Chemistry and Physics, 1998. **199**(10): p. 2165-2172.

272. Warner, P., Sutherland, R., *Electron demand in the transition state of the cyclopropylidene to allene ring opening.* The Journal of Organic Chemistry, 1992. **57**(23): p. 6294-6300.

273. Boeckman, R. K. Jr., Shao, P., Mullins, J. J., *THE DESS-MARTIN PERIODINANE: 1,1,1-TRIACETOXY-1,1-DIHYDRO-1,2-BENZIODOXOL-3(1H)-ONE.* Org. Synth., 2000. **77**: p. 141-146.

274. Harrar, K., *Enantioselective Synthesis of (-)-Paeonilide.* Dissertation, 2011.

275. Beumer, R., *Enantio- und diastereoselektive Synthese von β-Aminocyclopropancarbonsäurederivaten und deren Verwendung als Peptidbausteine.* Dissertation, 2000.

G Appendix

1 NMR spectra

^{1}H-NMR spectra: upper image

^{13}C-NMR spectra (DEPT 135 integrated):   lower image

Solvent and frequency are stated each spectrum.

(*S*)-*N*-Benzyl-4-*iso*-propyl-4,5-dihydrooxazol-2-amine (**82**)

CDCl$_3$, 300 MHz
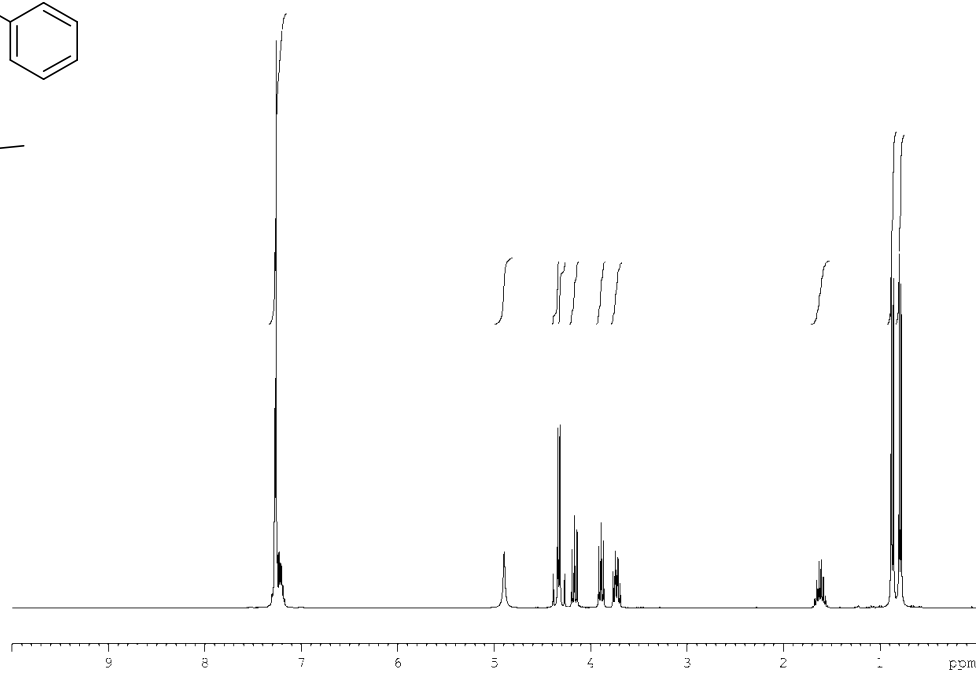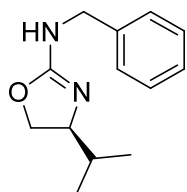
CDCl$_3$, 75 MHz
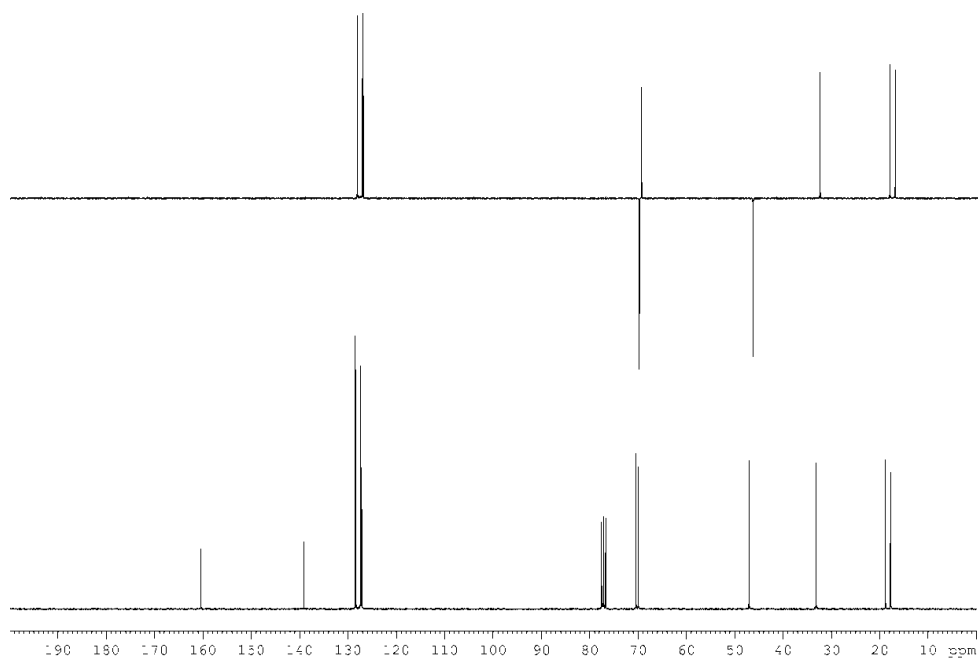
(1*S*,5*S*,6*S*)-di-*tert*-Butyl-2-azabicyclo[3.1.0]hex-3-ene-2,6-dicarboxylate ((*S*,*S*,*S*)-(-)-**103**)

CDCl$_3$, 600 MHz
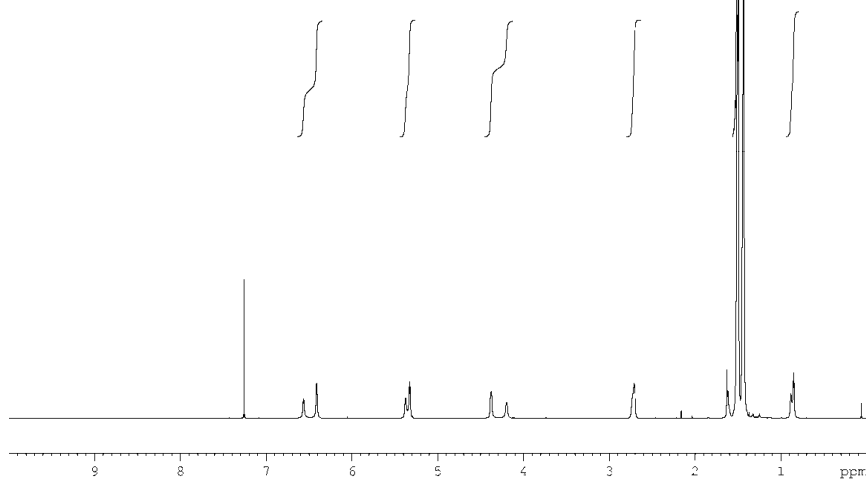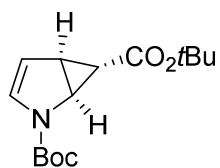
CDCl$_3$, 151 MHz
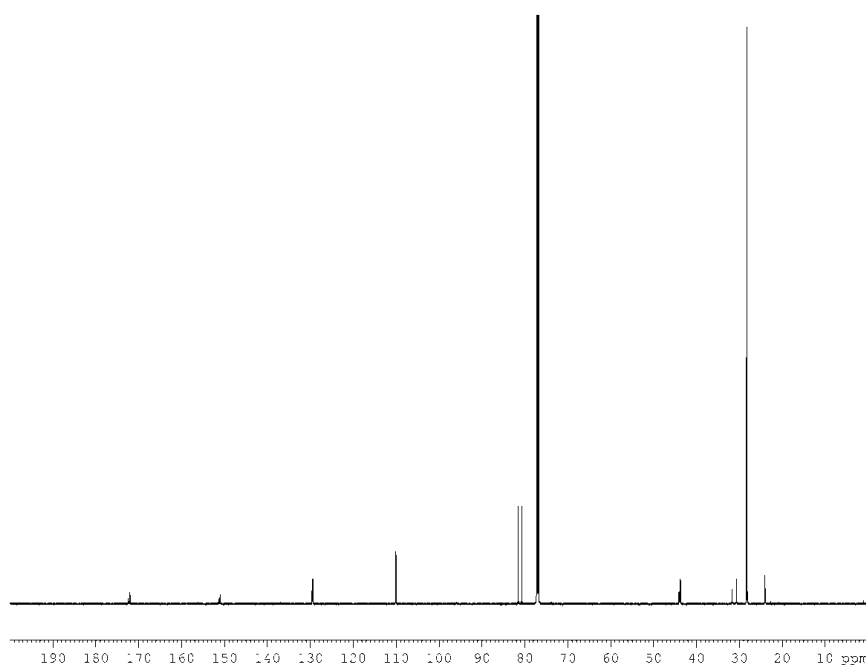
(1*S*,2*S*,3*S*,4*S*,6*S*,7*S*)-tri-*tert*-Butyl-5-azatricyclo[4.1.0.0^{2,4}]heptane-3,5,7-tricarboxylate (**104**)

CDCl$_3$, 300 MHz
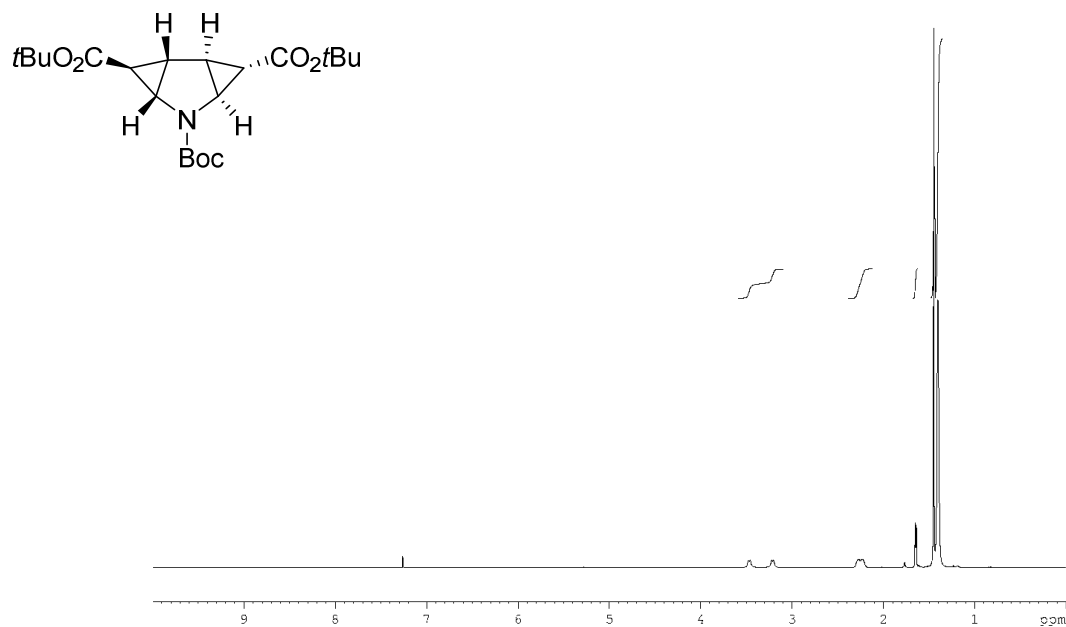
CDCl$_3$, 75 MHz
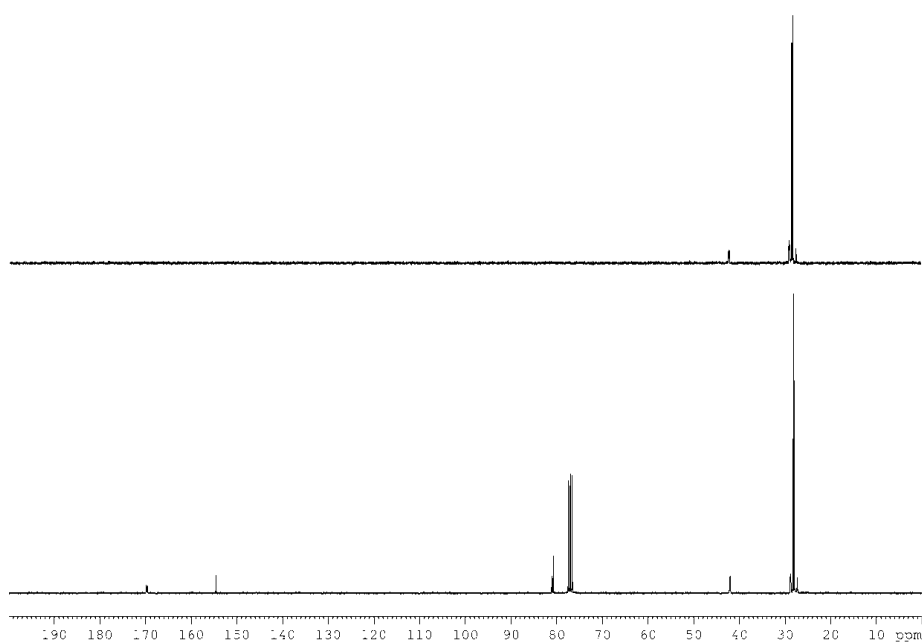
(1*S*,5*S*,6*S*)-di-*tert*-Butyl-2-azabicyclo[3.1.0]hexane-2,6-dicarboxylate (**149**)

CDCl$_3$, 300 MHz

CDCl$_3$, 75 MHz

(1*S*,5*S*,6*S*)-di-*tert*-Butyl-2-azabicyclo[3.1.0]hexane-2,6-dicarboxylate (**149**)
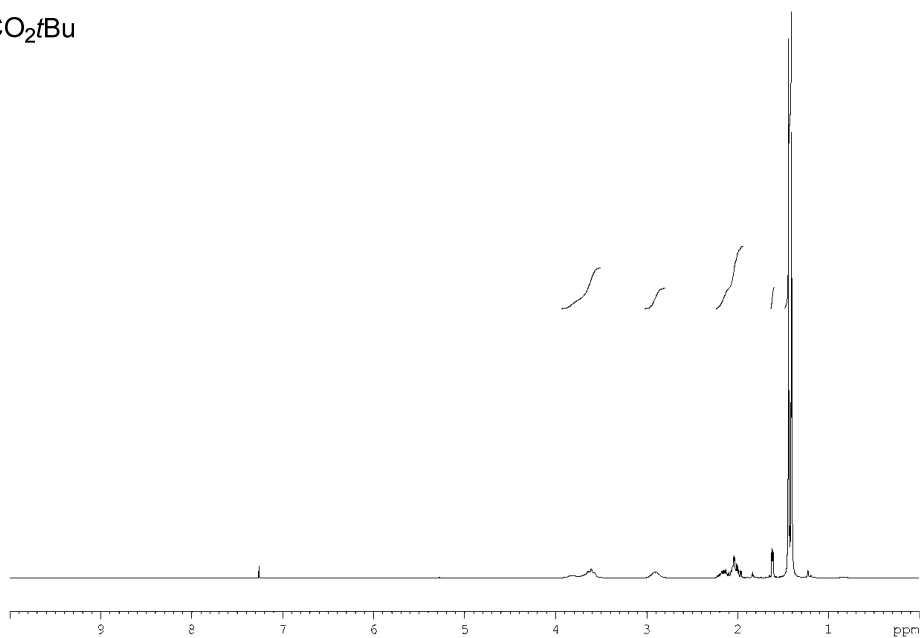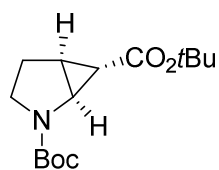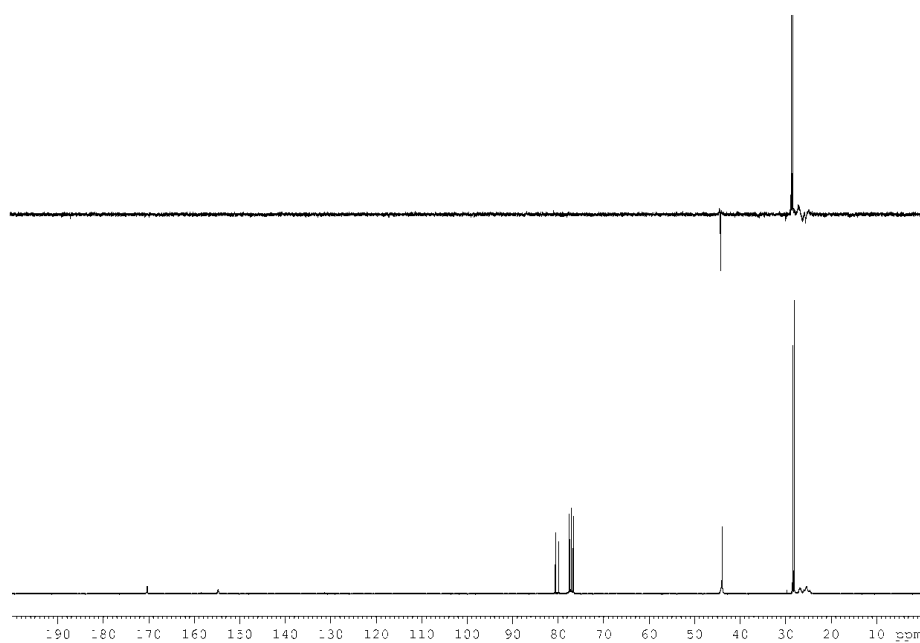
(*S*)-*tert*-Butyl-3-(2-(*tert*-butoxy)-2-oxoethyl)pyrrolidine-1-carboxylate (**150**)

CDCl$_3$, 300 MHz
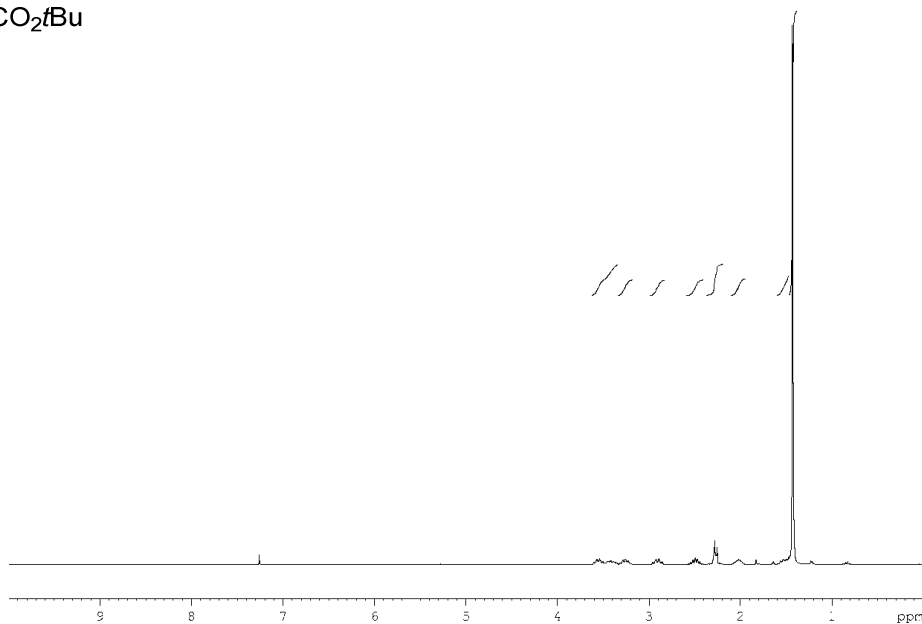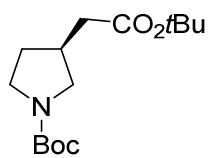
CDCl$_3$, 75 MHz
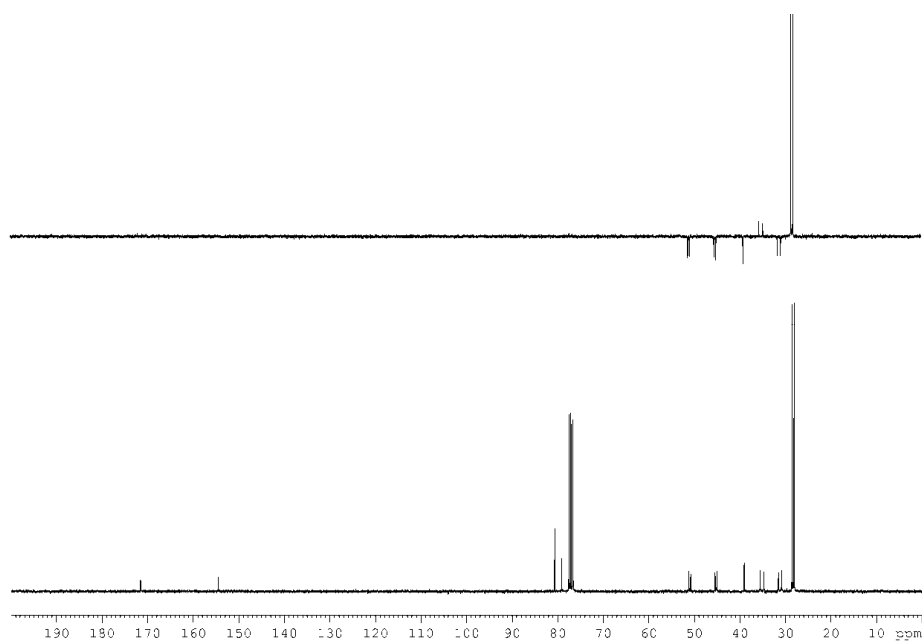
(1*S*,5*R*,6*S*)-di-*tert*-Butyl-4-((1*S*,5*S*,6*S*)-2,6-bis(*tert*-butoxycarbonyl)-2-azabicyclo[3.1.0]hexan-3-yl)-2-azabicyclo[3.1.0]hex-3-ene-2,6-dicarboxylate (**151**)

CDCl$_3$, 300 MHz
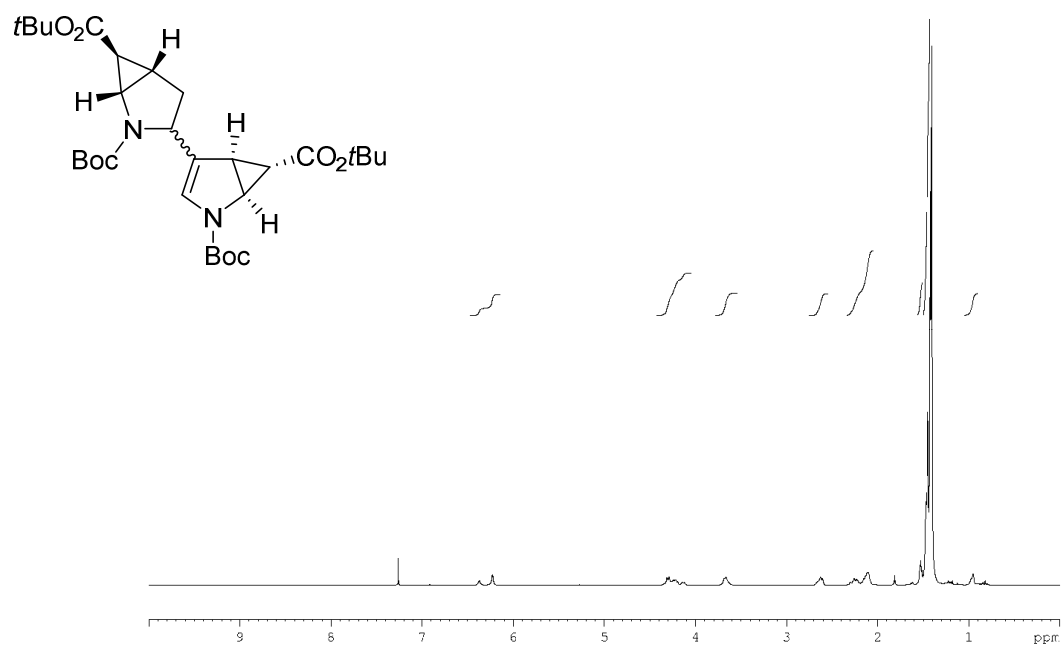
CDCl$_3$, 75 MHz
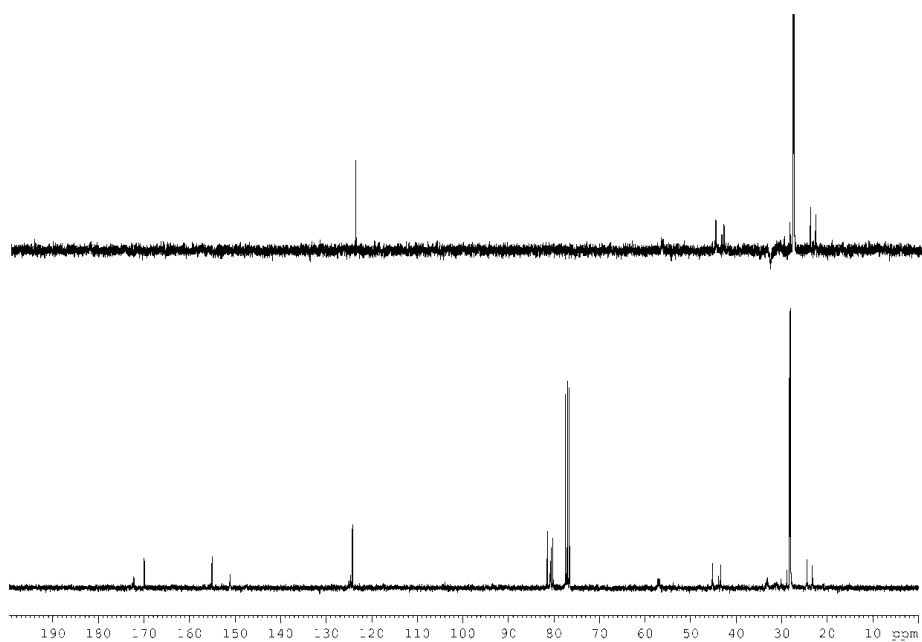
(1*S*,3*S*,5*S*,6*S*)-di-*tert*-Butyl-3-(*tert*-butylcarbamoyl)-2-azabicyclo[3.1.0]hexane-2,6-dicarboxylate (**165a**)

CDCl$_3$, 300 MHz
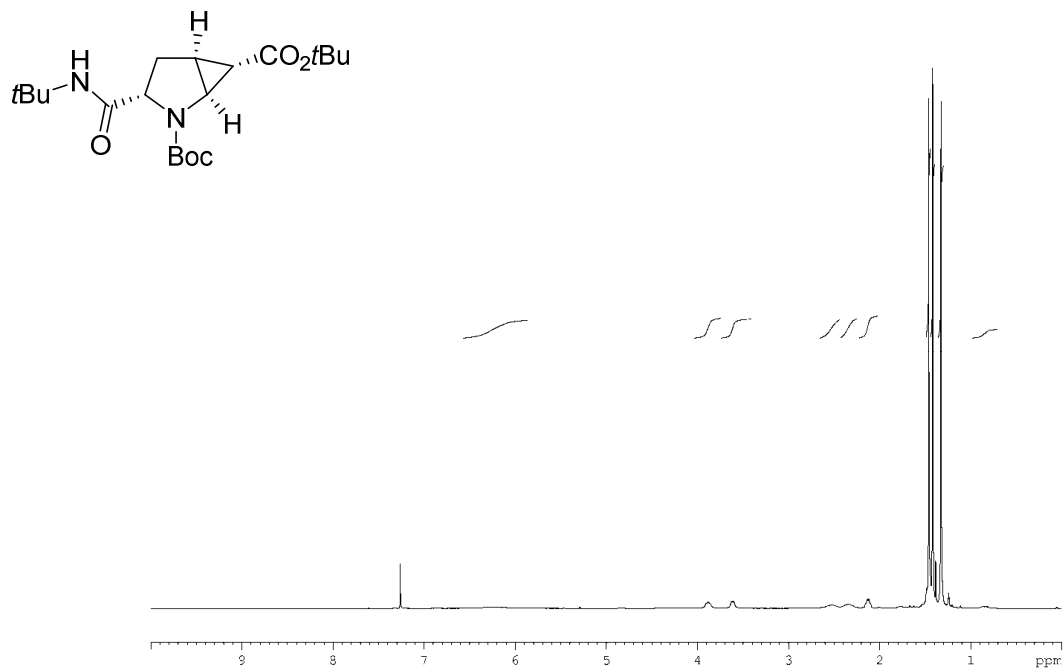
CDCl$_3$, 151 MHz
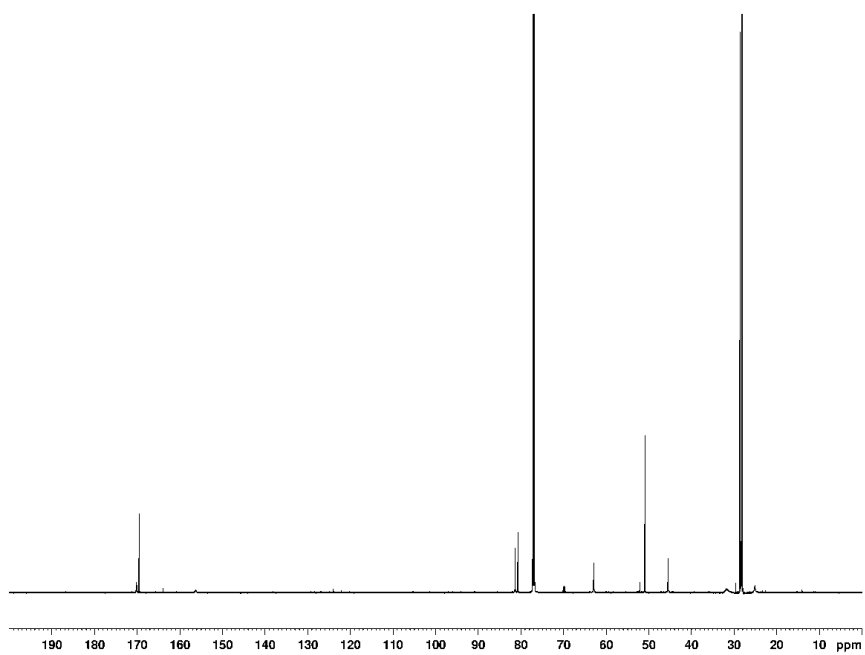
(1*S*,3*R*,5*S*,6*S*)-di-*tert*-Butyl-3-(*tert*-butylcarbamoyl)-2-azabicyclo[3.1.0]hexane-2,6-dicarboxylate (**165b**)

CDCl$_3$, 400 MHz, 223 K
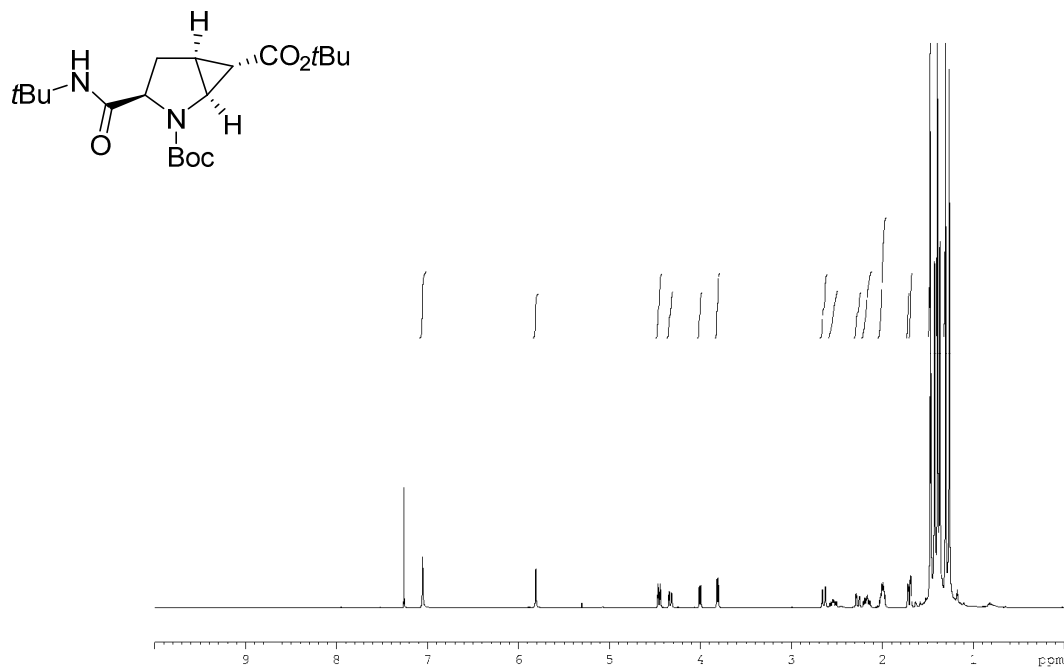
CDCl$_3$, 101 MHz, 223 K
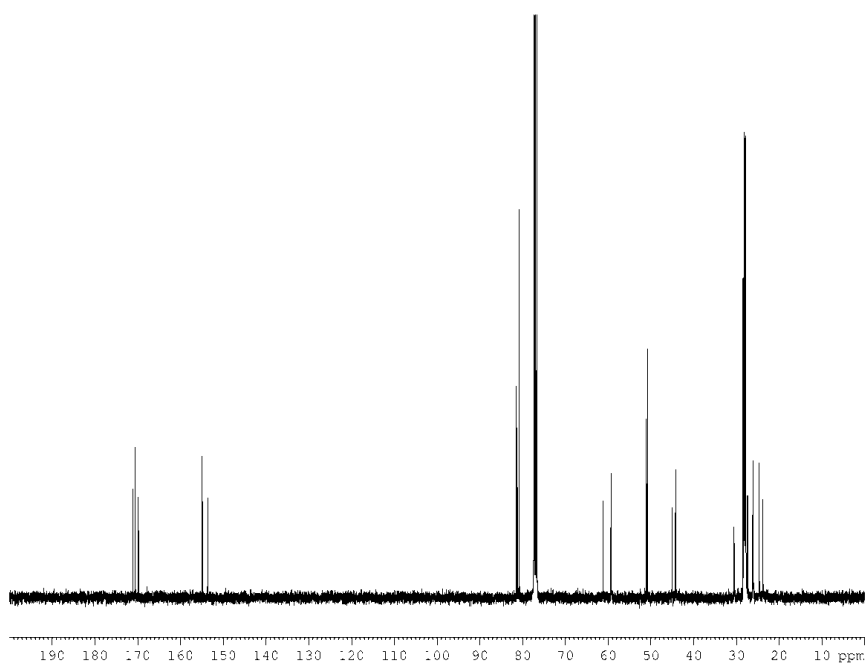
di-*tert*-Butyl-(1*S*,5*S*,6*S*)-3-(2,4,6-trimethoxyphenyl)-2-azabicyclo[3.1.0]hexane-2,6-dicarboxylate (**172**)

CDCl$_3$, 400 MHz
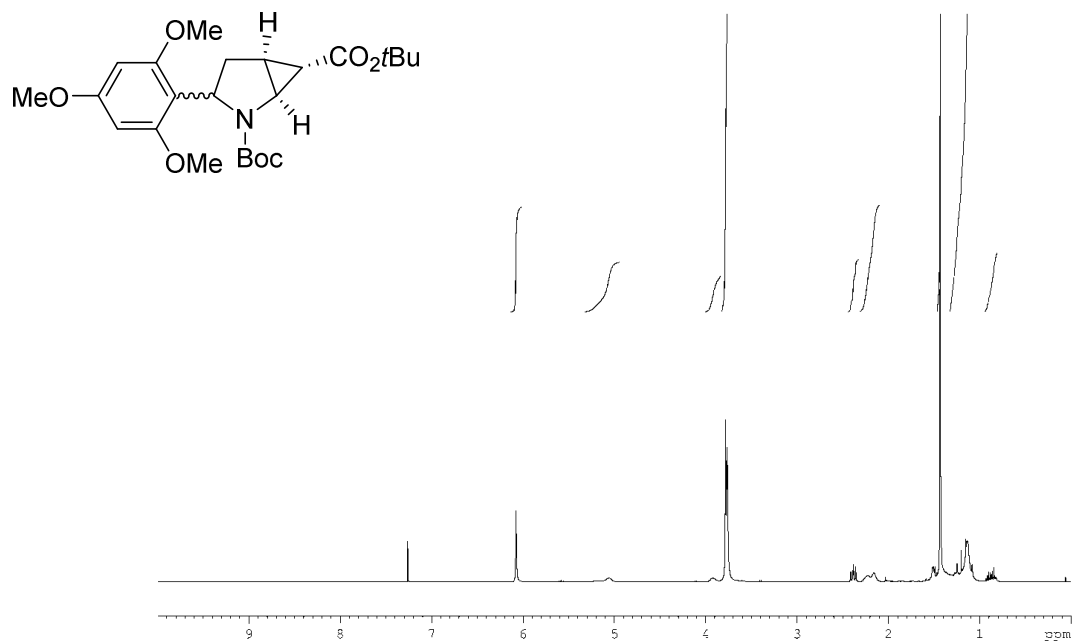
CDCl$_3$, 101 MHz
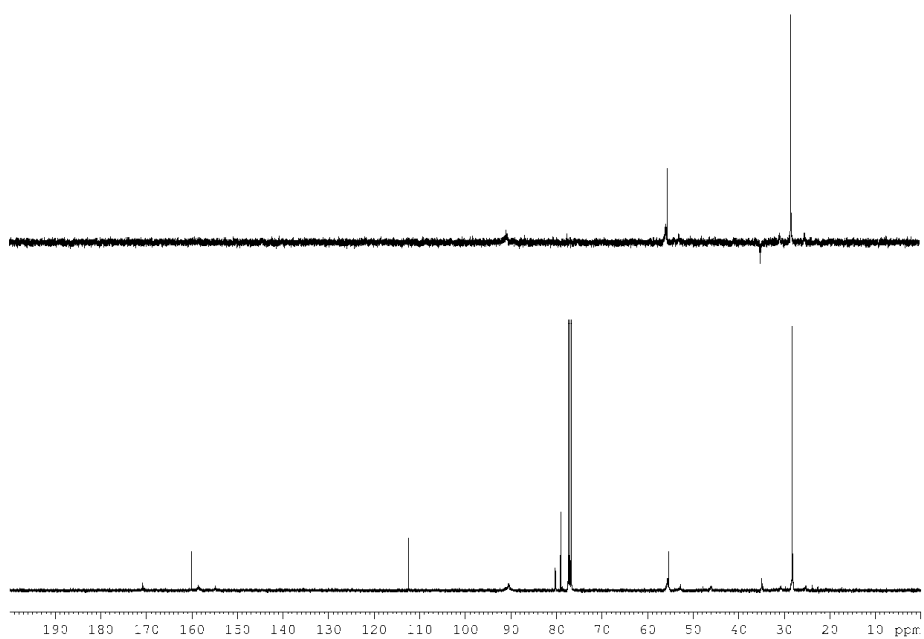
((1*S*,2*S*,3*S*,4*S*,6*S*,7*S*)-5-(*tert*-Butoxycarbonyl)-5-azatricyclo[4.1.0.02,4]heptane-3,7-diyl)bis(methylene) diacetate (**187**)

CDCl$_3$, 300 MHz

CDCl$_3$, 75 MHz

((1*S*,2*S*,3*S*,4*S*,6*S*,7*S*)-5-(*tert*-Butoxycarbonyl)-5-azatricyclo[4.1.0.02,4]heptane-3,7-diyl)bis(methylene) diacetate (**187**)
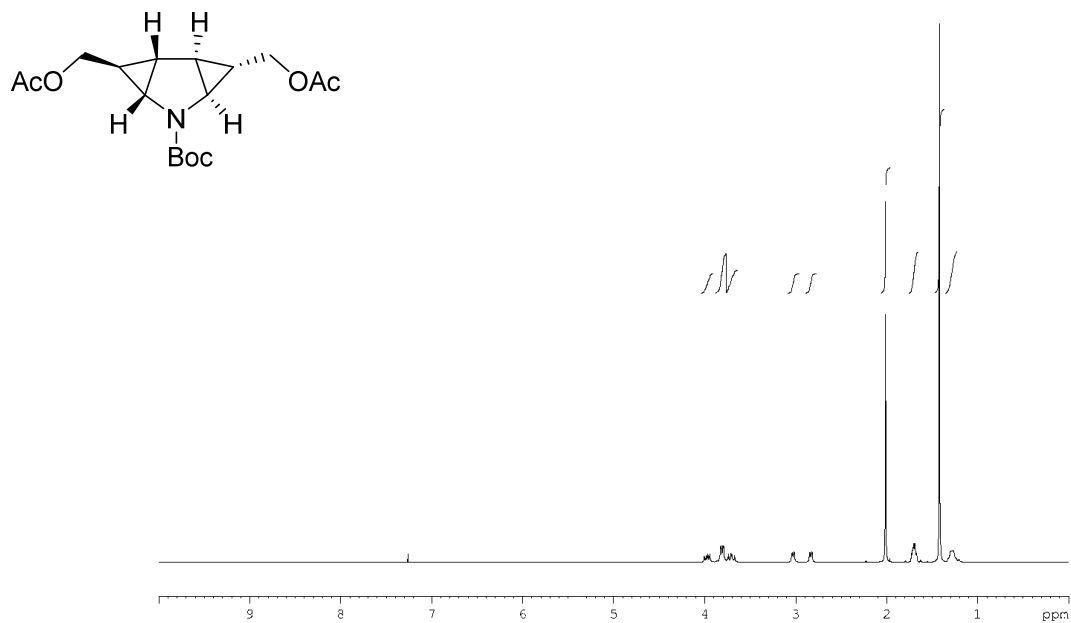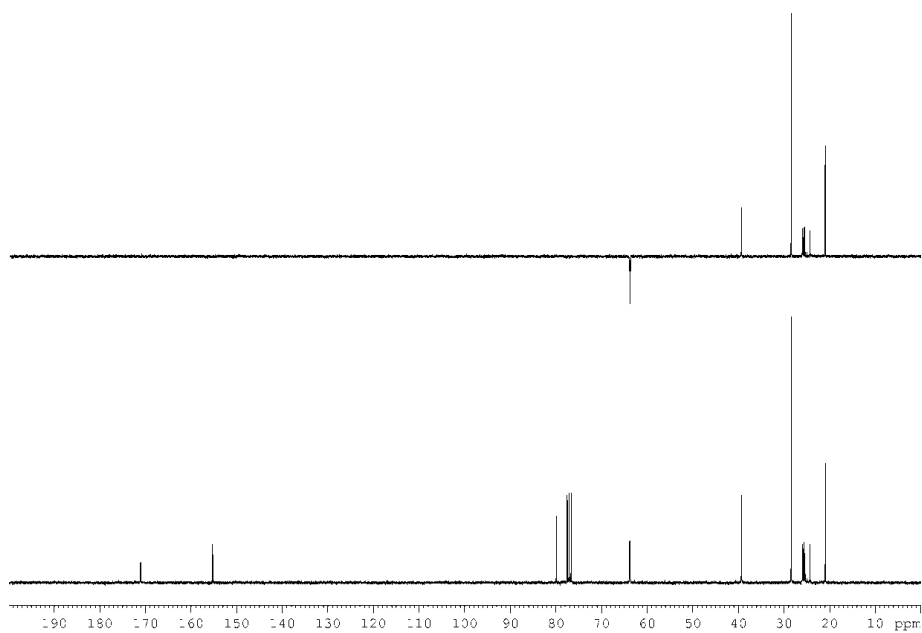
2 HPLC chromatograms

di-*tert*-Butyl-2-azabicyclo[3.1.0]hex-3-ene-2,6-dicarboxylate ((*rac*)-(±)-**103**)
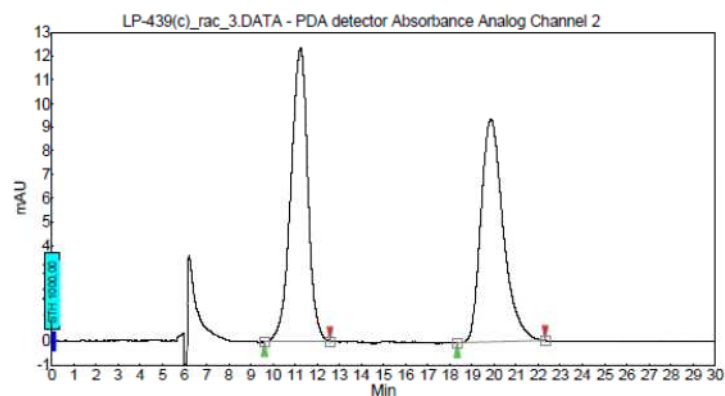
(1*S*,5*S*,6*S*)-di-*tert*-Butyl-2-azabicyclo[3.1.0]hex-3-ene-2,6-dicarboxylate ((*S*,*S*,*S*)-(-)-**103**)

(1*R*,5*R*,6*R*)-di-*tert*-Butyl-2-azabicyclo[3.1.0]hex-3-ene-2,6-dicarboxylate ((*R,R,R*)-(+)-**103**)

Vail : 77
Method : Phex-Cel2_98-2_0.5
Run time : 30,00 min
Inj. vol. : 10,000 µl

λ : 254 nm

Column : Phenomenex Lux Cellulose-2,
4.6 x 250 mm, 5 µm
Eluents : A = n-Heptane
B = i-Propanol
Flow : 0.5 ml/min

LP-mono-Cp_6.DATA - PDA detector Absorbance Analog Channel 2
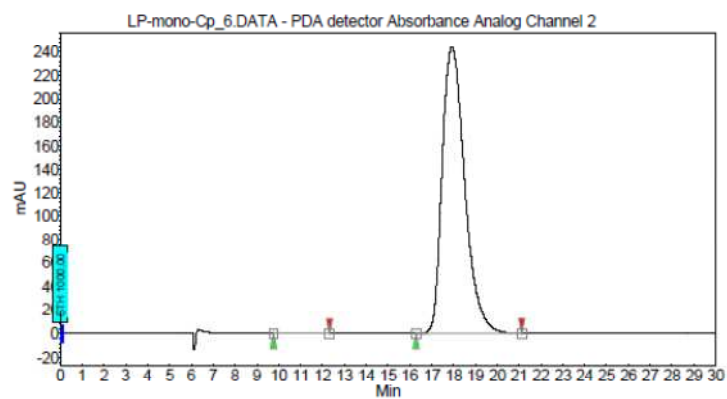
Peak Results :

Index	Name	Time [Min]	Quantity [% Area]	Height [mAU]	Area [mAU.Min]	Area % [%]
2	UNKNOWN	11,17	0,25	0,7	0,7	0,252
1	UNKNOWN	17,93	99,75	244,0	291,7	99,748
Total			100,00	244,8	292,4	100,000

tri-*tert*-Butyl-5-azatricyclo[4.1.0.0^{2,4}]heptane-3,5,7-tricarboxylate ((*rac*)-(±)-**104**)

Vail : 173
Method : Phex-Cel2_98-2_0.5
Run time : 60,00 min
Inj. vol. : 10,000 µl

λ : 215 nm

Column : Phenomenex Lux Cellulose-2,
4.6 x 250 mm, 5 µm
Eluents : A = n-Heptane
B = i-Propanol
Flow : 0.5 ml/min

LP-156(cryst)_rac_4.DATA - PDA detector Absorbance Analog Channel 1
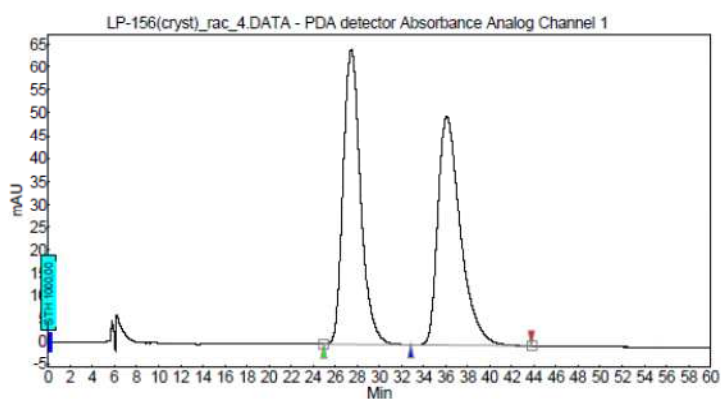
Peak Results :

Index	Name	Time [Min]	Quantity [% Area]	Height [mAU]	Area [mAU.Min]	Area % [%]
1	UNKNOWN	27,46	49,95	64,4	117,8	49,947
2	UNKNOWN	36,10	50,05	50,0	118,0	50,053
Total			100,00	114,3	235,8	100,000

(1*S*,2*S*,3*S*,4*S*,6*S*,7*S*)-tri-*tert*-Butyl-5-azatricyclo[4.1.0.0^{2,4}]heptane-3,5,7-tricarboxylate

((*S*,*S*,*S*,*S*,*S*,*S*)-(+)-**104**, 41% *ee*)

Vail : 186
Method : Phex-Cel2_98-2_0.5
Run time : 60,00 min
Inj. vol. : 10,000 µl

λ : 215 nm

Column : Phenomenex Lux Cellulose-2,
        4.6 x 250 mm, 5 µm
Eluents : A = n-Heptane
         B = i-Propanol
Flow : 0.5 ml/min

LP-102_R_1.DATA - PDA detector Absorbance Analog Channel 1
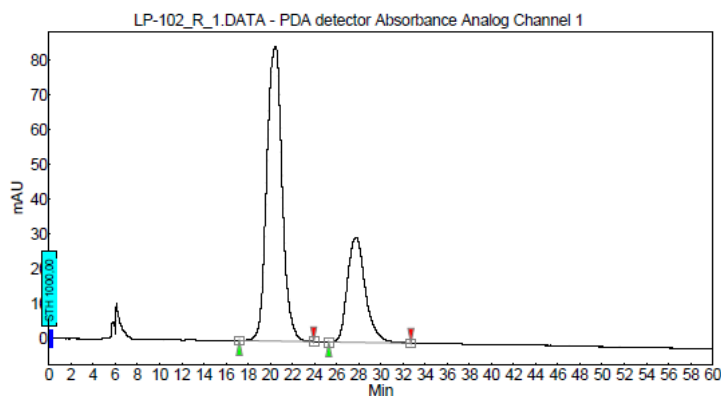
Peak Results :

Index	Name	Time [Min]	Quantity [% Area]	Height [mAU]	Area [mAU.Min]	Area % [%]
1	UNKNOWN	20,48	70,67	84,8	136,7	70,665
2	UNKNOWN	27,77	29,33	30,2	56,7	29,335
Total			100,00	115,1	193,4	100,000

di-*tert*-Butyl-2-azabicyclo[3.1.0]hexane-2,6-dicarboxylate ((*rac*)-(±)-**149**)

Vail : 65
Method : Phex-Cel2_70-30_0.5
Run time : 38,00 min
Inj. vol. : 10,000 µl

λ : 215 nm

Column : Phenomenex Lux Cellulose-2,
        4.6 x 250 mm, 5 µm
Eluents : A = n-Heptane
         B = i-Propanol
Flow : 0.5 ml/min

LP-442_rac_2.DATA - PDA detector Absorbance Analog Channel 1
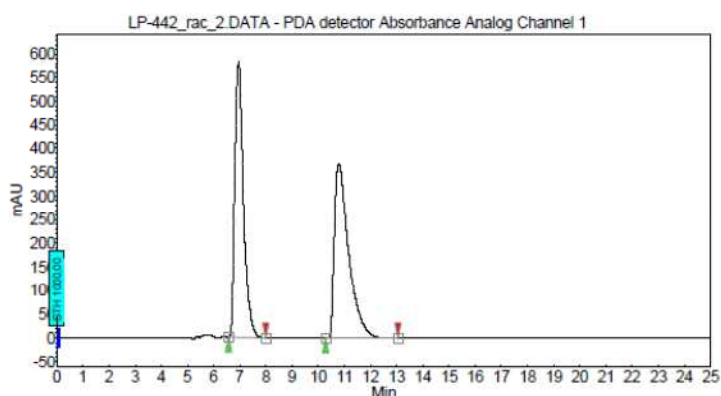
Peak Results :

Index	Name	Time [Min]	Quantity [% Area]	Height [mAU]	Area [mAU.Min]	Area % [%]
1	UNKNOWN	6,95	48,98	582,5	222,6	48,979
2	UNKNOWN	10,79	51,02	368,5	231,9	51,021
Total			100,00	950,9	454,5	100,000

149

(1*S*,5*S*,6*S*)-di-*tert*-Butyl-2-azabicyclo[3.1.0]hexane-2,6-dicarboxylate ((*S*,*S*,*S*)-(-)-**149**)

Vail : 145
Method : Phex-Cel2_70-30_0.5
Run time : 25,00 min
Inj. vol. : 10,000 µl

λ : 215 nm

Column : Phenomenex Lux Cellulose-2,
4.6 x 250 mm, 5 µm
Eluents : A = n-Heptane
B = i-Propanol
Flow : 0.5 ml/min

LP-448.DATA - PDA detector Absorbance Analog Channel 1
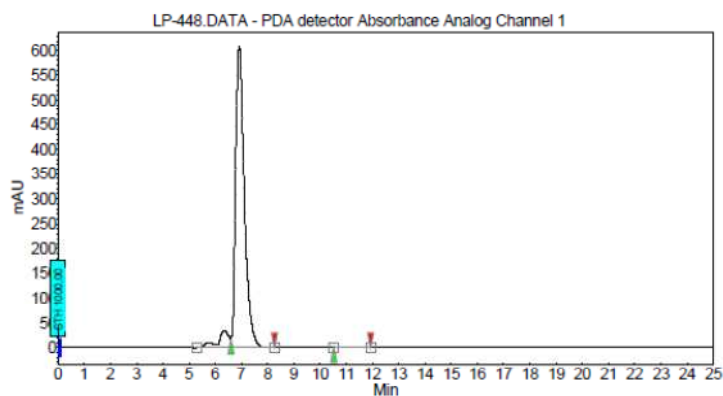
Peak Results :

Index	Name	Time [Min]	Quantity [% Area]	Height [mAU]	Area [mAU.Min]	Area % [%]
2	UNKNOWN	6,92	99,79	607,9	234,2	99,788
1	UNKNOWN	11,00	0,21	0,9	0,5	0,212
Total			100,00	608,8	234,7	100,000

tert-Butyl-3-(2-(*tert*-butoxy)-2-oxoethyl)pyrrolidine-1-carboxylate ((*rac*)-(±)-**150**)

Vail : 21
Method : NOT DEFINED
Run time : 0,00 min
Inj. vol. : 3,000 µl

Column : Phenomenex Lux Cellulose-1,
4.6 x 250 mm, 5 µm
Eluents : A = n-Heptane
B = i-Propanol
Flow : 0.5 ml/min

LP-446_rac_35.DATA - 200,00 nm
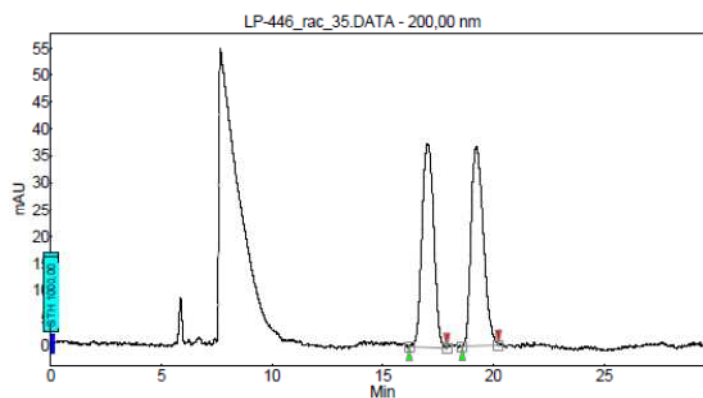
Peak Results :

Index	Name	Time [Min]	Quantity [% Area]	Height [mAU]	Area [mAU.Min]	Area % [%]
1	UNKNOWN	17,03	49,34	37,7	23,1	49,341
2	UNKNOWN	19,25	50,66	36,7	23,7	50,659
Total			100,00	74,3	46,8	100,000

(*S*)-*tert*-Butyl-3-(2-(*tert*-butoxy)-2-oxoethyl)pyrrolidine-1-carboxylate ((*S*)-(+)-**150**, 73% *ee*)

Vail : 22
Method : NOT DEFINED
Run time : 0,00 min
Inj. vol. : 3,000 µl

Column : Phenomenex Lux Cellulose-1,
    4.6 x 250 mm, 5 µm
Eluents : A = n-Heptane
    B = i-Propanol
Flow : 0.5 ml/min

LP-449.DATA - 200,00 nm
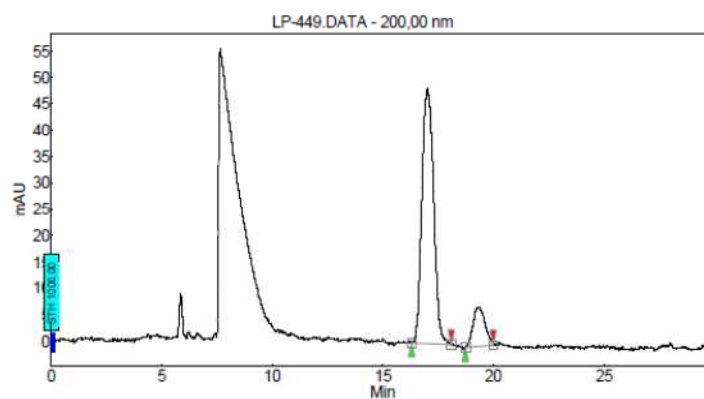
Peak Results :

| Index	Name	Time [Min]	Quantity [% Area]	Height [mAU]	Area [mAU.Min]	Area % [%]
1	UNKNOWN	17,03	86,46	48,3	29,6	86,465
2	UNKNOWN	19,31	13,54	7,5	4,6	13,535
Total			100,00	55,7	34,2	100,000

3 X-ray crystallographic data

(1*S*,5*S*,6*S*)-di-*tert*-Butyl-2-azabicyclo[3.1.0]hex-3-ene-2,6-dicarboxylate (((*S*,*S*,*S*)-(-)-**103**)
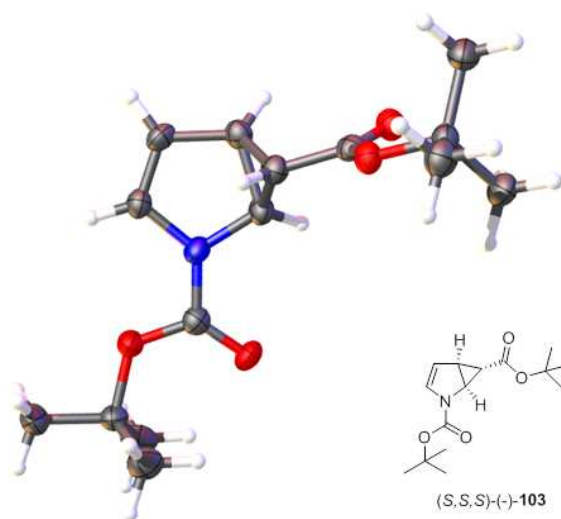
(*S*,*S*,*S*)-(-)-**103**

Table 1. Crystal data and structure refinement for (*S*,*S*,*S*)-(-)-**103**.

Empirical formula	$C_{15}H_{23}NO_4$
Formula weight	281.34
Temperature/K	123.0
Crystal system	monoclinic
Space group	$P2_1$
a/Å	9.4639(3)
b/Å	6.1799(2)
c/Å	13.1692(5)
α/°	90
β/°	90.131(4)
γ/°	90
Volume/Å^3	770.21(5)
Z	2
ρ_{calc}mg/mm^3	1.213
m/mm^{-1}	0.715
F(000)	304.0
Crystal size/mm^3	$0.53 \times 0.081 \times 0.0264$
Radiation	CuKα (λ = 1.54184)
2Θ range for data collection	6.72 to 149.3°
Index ranges	$-11 \leq h \leq 11, -6 \leq k \leq 7, -16 \leq l \leq 14$
Reflections collected	3296
Independent reflections	2115 [R_{int} = 0.0341, R_{sigma} = 0.0469]

Data/restraints/parameters	2115/1/187
Goodness-of-fit on F^2	1.104
Final R indexes [I>=2σ (I)]	$R_1 = 0.0610$, $wR_2 = 0.1569$
Final R indexes [all data]	$R_1 = 0.0630$, $wR_2 = 0.1602$
Largest diff. peak/hole / e $\mathring{A}^{-3}$	0.36/-0.29
Flack parameter	0.0(3)

Table 2. Fractional atomic coordinates ($\times 10^4$) and equivalent isotropic displacement parameters ($\mathring{A}^2 \times 10^3$) for (*S*,*S*,*S*)-(-)-**103**. U_{eq} is defined as 1/3 of the trace of the orthogonalised U_{IJ} tensor.

Atom	x	y	z	U(eq)
O1	-8000(2)	-8004(4)	846.3(15)	35.3(6)
O2	-7734(2)	-4482(3)	376.9(15)	34.5(6)
O3	-7369(2)	-4381(3)	-3711.7(14)	31.4(5)
O4	-5183(2)	-3471(4)	-3128.7(16)	34.8(6)
N1	-6701(3)	-7226(4)	-498.4(18)	31.3(7)
C1	-7512(3)	-6395(5)	264(2)	30.6(8)
C2	-6332(3)	-9414(5)	-675(2)	29.9(7)
C3	-5449(3)	-9566(5)	-1450(2)	31.8(8)
C4	-5179(3)	-7407(5)	-1889(2)	32.1(8)
C5	-6031(3)	-5882(5)	-1248(2)	30.7(7)
C6	-6497(3)	-6301(5)	-2341(2)	31.1(7)
C7	-6252(3)	-4558(5)	-3088.7(18)	29.2(7)
C8	-7402(3)	-2753(5)	-4532(2)	30.6(7)
C9	-6213(4)	-3113(6)	-5289(2)	37.9(9)
C10	-7367(4)	-484(5)	-4085(2)	36.7(8)
C11	-8837(3)	-3181(6)	-5022(2)	38.2(8)
C12	-8986(3)	-7606(5)	1684(2)	32.8(8)
C13	-10304(3)	-6475(6)	1293(3)	42.8(9)
C14	-8242(3)	-6328(7)	2510(2)	43.1(9)
C15	-9359(5)	-9876(6)	2033(3)	49.0(11)

Table 3. Anisotropic displacement parameters ($\mathring{A}^2 \times 10^3$) for (*S*,*S*,*S*)-(-)-**103**. The anisotropic displacement factor exponent takes the form: $-2\pi^2[h^2a^{*2}U_{11}+2hka^*b^*U_{12}+\ldots]$.

Atom	U_{11}	U_{22}	U_{33}	U_{23}	U_{13}	U_{12}
O1	44.1(11)	27.7(10)	34.1(9)	1.3(8)	9.6(8)	2.4(9)
O2	40.2(10)	23.2(10)	40.2(10)	-3.0(9)	-1.0(9)	6.2(9)

O3	34.4(9)	27.6(10)	32.2(9)	0.9(8)	-2.4(8)	-4.9(8)
O4	35.9(10)	32.1(11)	36.3(9)	-0.2(8)	0.1(8)	-6.3(9)
N1	40.0(12)	24.3(12)	29.6(10)	-3.2(9)	1.9(9)	2.2(10)
C1	30.8(13)	31.5(15)	29.5(11)	0.4(11)	-2.5(10)	0.8(11)
C2	33.6(13)	24.6(13)	31.4(12)	0.7(11)	-2.1(10)	-1.9(11)
C3	34.1(13)	26.8(14)	34.4(12)	-2.8(11)	-2.4(10)	7.4(12)
C4	29.2(13)	32.5(14)	34.6(12)	1.1(12)	0.9(11)	-3.4(12)
C5	35.8(13)	24.8(13)	31.5(12)	-0.6(10)	-0.4(11)	-3.4(11)
C6	32.5(13)	27.9(13)	32.8(12)	-1.6(11)	0.6(10)	-3.1(11)
C7	33.0(13)	26.1(12)	28.5(11)	-6.9(10)	0.8(10)	-0.6(12)
C8	36.5(14)	25.1(13)	30.3(11)	1.7(10)	1.0(11)	-0.8(11)
C9	44.9(16)	35.4(16)	33.3(13)	-0.6(12)	2.8(12)	1.5(13)
C10	42.5(15)	26.6(14)	41.1(14)	-4.2(11)	1.3(12)	-1.5(12)
C11	41.2(15)	35.1(15)	38.4(13)	1.4(13)	-6.4(12)	0.7(13)
C12	35.1(13)	31.2(14)	32.2(12)	-1.1(11)	6.0(11)	2.9(13)
C13	33.4(15)	46.0(18)	49.0(16)	-4.0(15)	-1.4(13)	2.5(15)
C14	36.2(15)	58(2)	35.1(13)	-6.3(15)	2.3(12)	0.5(15)
C15	58(2)	37.4(18)	51.8(17)	7.6(15)	20.8(16)	0.1(17)

Table 4. Bond lengths for (*S*,*S*,*S*)-(-)-**103**.

Atom	Atom	Length/Å	Atom	Atom	Length/Å
O1	C1	1.339(4)	C4	C5	1.501(4)
O1	C12	1.467(3)	C4	C6	1.541(4)
O2	C1	1.210(4)	C5	C6	1.527(4)
O3	C7	1.341(3)	C6	C7	1.478(4)
O3	C8	1.477(3)	C8	C9	1.521(4)
O4	C7	1.216(4)	C8	C10	1.521(4)
N1	C1	1.365(4)	C8	C11	1.525(4)
N1	C2	1.416(4)	C12	C13	1.519(4)
N1	C5	1.439(4)	C12	C14	1.516(4)
C2	C3	1.324(4)	C12	C15	1.518(5)
C3	C4	1.477(4)			

Table 5. Bond angles for (*S,S,S*)-(-)-**103**.

Atom	Atom	Atom	Angle/°	Atom	Atom	Atom	Angle/°
C1	O1	C12	121.8(2)	C4	C6	C7	116.9(2)
C7	O3	C8	121.2(2)	C5	C6	C7	117.3(2)
C1	N1	C2	128.3(2)	O3	C7	O4	125.7(3)
C1	N1	C5	122.5(2)	O3	C7	C6	110.0(2)
C2	N1	C5	109.2(2)	O4	C7	C6	124.3(3)
O1	C1	O2	126.5(3)	O3	C8	C9	111.4(2)
O1	C1	N1	109.7(3)	O3	C8	C10	110.2(2)
O2	C1	N1	123.8(3)	O3	C8	C11	102.1(2)
N1	C2	C3	110.5(3)	C9	C8	C10	111.9(3)
C2	C3	C4	110.4(3)	C9	C8	C11	110.9(2)
C3	C4	C5	104.7(2)	C10	C8	C11	110.0(3)
C3	C4	C6	114.3(2)	O1	C12	C13	110.2(2)
C5	C4	C6	60.23(18)	O1	C12	C14	109.4(2)
N1	C5	C4	105.2(2)	O1	C12	C15	102.8(3)
N1	C5	C6	115.0(2)	C13	C12	C14	112.5(3)
C4	C5	C6	61.17(18)	C13	C12	C15	109.7(3)
C4	C6	C5	58.61(18)	C14	C12	C15	111.8(3)

Table 6. Hydrogen bonds for (*S,S,S*)-(-)-**103**.

D	H	A	d(D-H)/Å	d(H-A)/Å	d(D-A)/Å	D-H-A/°
C3	H3	O4[1]	0.9500	2.4800	3.283(4)	142.00
C9	H9A	O4	0.9800	2.4300	3.013(3)	118.00
C10	H10C	O4	0.9800	2.4700	3.042(4)	117.00
C13	H13A	O2	0.9800	2.3900	2.984(4)	118.00
C13	H13C	O2[2]	0.9800	2.4700	3.423(4)	165.00
C14	H14C	O2	0.9800	2.4900	3.071(4)	118.00

[1]+X,-1+Y,+Z; [2]-2-X,-1/2+Y,-Z

Table 7. Torsion angles for (*S,S,S*)-(-)-**103**.

A	B	C	D	Angle/°	A	B	C	D	Angle/°
N1	C2	C3	C4	-1.7(3)	C3	C4	C6	C7	-159.4(2)
N1	C5	C6	C4	-94.2(3)	C4	C5	C6	C7	-106.4(3)
N1	C5	C6	C7	159.5(3)	C4	C6	C7	O3	154.1(2)

C1	O1	C12	C13	57.0(3)	C4	C6	C7	O4	-25.3(4)
C1	O1	C12	C14	-67.2(3)	C5	N1	C1	O1	180.0(2)
C1	O1	C12	C15	173.9(3)	C5	N1	C1	O2	-0.2(4)
C1	N1	C2	C3	-175.7(3)	C5	N1	C2	C3	2.1(3)
C1	N1	C5	C4	176.3(3)	C5	C4	C6	C7	107.1(3)
C1	N1	C5	C6	-118.8(3)	C5	C6	C7	O3	-139.2(2)
C2	N1	C1	O1	-2.5(4)	C5	C6	C7	O4	41.4(4)
C2	N1	C1	O2	177.3(3)	C6	C4	C5	N1	110.5(3)
C2	N1	C5	C4	-1.6(3)	C7	O3	C8	C9	61.2(3)
C2	N1	C5	C6	63.3(3)	C7	O3	C8	C10	-63.6(3)
C2	C3	C4	C5	0.6(3)	C7	O3	C8	C11	179.6(2)
C2	C3	C4	C6	-63.0(3)	C8	O3	C7	O4	-0.7(4)
C3	C4	C5	N1	0.6(3)	C8	O3	C7	C6	179.9(2)
C3	C4	C5	C6	-109.9(2)	C12	O1	C1	O2	4.5(4)
C3	C4	C6	C5	93.6(3)	C12	O1	C1	N1	-175.6(2)

Table 8. Hydrogen atom coordinates ($\text{Å}\times10^4$) and isotropic displacement parameters ($\text{Å}^2\times10^3$) for (S,S,S)-(-)-**103**.

Atom	x	y	z	U(eq)
H2	-6672	-10606	-291	36
H3	-5046	-10878	-1690	38
H4	-4211	-6998	-2125	39
H5	-5634	-4442	-1051	37
H6	-7354	-7222	-2442	37
H9A	-5302	-2873	-4953	57
H9B	-6317	-2098	-5856	57
H9C	-6256	-4601	-5546	57
H10A	-8134	-325	-3592	55
H10B	-7487	581	-4630	55
H10C	-6458	-245	-3745	55
H11A	-8869	-4671	-5275	57
H11B	-8979	-2175	-5589	57
H11C	-9585	-2969	-4518	57
H13A	-10055	-5027	1049	64
H13B	-10994	-6353	1844	64
H13C	-10714	-7316	735	64
H14A	-7383	-7095	2719	65
H14B	-8872	-6170	3095	65

H14C	-7990	-4893	2250	65
H15A	-9770	-10686	1465	74
H15B	-10044	-9794	2588	74
H15C	-8503	-10612	2270	74

(1*S*,2*S*,3*S*,4*S*,6*S*,7*S*)-tri-*tert*-Butyl-5-azatricyclo[4.1.0.0^{2,4}]heptane-3,5,7-tricarboxylate (**104**)
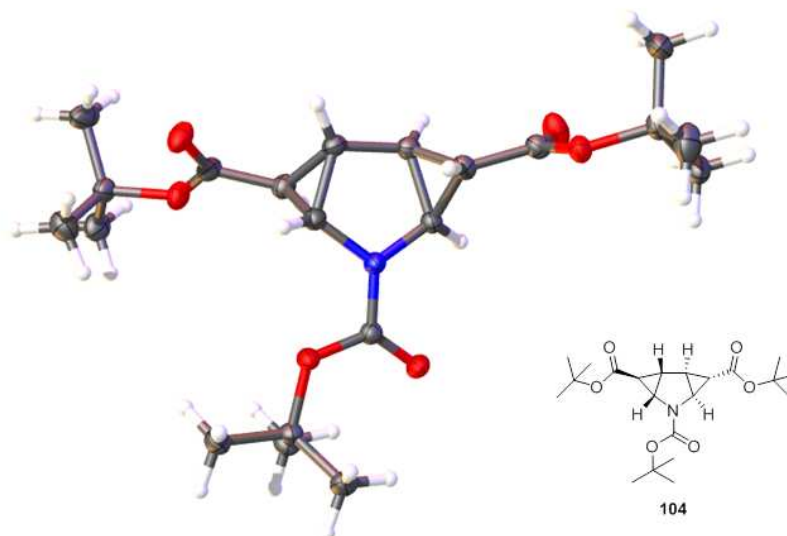
Table 1. Crystal data and structure refinement for **104**.

Empirical formula	$C_{21}H_{33}NO_6$
Formula weight	395.48
Temperature/K	123.0
Crystal system	monoclinic
Space group	P2$_1$/c
a/Å	5.7733(2)
b/Å	9.1531(4)
c/Å	41.7797(19)
α/°	90
β/°	91.716(4)
γ/°	90
Volume/Å^3	2206.80(16)
Z	4
ρ_{calc}mg/mm^3	1.190
m/mm^{-1}	0.708
F(000)	856.0
Crystal size/mm^3	$0.3002 \times 0.1264 \times 0.0446$
Radiation	CuKα (λ = 1.54184)
2Θ range for data collection	8.46 to 150.78°
Index ranges	-7 ≤ h ≤ 5, -11 ≤ k ≤ 10, -52 ≤ l ≤ 51
Reflections collected	8423
Independent reflections	4381 [R$_{int}$ = 0.0306, R$_{sigma}$ = 0.0357]
Data/restraints/parameters	4381/0/262

Goodness-of-fit on F^2	1.037
Final R indexes [I>=2σ (I)]	$R_1 = 0.0498$, $wR_2 = 0.1337$
Final R indexes [all data]	$R_1 = 0.0564$, $wR_2 = 0.1421$
Largest diff. peak/hole / e Å^{-3}	0.24/-0.34
Flack parameter	.

Table 2. Fractional atomic coordinates ($\times 10^4$) and equivalent isotropic displacement parameters (Å$^2 \times 10^3$) for **104**. U_{eq} is defined as 1/3 of the trace of the orthogonalised U_{IJ} tensor.

Atom	x	y	z	U(eq)
O1	9298.9(16)	7580.4(12)	646.7(2)	23.2(3)
O2	5881.0(17)	8358.1(12)	849.4(2)	26.2(3)
O3	12033.9(18)	3358.8(11)	1108.9(3)	27.4(3)
O4	14891.9(18)	4860.0(13)	1298.7(3)	33.4(3)
O5	8016.3(18)	11151.3(11)	1975.2(2)	24.9(3)
O6	6120(2)	9064.8(13)	2100.3(3)	38.1(4)
N1	9050(2)	7899.7(13)	1170.1(3)	21.3(3)
C1	7880(2)	7966.8(14)	883.0(3)	20.8(4)
C2	11206(2)	7129.6(15)	1224.6(3)	22.0(4)
C3	10923(2)	5544.1(16)	1333.3(3)	24.6(4)
C4	12863(3)	4568.6(16)	1251.7(3)	25.2(4)
C5	13575(3)	2217.9(16)	983.6(3)	27.0(4)
C6	11860(3)	1128.8(18)	840.6(4)	34.7(5)
C7	14997(3)	1544.3(19)	1256.0(4)	39.2(5)
C8	15081(3)	2857(2)	727.2(4)	37.5(5)
C9	11395(2)	6761.7(16)	1573.0(3)	22.9(4)
C10	9286(2)	7372.8(16)	1725.8(3)	23.6(4)
C11	7849(2)	8057.8(15)	1466.0(3)	21.2(4)
C12	9069(3)	9028.2(16)	1715.8(3)	23.4(4)
C13	7564(3)	9723.0(16)	1954.0(3)	24.7(4)
C14	6848(3)	12092.5(17)	2210.3(3)	28.2(4)
C15	7772(3)	13601.1(19)	2130.0(5)	41.7(5)
C16	7618(3)	11625(2)	2544.0(4)	41.8(5)
C17	4237(3)	12068(2)	2162.9(4)	36.0(5)
C18	8389(2)	7500.2(16)	314.9(3)	22.8(4)
C19	10538(3)	7119.5(18)	130.6(3)	30.1(4)
C20	6615(3)	6284.6(18)	289.1(4)	31.6(4)
C21	7419(3)	8972.3(18)	206.3(4)	30.7(4)

Table 3. Anisotropic displacement parameters ($\text{Å}^2 \times 10^3$) for **104**. The anisotropic displacement factor exponent takes the form: $-2\pi^2[h^2a^{*2}U_{11}+2hka^*b^*U_{12}+\ldots]$.

Atom	U_{11}	U_{22}	U_{33}	U_{23}	U_{13}	U_{12}
O1	18.7(5)	31.0(5)	19.8(5)	-2.8(4)	-1.9(4)	3.1(4)
O2	20.2(5)	32.8(6)	25.5(5)	-0.5(4)	-1.7(4)	6.3(4)
O3	24.1(5)	21.8(5)	36.3(5)	-5.3(4)	-0.8(4)	2.1(4)
O4	22.6(6)	30.7(6)	46.5(6)	-8.4(5)	-6.5(4)	4.3(4)
O5	25.8(5)	23.3(5)	25.7(5)	-4.2(4)	2.3(4)	0.6(4)
O6	44.9(7)	30.4(6)	40.0(6)	-3.0(5)	19.9(5)	-5.1(5)
N1	18.0(6)	26.1(6)	19.6(5)	-1.3(4)	-0.8(4)	2.6(4)
C1	20.7(7)	20.2(6)	21.4(6)	-0.7(5)	-0.8(5)	0.3(5)
C2	19.2(7)	23.9(7)	22.6(6)	-1.8(5)	-1.9(5)	1.1(5)
C3	22.5(7)	23.4(7)	27.8(6)	-1.7(5)	-1.8(5)	0.3(5)
C4	24.2(7)	23.0(7)	28.1(6)	0.3(5)	-3.9(5)	2.0(5)
C5	29.9(8)	23.4(7)	27.6(7)	-2.2(5)	-1.1(6)	5.9(6)
C6	37.5(9)	26.8(8)	39.6(8)	-7.6(6)	-2.7(7)	1.6(6)
C7	53.7(11)	29.3(8)	33.7(8)	-3.1(6)	-12.1(7)	12.2(8)
C8	39.3(10)	40.9(9)	32.5(8)	-2.6(7)	6.1(7)	-0.6(7)
C9	22.2(7)	23.6(7)	22.8(6)	0.9(5)	-3.2(5)	1.7(5)
C10	25.3(7)	23.6(7)	21.7(6)	0.2(5)	-0.8(5)	0.2(5)
C11	20.7(7)	22.3(6)	20.5(6)	-1.6(5)	1.0(5)	1.0(5)
C12	25.4(7)	23.1(7)	21.9(6)	-1.5(5)	1.8(5)	-0.6(5)
C13	27.0(7)	25.1(7)	21.9(6)	-0.6(5)	0.9(5)	-0.7(6)
C14	29.8(8)	28.2(7)	26.4(7)	-7.6(6)	-0.2(6)	5.3(6)
C15	40.5(10)	29.1(8)	55.7(10)	-10.7(7)	6.0(8)	0.8(7)
C16	48.7(11)	49.9(10)	26.3(7)	-10.9(7)	-6.5(7)	18.4(8)
C17	30.0(9)	42.7(9)	35.3(8)	-8.8(7)	0.1(6)	6.3(7)
C18	20.8(7)	27.4(7)	19.9(6)	-1.5(5)	-3.4(5)	1.6(5)
C19	28.7(8)	38.2(8)	23.3(6)	-2.9(6)	1.3(5)	3.8(6)
C20	28.4(8)	32.4(8)	33.6(7)	-7.0(6)	-3.8(6)	-3.3(6)
C21	34.1(8)	31.7(8)	26.3(7)	3.7(6)	-0.7(6)	6.4(6)

Table 4. Bond lengths for **104**.

Atom	Atom	Length/Å	Atom	Atom	Length/Å
O1	C1	1.3488(15)	C3	C9	1.5175(19)
O1	C18	1.4695(15)	C5	C6	1.515(2)
O2	C1	1.2125(15)	C5	C7	1.514(2)

O3	C4	1.3395(18)	C5	C8	1.517(2)
O3	C5	1.4779(19)	C9	C10	1.4998(17)
O4	C4	1.212(2)	C10	C11	1.4851(18)
O5	C13	1.3356(18)	C10	C12	1.521(2)
O5	C14	1.4838(18)	C11	C12	1.5265(19)
O6	C13	1.209(2)	C12	C13	1.484(2)
N1	C1	1.3603(17)	C14	C15	1.521(2)
N1	C2	1.4426(17)	C14	C16	1.512(2)
N1	C11	1.4427(17)	C14	C17	1.515(2)
C2	C3	1.531(2)	C18	C19	1.520(2)
C2	C9	1.4949(18)	C18	C20	1.514(2)
C3	C4	1.480(2)	C18	C21	1.523(2)

Table 5. Bond angles for **104**.

Atom	Atom	Atom	Angle/°	Atom	Atom	Atom	Angle/°
C1	O1	C18	119.72(10)	C3	C9	C10	115.01(10)
C4	O3	C5	122.08(12)	C9	C10	C11	106.81(10)
C13	O5	C14	121.36(11)	C9	C10	C12	115.29(12)
C1	N1	C2	124.37(11)	C11	C10	C12	61.02(9)
C1	N1	C11	120.82(11)	N1	C11	C10	108.16(10)
C2	N1	C11	110.38(11)	N1	C11	C12	114.86(11)
O1	C1	O2	126.12(11)	C10	C11	C12	60.64(9)
O1	C1	N1	109.71(10)	C10	C12	C11	58.33(9)
O2	C1	N1	124.14(12)	C10	C12	C13	117.26(12)
N1	C2	C3	114.25(10)	C11	C12	C13	116.13(14)
N1	C2	C9	107.53(10)	O5	C13	O6	126.20(14)
C3	C2	C9	60.19(9)	O5	C13	C12	110.29(13)
C2	C3	C4	114.54(11)	O6	C13	C12	123.50(14)
C2	C3	C9	58.73(9)	O5	C14	C15	102.22(12)
C4	C3	C9	118.22(11)	O5	C14	C16	108.61(13)
O3	C4	O4	125.81(14)	O5	C14	C17	112.04(12)
O3	C4	C3	109.79(13)	C15	C14	C16	111.39(14)
O4	C4	C3	124.36(13)	C15	C14	C17	109.80(14)
O3	C5	C6	102.20(13)	C16	C14	C17	112.35(13)
O3	C5	C7	109.88(11)	O1	C18	C19	102.43(10)
O3	C5	C8	109.97(12)	O1	C18	C20	109.02(11)
C6	C5	C7	111.20(13)	O1	C18	C21	110.78(12)
C6	C5	C8	110.91(12)	C19	C18	C20	110.86(12)

C7	C5	C8	112.23(14)	C19	C18	C21	110.50(12)
C2	C9	C3	61.08(9)	C20	C18	C21	112.77(12)
C2	C9	C10	107.09(10)				

Table 6. Hydrogen bonds for **104**.

D	H	A	d(D-H)/Å	d(H-A)/Å	d(D-A)/Å	D-H-A/°
C2	H2	O2[1]	1.0000	2.3600	3.3556(16)	175.00
C3	H3	O4[2]	1.0000	2.5700	3.5365(16)	163.00
C6	H6C	O2[3]	0.9800	2.5700	3.438(2)	148.00
C7	H7B	O4	0.9800	2.4600	3.041(2)	117.00
C7	H7C	O2[3]	0.9800	2.5500	3.421(2)	147.00
C8	H8B	O4	0.9800	2.4600	3.015(2)	115.00
C16	H16B	O6	0.9800	2.5400	3.095(2)	115.00
C16	H16C	O6[4]	0.9800	2.5800	3.471(2)	151.00
C17	H17B	O6	0.9800	2.3700	2.970(2)	119.00
C20	H20A	O2	0.9800	2.4600	3.0530(19)	118.00
C21	H21B	O2	0.9800	2.3400	2.9097(19)	116.00

[1]1+X,+Y,+Z; [2]-1+X,+Y,+Z; [3]1+X,-1+Y,+Z; [4]1-X,1/2+Y,1/2-Z

Table 7. Torsion angles for **104**.

A	B	C	D	Angle/°	A	B	C	D	Angle/°
N1	C2	C3	C4	153.63(11)	C4	C3	C9	C10	-160.49(12)
N1	C2	C3	C9	-97.05(12)	C5	O3	C4	O4	-1.1(2)
N1	C2	C9	C3	108.39(11)	C5	O3	C4	C3	176.50(11)
N1	C2	C9	C10	-1.21(14)	C9	C2	C3	C4	-109.32(12)
N1	C11	C12	C10	-97.67(12)	C9	C3	C4	O3	163.68(12)
N1	C11	C12	C13	155.07(12)	C9	C3	C4	O4	-18.7(2)
C1	O1	C18	C19	177.06(12)	C9	C10	C11	N1	-1.19(15)
C1	O1	C18	C20	-65.45(16)	C9	C10	C11	C12	-110.04(12)
C1	O1	C18	C21	59.20(15)	C9	C10	C12	C11	95.97(12)
C1	N1	C2	C3	-91.36(15)	C9	C10	C12	C13	-158.70(13)
C1	N1	C2	C9	-155.93(12)	C10	C11	C12	C13	-107.26(13)
C1	N1	C11	C10	157.83(12)	C10	C12	C13	O5	163.34(12)
C1	N1	C11	C12	-136.80(13)	C10	C12	C13	O6	-17.9(2)
C2	N1	C1	O1	-17.02(17)	C11	N1	C1	O1	-171.12(11)

C2	N1	C1	O2	164.89(13)	C11	N1	C1	O2	10.8(2)
C2	N1	C11	C10	0.45(15)	C11	N1	C2	C3	65.05(14)
C2	N1	C11	C12	65.82(15)	C11	N1	C2	C9	0.48(15)
C2	C3	C4	O3	-130.06(12)	C11	C10	C12	C13	105.33(15)
C2	C3	C4	O4	47.61(18)	C11	C12	C13	O5	-130.55(13)
C2	C3	C9	C10	96.48(12)	C11	C12	C13	O6	48.3(2)
C2	C9	C10	C11	1.46(15)	C12	C10	C11	N1	108.86(12)
C2	C9	C10	C12	-63.90(14)	C13	O5	C14	C15	-176.27(13)
C3	C2	C9	C10	-109.60(11)	C13	O5	C14	C16	65.91(17)
C3	C9	C10	C11	-64.03(15)	C13	O5	C14	C17	-58.78(17)
C3	C9	C10	C12	-129.39(12)	C14	O5	C13	O6	4.9(2)
C4	O3	C5	C6	-178.49(13)	C14	O5	C13	C12	-176.37(12)
C4	O3	C5	C7	63.37(17)	C18	O1	C1	O2	-4.9(2)
C4	O3	C5	C8	-60.65(17)	C18	O1	C1	N1	177.03(11)
C4	C3	C9	C2	103.04(13)					

Table 8. Hydrogen atom coordinates ($Å \times 10^4$) and isotropic displacement parameters ($Å^2 \times 10^3$) for **104**.

Atom	x	y	z	U(eq)
H2	12616	7429	1108	26
H3	9325	5122	1323	30
H6A	10811	801	1006	52
H6B	10960	1594	666	52
H6C	12699	287	757	52
H7A	13961	1196	1421	59
H7B	16056	2279	1348	59
H7C	15893	721	1175	59
H8A	14106	3390	571	56
H8B	16216	3527	826	56
H8C	15894	2067	619	56
H9	12934	6819	1689	28
H10	8521	6809	1898	28
H11	6124	7954	1466	25
H12	10448	9595	1646	28
H15A	7306	13853	1909	62
H15B	9467	13599	2152	62
H15C	7138	14323	2277	62
H16A	9314	11598	2559	63

H16B	7000	10652	2589	63
H16C	7038	12324	2700	63
H17A	3822	12365	1943	54
H17B	3662	11077	2201	54
H17C	3539	12745	2314	54
H19A	11174	6189	209	45
H19B	11701	7891	162	45
H19C	10126	7034	-98	45
H20A	5310	6511	425	47
H20B	7331	5363	359	47
H20C	6056	6193	66	47
H21A	8558	9740	255	46
H21B	5988	9176	319	46
H21C	7086	8948	-25	46

(*S*)-*tert*-Butyl-3-(2-(*tert*-butoxy)-2-oxoethyl)pyrrolidine-1-carboxylate (**150**)
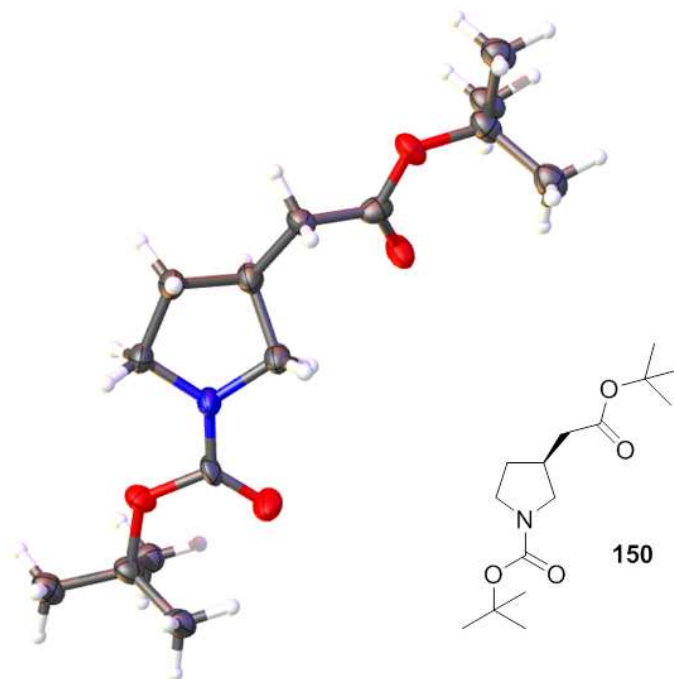
Table 1. Crystal data and structure refinement for **150**.

Empirical formula	$C_{15}H_{27}NO_4$
Formula weight	285.37
Temperature/K	123.00(10)
Crystal system	orthorhombic
Space group	$P22_12_1$
a/Å	6.02696(12)
b/Å	8.52370(17)
c/Å	15.8573(3)
α/°	90
β/°	90
γ/°	90
Volume/Å^3	814.62(3)
Z	2
ρ_{calc}mg/mm^3	1.163
m/mm^{-1}	0.676
F(000)	312.0
Crystal size/mm^3	$0.1519 \times 0.1343 \times 0.0933$
Radiation	CuKα (λ = 1.54184)
2Θ range for data collection	11.16 to 140.508°

Index ranges	$-7 \le h \le 7, -10 \le k \le 9, -17 \le l \le 19$
Reflections collected	4025
Independent reflections	1515 [$R_{int} = 0.0498$, $R_{sigma} = 0.0348$]
Data/restraints/parameters	1515/63/187
Goodness-of-fit on F^2	1.031
Final R indexes [I>=2σ (I)]	$R_1 = 0.0289$, $wR_2 = 0.0757$
Final R indexes [all data]	$R_1 = 0.0308$, $wR_2 = 0.0767$
Largest diff. peak/hole / e Å^{-3}	0.10/-0.13
Flack parameter	0.10(17)

Table 2. Fractional atomic coordinates ($\times 10^4$) and equivalent isotropic displacement parameters ($\text{Å}^2 \times 10^3$) for **150**. U_{eq} is defined as 1/3 of the trace of the orthogonalised U_{IJ} tensor.

Atom	x	y	z	U(eq)
O3	6310(19)	980(20)	6363(8)	31.4(15)
O4	9274(6)	2744(5)	6208(2)	44.9(9)
C12	7320(14)	2409(9)	6054(5)	28.9(16)
C4	3650(7)	2887(5)	5403(3)	32.4(8)
C1	6645(4)	4803(3)	5269.3(19)	34.6(6)
N1	5936(6)	3310(3)	5624.7(18)	30.9(6)
C2	4881(4)	5168(3)	4616.7(19)	30.6(6)
C3	2806(4)	4386(3)	4981.1(19)	32.0(6)
O1	8344(8)	7151(5)	3969(3)	40.2(10)
C6	6480(10)	7710(11)	4007(5)	32.4(18)
O2	5910(20)	9010(20)	3746(9)	32.8(16)
C7	4554(9)	6899(5)	4424(2)	28.8(8)
C10	8650(20)	9572(12)	2430(7)	37.8(18)
C9	9394(19)	10740(20)	3795(8)	45(2)
C8	7534(17)	10200(13)	3218(6)	32.2(16)
C11	5830(30)	11480(16)	3072(8)	38(2)
C15	8500(30)	691(14)	7472(7)	45(2)
C14	9100(17)	-838(19)	6065(7)	36.7(18)
C13	7527(17)	-112(14)	6703(6)	31.8(16)
C16	5940(30)	-1327(17)	7055(9)	43(2)

Table 3. Anisotropic displacement parameters ($\mathring{A}^2 \times 10^3$) for **150**. The anisotropic displacement factor exponent takes the form: $-2\pi^2[h^2a^{*2}U_{11}+2hka^*b^*U_{12}+\ldots]$.

Atom	U_{11}	U_{22}	U_{33}	U_{23}	U_{13}	U_{12}
O3	39(3)	25.8(19)	29(3)	5(2)	-16(2)	8(3)
O4	30(2)	33.3(15)	72(2)	11.0(13)	-14.2(15)	-1.6(15)
C12	35(5)	14(3)	37(2)	4.4(18)	0(4)	-7(3)
C4	26(2)	29.8(17)	41(2)	6.7(15)	-4.8(16)	-7.2(18)
C1	28.6(12)	24.9(14)	50.3(17)	6.1(14)	-5.5(11)	-3.4(12)
N1	23.9(15)	23.1(14)	45.7(15)	7.5(12)	-5.2(13)	-3.1(12)
C2	28.3(12)	24.8(13)	38.8(12)	2.2(12)	0.9(11)	-1.9(11)
C3	25.6(11)	34.0(12)	36.5(11)	6.3(14)	-1.7(12)	-4.8(10)
O1	32(3)	26.6(18)	63(2)	12.4(16)	5.4(19)	1(2)
C6	32(4)	30(3)	35(2)	-6.0(19)	-5(3)	9(3)
O2	42(4)	23.4(17)	33(3)	10(2)	17(2)	-7(3)
C7	31(3)	23.8(19)	31.4(18)	4.7(13)	0(2)	2(2)
C10	52(3)	26(3)	36(3)	-2(3)	15(2)	-7(3)
C9	60(4)	36(3)	37(4)	0(3)	4(3)	-7(3)
C8	45(3)	22(2)	30(2)	9(2)	3(2)	-10(2)
C11	55(3)	21(3)	39(3)	6(3)	5(3)	10(2)
C15	55(3)	37(4)	43(3)	10(2)	-13(2)	11(3)
C14	48(3)	30(3)	32(3)	-1(2)	0(2)	4(2)
C13	43(3)	22(3)	30(2)	3(2)	-5(2)	-5(2)
C16	53(4)	33(4)	42(4)	-2(2)	-6(3)	-5(3)

Table 4. Bond lengths for **150**.

Atom	Atom	Length/Å	Atom	Atom	Length/Å
O3	C12	1.44(2)	O1	C6	1.222(6)
O3	C13	1.30(2)	C6	O2	1.23(2)
O4	C12	1.236(8)	C6	C7	1.505(8)
C12	N1	1.322(9)	O2	C8	1.64(2)
C4	N1	1.467(4)	C10	C8	1.5176(18)
C4	C3	1.529(5)	C9	C8	1.5179(18)
C1	N1	1.456(4)	C8	C11	1.5176(18)
C1	C2	1.516(4)	C15	C13	1.5176(18)
C2	C3	1.530(3)	C14	C13	1.5178(18)
C2	C7	1.519(5)	C13	C16	1.5176(18)

Table 5. Bond angles for **150**.

Atom	Atom	Atom	Angle/°	Atom	Atom	Atom	Angle/°
C13	O3	C12	120.4(10)	O2	C6	C7	110.1(7)
O4	C12	O3	121.9(7)	C6	O2	C8	123.9(9)
O4	C12	N1	124.6(6)	C6	C7	C2	115.7(5)
N1	C12	O3	113.4(7)	C10	C8	O2	117.9(9)
N1	C4	C3	102.2(3)	C10	C8	C9	106.0(9)
N1	C1	C2	103.8(2)	C9	C8	O2	108.8(10)
C12	N1	C4	125.0(5)	C11	C8	O2	96.7(9)
C12	N1	C1	121.5(4)	C11	C8	C10	115.4(10)
C1	N1	C4	113.4(3)	C11	C8	C9	112.0(11)
C1	C2	C3	103.0(2)	O3	C13	C15	103.1(10)
C1	C2	C7	115.3(2)	O3	C13	C14	111.6(11)
C7	C2	C3	113.2(3)	O3	C13	C16	106.6(11)
C4	C3	C2	104.9(2)	C15	C13	C14	118.5(10)
O1	C6	O2	126.3(9)	C15	C13	C16	104.8(10)
O1	C6	C7	123.5(8)	C16	C13	C14	111.2(11)

Table 6. Torsion angles for **150**.

A	B	C	D	Angle/°	A	B	C	D	Angle/°
O3	C12	N1	C4	-5.4(9)	C3	C4	N1	C12	175.8(4)
O3	C12	N1	C1	179.5(7)	C3	C4	N1	C1	-8.8(4)
O4	C12	N1	C4	176.7(5)	C3	C2	C7	C6	-175.8(4)
O4	C12	N1	C1	1.6(9)	O1	C6	O2	C8	5(2)
C12	O3	C13	C15	62.8(14)	O1	C6	C7	C2	-14.4(9)
C12	O3	C13	C14	-65.5(14)	C6	O2	C8	C10	54.4(18)
C12	O3	C13	C16	172.9(11)	C6	O2	C8	C9	-66.2(16)
C1	C2	C3	C4	-36.0(3)	C6	O2	C8	C11	177.8(13)
C1	C2	C7	C6	65.9(5)	O2	C6	C7	C2	168.1(8)
N1	C4	C3	C2	27.4(4)	C7	C2	C3	C4	-161.2(3)
N1	C1	C2	C3	29.9(3)	C7	C6	O2	C8	-177.2(10)
N1	C1	C2	C7	153.6(3)	C13	O3	C12	O4	-10.9(17)
C2	C1	N1	C12	162.2(4)	C13	O3	C12	N1	171.2(10)
C2	C1	N1	C4	-13.5(4)					

Table 7. Hydrogen atom coordinates ($Å\times10^4$) and isotropic displacement parameters ($Å^2\times10^3$) for **150**.

Atom	x	y	z	U(eq)
H4A	2768	2628	5911	39
H4B	3612	1987	5009	39
H1A	8125	4709	5004	42
H1B	6701	5628	5708	42
H2	5282	4620	4081	37
H3A	2077	5079	5398	38
H3B	1732	4135	4528	38
H7A	3237	7009	4056	35
H7B	4223	7450	4959	35
H10A	9795	8809	2590	57
H10B	9341	10441	2121	57
H10C	7545	9061	2071	57
H9A	8766	11112	4329	67
H9B	10214	11595	3524	67
H9C	10402	9861	3905	67
H11A	4631	11074	2715	58
H11B	6537	12374	2791	58
H11C	5214	11820	3614	58
H15A	9507	1529	7292	67
H15B	9324	-77	7810	67
H15C	7301	1139	7813	67
H14A	8249	-1247	5587	55
H14B	9924	-1696	6331	55
H14C	10144	-38	5865	55
H16A	4909	-821	7449	64
H16B	6777	-2143	7350	64
H16C	5094	-1802	6592	64

Table 8. Atomic occupancy for **150**.

Atom	*Occupancy*	Atom	*Occupancy*	Atom	*Occupancy*
O3	0.5	O4	0.5	C12	0.5
C4	0.5	H4A	0.5	H4B	0.5
C1	0.5	H1A	0.5	H1B	0.5
N1	0.5	C2	0.5	H2	0.5

C3	0.5	H3A	0.5	H3B	0.5
O1	0.5	C6	0.5	O2	0.5
C7	0.5	H7A	0.5	H7B	0.5
C10	0.5	H10A	0.5	H10B	0.5
H10C	0.5	C9	0.5	H9A	0.5
H9B	0.5	H9C	0.5	C8	0.5
C11	0.5	H11A	0.5	H11B	0.5
H11C	0.5	C15	0.5	H15A	0.5
H15B	0.5	H15C	0.5	C14	0.5
H14A	0.5	H14B	0.5	H14C	0.5
C13	0.5	C16	0.5	H16A	0.5
H16B	0.5	H16C	0.5		

(1*S*,2*S*,3*S*)-2-((*tert*-Butoxycarbonyl)amino)-3-(methoxycarbonyl)cyclopropane-1-carboxylic acid (**33**)
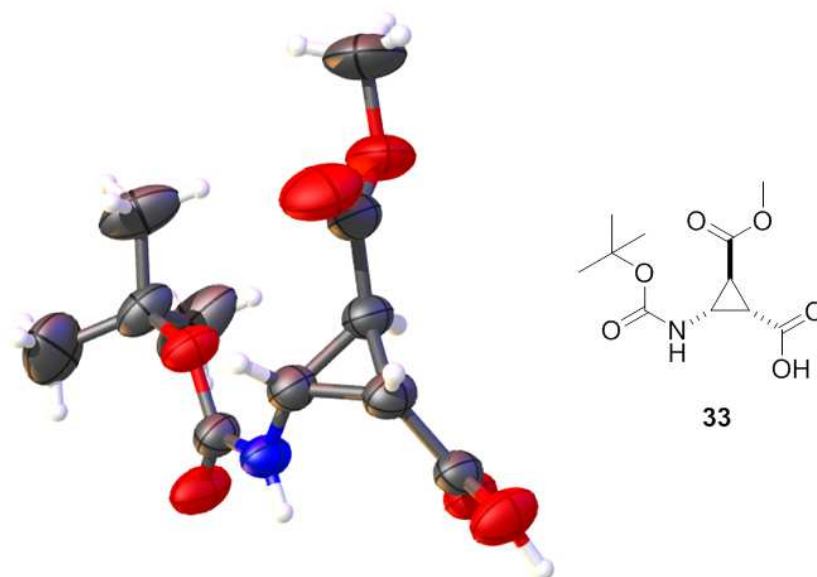
Table 1. Crystal data and structure refinement for **33**.

Empirical formula	$C_{11}H_{17}NO_6$
Formula weight	259.26
Temperature/K	293.0
Crystal system	monoclinic
Space group	$P2_1/c$
a/Å	5.6612(1)
b/Å	14.8842(3)
c/Å	16.2863(3)
α/°	90
β/°	92.0278(16)
γ/°	90
Volume/Å^3	1371.46(4)
Z	4
ρ_{calc}mg/mm^3	1.256
m/mm^{-1}	0.874
F(000)	552.0
Crystal size/mm^3	$0.4343 \times 0.1419 \times 0.082$
Radiation	CuKα (λ = 1.54184)
2Θ range for data collection	8.04 to 151.28°
Index ranges	-7 ≤ h ≤ 5, -18 ≤ k ≤ 16, -20 ≤ l ≤ 20
Reflections collected	5139

Independent reflections	2725 [R_{int} = 0.0153, R_{sigma} = 0.0189]
Data/restraints/parameters	2725/0/169
Goodness-of-fit on F^2	1.086
Final R indexes [I>=2σ (I)]	R_1 = 0.0539, wR_2 = 0.1602
Final R indexes [all data]	R_1 = 0.0583, wR_2 = 0.1676
Largest diff. peak/hole / e $Å^{-3}$	0.20/-0.21
Flack parameter	.

Table 2. Fractional atomic coordinates ($\times 10^4$) and equivalent isotropic displacement parameters ($Å^2 \times 10^3$) for **33**. U_{eq} is defined as 1/3 of the trace of the orthogonalised U_{IJ} tensor.

Atom	x	y	z	U(eq)
O1	3937(3)	2590.3(8)	190.9(9)	77.6(5)
O2	6449(2)	2332.2(8)	1279.3(8)	60.9(4)
O3	8572(3)	6204.0(9)	633.1(9)	74.7(5)
O4	5295(2)	5429.0(8)	866.1(7)	59.7(4)
O5	11855(3)	3891.4(13)	2578.9(11)	98.8(7)
O6	8580(4)	3788.0(13)	3293.1(9)	96.2(7)
N1	6841(3)	3567.5(9)	551.2(8)	53.8(4)
C1	8707(3)	3849.6(10)	1100.1(9)	51.0(5)
C2	9057(3)	4829.9(11)	1281.1(10)	54.5(5)
C3	8123(3)	4202.8(11)	1929.7(9)	54.4(5)
C4	5618(3)	2807.6(10)	646.4(10)	53.6(5)
C5	5324(3)	1497.3(12)	1554.0(13)	66.8(6)
C6	5702(8)	784.9(17)	921(2)	124.6(17)
C7	2793(4)	1650(2)	1731(3)	126.9(16)
C8	6698(5)	1288(2)	2335.9(17)	101.7(10)
C9	7424(3)	5507.4(10)	915.2(9)	52.4(5)
C10	9757(4)	3952.8(12)	2621.5(11)	66.7(6)
C11	10011(8)	3478(3)	3996.8(16)	132.4(17)

Table 3. Anisotropic displacement parameters ($Å^2 \times 10^3$) for **33**. The anisotropic displacement factor exponent takes the form: $-2\pi^2[h^2a^{*2}U_{11}+2hka^*b^*U_{12}+...]$.

Atom	U_{11}	U_{22}	U_{33}	U_{23}	U_{13}	U_{12}
O1	99.3(10)	47.6(7)	82.8(9)	13.3(6)	-39.5(8)	-19.6(6)
O2	60.1(7)	52.3(7)	69.4(7)	20.9(5)	-10.2(5)	-6.5(5)
O3	80.7(9)	53.9(7)	88.0(9)	24.1(6)	-19.1(7)	-16.6(6)
O4	66.0(7)	53.7(7)	59.0(7)	9.9(5)	-4.6(5)	1.3(5)

O5	82.4(11)	109.9(13)	101.2(12)	25.8(10)	-37.0(9)	-3.9(9)
O6	131.2(15)	104.1(13)	52.4(8)	19.3(7)	-9.5(8)	22.3(10)
N1	70.2(8)	42.3(7)	47.9(7)	7.1(5)	-11.2(6)	-7.4(6)
C1	55.4(8)	45.7(8)	51.4(8)	5.0(6)	-5.6(6)	-0.7(6)
C2	60.2(9)	47.5(8)	54.9(8)	6.5(6)	-11.3(6)	-7.7(6)
C3	65.5(9)	47.9(8)	49.1(8)	6.0(6)	-9.2(7)	-2.0(7)
C4	65.3(9)	40.6(8)	54.0(8)	4.4(6)	-8.7(7)	-0.8(6)
C5	56.9(9)	51.7(9)	91.4(13)	25.9(9)	-0.7(8)	-1.4(7)
C6	190(4)	50.8(13)	133(3)	9.3(14)	8(2)	-2.1(16)
C7	63.0(13)	114(2)	205(4)	80(2)	23.5(16)	10.6(13)
C8	86.6(15)	106.9(19)	110.9(19)	64.9(16)	-7.6(13)	-12.0(13)
C9	69.5(10)	42.5(8)	44.4(7)	1.6(6)	-9.4(6)	-7.2(6)
C10	89.4(14)	49.0(9)	59.9(10)	4.7(7)	-21.1(9)	-1.3(8)
C11	196(4)	133(3)	65.2(14)	29.5(15)	-37.8(18)	23(2)

Table 4. Bond lengths for **33**.

Atom	Atom	Length/Å	Atom	Atom	Length/Å
O1	C4	1.229(2)	N1	C4	1.338(2)
O2	C4	1.323(2)	C1	C2	1.500(2)
O2	C5	1.473(2)	C1	C3	1.498(2)
O3	C9	1.315(2)	C2	C3	1.519(2)
O4	C9	1.211(2)	C2	C9	1.479(2)
O5	C10	1.196(3)	C3	C10	1.480(3)
O6	C10	1.324(3)	C5	C6	1.500(4)
O6	C11	1.455(4)	C5	C7	1.489(3)
N1	C1	1.423(2)	C5	C8	1.501(3)

Table 5. Bond angles for **33**.

Atom	Atom	Atom	Angle/°	Atom	Atom	Atom	Angle/°
C4	O2	C5	122.83(13)	O2	C4	N1	111.79(14)
C10	O6	C11	115.3(2)	O2	C5	C6	108.30(19)
C1	N1	C4	123.53(13)	O2	C5	C7	111.06(17)
N1	C1	C2	120.03(14)	O2	C5	C8	102.48(16)
N1	C1	C3	119.19(14)	C6	C5	C7	113.8(3)
C2	C1	C3	60.87(11)	C6	C5	C8	110.7(2)
C1	C2	C3	59.48(10)	C7	C5	C8	109.9(2)

C1	C2	C9	120.50(14)	O3	C9	O4	123.78(15)
C3	C2	C9	118.12(14)	O3	C9	C2	111.64(15)
C1	C3	C2	59.66(10)	O4	C9	C2	124.57(14)
C1	C3	C10	116.53(15)	O5	C10	O6	124.3(2)
C2	C3	C10	117.42(15)	O5	C10	C3	124.79(18)
O1	C4	O2	125.16(15)	O6	C10	C3	110.88(19)
O1	C4	N1	123.04(15)				

Table 6. Hydrogen bonds for **33**.

D	H	A	d(D-H)/Å	d(H-A)/Å	d(D-A)/Å	D-H-A/°
N1	H1N	O4[1]	0.83(2)	2.16(2)	2.9705(18)	167(2)
O3	H3O	O1[1]	0.92(2)	1.72(3)	2.628(2)	172(2)
C6	H6A	O1	0.9600	2.5200	3.090(3)	118.00
C7	H7B	O1	0.9600	2.3500	2.964(5)	121.00

[1]1-X,1-Y,-Z

Table 7. Torsion angles for **33**.

A	B	C	D	Angle/°	A	B	C	D	Angle/°
N1	C1	C2	C3	108.83(17)	C3	C1	C2	C9	-106.72(17)
N1	C1	C2	C9	2.1(2)	C3	C2	C9	O3	154.88(14)
N1	C1	C3	C2	-110.17(16)	C3	C2	C9	O4	-26.3(2)
N1	C1	C3	C10	142.12(15)	C4	O2	C5	C6	70.1(2)
C1	N1	C4	O1	176.49(16)	C4	O2	C5	C7	-55.5(3)
C1	N1	C4	O2	-3.8(2)	C4	O2	C5	C8	-172.87(17)
C1	C2	C3	C10	106.22(17)	C4	N1	C1	C2	-144.59(16)
C1	C2	C9	O3	-135.82(15)	C4	N1	C1	C3	-73.3(2)
C1	C2	C9	O4	43.0(2)	C5	O2	C4	O1	-4.6(3)
C1	C3	C10	O5	37.2(3)	C5	O2	C4	N1	175.71(14)
C1	C3	C10	O6	-141.58(16)	C9	C2	C3	C1	110.67(16)
C2	C1	C3	C10	-107.71(17)	C9	C2	C3	C10	-143.11(15)
C2	C3	C10	O5	-30.7(3)	C11	O6	C10	O5	-2.7(3)
C2	C3	C10	O6	150.58(16)	C11	O6	C10	C3	176.1(2)

Table 8. Hydrogen atom coordinates ($Å\times10^4$) and isotropic displacement parameters ($Å^2\times10^3$) for **33**.

Atom	x	y	z	U(eq)
H1	10159	3493	1083	61
H1N	6460(40)	3884(14)	148(14)	65
H2	10700	5024	1368	65
H3	6444	4255	2049	65
H3O	7570(40)	6599(17)	362(16)	90
H6A	4924	957	412	150
H6B	5061	226	1105	150
H6C	7365	716	841	150
H7A	2112	1101	1923	152
H7B	1957	1842	1238	152
H7C	2677	2105	2145	152
H8A	8355	1271	2230	122
H8B	6210	716	2542	122
H8C	6409	1745	2736	122
H11A	11178	3923	4142	159
H11B	10783	2926	3859	159
H11C	9016	3378	4453	159

4 Curriculum Vitae

Ludwig Konrad Alois Pilsl

Personal Data

Date of Birth	07/26/1985
Marital status	Unmarried
Nationality	German
Email	ludwig.pilsl@ur.de

Education

02/2014 – Current	Postdoctoral fellow in the group of *Prof. A. J. Wilson* (School of Chemistry, University of Leeds, UK)
10/2010 – 01/2014	PhD thesis in the group of *Prof. O. Reiser* (University of Regensburg, Germany)
09/2011 – 10/2011	Research stay with *Prof. R. M. Ortuño* (Universitat Autònoma de Barcelona, Spain)
09/2010	Master of Science in Chemistry
01/2010 – 09/2010	Master of Science thesis in the research groups of *Prof. O. Reiser* and *Prof. T. A. Martinek / Prof. F. Fülöp* (University of Szeged, Hungary)
11/2008 – 12/2009	Internship in the research group of *Prof. O. Reiser*
10/2008 – 09/2009	Advanced studies in Organic Chemistry
09/2008	Bachelor of Science in Chemistry
03/2008 – 06/2008	Bachelor of Science thesis in the research group of *Prof. O. Reiser*
10/2005 – 09/2010	Studies in Chemistry, University of Regensburg, Germany
09/1996 – 07/2005	Abitur (*A-levels*) Gymnasium (secondary school) Kelheim, Germany, *High school Certificate equivalent.*

Referees

Prof. Dr. Oliver Reiser

Institut für Organische Chemie

Universität Regensburg, Universitätsstr. 31

D-93053 Regensburg, Germany

oliver.reiser@ur.de

Prof. Dr. Tamás A. Martinek

Institute of Pharmaceutical Chemistry

University of Szeged, Eötvös u. 6

H-6720 Szeged, Hungary

martinek@pharm.u-szeged.hu

Prof. Dr. Rosa M. Ortuño Mingarro

Department of Chemistry

Universitat Autònoma de Barcelona

Cerdanyola del Vallès

E-08193 Barcelona, Spain

rosa.ortuno@uab.es

List of publications

1. **Enantioselective cyclopropanation of *N*-Boc-pyrrole – synthesis of homo-β-proline.**
    L. Pilsl, T. Ertl, O. Reiser, *manuscript in preparation.*

2. **Larvae of the parasitoid wasp *Ampulex compressa* sanitize their host, the American cockroach, with a blend of antimicrobials.**
    G. Herzner, A. Schlecht, V. Dollhofer, C. Parzefall, K. Harrar, A. Kreuzer, **L. Pilsl**, J. Ruther, *Proc. Natl. Acad. Sci.* U. S. A. **2013**, *110*, 1369-1374.

3. **Unique *α,β*- and *α,α,β,β*-peptide foldamers based on cis-*β*-aminocyclopentanecarboxylic acid.**
    Ł. Berlicki, **L. Pilsl**, E. Wéber, I. M. Mándity, C. Cabrele, T. A. Martinek, F. Fülöp, O. Reiser, *Angew. Chem.* **2012**, *124*, 2251-2255; *Angew. Chem. Int. Ed.* **2012**, *51*, 2208-2212.

4. **α/β-Peptide foldamers: state of the art.**
    L. Pilsl, O. Reiser, *Amino Acids* **2011**, *41*, 709-718.

Conferences

Foldamers: From Design to Protein Recognition – European Institute of Chemistry and Biology, Bordeaux-Pessac (France), January 25-28, 2010. *"Synthesis of new unnatural amino acids for foldamers and neuropeptide Y (NPY) analogues as selective ligands for NPY receptors"* (poster).

Peptidkémia – Balatonszemes (Hungary), May 26-28, 2010.

Foldamers: Design, Synthesis and Applications – Alma Mater Studiorum Universita di Bologna (Italy), October 6-8, 2010. *"De Novo design of new α,α,β,β-peptide foldamers"* (oral communication, 20 min).

10th German Peptide Symposium – Freie Universität Berlin (Germany), March 7-10, 2011. *"De Novo design of new α,α,β,β-peptide foldamers"* (short lecture 3 min + poster).

Foldamers: Synthesis and Structure of Functional Materials – Casa de Convalescència, Barcelona (Spain), April 7-9, 2011. *"De Novo design of α/β-peptide foldamers"* (short lecture 5 min + poster).

4th EuCheMS Chemistry Congress – Prague Congress Centre, Prague (Czech Republic), August 26-30, 2012. *"Copper-catalyzed enantioselective cyclopropanations of heterocyclic compounds using diazoacetates"* (poster).

Foldamers: Synthesis and Structure of Functional Materials – Universität Regensburg (Germany), August 30 – September , 2012. *"Asymmetric cyclopropanation reactions of heterocyclic substrates – toward β-aminocycopropanecarboxylic acids (β-ACCs)"* (short lecture 5 min + poster).

11th German Peptide Symposium – Technische Universität München (Germany), March 18-21, 2013. *"De Novo design of secondary structure motifs from mixed α/β–peptide foldamers"* (short lecture 3 min + poster).

Paris 2013 Symposium on Foldamers – Les Cordeliers Paris (France), April 10-12, 2013. *"Foldamers under pressure"* (poster).

15th International Conference 'Heterocycles in Bio-organic Chemistry' – Latvian Institute of Organic Synthesis Riga (Latvia), May 27-30, 2013. *"Asymmetric cyclopropanation of heterocycles"* (oral communication 15 min + poster).

H Acknowledgments – Danksagung

Herzlich bedanken möchte ich mich bei:

- Prof. Oliver Reiser für die interessante Themenstellung, die beständige Unterstützung während der gesamten Arbeit und die Ermöglichung meines Auslandsaufenthalts.

- Prof. Rosa M. Ortuño, Dr. Ona Illa, sowie allen Mitarbeitern für die freundliche Aufnahme in den Arbeitskreis in Barcelona.

- Prof. Dr. Dr. Hans-Robert Kalbitzer und Prof. Dr. Werner Kremer für die Messungen der NMR Spektren unter Hochdruck.

- Prof. Dr. Roland Winter für die Messungen der FTIR Spektren unter Hochdruck und Hilfe bei deren Auswertung.

- Dr. Peter Kreitmeier, Dr. Sabine Amslinger und besonders Prof. Dr. Kirsten Zeitler für fachkundige Diskussionen und Hilfestellungen bei Problemen jeglicher Art.

- Allen Mitarbeitern der Zentralen Analytik der Universität Regensburg für sämtliche Messungen und bereitwillige Hilfestellung bei Problemen.

- Georg Adolin, Klaus Döring, Helena Konkel, besonders Roxanne Harteis für synthetische Hilfestellungen, sowie unseren Sekretärinnen Antje Weigert, Young Rothermund und Hedwig Ohli für die stete Hilfsbereitschaft bei Problemen jedweder Art.

- Meinen Freunden und Laborkollegen Daniel Rackl, Andreas Okun, Dr. Klaus Harrar und Dr. Markus Hager, sowie Dr. Gang Xu, Dr. Yudha S. Salprima, Dr. Woraluk Mansawat für die stets lockere und angenehme Atmosphäre im Labor.

- Dr. Georgiy Kachkovskyi für seine Ratschläge, Hilfestellungen und interessante Diskussionen über Chemie und andere Dinge.

- Matthias Knorn für die Bereitstellung der Isonitrile und Oxazoline.

- Karin, Andi, Tom, Jimmy, Corina, Soraia, Francesca (Franzi), Roland, Paul, Christian, Matze, Hana Seo, Sudipta, Sebastian, Michl, Julian, Pietro, Mattia Marchini, Marco

Durini, Qurin, Andreas Bergmann, sowie allen aktuellen und ehemaligen Mitgliedern des Arbeitskreises.

- Thomas Ertl für seine Freundschaft, gute Laune, morgendlichen Kaffee, Ertl Bräu und alle Unterstützung und Hilfe während der letzten Jahre.

- Soraia Fernandes für ihre Freundschaft, Offenheit, Lebensfreude und die Einführung in portugiesische Kultur (*bacalhau*, *fado* usw.)

- Martin (Jimmy) Hofmann, Corina Eichenseer, Daniel Rackl und Thomas Ertl für das Korrekturlesen dieser Arbeit.

- Meinen ehemaligen Bachelorstudenten und Forschungspraktikanten Max Halder, Thomas Hausler, Yannick Mousli, Marco Peteranderl, Thomas Ertl und Uwe Faltermeier für synthetische Unterstützung und anregende Diskussionen.

- Meinen Freunden Agnes und Klaus, Judith und Markus, Hans, Flo, Alex, Ignaz, Micha und Wolle, Heike und Patrick, Matt und Caro, Julia und Carlos, Michel und Anni.

- Meinen Kollegen und Freunden aus Barcelona Jimena, Fernando, Alessandro, Raquel, Enric, Marta und Adaris.

- Prof. Tamás A. Martinek, Dr. István M. Mándity und Dr. Edit Wéber für die freundliche Aufnahme an den Arbeitskreis in Szeged, die langjährige Freundschaft, sowie Hilfestellungen jeglicher Art.

- Meinen Eltern, Anna und Ludwig, sowie Lisa, den 'Passauern' und meiner gesamten Familie für die ganze Unterstützung im Laufe der Jahre.

- Meiner Verlobten Berni für die unermessliche Hilfe, Unterstützung und Geduld in den letzten Jahren.

Declaration

Herewith I declare that I have made this existing work single-handed. I have only used the stated utilities.

Regensburg, February 14, 2014

Ludwig K. A. Pilsl